

User-oriented Solutions for Improved Monitoring and Management of Biodiversity and Ecosystem services in vulnerable European Seas

Deliverable 3.1 Report on temporal trends and spatial patterns of multiple biodiversity indicators



Deliverable Title: Report on temporal trends and spatial patterns of multiple

biodiversity indicators

Work package: 3 Biodiversity status and cumulative impacts

Deliverable no: D3.1

Lead beneficiary: DTU Aqua

Lead responsible for the report: Martin Lindegren (DTU)

mli@aqua.dtu.dk

Submission date: 30th September 2025

Authors and citation:

Martin Lindegren, Manuel Hidalgo, Marcel Montanyes, Federico Maioli, Benjamin Weigel, Daniel van Denderen, Gleb Tikhnov, Otso Ovaskainen, Baptiste Degueurce, Tim Jimenez, Francesco Golin, Ingibjörg G. Jónsdóttir, Haseeb Randhawa, Julian Burgos, Walter Zupa, Antonella Consiglio, Matteo Chiarini, Maria Teresa Spedicato, Patricia Puerta, Alicia Gran, Shannon Moore, Laurene Pecuchet, Murray Thompson, Lily Greig, Keith Cooper, Georg Engelhard, Justin Tiago, Marcel Rozemeijer, Sofia Henriques, André Martins, Corina Chaves, Rita Vasconcelos, Teresa Moura (2025) – B-USEFUL. Report on temporal trends and spatial patterns of multiple biodiversity indicators. Technical University of Denmark.

Dissemination Level: PU

PU: Public

PP: Restricted to other programme participants (including the Commission Services)

RE: Restricted to a group specified by the consortium (including the Commission Services)

CO: Confidential, only for partners of the consortium (including the Commission Services)

Executive summary

The goal of the B-USEFUL project is to contribute to achieve policy goals of EU Green Deal and the Biodiversity Strategy 2030 by developing user-oriented tools and solutions to conserve and protect marine biodiversity, effectively building and improving upon existing European data infrastructures and governance frameworks. The role of this deliverable is to report on key outcomes of extensive modelling activities undertaken by partners under Task 3.1. The modelling of marine species distribution, composition and overall diversity featured within this deliverable report represent a broad range of marine ecosystems and organisms sampled along European shelf seas from the Eastern Mediterranean Sea to Greenland and Barents Sea. Consequently, the organisms and areas considered are exposed to very different regional and local environmental conditions, both in terms of climate and hydrography, but also with regards to the type and level of human activities and their associated pressures. Furthermore, the model development relies on available monitoring data that may differ in terms of the spatio-temporal extent, as well as the amount and resolution of species occurrence and abundances data and their associated trait information. Despite these differences, the model results allows us to compare key outputs across areas and organism groups.

In terms of environmental drivers we found that ocean climate and hydrography are primary determinants of species distributions and community composition. Among these, bottom temperature stands out as a key predictor throughout most areas, with species responding both positively and negatively to increasing temperature. In addition to the broad and ubiquitous effect of temperature, we found a number of environmental variables with more regional and local impacts, including depth and salinity. Taken together, the broad range of studies indicate that environmental filtering, conditioned on drivers and conditions operating across both larger and local spatial scales is a primary community assembly process determining the past, current, but also future distribution and composition of marine organisms throughout European Seas. However, while a large degree of variation in species distribution and abundance can be explained by the set of environmental conditions included, the importance of spatial random effects across our models underscore the importance of other drivers and assembly processes. These include a range of largely unmeasured environmental covariates not yet accounted for in our modelling setup, but also potential biotic effects channelled through competitive or predator-prey interactions. Hence, we recommend further efforts compiling data and information on such candidate drivers, as well as studies examining the role and relative importance of local biotic interactions, partly reflected by the pair-wise residual associations of our models.

The set of biodiversity indicators estimated from the fitted and validated models, or from data analysis, include both species and community-level indicators (i.e., reflecting the overall taxonomic and functional richness, evenness and dispersion). These indicators show marked spatial variation in terms of patterns and trends both within and among regions and metrics. Taken together, the differences and similarities in patterns and trends among these "Essential Biodiversity Variables" (EBVs) may challenge end-users and managers involved in Marine Spatial Planning (MSP), especially since hotspots or broader regions of "high biodiversity" may seem contingent on the set of indicators and metrics considered. Hence, we advocate a broader and holistic perspective aiming to embrace this complexity when identifying candidate locations and areas for protection under different scenarios of change.

Index

E)	xecutive summary	3
In	dex	4
1.	The role of this deliverable	7
	Acronyms and abbreviations	8
2.	Introduction	9
	2.1 Background and overview	
	2.2 Biodiversity: from definitions to indicators	
	2.3 Community assembly rules	
	2.4 Joint species distribution models	. 12
	2.5 Application of other data driven approach for biodiversity assessments	. 14
	2.5 Application of species distribution modelling in B-USEFUL	. 15
	2.6 References	. 16
3.	Summary of model results across areas	19
٠.	3.1 North East Atlantic fish model	
	3.1.1. Study area and data availability	
	3.1.2. Model fitting, validation and predictions	
	3.1.3. Model diagnostics and performance	
	3.1.4. Species responses to drivers	
	3.1.5. Patterns and trends in biodiversity	
	3.1.6. Summary	
	3.1.7. References	
	3.2 North Sea fish model	
	3.2.1. Study area and data availability	
	3.2.2. Model setup, fitting and validation	
	3.2.3. Model diagnostics and performance	
	3.2.4. Species and trait responses to drivers	
	3.2.5. Patterns and trends in biodiversity	
	3.2.6. Summary	
	3.2.7. References	
	3.3 Baltic Sea fish model	
	3.3.1. Study area and data availability	

3.3.2. Model setup, fitting and validation	37
3.3.3. Model diagnostics and performance	38
3.3.4. Species and trait responses to drivers	38
3.3.5. Patterns and trends in biodiversity	40
3.3.6. Summary	42
3.3.7. References	42
3.4 Baltic Sea benthos model	43
3.4.1. Study area and data availability	43
3.4.2. Model setup, fitting and validation	44
3.4.3. Model diagnostics and performance	44
3.4.4. Species and trait responses to drivers	45
3.4.5. Patterns and trends in biodiversity	46
3.4.6. Summary	48
3.4.7. References	48
3.5 Icelandic fish model	49
3.5.1. Study area and data availability	49
3.5.2. Model setup, fitting and validation	51
3.5.3. Model diagnostics and performance	51
3.5.4. Species and trait responses to drivers	52
3.5.5. Patterns and trends in biodiversity	54
3.5.6. Summary	56
3.5.6. References	57
3.6 Central-Eastern Mediterranean Sea model	59
3.6.1. Study area and data availability	59
3.6.2. Model setup, fitting and validation	61
3.6.3. Model diagnostics and performance	63
3.6.4. Species and trait responses to drivers	65
3.6.5. Patterns and trends in biodiversity	68
3.6.6. Summary	70
3.6.7. References	71
3.7. Western Mediterranean model	<i>75</i>
3.7.1. Study area and data availability	<i>75</i>
3.7.2. Model fitting, validation and predictions	76
3.7.3. Model diganostics and performance	77

	3.7.4. Species and trait responses to drivers	. 79
	3.7.5. Patterns and trends in biodiversity	. 80
	3.7.6. Summary	. 82
	3.7.7. References	. 83
	3.8 Barents Sea fish model	. 85
	3.8.1. Study area and data availability	. 85
	3.8.2. Model setup, fitting and validation	. 86
	3.8.3. Model diagnostics and performance	. 87
	3.8.5. Patterns and trends in biodiversity	. 91
	3.8.6. Summary	. 92
	3.8.7. References	. 93
4.	Alternative approaches to biodiversity assessments	94
	4.1. Biodiversity assessment across organism groups in the Greater North Sea	. 94
	4.1.1. Study area and data	. 94
	4.1.2. Methods and indicators	. 95
	4.1.3. Results	. 96
	4.1.4. Summary	. 98
	4.1.5. References	. 98
	4.2 Data driven analysis on biodiversity indicators of North Sea invertebrates	. 99
	4.2.1. Study area and data availability	. 99
	4.2.2. Results	101
	3.7.3. Discussion	103
	3.5.6. Summary	105
	3.7.6. References	105
	4.3 Data driven analysis on fish biodiversity in the Iberian Coasts	106
	4.3.1. Study area and data availability	106
	4.3.2. Results	107
	4.3.3. References	108
5.	Summary and perspectives	.109
	,	
6.	Appendices	.112
V	ersion History	.112

1. The role of this deliverable

The goal of the B-USEFUL project is to contribute to achieve policy goals of EU Green Deal and the Biodiversity Strategy 2030 by developing user-oriented tools and solutions to conserve and protect marine biodiversity, effectively building and improving upon existing European data infrastructures and governance frameworks. The role of this deliverable is to report on key outcomes of extensive modelling activities undertaken by partners under Task 3.1. The set of methods rely primarily on advanced joint-species distribution models (jSDM) capable of integrating multiple sources of data (e.g., observations of species composition and abundances, environmental covariates, species traits and phylogeny) derived from data collection and standardization performed under WP2. After proper cross-validation, the set of trained and parameterized models are used to generate community-level outputs of biodiversity indicators, reflecting a suite of "essential biodiversity variables" (EBVs) deemed important by end-users (from workshops under WP1; D1.2). These include both spatial patterns and trends in indicators across European Seas and for different organism groups (e.g., fish, benthic invertebrates, cephalopods). The activities build on training activities and knowledge sharing among partners achieved through dedicated workshops together with key experts in the field (Milestone 3.1). Beyond this deliverable, the developed models will be used in downstream WPs, notably WP5 where scenario testing of conservation and management strategies supporting Marine spatial planning (MSP), including Marine Protected Areas (MPAs) will be performed and later visualized as part of decision-support tools (DST) developed under WP6. The deliverable is structured to first provide a brief background of the field, followed by a description of the key methods used and its setup and implementation across areas and organism groups. The section represent primarily manuscript in preparation, or in review, with a single contribution published prior to submission of this report (see section 3.2; Montanyes et al., 2023).



Figure 1.1. Participants of a training event organized in Barcelona (22-24th Feb 2023) focused on Hierarchical Modelling of Species Communities (HMSC).



Acronyms and abbreviations

EBVs: Essential Biodiversity Variables

MSP: Marine Spatial Planning

MPAs: Marine Protected Areas

SDM: Species Distribution Modelling

JSDM: Joint Species Distribution Modelling

HMSC: Hierarchical Modelling of Species Communities

BTS: Beam Trawl Surveys

DATRAS: online database of trawl surveys at ICES

DOI: Digital Identifier of an Object

EMODnet: European Marine Observation and Data Network

GFCM: General Fisheries Commission for the Mediterranean

GFW: Global Fishing Watch

GSA: GFCM Geographical Sub Area

IBTS: International Bottom Trawl Surveys

ICES: International Council for the Exploration of the Sea

IPCC: Intergovernmental Panel on Climate Change

IUCN: International Union for the Conservation of Nature

MEDITS: Mediterranean International Bottom Trawl Survey

MSFD: Marine Strategy Framework Directive

OSPAR: Convention for the Protection of the Marine Environment of the North-East Atlantic

PT-IBTS: International Bottom Trawl Survey in Portugal

SP-NORTH: Spanish North Coast Bottom Trawl Survey

SST: Sea Surface Temperature

VMS: Vessel Monitoring Systems

2. Introduction

2.1 Background and overview

We are currently experiencing a rapid and accelerating loss of biodiversity worldwide, largely due overexploitation, habitat loss and climate change (Butchart et al., 2010; IPBES, 2019; Lee et al., 2023; Pimm et al., 2014). Global warming has also caused shifts in species distribution, primarily towards higher latitudes, as species follow their thermal niche (Dulvy et al., 2008; Freeman et al., 2018; Pinsky et al., 2013). The rate of extinctions and distributional shifts varies between taxa (Perry et al., 2005; Poloczanska et al., 2013), suggesting that community composition, as well as the structure and functioning of ecosystems may be profoundly altered (Harley et al., 2006). Consequently, understanding the key drivers and underlying assembly processes determining species distribution and composition is essential to anticipate the effects of a changing environment on biodiversity and ecosystem functioning (Harley et al., 2006; McGill et al., 2006; Micheli et al., 2017; Mouillot et al., 2013). Furthermore, more accurate predictions of biodiversity changes may allow us to evaluate and devise effective management actions to halt the current loss of biodiversity worldwide (Mace et al., 2005; Pimm et al., 2014). The accomplishment of this ambitious policy goal is regarded to be achievable through an effective and well-connected system of protected areas jointly covering 30% of the land and ocean space (Convention on Biological Diversity, 2021; European Commission, 2020; Hermoso et al., 2022). However, the designation of protected areas, especially towards "areas of particular importance for biodiversity" (European Commission, 2020) needs to be based on a suite of indicators reflecting the multiple facets of biodiversity (Cavender-Bares et al., 2020; Pereira et al., 2013). This requires robust modelling frameworks capable of mapping the status and trends in key biodiversity indicators to inform decisionmakers and managers (Jetz et al., 2019), while at the same time providing improved process understanding of the underlying drivers and community assembly processes determining patterns and changes in the distribution and composition of marine communities. In the following sections we will briefly introduce: (i) the field of biodiversity and the key indicators in place to represent this diversity; (ii) the concept of community assembly rules underlying biodiversity; and (iii) the modelling frameworks in place to provide indicators while addressing the underlying drivers and community assembly processes.

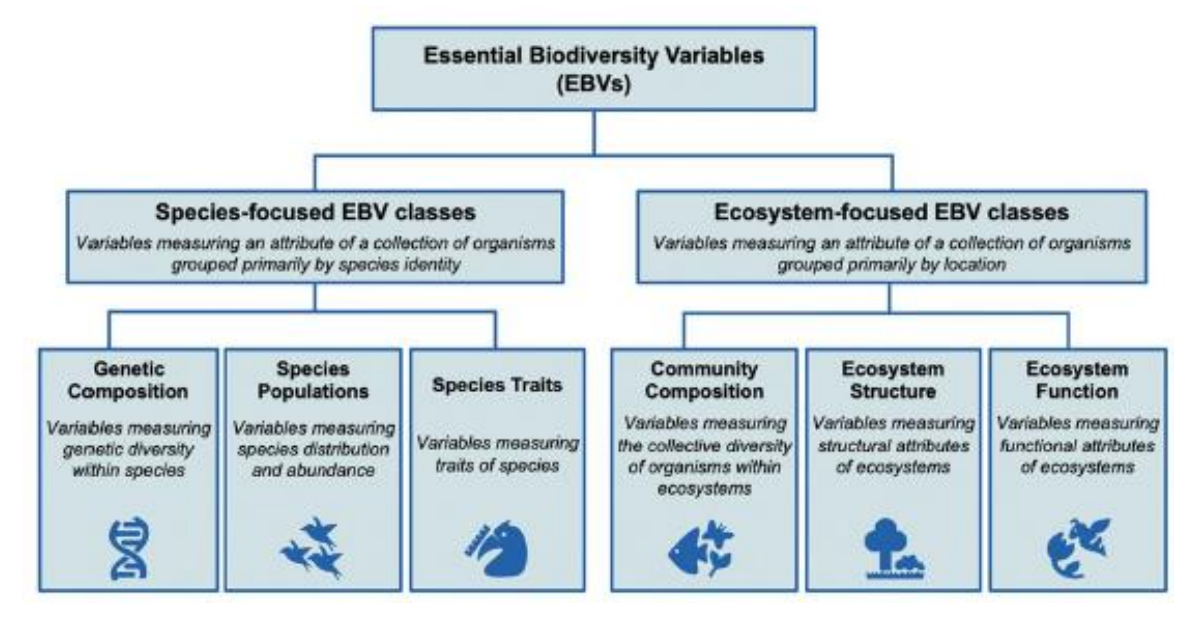


Figure 2.1. Essential Biodiversity Variables and their categories (source: Cavender-Bares et al. 2020).

2.2 Biodiversity: from definitions to indicators

The variety of life on Earth, defined by the term biodiversity, spans diverse levels of organization, encompassing genes, species, traits, communities, and entire ecosystems (Rawat & Agarwal, 2015). This manifestation of biological diversity occurs within specific spatio-temporal contexts, reflecting the complexity of a multifaceted concept. Therefore, when addressing biodiversity, we delve into a comprehensive concept that embraces multiple perspectives and dimensions. Traditionally, biodiversity has been quantified by assessing the number and identity of species within an ecosystem. However, contemporary ecology recognizes that each facet of biodiversity holds significance, offering unique perspectives and illuminating diverse ecological processes. The complexity inherent in biodiversity poses challenges in effectively communicating key information and indicators (Magurran & McGill, 2010), potentially leading to misguided management and conservation efforts. Therefore, establishing a common language for sharing biodiversity knowledge is crucial for managers, researchers and stakeholders in order to optimize resource utilization (Jetz et al., 2019; Pereira et al., 2013). More specifically, we require a consistent framework for characterizing biodiversity that better facilitates the monitoring process, and the integration and sharing of data and outputs across different habitats, regions, and over time (Navarro et al., 2017). To that end, the Essential Biodiversity Variables (EBV) (Pereira et al., 2013) provide a conceptual framework that aims to clearly identify key biodiversity indicators that can be easily implemented, harmonized and that facilitates communication, among scientist but also with institutions. The EBV comprise six classes of variables that describe different aspects of biodiversity, such as genetic composition, species populations, species traits, community composition, ecosystem structure and ecosystem function (Figure 2.1). These are a set of biological indicators complementary to each other that allow detection and evaluation of patterns, changes, trends and processes in biodiversity (Pereira et al., 2013). The EBVs act as the guiding framework for B-USEFUL when selecting and modelling biodiversity indicators.

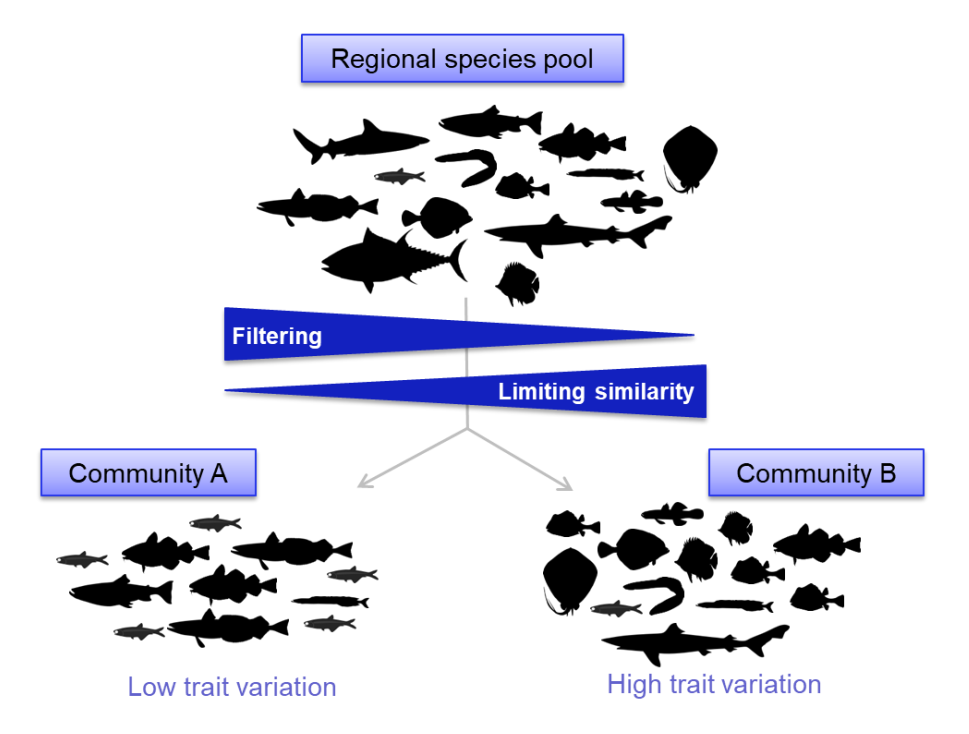


Figure 2.2. Illustration of the community assembly rule concept where species from a regional pool are selected through a filtering process conditioned on their traits. (Adapted from Mouillot et al., 2007).

2.3 Community assembly rules

Patterns and changes in biodiversity emerge from diverse processes operating across various scales. To effectively manage natural areas and allocate resources for conservation, it is imperative to comprehend the inherent dynamics of these processes and their role in shaping natural communities. Once we are able to disentangle the dynamics of these processes, we can study, understand and anticipate the potential impacts of stressors on biodiversity, such as climate change. The community assembly processes framework is one of the main standing ecology theories. The assembly processes theory describes that the communities that we observe in nature are determined by the joint action of a set of filters, which act at different spatio-temporal scales (Figure 2.2). From a global pool of species, the evolutionary history and the dispersal capabilities of such species will determine a subset that is able to reach a certain region (Cadotte & Tucker, 2017; Keddy, 1992). Then, from the regional pool of species, those that are not adapted to the specific abiotic conditions of the region (i.e., the environment) will be filtered out. Furthermore, biotic interactions will modify the subset of species that have gone through the environmental filter, either excluding species through competitive interactions, or including them through facilitative processes (Bruno et al., 2003; Diamond, 1975; Zobel, 1997). The set of species that has gone through all the filters will comprise the local pool of species and thus the actual assemblage of species that we observe in a specific time and location. Traditionally, the study of the assembly processes has been centered on the taxonomic identity and diversity of the species forming communities. However, what determines if species can adapt to the local environment, how they interact with other species, and their specific dispersal capabilities are all linked to their functional characteristics, their so-called traits. The above-described filters will exclude species that lack certain traits (or their combination) and are therefore poorly adapted to the specific local conditions (Götzenberger et al., 2012; Keddy, 1992; Zobel, 1997). Moreover, this trait perspective enables to find rules that determine community composition and structure between communities with completely different species, enabling to make comparisons and predictions (Keddy, 1992; McGill et al., 2006).

Anthropogenic activities have an impact on the filtering process of the community assembly rules. For instance, climate change is modifying the environmental characteristics of the whole Earth system through e.g., warming, which directly affects the local pool of species as they follow their thermal niche towards higher latitudes or deeper and colder waters (Dulvy et al., 2008; Perry et al., 2005). A second example is the introduction of non-indigenous species (NIS), which can lead to competitive exclusion of some native species (Clavero et al., 2022; Thomsen et al., 2014). Lastly, habitat destruction can combine the effects on both environmental and biotic filtering through the modification of the physical conditions of a community such as the habitat complexity. For instance, if the habitat is formed by an organism (e.g., biogenic reefs), its destruction can have severe implications for species interactions if there were some dependencies, but also leaving a bare substrate that can now be colonized by other habitatforming species (Stachowicz et al., 2007). A better understanding of the processes and underlying drivers that shape marine communities can improve our knowledge on marine ecosystems and how to better manage and conserve them and their services (Thompson et al., 2022). Species distribution models can be useful tools that, when applied to the extensive datasets available in time and space, can reveal relevant insights on these processes at both single-species and whole-community levels (Brown, 2014; Ovaskainen et al., 2017; Thuiller,

2015). Moreover, the inclusion of traits in modelling exercises can also shed light on trait-environment relationships within communities and may inform about some mechanisms driving community composition and changes. Such modelling tools can produce predictions on how single species, and whole communities, will change under certain climate change scenarios, which can provide important knowledge for management and conservation (Botkin et al., 2010; Franklin, 2023; Urban et al., 2016). This can in fact allow us to anticipate future situations and take the necessary actions for safeguarding healthy ecosystems which can sustain the goods and services that humankind benefits from. Below we will provide a brief background of such models and their application within B-USEFUL.

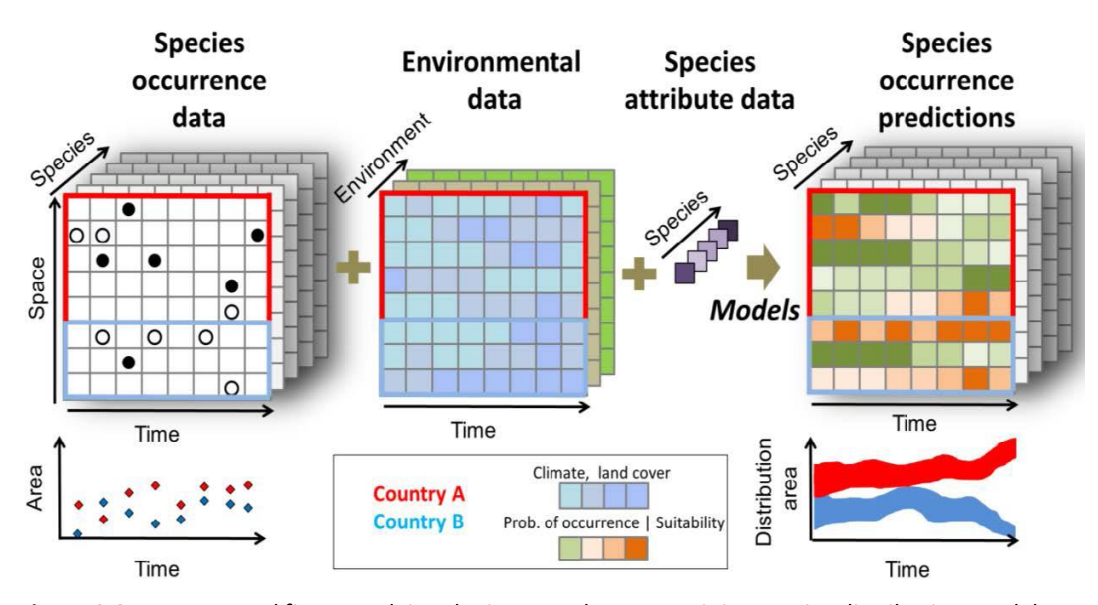


Figure 2.3. A conceptual figure outlying the input and output to joint species distribution models used to improve our understanding or drivers and community assembly rules, while at the same time providing estimates of EBVs relevant for assessing the status and trends in biodiversity. (From: Jetz et al. 2019).

2.4 Joint species distribution models

Species distribution models (SDMs), also known as ecological niche models or habitat models, are a widespread tool used in ecology to understand and estimate the relationship between species occurrence or abundance (or biomass) and environmental conditions, i.e., represent the species realized niche. There are many different methods for performing SDMs (e.g., Generalized Additive Models, Random Forest, Support Vector Machines) each with their advantages and disadvantages (Yates et al., 2018). Moreover, SDMs allow predicting species occurrence or abundance under certain environmental conditions, which can be useful for exploring the outcomes of specific scenarios (e.g., climate change). When the models for making predictions, it is important to test for its predictive power, i.e., how good does the model predict for data that has not been used to fit the model (Charney et al., 2021; Petchey et al., 2015; Yates et al., 2018). A typical approach for that is to perform a k-fold crossvalidation (Roberts et al., 2017). For instance, in a 2-fold cross-validation, the available data would be divided into two sets, one for fitting or training the model (training data) and one for testing its predictive performance (testing data). To assess the predictive performance, the fitted model is used to predict e.g., species occurrence under the specific environmental conditions of the testing data, and then such predictions are compared to the true known

occurrences. The process is then repeated but the data that was used for training in the first fold is now used for testing and vice versa. Traditionally, community predictions have been addressed by combining (i.e., stacking) the single-species predictions from SDMs (Grenié et al., 2020). This approach models species individually and thus assumes that they have independent responses to the environment (Guisan & Rahbek, 2011).

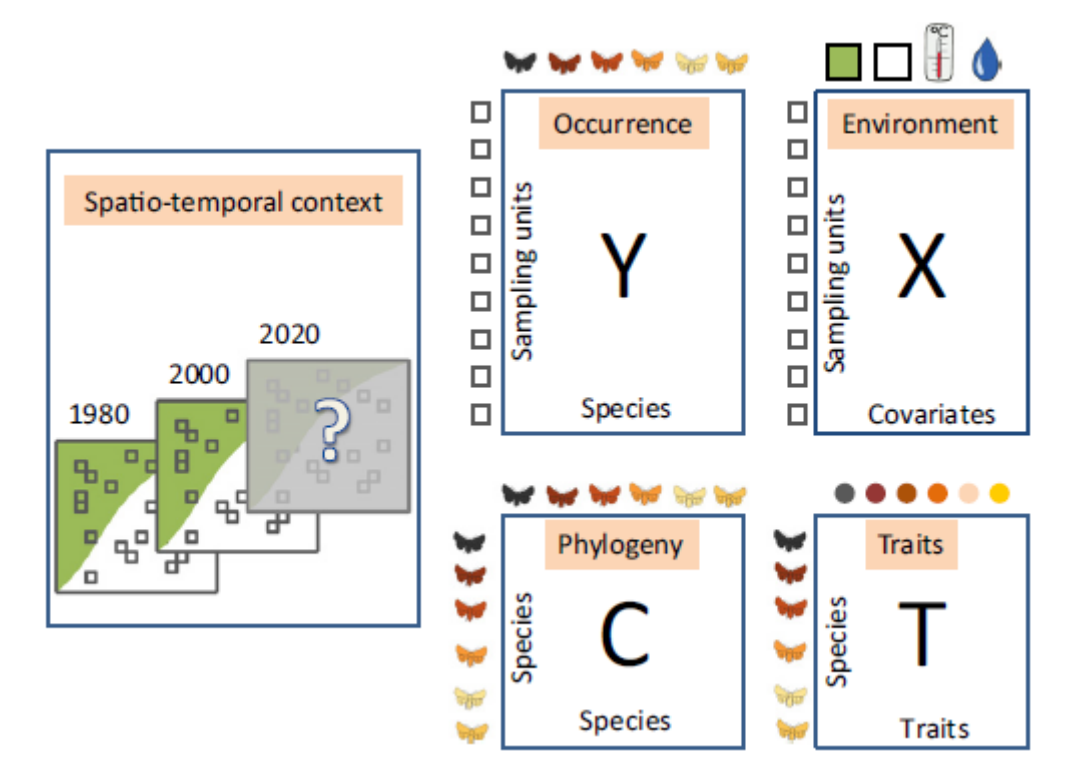


Figure 2.4. Key inputs to the HMSC modelling framework used in B-USEFUL. The occurrence data (denoted as the Y matrix) includes the occurrences of the species recorded in a set of temporal and/or spatial sampling units. The environmental data (denoted as the X matrix) consists of the environmental covariates measured over the sampling units. The traits data (denoted as the T matrix) consists of a set of traits measured for the species present in the Y matrix. To account for the phylogenetic dependencies among the species, we can include a fourth matrix consisting of the phylogenetic correlations among the species (denoted as the C matrix). The spatiotemporal context includes location and time information about the samples. (From Ovaskainen et al. 2017).

A more recent development in statistical modelling are the Joint Species Distribution Models (JSDMs), which unlike SDMs consider all species simultaneously and account for the multivariate nature of biological communities (Figure 2.3). There is a wide variety of JSDM frameworks (e.g., HMSC, BORAL, JDSDM, GJAM, GLLVM, ANN) with different implementation and statistical foundations (Bourhis et al., 2023; Clark et al., 2017b; Hui, 2016; Niku et al., 2019; Ovaskainen & Abrego, 2020; Thorson et al., 2016). The Hierarchical Modelling of Species Communities (HMSC) is a JSDM framework fitted with Bayesian inference (Figure 2.4), and conceptually and theoretically rooted on the community assembly processes (Ovaskainen & Abrego, 2020). The framework can incorporate random effects which capture the signal from processes such as biotic filtering, dispersal limitation and environmental filtering not included in the fixed effects, which usually include the environmental predictors. The random effects can be defined by a spatio-temporal structure, aiming to capture processes at a given scale, and are computed through latent variables (similar to a PCA ordination) that can yield a

species-to-species residual association matrix. This association matrix reflects co-occurrence patterns of the species within the community that cannot be explained by the environmental niche, i.e., the fixed effects. Consequently, a positive association between two species' occurrence indicates that those species co-occur more often than expected after considering their environmental niche. Whether the underlying process that leads to such pattern is biotic filtering, dispersal limitation or unaccounted environmental filtering in the fixed effects, cannot be disentangled with JSDMs. This is not a shortcoming of JSDMs as such, but rather a result from the type of data used. Nonetheless, the incorporation of such random effects can provide relevant information on potential underlying processes and puts the understanding and knowledge that we have from species niches into perspective (Ovaskainen et al., 2017).

Another interesting feature from HMSC is that it enables including information on species traits. Incorporating traits into the model, not only allows identifying trait-environment relationships, but it actually improves the model performance for some species, typically rare, as it allows information to be shared across species (Norberg et al., 2019; Ovaskainen & Soininen, 2011). In a study comparing the predictive performance of different modelling frameworks (i.e., different stacked SDMs and JSDMs) HMSC was consistently ranked among the best performing, especially when rare species were considered (Norberg et al., 2019). Lastly, HMSC can also incorporate information on species phylogenetic relationship, which accounts for the non-independence of traits among species, i.e. closely related species are likely to share more similar traits than non related species. A strong phylogenetic signal in the model is indicative of a common response towards the environment of closely related species. Hence, following the niche conservatism theory the presence of a phylogenetic signal signifies that there are traits that have not been included in the model that show some relationship with the environment of the studied community. Similar to random effects, the specific traits associated with this signal cannot be disentangled with this method, but finding a phylogenetic signal can highlight the need for further research into trait-environment relationships and generally indicates that closely related species share common responses to the environment, opening avenues for targeted conservation strategies.

2.5 Application of other data driven approach for biodiversity assessments

While the application of SDMs and JSDM can provide a means to assess and predict patterns and changes in overall biodiversity, data driven approaches based on rarefaction can offer an alternative framework to quantify the multidimensional and scale-dependent properties of biodiversity, including alpha-, beta- and gamma-diversity (i.e. sample-level species richness, regional differences in species composition between samples, and regional species richness, respectively; Chao et al., 2014; Chao et al. 2023; Thompson et al. 2021). Since data-driven studies have previously been carried out and published by partners in many areas, such as the Barents Sea, North Sea and Baltic Sea (e., Wiedmann et al 2014; Pecuchet et al. 2016; Dencker et al. 2017) we present results from areas and/or organism groups that have not been extensively featured in such previous work. More information on the methods and derived results from these studies are presented in section 4.

2.5 Application of species distribution modelling in B-USEFUL

The above-mentioned modelling frameworks were used within B-USEFUL to improve our process understanding of drivers and assembly rules affecting past and current distribution and composition of marine communities, as well as assess the current status and trends in biodiversity indicators throughout European Seas (Figure 2.5). While the primary focus is on demersal (bottom-living) fish and benthic invertebrates that a more place bound and therefore impacted by spatial management actions (e.g., MPAs and other trawling restrictions), the work presented include also examples of cephalopods, as well as plankton. In the following sections 3-4 we will describe the collective efforts of partners setting up, parameterizing and validating JSDMs under task 3.1 on the basis of data collected and standardized through WP2. Moreover, we present and discuss pattern and changes in multiple biodiversity indicators, reflecting both species and community-level EBVs estimated for each area and organism group in question. We acknowledge that differences among these EBVs may challenge end-users and managers involved in MSP and MPA planning, especially since hotspots or broader regions of "high biodiversity" may seem contingent on the set of indicators and metrics considered. Hence, we advocate a broader and holistic perspective aiming to embrace this complexity when identifying candidate locations and areas for protection (especially under WP5-WP6). This can involve the joint considerations across a suite of EBVs, combined with more composite metrics and indicators simultaneously accounting for richness, abundances and traits, such as Hill numbers (Hill 1973; Chao et al., 2014; Chao et al. 2023) that are readily available from model outputs, but not presented in this particular report. Specific details and information regarding model diagnostics etc are provided in the associated appendices.

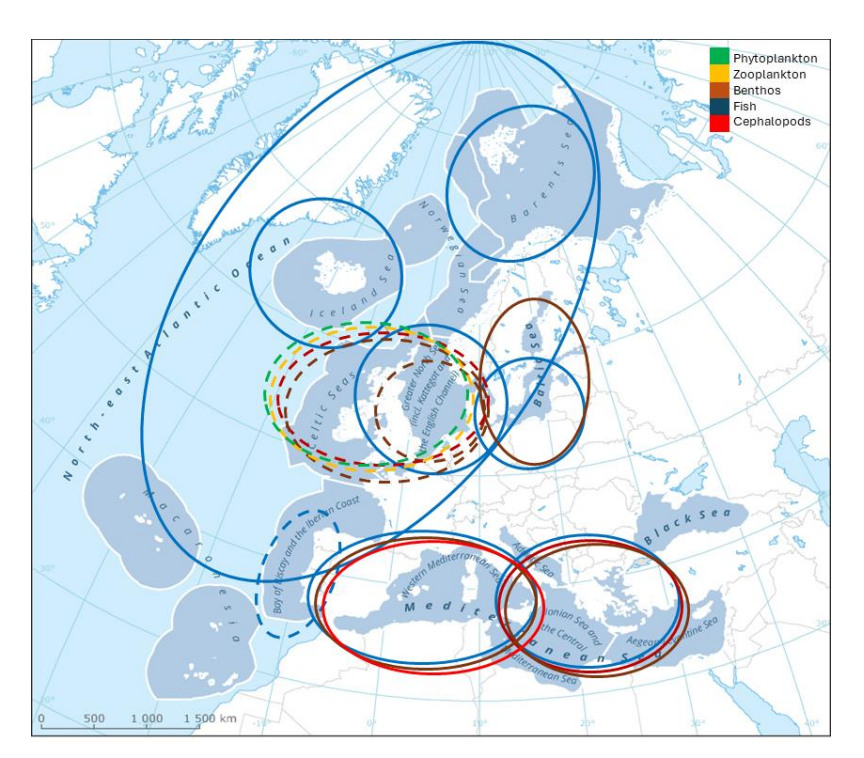


Figure 2.5. Map of European Seas including case study areas where JSDMs (solid circles) and/or data analysis (dashed circles) featured within this report present underlying drivers and processes of species distributions, as well as derived patterns and changes in biodiversity indicators across organism groups (colours). While the primary focus of the B-USEFUL project is on marine fish and benthic invertebrate communities, some of the modelling activities include also cephalopods and plankton.

2.6 References

Botkin, D. B., Saxe, H., Araújo, M. B., Betts, R., Bradshaw, R. H. W., Cedhagen, T., ... Stockwell, D. R. B. (2010). Forecasting the Effects of Global Warming on Biodiversity. 57, 227–236.

Bourhis, Y., Bell, J. R., Shortall, C. R., Kunin, W. E., & Milne, A. E. (2023). Explainable neural networks for trait-based multispecies distribution modelling—A case study with butterflies and moths. Methods in Ecology and Evolution, 14, 1531–1542.

Brown, J. L. (2014). SDMtoolbox: a python-based GIS toolkit for landscape genetic, biogeographic and species distribution model analyses. 694–700.

Butchart, S. H. M., Walpole, M., Collen, B., Strien, A. van, Scharlemann, J. P. W., Almond, R. E. A., ... Watson, R. (2010). Global Biodiversity: Indicators of. Science, 328, 1164–1168.

Cadotte, M. W., & Tucker, C. M. (2017). Should Environmental Filtering be Abandoned? Trends in Ecology and Evolution, 32, 429–437.

Cavender-Bares, J., Gamon, J. A., & Townsend, P. A. (2020). Remote sensing of plant biodiversity.

Chao, A., Chiu, C.-H., Hu, K.-H., van der Plas, F., Cadotte, M. W., Mitesser, O., Thorn, S., Mori, A. S., Scherer-Lorenzen, M., Eisenhauer, N., Bässler, C., Delory, B. M., Feldhaar, H., Fichtner, A., Hothorn, T., Peters, M. K., Pierick, K., von Oheimb, G., & Müller, J. (2024). Hill—Chao numbers allow decomposing gamma multifunctionality into alpha and beta components. Ecology Letters, 27(1), e14336.

Chao, A., Gotelli, N. J., Hsieh, T. C., Sander, E. L., Ma, K. H., Colwell, R. K., & Ellison, A. M. (2014). Rarefaction and extrapolation with Hill numbers: a framework for sampling and estimation in species diversity studies. Ecological Monographs, 84(1), 45–67. https://doi.org/10.1890/13-0133.1

Charney, N. D., Record, S., Gerstner, B. E., Merow, C., Zarnetske, P. L., & Enquist, B. J. (2021). A Test of Species Distribution Model Transferability Across Environmental and Geographic Space for 108 Western North American Tree Species. Frontiers in Ecology and Evolution, 9, 1–16.

Clark, J. S., Nemergut, D., Seyednasrollah, B., Turner, P. J., & Zhang, S. (2017a). Generalized joint attribute modeling for biodiversity analysis: median-zero, multivariate, multifarious data. Ecological Monographs, 87, 34–56.

Clark, J. S., Nemergut, D., Seyednasrollah, B., Turner, P. J., & Zhang, S. (2017b). Generalized joint attribute modeling for biodiversity analysis: Median-zero, multivariate, multifarious data. Ecological Monographs, 87, 34–56.

Clavero, M., Franch, N., Bernardo-Madrid, R., López, V., Abelló, P., Queral, J. M., & Mancinelli, G. (2022). Severe, rapid and widespread impacts of an Atlantic blue crab invasion. Marine Pollution Bulletin, 176.

Convention on Biological Diversity. (2021). First Draft of the Post-2020 Global Biodiversity Framework. CBD/WG2020/3/3. 2021, pp. 1–12.

Dencker, T. S., Pecuchet, L., Beukhof, E., Richardson, K., Payne, M. R. and Lindegren, M. 2017. Temporal and spatial differences between taxonomic and trait biodiversity in a large marine ecosystem: causes and consequences. – PLoS One 12: 1–19.

Dulvy, N. K., Rogers, S. I., Jennings, S., Stelzenmüller, V., Dye, S. R., & Skjoldal, H. R. (2008). Climate change and deepening of the North Sea fish assemblage: A biotic indicator of warming seas. Journal of Applied Ecology, 45, 1029–1039.

European Commission. (2020). EU Biodiversity Strategy for 2030. 2020, pp. 1–22.

Franklin, J. (2023). Species distribution modelling supports the study of past, present and future biogeographies. Journal of Biogeography, 50, 1533–1545.

Freeman, B. G., Lee-Yaw, J. A., Sunday, J. M., & Hargreaves, A. L. (2018). Expanding, shifting and shrinking: The impact of global warming on species' elevational distributions. Global Ecology and Biogeography, 27, 1268–1276.

Grenié, M., Violle, C., & Munoz, F. (2020). Is prediction of species richness from stacked species distribution models biased by habitat saturation? Ecological Indicators, 111, 105970.

Guisan, A., & Rahbek, C. (2011). SESAM - a new framework integrating macroecological and species distribution models for predicting spatio-temporal patterns of species assemblages. Journal of Biogeography, 38, 1433–1444.

Götzenberger, L., de Bello, F., Bråthen, K. A., Davison, J., Dubuis, A., Guisan, A., ... Zobel, M. (2012). Ecological assembly rules in plant communities-approaches, patterns and prospects. Biological Reviews, 87, 111–127.

Harley, C. D. G., Hughes, A. R., Hultgren, K. M., Miner, B. G., Sorte, C. J. B., Thornber, C. S., ... Williams, S. L. (2006). The impacts of climate change in coastal marine systems. Ecology Letters, 9, 228–241.

Hermoso, V., Carvalho, S. B., Giakoumi, S., Goldsborough, D., Katsanevakis, S., Leontiou, S., ... Yates, K. L. (2022). The EU Biodiversity Strategy for 2030: Opportunities and challenges on the path towards biodiversity recovery. Environmental Science and Policy, 127, 263–271.

Hill, M. O. (1973). "Diversity and evenness: a unifying notation and its consequences". Ecology. 54 (2): 427–432.

Hui, F. K. C. (2016). boral – Bayesian Ordination and Regression Analysis of Multivariate Abundance Data in r. Methods in Ecology and Evolution, 7, 744–750.

IPBES. (2019). The global assessment report on Biodiversity and Ecosystem services.

Jetz, W., McGeoch, M. A., Guralnick, R., Ferrier, S., Beck, J., Costello, M. J., ... Turak, E. (2019). Essential biodiversity variables for mapping and monitoring species populations. Nature Ecology and Evolution, 3, 539–551.

Keddy, P. A. (1992). Assembly and response rules: two goals for predictive community ecology. Journal of Vegetation Science, 3, 157–164.

Lee, H., Calvin, K., Dasgupta, D., Krinner, G., Mukherji, A., Thorne, P., ... Blanco, G. (2023). Climate Change 2023: Synthesis Report. Contribution of Working Groups I, II and III to the Sixth Assessment Report of the Intergovernmental Panel on Climate Change. 184 pp. Geneva, Switzerland.

Mace, G., Masundire, H., & Baillie, J. E. M. (2005). Biodiversity. Ecosystems and human well-being: current state and trends. H. Hassan, R. Scholes, & N. Ash (Eds.). Washington DC.

Magurran, A.E., McGill, B.J. (Eds.) 2010. Biological diversity: frontiers in measurement and assessment. OUP Oxford.

McGill, B. J., Enquist, B. J., Weiher, E., & Westoby, M. (2006). Rebuilding community ecology from functional traits. Trends in Ecology and Evolution, 21, 178–185.

Micheli, F., Halpern, B. S., Lindegren, M., Holt, B. G., MacKenzie, B. R., Rahbek, C., ... Hui, F. K. C. (2017). Body size-dependent responses of a marine fish assemblage to climate change and fishing over a century-long scale. Ecology Letters, 27, 1–19.

Montanyès, M., Weigel, B., & Lindegren, M. (2023). Community assembly processes and drivers shaping marine fish community structure in the North Sea. Ecography, 2023(10), Article e06642. https://doi.org/10.1111/ecog.06642

Mouillot, D., Dumay, O., & Tomasini, J. A. (2007). Limiting similarity, niche filtering and functional diversity in coastal lagoon fish communities. Estuarine, Coastal and Shelf Science, 71, 443–456.

Mouillot, D., Graham, N. A. J., Villéger, S., Mason, N. W. H., & Bellwood, D. R. (2013). A functional approach reveals community responses to disturbances. Trends in Ecology and Evolution, 28, 167–177.

Niku, J., Hui, F. K. C., Taskinen, S., & Warton, D. I. (2019). gllvm: Fast analysis of multivariate abundance data with generalized linear latent variable models in r. Methods in Ecology and Evolution, 10, 2173–2182.

Norberg, A., Abrego, N., Blanchet, F. G., Adler, F. R., Anderson, B. J., Anttila, J., ... Ovaskainen, O. (2019). A comprehensive evaluation of predictive performance of 33 species distribution models at species and community levels. Ecological Monographs, 89, 1–24.

Ovaskainen, O., & Soininen, J. (2011). Making more out of sparse data: Hierarchical modeling of species communities. Ecology, 92, 289–295.

Ovaskainen, O., & Abrego, N. (2020). Joint Species Distribution Modelling: With Applications in R. Cambridge University Press.

Ovaskainen, O., Tikhonov, G., Norberg, A., Guillaume Blanchet, F., Duan, L., Dunson, D., ... Abrego, N. (2017). How to make more out of community data? A conceptual framework and its implementation as models and software. Ecology Letters, 20, 561–576.

Pecuchet L, ToÈrnroos A, Lindegren M. Patterns and drivers of fish community assembly in a large marine ecosystem. Mar Ecol Prog Ser. 2016; 546:239±48.

Pereira, H. M., Ferrier, S., Walters, M., Geller, G. N., Jongman, R. H. G., Scholes, R. J., ... Wegmann, M. (2013). Essential Biodiversity Variables. Science, 339, 277–278.

Perry, A. L., Low, P. J., Ellis, J. R., & Reynolds, J. D. (2005). Climate change and distribution shifts in marine fishes. Science, 308, 1912–1915.

Petchey, O. L., Pontarp, M., Massie, T. M., Kéfi, S., Ozgul, A., Weilenmann, M., ... Pearse, I. S. (2015). The ecological forecast horizon, and examples of its uses and determinants. Ecology Letters, 18, 597–611.

Pimm, S. L., Jenkins, C. N., Abell, R., Brooks, T. M., Gittleman, J. L., Joppa, L. N., ... Sexton, J. O. (2014). The biodiversity of species and their rates of extinction, distribution, and protection. Science, 344.

Poloczanska, E. S., Brown, C. J., Sydeman, W. J., Kiessling, W., Schoeman, D. S., Moore, P. J., ... Richardson, A. J. (2013). Global imprint of climate change on marine life. Nature Climate Change, 3, 919–925.

Rawat, U. S., & Agarwal, N. K. (2015). Biodiversity: Concept, threats and conservation. Environment Conservation Journal, 16, 19–28.

Roberts, D. R., Bahn, V., Ciuti, S., Boyce, M. S., Elith, J., Guillera-arroita, G., ... Dormann, C. F. (2017). Cross-validation strategies for data with temporal, spatial, hierarchical, or phylogenetic structure. 913–929.

Stachowicz, J. J., Bruno, J. F., & Duffy, J. E. (2007). Understanding the effects of marine biodiversity on communities and ecosystems. Annual Review of Ecology, Evolution, and Systematics, 38, 739–766.

Thomsen, M. S., Byers, J. E., Schiel, D. R., Bruno, J. F., Olden, J. D., Wernberg, T., & Silliman, B. R. (2014). Impacts of marine invaders on biodiversity depend on trophic position and functional similarity. Marine Ecology Progress Series, 495, 39–47.

Thompson, M. S. A., Couce, E., Webb, T. J., Grace, M., Cooper, K. M., & Schratzberger, M. (2021). What's hot and what's not: Making sense of biodiversity 'hotspots.' Global Change Biology, 27(3), 521–535. https://doi.org/10.1111/gcb.15443

Thompson, P. L., Anderson, S. C., Nephin, J., Haggarty, D. R., Peña, M. A., English, P. A., ... Rubidge, E. (2022). Disentangling the impacts of environmental change and commercial fishing on demersal fish biodiversity in a northeast Pacific ecosystem. 689, 137–154.

Thorson, J. T., Ianelli, J. N., Larsen, E. A., Ries, L., Scheuerell, M. D., Szuwalski, C., & Zipkin, E. F. (2016). Joint dynamic species distribution models: a tool for community ordination and spatio-temporal monitoring. Global Ecology and Biogeography, 25, 1144–1158.

Thuiller, W. (2015). Editorial commentary on 'BIOMOD – optimizing predictions of species distributions and projecting potential future shifts under global change '. 3591–3592.

Urban, M. C., Bocedi, G., Hendry, A. P., Mihoub, J.-B., Pe'er, G., Singer, A., ... Travis, J. M. J. (2016). Improving the forecast for biodiversity under climate change. 353.

Wiedmann M, Aschan M, Certain G, Dolgov A, Greenacre M, Johannesen E, et al. Functional diversity of the Barents Sea fish community. Mar Ecol Prog Ser. 2014; 495:205±18.

Yates, K. L., Bouchet, P. J., Caley, M. J., Mengersen, K., Randin, C. F., Parnell, S., ... Sequeira, A. M. M. (2018). Outstanding Challenges in the Transferability of Ecological Models. Trends in Ecology and Evolution, 33, 790–802.

Zobel, M. (1997). The relative role of species pools in determining plant species richness: An alternative explanation of species coexistence? Trends in Ecology and Evolution, 12, 266–269.



3. Summary of model results across areas

3.1 North East Atlantic fish model

Authors: Marcel Montanyès, Benjamin Weigel, Federico Maioli, Gleb Tikhonov, Pieter Daniël van Denderen, Otso Ovaskainen, Martin Lindegren

3.1.1. Study area and data availability

We gathered a comprehensive data set on fish species distribution and biomass from 13 scientific bottom-trawl surveys conducted across the North and North-east Atlantic Ocean (Appendix 1; Table S1). The data set encompass 90,029 unique hauls spanning 33 years (1989-2021), thus capturing the active period for most surveys and providing an extensive spatio-temporal coverage of our study area (Figure 3.1.1). We focused our analysis solely on fish taxa (i.e., *Elasmobranchii*, *Actinopteri*, *Holocephali*, *Myxini*, *Petromyzonti* and *Teleostei*) identified at the species level and that exhibited a minimum prevalence of 0.1% (i.e., > 90 occurrences), resulting in a selection of 151 species. The species names were cross-referenced and updated using the World Register of Marine Species (WoRMS Editorial Board 2022). For each of the hauls we recorded the presence-absence of species, as well as their biomass standardized for sampling area (km²) and trawl gear catchability following methodologies detailed in previous studies (van Denderen et al. 2023; Maureaud et al. 2019; Walker et al. 2017).

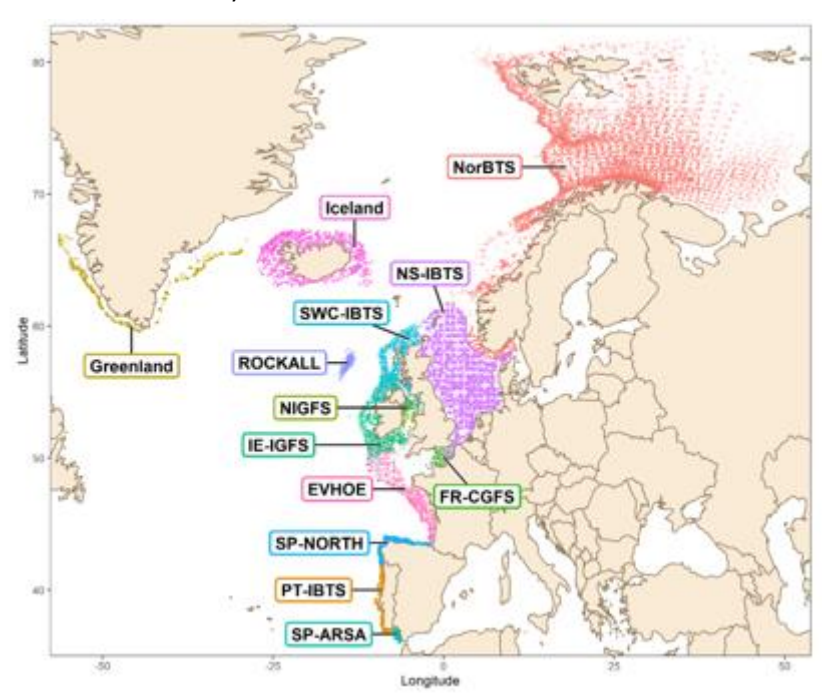


Figure 3.1.1. Position of all unique hauls from the different surveys performed in the North East Atlantic model domain between 1989 and 2021.

To account for functional (trait) aspects of biodiversity, we selected 6 traits that broadly represent the life history, reproduction, morphology and diet of species (Dencker et al. 2017) following a formal framework developed for other marine organisms (Litchman, Ohman, and Kiørboe 2013). Trait information was retrieved from the database by Beukhof et al. (2019). The life history of each species was characterized by two parameters: age of maturity (in years) and the von Bertalanffy growth coefficient K (measured in year-1), while

the reproductive traits were represented by offspring size, i.e. egg diameter (measured in mm). Morphological characteristics were assessed through maximum length (in cm) and the caudal fin aspect ratio as a proxy for mobility. Lastly, we considered diet by including the trophic level of each species. To represent the environmental conditions at each unique haul, we retrieved environmental and physical variables from the model re-analysis products of the NEMO-MEDUSA model (Gurvan et al. 2022; Yool et al. 2013). This provided us with surface and bottom details concerning temperature (°C), salinity (PSU), detritus concentration (mmol N per m³), chlorophyll a concentration (Chl a; mmol N per m³) and dissolved inorganic nitrogen concentration (DIN; mmol N per m³), as well as depth (m). Additionally, we computed the annual standard deviation for temperature, salinity, and Chl a at each location, as a proxy for seasonal variation (Beukhof et al. 2019; Dencker et al. 2017; Maureaud et al. 2019). Due to the lack of available long-term data on fishing effort throughout the area, the potential effects of commercial fishing were not explicitly accounted for. However, previous large-scale studies on marine fish communities in the area found no, or only weak effects on the species distribution and community trait composition (Beukhof et al. 2019; Dencker et al. 2017). After checking for potential collinearity we omitted highly correlated variables, i.e., with Pearson coefficient > 0.7 (Appendix 1; Figure S1). The final set of environmental covariates comprises sea bottom temperature (SBT), SBT seasonality, sea bottom salinity (SBS), SBS seasonality, seafloor detritus, surface DIN, surface Chl a, surface Chl a seasonality, seafloor Chl a seasonality, and depth.

3.1.2. Model fitting, validation and predictions

We employed HMSC to model the fish communities, treating each unique sample event as a response variable. Given the zero-inflated nature of the data, we adopted a hurdle approach. This involved utilizing one model for presence-absence (probit regression) and another model for biomass conditional on presence (log-linear regression). As fixed effects we incorporated the environmental covariates detailed above, including quadratic terms for sea bottom temperature (SBT) and sea bottom salinity (SBS) to account for potential nonlinear species' responses. To account for potential seasonal differences in distribution and biomass (i.e., linked to migrations and spawning) we further included spring/summer and autumn/winter as a fixed factor. In addition to the fixed effects, the models encompassed spatially- (Ovaskainen et al. 2016) and temporally (yearly) structured latent variables. Spatial units were represented by hexagonal cells (N=574 cells), each covering an area of 7,774 km². To determine the relative importance of the environmental covariates we partitioned the explained variation among the fixed and random effects (Ovaskainen et al. 2017; Ovaskainen and Abrego 2020). The model was fitted with four Markov chain Monte Carlo (MCMC) chains taking 250 samples per chain, resulting in 1,000 posterior samples. The thinning applied was specific to each model with the aim of achieving a good model convergence with a reasonable use of computational resources. We assessed MCMC convergence by examining the potential scale reduction factors (PSRFs; Gelman and Rubin 1992) of model parameters where values <1.1 indicate satisfactory convergence (Tikhonov et al. 2020). To assess the predictive performance of our models we partitioned the data into three decades (1989-1999, 2000-2009, 2010-2021) and trained separate models on each decade. To evaluate the explanatory power of these trained models, we employed metrics such as AUC and Tjur R2 for species presence-absence, R2 for biomass conditional on presence, and root mean

square error (RMSE) for both (Ovaskainen & Abrego, 2020). Subsequently, we tested the models on the remaining decades to assess their out-of-sample predictive performances.

After model diagnostics and cross-validation we computed a suite of six complementary EBVs based on model predictions of species occurrence and biomass across locations and years. The selected set of EBVs aim to represent multiple aspects of biodiversity (Pereira et al. 2013), including taxonomic and functional richness, evenness and dispersion. To reflect the taxonomic richness of communities the total number of species in a given location was calculated based on the maximum probability of occurrence of a given species throughout a year, where monthly probabilities equal or higher than 0.5 were considered to represent presence. The same approach was used for computing richness of threatened species, classified as Vulnerable, Endangered or Critically Endangered (IUCN 2023). Species lacking classifications were assigned as "Not evaluated". To account for differences in species evenness we calculated Pielou's evenness using the mean annual estimates of species biomasses in each location. To calculate the functional diversity indices we computed a multidimensional space with a PCoA based on trait-based (Gower) distances (Mouillot et al. 2013). We then used the first 5 PCs (cumulative explained variance of 82%) to compute the functional richness, evenness and dispersion for each year and location. These represent the proportion of functional space filled by the species in the community, the regularity of biomass distribution in the functional space, and the biomass-weighted mean distance to the biomass-weighted mean trait values of the community, respectively (Mouillot et al. 2013). Taxonomic EBV were carried with 'vegan' package (Oksanen et al. 2022), and functional EBVs with 'mFD' package (Magneville et al. 2022), while the species conservation classifications were retrieved with the 'rredlis' package (Gearty and Chamberlain 2023) and complemented with information from the website (IUCN 2023).

Table 3.1.1. Models' explanatory (diagonal) and predictive (off-diagonal) power for occurrence and biomass models. Columns indicate the training decade and rows the testing decade. The right-most column indicates the explanatory power for the whole-period model fitted on all years.

Model	Testing	Training decade			Whole period
Wiodei	decade	1990	2000	2010	whole period
Occurrence	1990	0.90	0.87	0.86	
(AUC)	2000	0.88	0.91	0.90	0.91
(ACC)	2010	0.86	0.89	0.91	
Biomass	1990	0.23	0.13	0.14	
(R ²)	2000	0.13	0.22	0.16	0.21
(/	2010	0.11	0.15	0.22	

3.1.3. Model diagnostics and performance

The MCMC convergence for the whole-period and decadal models was overall satisfactory, indicated by the mean of the PSRF being <1.1 (Appendix 1, Figure S2-S3). In terms of

explanatory power, the occurrence models showed high performance overall, indicated by AUC values equal to or exceeding 0.9 for all decadal models (diagonal in Table 3.1), as well as for the whole-period full- (0.95) and environment-only (0.91) models. Conversely, the biomass models show more moderate explanatory power with R² values amounting to >0.22 for the decadal models, and 0.34 and 0.21 for the full and environment whole-period models, respectively. The decadal cross-validation routine shows high predictive performance for all occurrence models, indicated by AUC values ranging from 0.86-0.90 for the testing decades not used for model training (off-diagonal in Table 3.1.1). Conversely, the biomass models demonstrate considerably lower predictive power for decades used for testing with R2 values ranging from 0.11 to 0.16 (off-diagonal in Table 3.1.1).

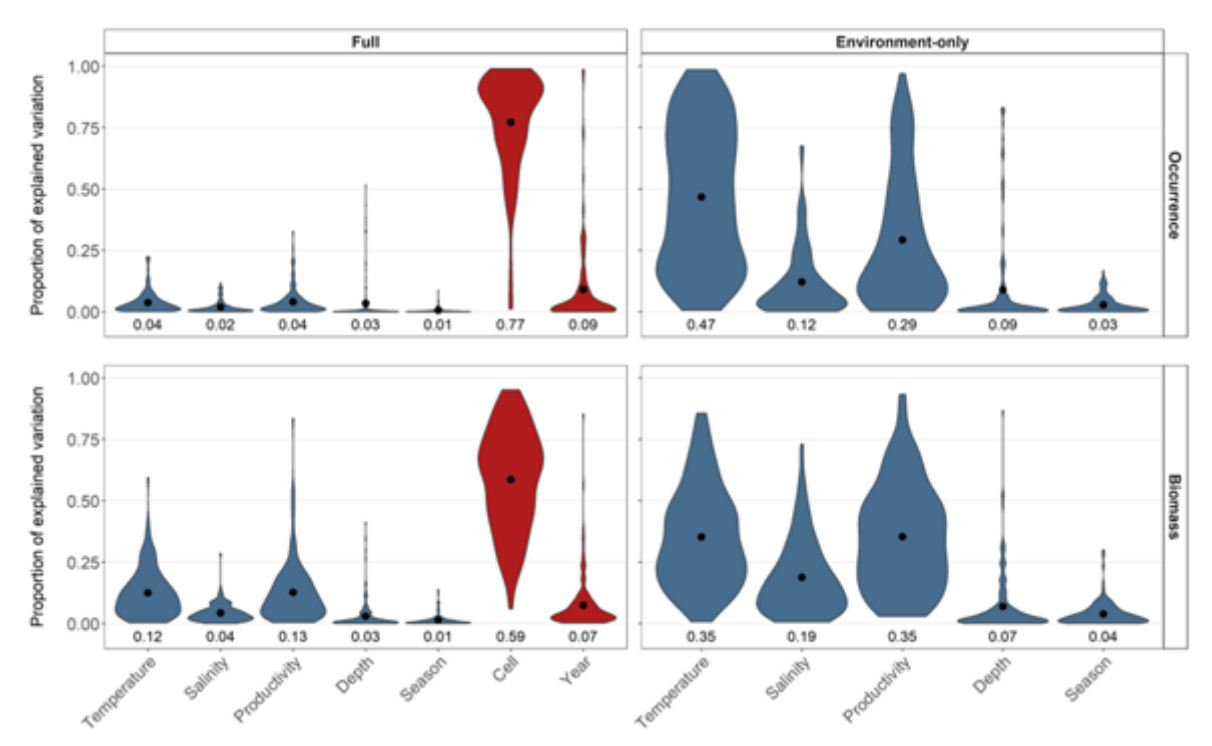


Figure 3.1.1. Variance partitioning of fixed (blue) and random (red) effects for the full (left) and environment-only models (right) for occurrence (top) and biomass (bottom). The mean value for each violin plot is denoted by a black dot, with values indicated below.

The variance partitioning for the environment-only models show that temperature- and productivity-associated covariates explain most of the variation in species distributions and biomass (Figure 3.1.2). For the full models more than half of the variance is instead attributed to the spatial and temporal random effects. This has direct implications for model forecasting since random effects are assumed to remain constant during predictions (Ovaskainen & Abrego, 2020). This means that even in the presence of pronounced environmental changes, model predictions of species distributions will be more static and less suitable to represent species range shifts and changes in overall composition and diversity. Hence, since both MCMC convergence and performance of the environment-only models was equal to, or even better compared to the considerably more complex and computationally demanding random effect models we decided to present results and predictions exclusively on the basis of the environment-only models.

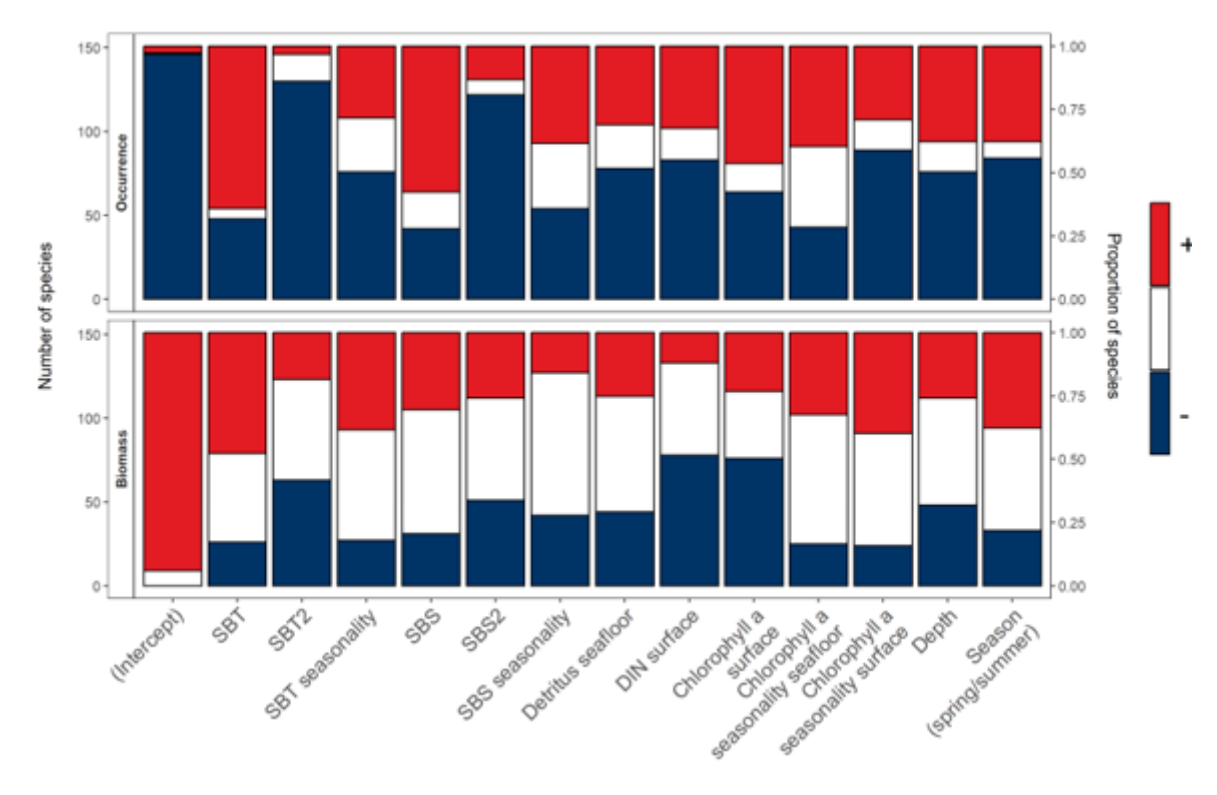


Figure 3.1.3. Number and proportion of species with positive (red), negative (blue) or no response (white) to each environmental variable, for the occurrence (top) and biomass (bottom) environment-only models.

3.1.4. Species responses to drivers

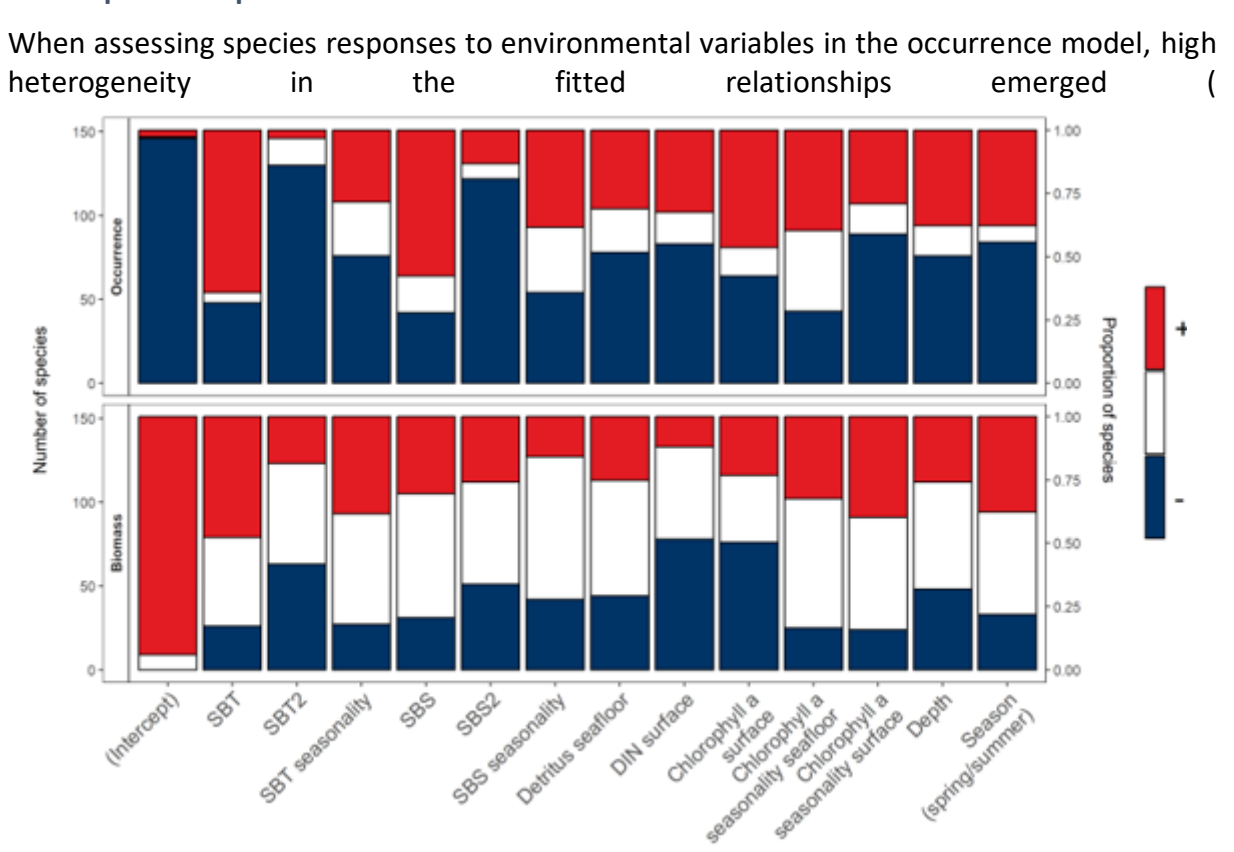


Figure **3.1.3**.1.3). Notably, over 60% of species exhibited a positive linear response to SBT, but a negative response to the quadratic term (SBT2). Similar responses were observed for SBS and its quadratic term. This indicates that a majority of species demonstrate a bell-shaped response to temperature and salinity, albeit with different peak values and spread. This in turn reflects the different environmental niches of marine fish species (i.e., warm- vs cold-water taxa), both in terms of their optimal conditions, but also the width and degree of tolerance, notably to temperature (Magnuson, Crowder, and Medvick 1979; Pörtner and Farrell 2008; Stuart-Smith, Edgar, and Bates 2017). Among the other environmental covariates, the proportion of species displaying a negative response to SBT seasonality, ChI α surface seasonality and depth surpassed those displaying a positive relationship. This indicates that most of the species considered prefer more stable environments with less seasonal changes, which corroborates previous findings on the role of seasonality and depth as primary filtering mechanisms determining fish community structure (Beukhof et al. 2019; Pecuchet et al. 2017). In terms of the biomass model the proportion of species showing a positive or negative response to the environmental covariates was more balanced. However, a considerably larger number of species demonstrated no significant relationships, as expected from the much weaker explanatory power of the model.

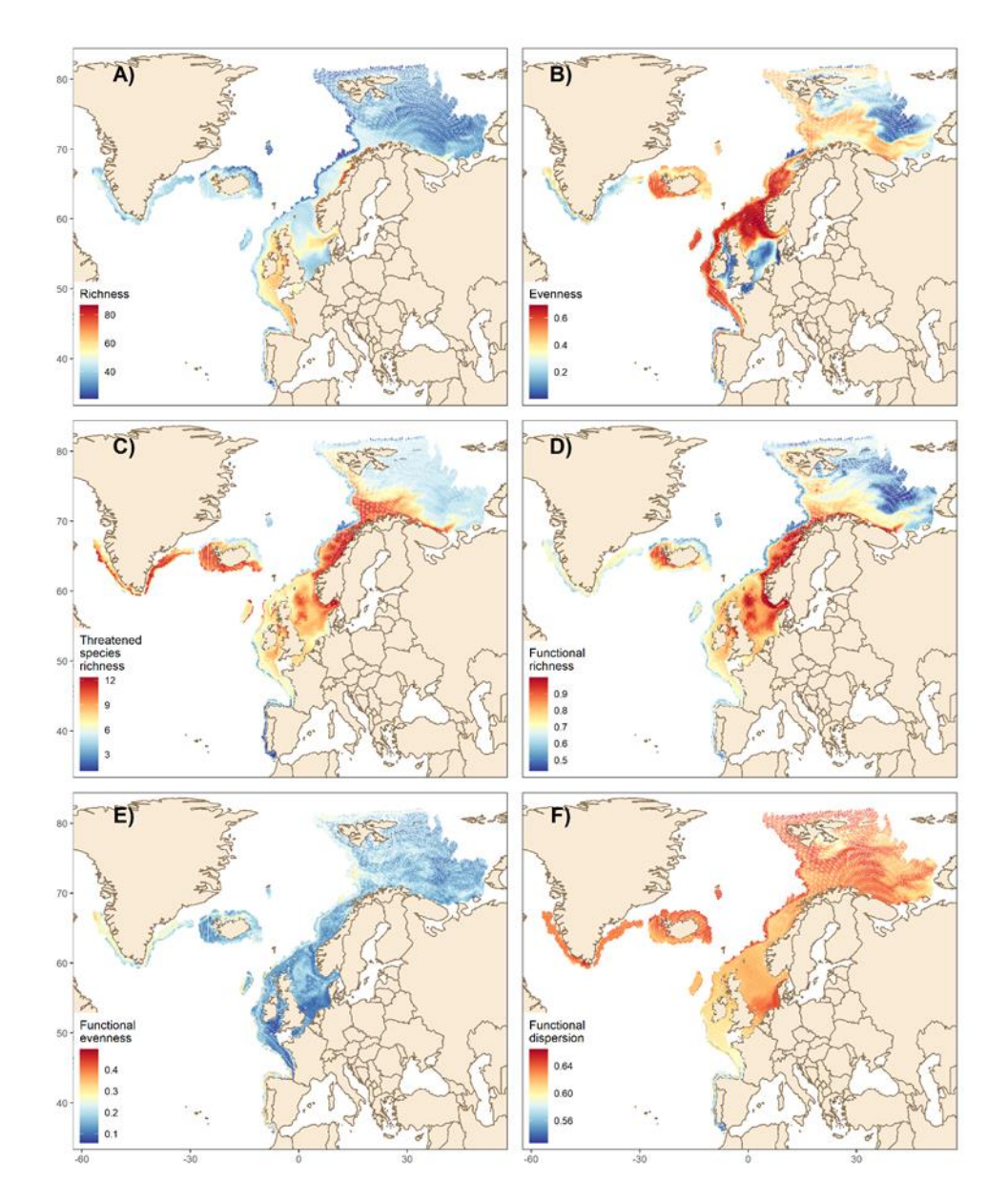


Figure 3.1.4. Mean estimates of multiple EBVs, including species richness and evenness (A, B), the number of threatened IUCN taxa (C), as well as the functional indicators of richness, evenness and dispersion (D-F) throughout the time period from 2000-2016.

3.1.5. Patterns and trends in biodiversity

The overall indicators of taxonomic and functional biodiversity estimated from model predictions of species occurrence and biomass combined with traits show marked spatial variation among the set of EBVs (Figure 3.1.4). In terms of species richness, we found the highest values in the Celtic Sea and Bay of Biscay, as well as the central North Sea, while the more northern areas, including the eastern Barents Sea, Iceland and Greenland show generally lower number of species. However, with regards to taxa deemed as threatened the above-mentioned areas around Greenland, as well as the Norwegian Sea and southern Barents Sea show relatively higher values, indicating the presence of more vulnerable species, primarily elasmobranchs in these areas. The presence of such shark and ray species, possessing traits and life-histories that are different from bony fish (Pecuchet et al. 2017) is

also evident in terms of the overall functional richness, showing higher values in the same areas. In terms of taxonomic and functional evenness, the patterns are largely different from richness with highest values in the northern North Sea, Norwegian Sea, as well as Iceland and the Celtic Sea. Finally, functional dispersion, reflecting the spread of functional traits among species in the communities demonstrate rather similar values throughout the area (i.e., ranging between 0.5-0.7), but with a slight tendency towards higher dissimilarity on the continental shelf breaks, as well as the southern North Sea. The pronounced spatial variation in mean biodiversity indicators is also evident in terms of recent temporal trends (Figure 3.1.5). More specifically, we observe a slight increase in richness, including both taxonomic and functional, as well as the number of threatened taxa throughout the area, except the Irish Sea, southern North Sea and the continental shelf breaks towards deeper areas. The trends in taxonomic and functional evenness and dispersion are more variable with fine-scaled structuring of areas with either increases or decreasing trends. This in turn reflect the complex underlying changes not only in species composition, but also in terms of their relative biomasses act in both time and space.

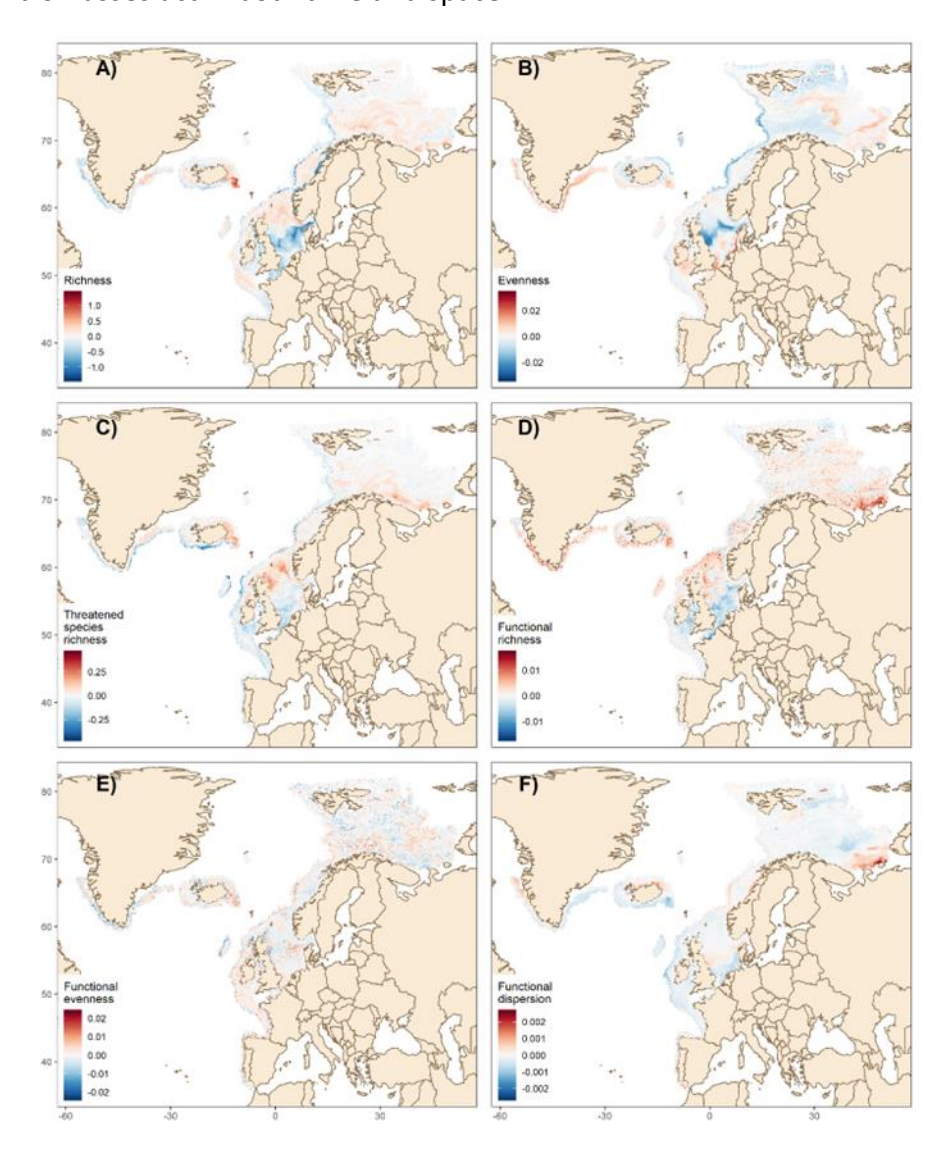


Figure 3.1.5. Temporal trends in EBVs, reflecting the regression slope of species richness and evenness (A, B), the number of threatened IUCN taxa ©, as well as the functional indicators of richness, evenness and dispersion (D-F) throughout the time period from 2000-2016.

3.1.6. Summary

Our large-scale modelling study of fish communities across the Northeast Atlantic shows that environmental filtering, primarily related to temperature and productivity, explains a large part of the variance in species distributions and community composition. This aligns with previous studies on key drivers and determinates of marine fish community structure in the area and beyond (Dencker et al. 2017; Beukhof et al. 2019b). Our study also demonstrates that model performance based on the set of environmental covariates included is rather robust across different decades used for training and validation. This indicates that the environmental niches of species are generally well described and parameterized within the models, at least to the extent that species distributions can be predicted in time periods not used for training. The overall performance and explanatory power of the models are worse in terms of biomass predictions, likely due to an inadequate representation of key processes that regulate the productivity and population dynamics of species, notably growth, reproduction and survival. However, the lower performance of predicting biomass is likely less of issue in terms of overall biodiversity predictions. This because the indicators rely either on presenceabsence predictions only (e.g., richness), or account for relative biomasses, rather than the absolute values predicted by the model. Hence, if the proportion of abundant or rare species remain well described the associated indicators relying on relative biomasses (e.g., evenness and dispersion) are likely robust to such uncertainty in absolute biomasses. Taken together we are confident that the models provides not only increased process understanding of the drivers and assembly rules structuring marine fish communities, but also a means to visualize and map patterns and changes in overall EBVs relevant for conservation and protection within the broader context of marine spatial planning.

3.1.7. References

Beukhof, E., Frelat, R., Pecuchet, L., Maureaud, A., Dencker, T. S., Sólmundsson, J., ... Lindegren, M. (2019a). Marine fish traits follow fast-slow continuum across oceans. Scientific reports, 9, 17878.

Beukhof, E., Dencker, T. S., Pecuchet, L., & Lindegren, M. (2019b). Spatio-temporal variation in marine fish traits reveals community-wide responses to environmental change. Marine Ecology Progress Series, 610, 205–222.

Beukhof, E., Dencker, T. S., Palomares, M. L. D. L. D., & Maureaud, A. (2019c). A trait collection of marine fish species from North Atlantic and Northeast Pacific continental shelf seas. PANGAEA

Dencker, T. S., Pecuchet, L., Beukhof, E., Richardson, K., Payne, M. R., & Lindegren, M. (2017). Temporal and spatial differences between taxonomic and trait biodiversity in a large marine ecosystem: Causes and consequences. PLoS ONE, 12, 1–19

Gearty, W., & Chamberlain, S. (2023). rredlist: 'IUCN' Red List Client

Gurvan, M., Bourdallé-Badie, R., Chanut, J., Clementi, E., Coward, A., Ethé, C., ... Moulin, A. (2022). NEMO ocean engine. Note du Pôle de modélisation. 2022, doi:10.5281/zenodo.1464816.

IUCN. (2023). The IUCN Red List of Threatened Species. Version 2023-1 https://www.iucnredlist.org (accessed Sep 5, 2023).

Litchman, E., Ohman, M. D., & Kiørboe, T. (2013). Trait-based approaches to zooplankton communities. Journal of Plankton Research, 35, 473–484

Magneville, C., Loiseau, N., Albouy, C., Casajus, N., Claverie, T., Escalas, A., ... Villeger, S. (2022). mFD: an R package to compute and illustrate the multiple facets of functional diversity.

Magnuson, J. J., Crowder, L. B., & Medvick, P. A. (1979). Temperature as an ecological resource. Integrative and Comparative Biology, 19, 331–343.

Maureaud, A., Hodapp, D., Daniël Van Denderen, P., Hillebrand, H., Gislason, H., Dencker, T. S., ... Lindegren, M. (2019). Biodiversity-ecosystem functioning relationships in fish communities: Biomass is related to evenness and the environment, not to species richness. Proceedings of the Royal Society B: Biological Sciences, 286.

Maureaud, A., Frelat, R., Pécuchet, L., Shackell, N., Mérigot, B., Pinsky, M. L., ... T. Thorson, J. (2021). Are we ready to track climate-driven shifts in marine species across international boundaries? - A global survey of scientific bottom trawl data. Global Change Biology, 27, 220–236.

Mouillot, D., Graham, N. A. J., Villéger, S., Mason, N. W. H., & Bellwood, D. R. (2013). A functional approach reveals community responses to disturbances. Trends in Ecology and Evolution, 28, 167–177.

Ovaskainen, O., & Abrego, N. (2020). Joint Species Distribution Modelling: With Applications in R. Cambridge University Press.

Ovaskainen, O., Tikhonov, G., Norberg, A., Guillaume Blanchet, F., Duan, L., Dunson, D., ... Abrego, N. (2017). How to make more out of community data? A conceptual framework and its implementation as models and software. Ecology Letters, 20, 561–576.

Ovaskainen, O., Roy, D. B., Fox, R., & Anderson, B. J. (2016). Uncovering hidden spatial structure in species communities with spatially explicit joint species distribution models. Methods in Ecology and Evolution, 7, 428–436.

Pecuchet, L., Lindegren, M., Hidalgo, M., Delgado, M., Esteban, A., Fock, H. O., ... Payne, M. R. (2017). From traits to life-history strategies: Deconstructing fish community composition across European seas. Global Ecology and Biogeography, 26, 812–822.

Pereira, H. M., Ferrier, S., Walters, M., Geller, G. N., Jongman, R. H. G., Scholes, R. J., ... Wegmann, M. (2013). Essential Biodiversity Variables. Science, 339, 277–278.

Pörtner, H. O., & Farrell, A. P. (2008). Physiology and Climate Change. Science, 322, 690-692.

Stuart-Smith, R. D., Edgar, G. J., & Bates, A. E. (2017). Thermal limits to the geographic distributions of shallow-water marine species. Nature Ecology and Evolution, 1, 1846–1852.

Yool, A., Popova, E. E., & Anderson, T. R. (2013). MEDUSA-2.0: An intermediate complexity biogeochemical model of the marine carbon cycle for climate change and ocean acidification studies. Geoscientific Model Development, 6, 1767–1811.

3.2 North Sea fish model

Authors: Marcel Montanyes, Benjamin Weigel, Martin Lindegren

3.2.1. Study area and data availability

We collected data from the North Sea International Bottom Trawl Survey (NS-IBTS) from the publicly available scientific monitoring survey DATRAS, hosted by the International Council for the Exploration of the Sea (ICES) (www.datras.ices.dk). The temporal span of the data was restricted to winter and summer surveys (i.e. first and third quarters of the calendar year) for the period 1986-2016, for which there is a good coverage of the entire study area. Spatially, the survey is structured on the basis of the ICES statistical rectangles; these are rectangles of 30' in latitude by 1º in longitude (approximately 56 by 64 km at the centre of the study area) that divide the area between 36°N and 85°30'N and 44°W and 68°30'E into grid cells (Figure 3.2.1).

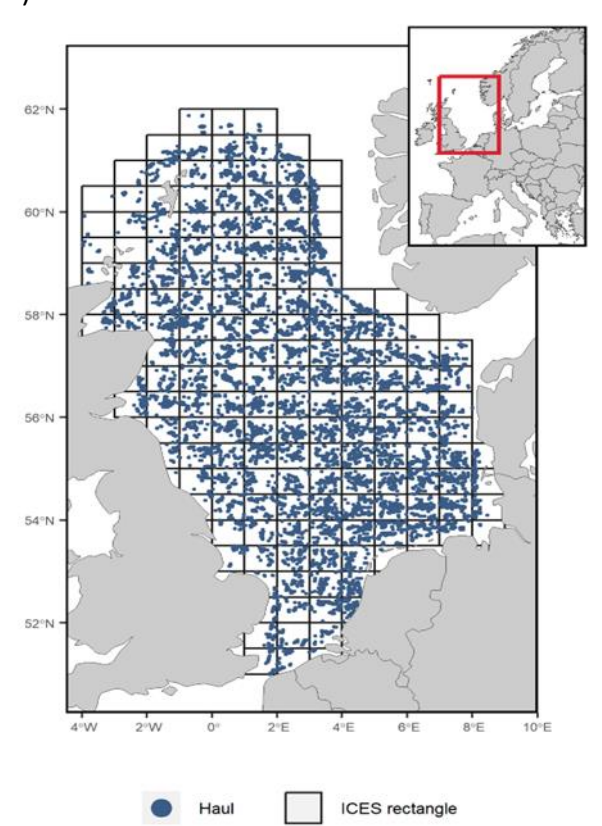


Figure 3.2.1. Position of all unique hauls of the IBTS surveys performed in the North Sea during the summer and winter seasons between 1986 and 2016. The grid represents the official ICES rectangles included in the study.

The ICES statistical rectangles gridding system is a formal spatial structure used in fisheries assessment and marine management advice within ICES. The DATRAS survey identifies catches at species level whenever possible, which we verified and updated with the World Register of Marine Species (WoRMS Editorial Board, 2022) whenever needed. Non-fish taxa were discarded and only organisms identified to species level from the following classes were kept: Actinopterygii, Elasmobranchii, Holocephali, Myxini and Petromyzonti. The data went through a quality check procedure where we removed invalid hauls and invalid species records, which resulted in presence-absence data for 247 species. Furthermore, we excluded rare species with less than 10 occurrence records in the entire data set (135 species), as well as those species where no trait or phylogenetic information was available (45 species), resulting in a total of 67 species stemming from 17319 unique hauls across 170 ICES rectangles. In addition to the community data we selected eleven traits to represent species'

morphology, life history, reproduction and diet (Dencker et al., 2017) (Appendix 2; Table S1). Trait values for each species were collected from available trait data bases (Beukhof et al. 2019b), supplemented with information from recent literature (Coulon et al., 2023)). Morphology of the species was described as body shape, caudal fin shape and maximum length (cm). Life history was characterized by the age of maturity (years) and the von Bertalanffy growth coefficient K (year-1), while reproduction was represented by spawning type, fecundity (number of eggs) and offspring size (egg diameter in mm). Dietary aspects were captured by diet and trophic level, while the position in the water column was included to represent a pelagic or demersal life style. Finally, we calculated phylogenetic relatedness among species using fishtree R package version 0.3.4. (Chang et al., 2019). The availability of in situ environmental data was limited to a few CTD records (i.e., 15% of the hauls) of temperature and salinity. Therefore, in order to ensure a complete and consistent coverage of both physical and environmental covariates across all unique sampling events we used model re-analysis products from the NEMO-MEDUSA coupled hydro-geochemical model runs (Yool et al., 2013). The available covariates included both surface and bottom temperature (°C), salinity (PSU), detritus (mmol N per m3), chlorophyll a (mmol N per m3), dissolved inorganic nitrogen (DIN; mmol N per m3) and depth. To reflect seasonality in environmental conditions, previously known to affect fish diversity and dynamics (Beukhof et al., 2019a; Dencker et al., 2017; Maureaud et al., 2019) we calculated temperature and salinity seasonality as the standard deviation in each corresponding sampling point and year. We acknowledge that relying on model-derived data may incur potential sources of uncertainty and errors, at least for variables less well-informed by in situ observations or remote sensing, such as sea bottom temperature (SBT). However, given the high correlation (r=0.87; p<0.001) between modelled data and the relatively few available CTD records of SBT measured prior to sampling we consider the risk of introducing errors as marginal. Moreover, seabed substrate composition, reflecting the benthic habitats corresponding to each sampling point was retrieved from EMODnet (European Marine Observation and Data network; www.emodnetgeology.eu; version September 2021) with a maximum spatial resolution of 4 km². Finally, to account for potential effects of exploitation, annual fishing effort data (fishing hours) per ICES statistical rectangle for both otter and beam trawlers was extracted (Couce et al., 2020). All the above-mentioned covariates were tested for multi-collinearity and when a correlation > 0.7 or < -0.7 was found, the variable which was least correlated with other covariates was kept for the analysis.

3.2.2. Model setup, fitting and validation

To examine the underlying community assembly rules acting on the North Sea fish community we used the HMSC framework (Ovaskainen et al., 2017; Tikhonov et al., 2020) through the R package Hmsc version 3.0-11 (Ovaskainen & Abrego, 2020; Tikhonov et al, 2021). More specifically, we fitted a presence-absence HMSC model with a probit link function using individual hauls as sampling unit. As linear fixed effects, we included SBT, SBT seasonality, sea bottom salinity (SBS) seasonality, seafloor detritus, surface chlorophyll a concentration, surface DIN concentrations, and fishing effort. Since fishing effort was represented by an annual total, we applied a one-year lag, as the possible effects of fishing are expected to be appreciable in the following year's community. Since species usually display optimum ranges in their environmental niches, especially for temperature, we also included a quadratic term for SBT in the model. The environmental covariate and trait matrices are scaled by default by

HMSC so that they have zero mean and unit variance over the columns. Such scaling is invisible to the user as the estimated parameters are back-transformed to the original scale when further processed. Finally, we included year and season within year (winter and summer) as temporal unstructured random effects, and the ICES statistical rectangles as spatially explicit random effect. All three random effects were treated independently, and the number of latent variables for each was constrained to a minimum of 1 and a maximum of 5. The model was fitted assuming the default priors described in Supporting Information of Tikhonov et al. (2020). Four Markov chain Monte Carlo (MCMC) chains were run, each collecting 250 samples, resulting in 1000 posterior samples. We applied a thinning of 100, resulting in 37,500 iterations per chain of which the first 12,500 were discarded as burn in. MCMC convergence was assessed by examining the potential scale reduction factors (Gelman & Rubin, 1992) of model parameters. MCMC convergence is considered satisfactory if the mean values do not exceed 1.1 (Tikhonov et al., 2020). The model performance was evaluated as explanatory and predictive power (through a 5-fold cross-validation) by means of the area under the receiver operating characteristic curve (AUC), Tjur R2 and root mean square error (RMSE). AUC is widely used to test SDMs discriminatory ability (i.e., the ability to distinguish between a presence and an absence) by evaluating its sensitivity (true positive rate) and specificity (true negative rate) (Fielding & Bell, 1997). Values of 0.5 suggest no discrimination, 0.7 to 0.8 as acceptable, 0.8 to 0.9 as excellent and > 0.9 as outstanding (Mandrekar, 2010). Likewise, Tjur R2 provides a measure of the model's discriminatory ability (Tjur, 2009), while RMSE is a measure of the accuracy (i.e., how close the measurement are to the true value). We conducted all statistical analyses in the R software, version 4.2.1 (R Core Team, 2022).

Table 3.2. Mean explanatory and predictive powers (from a 5-fold cross-validation) across all modelled species measured as AUC, Tjur R2 and RMSE.

	AUC	Tjur R ²	RMSE
Explanatory power	0.895	0.246	0.199
Predictive power	0.883	0.240	0.200

3.2.3. Model diagnostics and performance

The MCMC convergence was satisfactory indicated by the mean (and SD) of the potential scale reduction factor being < 1.1 for both beta and gamma parameters, reflecting species responses to the environment and the role of traits, respectively (Appendix 2; Figure S2). The effective sample size of the MCMC was close to the number of posterior samples, and we can therefore assume samples not being autocorrelated (Appendix 2; Figure S2). The explanatory power of the model had a mean AUC of 0.89, Tjur R2 of 0.246 and RMSE of 0.199, while the mean predictive power (based on a 5-fold cross validation) was of 0.88, 0.24 and 0.2, respectively (Appendix 2; Table S2). Although there are four exceptions (i.e., Pholis gunnellus for AUC, and *Phycis blennoides, Dicentrarchus labrax* and *Trachinus draco* for Tjur R2, being the difference of minimal), the explanatory power always outperformed the predicting power, showing no major signs of model overfitting (Appendix 2; Figure S3). The variance in species' occurrence explained by the model was attributed to both the fixed and random effects that

explained on average 35 and 65% of the variance, respectively (Figure 3.2.2). The spatial random effect was the variable that explained most variability across species, i.e. 50%. Subsequently, the temperature variables (i.e., SBT and SBT seasonality), explained 25% of the variance. Finally, year and productivity explained 12 and 7% of the variance, respectively. The remaining variables, namely season, sediment SBS seasonality and fishing, each explained ≤ 5% of the variance in species occurrences. Nonetheless, the contribution of each of each of the variables (both fixed and random) varies across species (Appendix 2; Figure S5). The species responses to the environmental variables were partially explained by the set of traits included in the model. The proportion of species responses to the different environmental variables explained by traits varied from a maximum of 61% for the mixed sediment, to a minimum of 11% for fishing effort (Appendix 2; Figure S4). From the thirteen environmental variables considered (HMSC treats each sediment type as an individual variable), traits explained more than 20% of the response in seven, and between 10-20% in six environmental variables.

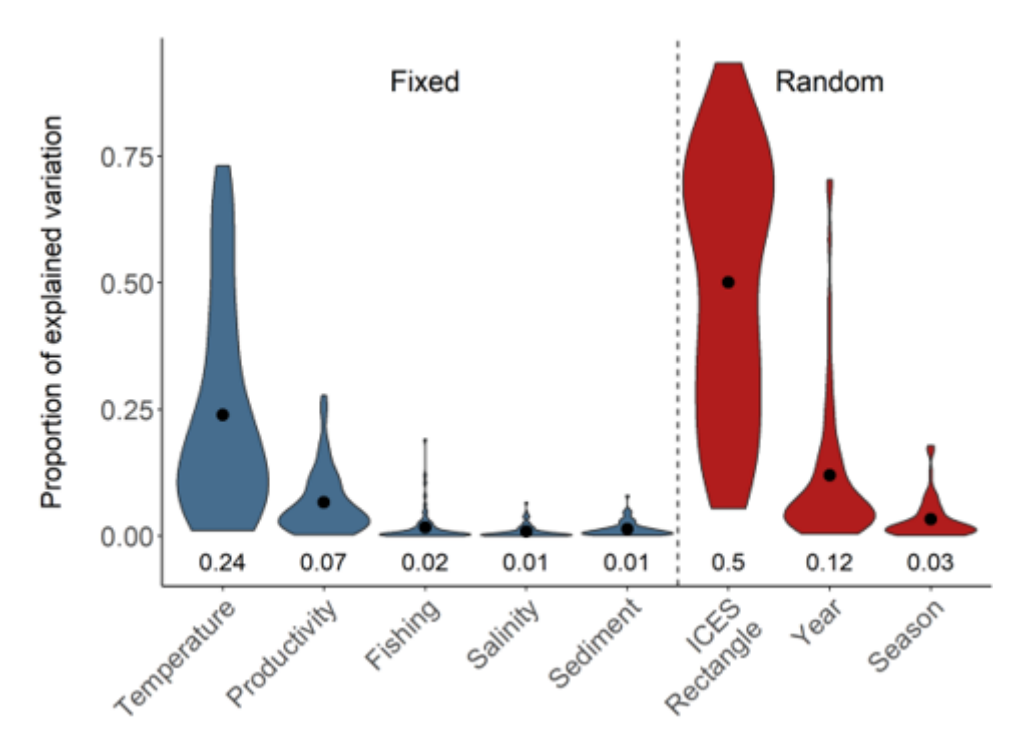


Figure 3.2.2. The proportion of total variation explained by each group of variables across species. The black dot denotes the mean variance explained by each covariate across the whole fish community, and the actual value is found below each violin plot. The variables belonging to the fixed and random parts of the model are shown on the left and right part of the model, respectively, and separated by a dashed line.

3.2.4. Species and trait responses to drivers

There is a great diversity of species-specific responses to the set of environmental variables included in the model with a high level of statistical support (posterior probability > 0.95), including negative, positive, or non-significant relationships (Figure 3.2.3), such as the derived SBT responses of Atlantic cod (*Gadus morhua*), sprat (*Sprattus sprattus*) and European eel (*Anguilla anguilla*). We found that among the total variance of individual species occurrences, 12.5% could be explained by traits. From the included traits, age at maturity, growth coefficient K, maximum length, body shape, caudal fin shape, feeding mode and habitat show a response to at least one of the environmental covariates (Figure 3.2.4). For example, the

growth coefficient K and age at maturity show a negative response to SBT, while age at maturity and maximum length demonstrate a negative or positive response to SBT seasonality, respectively. We found strong support for phylogenetic niche conservatism, with the phylogenetic correlation parameter rho being 0.82 (95% credible interval: 0.62 - 0.89). This indicates that a set of phylogenetically-structured traits, beyond the traits already included in the model, likely influence species niches.

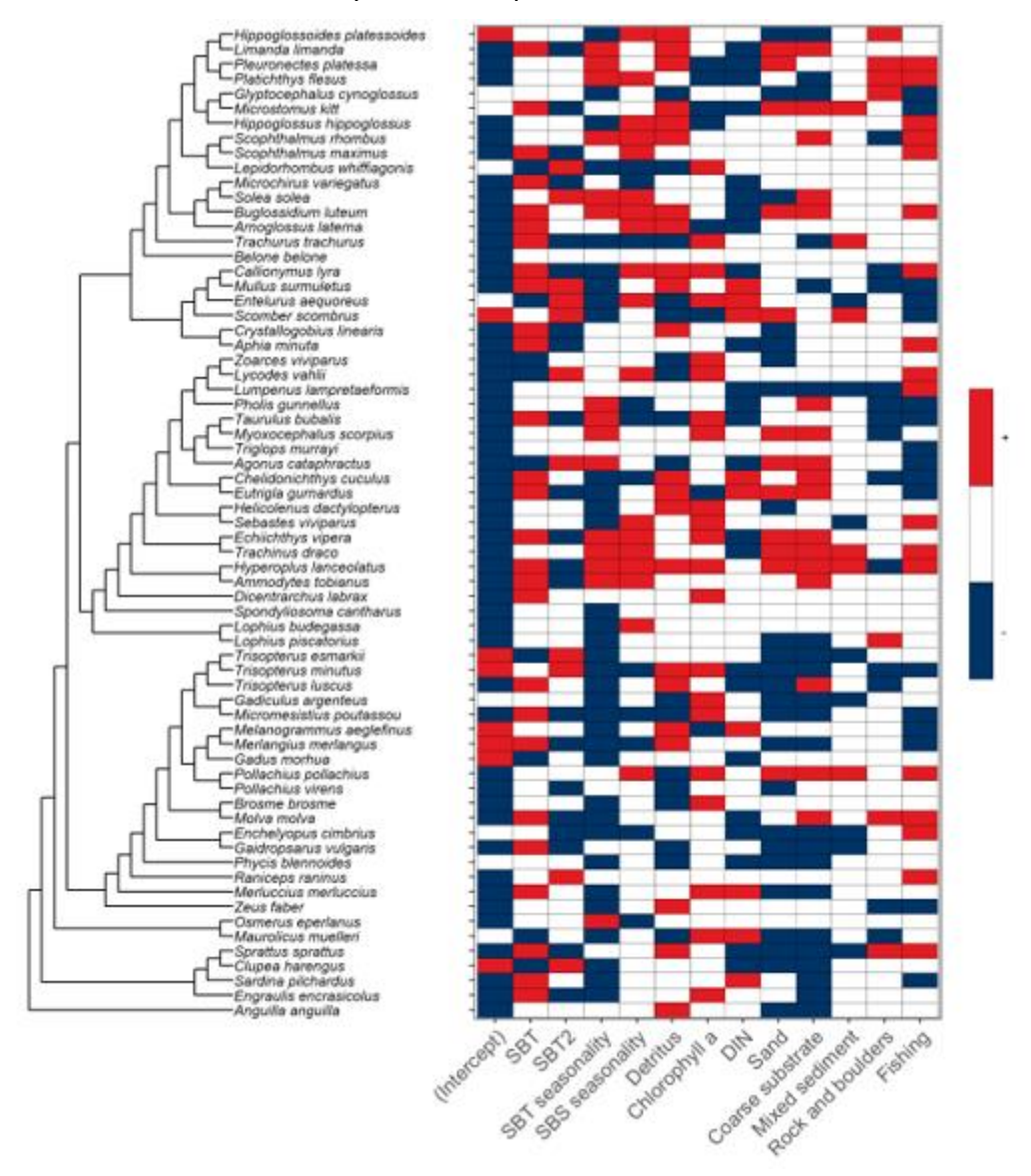


Figure 3.2.3. Heatmap of estimated beta coefficients indicating positive (red), negative (blue) or no relationships (blank) of species responses to the set of environmental covariates included (with at least a posterior probability of 0.95). Species are sorted vertically according to their phylogenetic relatedness.

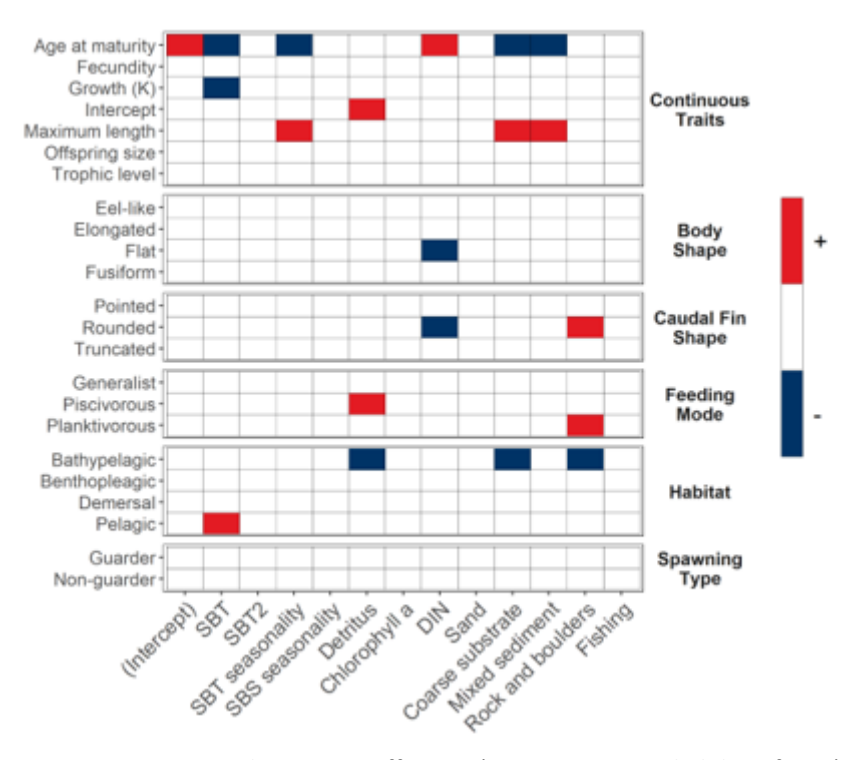


Figure 3.2.4. Estimated gamma coefficients (at a posterior probability of 0.95), indicating positive (red), negative (blue) or no relationships (blank) of traits to the set of environmental covariates included.

3.2.5. Patterns and trends in biodiversity

The overall indicators of taxonomic and functional biodiversity estimated from model predictions of species and community composition show pronounced spatio-temporal variation within and between metrics of richness and evenness (Figure 3.2.5). In terms of species richness, we found the highest values in the central North Sea, reflecting the mixing zone between the more shallow- and deep water communities dominating in the southern and northern part, respectively (Dencker et al. 2017). The geographic separation is also evident with regards to the Shannon index, showing communities with a more even distribution of abundances in the deeper northern part. The geographic patterns above are broadly reflected in terms of functional indicators, albeit with a less marked differences between areas, such as the more uniform distribution of functional richness. This highlights that while the number of species may differ between areas, the trait composition is more conserved (Dencker et al. 2017; Beukhof et al. 2019b). Nevertheless, the highest values observed across the central part of the area indicate that the higher number of species also lead to a more diverse community in terms of species traits. However, harbouring a higher trait richness does necessarily lead to a more uniform distribution of abundances, as indicated by the somewhat opposite pattern shown for functional evenness. Finally, the overall patterns described above are fairly consistent over the recent time period considered, albeit with a slight contraction of the area of high species richness in the central North Sea in recent years.

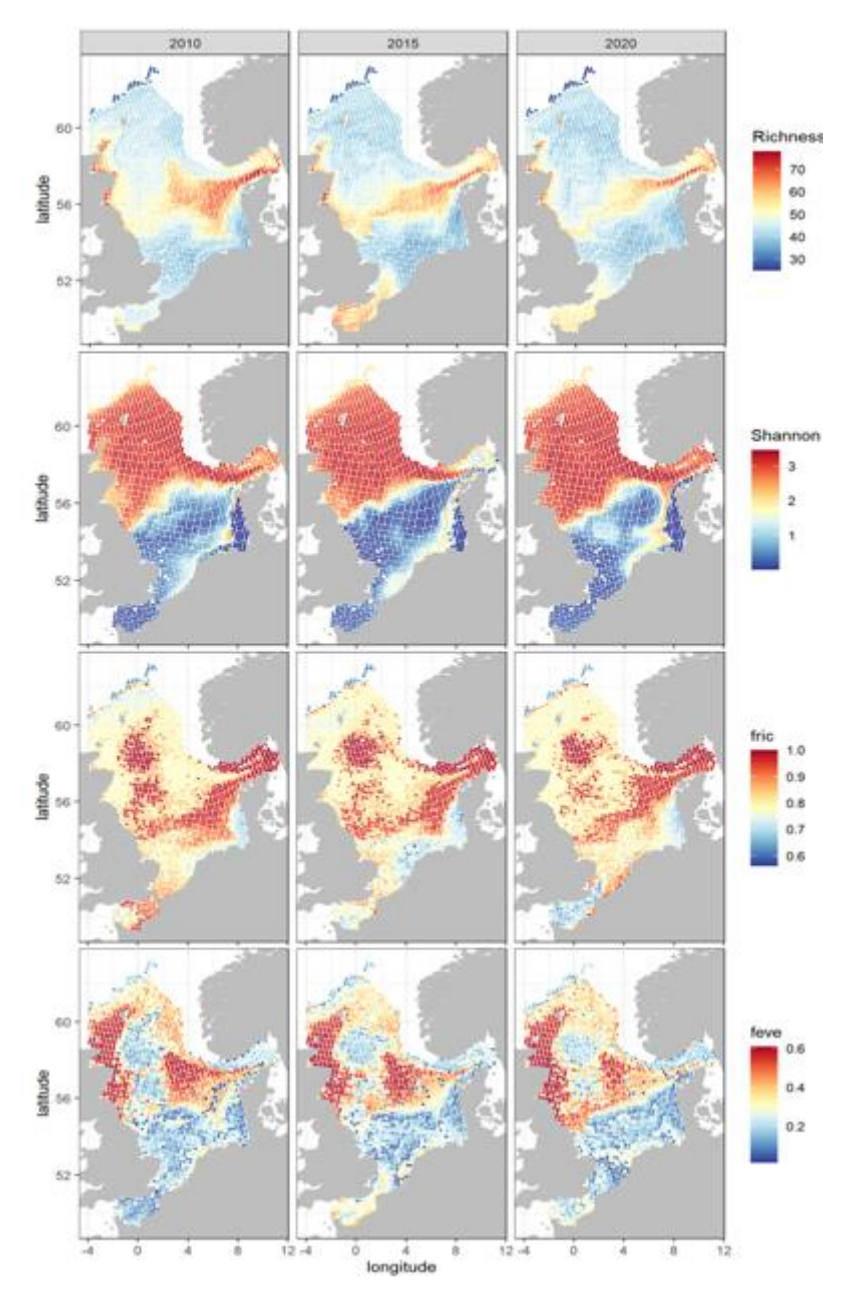


Figure 3.2.5. Spatial patterns of taxonomic and functional biodiversity indicators, including species richness (1st row), Shannon evenness (2nd row), functional richness (3rd row) and functional evenness (4th row). The indicators are based on model predictions for three selected years, including 2010 (left), 2015 (middle) and 2020 (right).

3.2.6. Summary

Our modelling study shows that environmental filtering, primarily related to temperature and seasonality, explains a large part of the variance in species distributions and community composition. This supports previous findings on drivers and determinates of marine fish community structure in the area and beyond (Dencker et al. 2017; Beukhof et al. 2019b). Our study also demonstrates that there are other assembly processes with a strong spatial structure playing a role in shaping these communities. Notably, we argue that biotic factors are likely important in this regard, but call for further research to better understand the underlying interactions involved. Furthermore, we stress the importance of accounting for species traits since their inclusion improves the mechanistic understanding on species responses to environmental change, while providing model predictions of key biodiversity indicators capable of informing spatial management and conservation efforts, such as the placement of marine protected areas.

3.2.7. References

Beukhof, E. et al. 2019a. Marine fish traits follow fast-slow continuum across oceans. - Sci. Rep. 9: 17878.

Beukhof, E. et al. 2019b. A trait collection of marine fish species from North Atlantic and Northeast Pacific continental shelf seas. in press.

Beukhof, E. et al. 2019c. Spatio-temporal variation in marine fish traits reveals community-wide responses to environmental change. - Mar. Ecol. Prog. Ser. 610: 205–222.

Couce, E. et al. 2020. Reconstructing three decades of total international trawling effort in the North Sea. - Earth Syst. Sci. Data 12: 373–386.

Coulon, N., Lindegren, M., Goberville, E., Toussaint, A., Receveur, A., & Auber, A. (2023). Threatened fish species in the Northeast Atlantic are functionally rare. Global Ecology and Biogeography, 32(10), 1827–1845.

Chang, J. et al. 2019. An r package and online resource for macroevolutionary studies using the ray-finned fish tree of life. - Methods Ecol. Evol. 10: 1118–1124.

Dencker, T. S. et al. 2017. Temporal and spatial differences between taxonomic and trait biodiversity in a large marine ecosystem: Causes and consequences. - PLoS One 12: 1–19.

Fielding, A. H. and Bell, J. F. 1997. A review of methods for the assessment of prediction errors in conservation presence/absence models. - Environ. Conserv. 24: 38–49.

Mandrekar, J. N. 2010. Receiver operating characteristic curve in diagnostic test assessment. - J. Thorac. Oncol. 5: 1315–1316.

Maureaud, A. et al. 2019. Biodiversity-ecosystem functioning relationships in fish communities: Biomass is related to evenness and the environment, not to species richness. - Proc. R. Soc. B Biol. Sci. in press.

Ovaskainen, O. et al. 2017. How to make more out of community data? A conceptual framework and its implementation as models and software. - Ecol. Lett. 20: 561–576.

Ovaskainen, O. and Abrego, N. 2020. Joint Species Distribution Modelling. - Cambridge University Press.

R Core Team 2022. R: A language and environment for statistical computing. R Foundation for Statistical Computing, Vienna, Austria. URL https://www.R-project.org/. in press.

Tikhonov, G., Opedal, Ø. H., Abrego, N., Lehikoinen, A., de Jonge, M. M. J., Oksanen, J., & Ovaskainen, O. (2020). Joint species distribution modelling with the r-package Hmsc. Methods in Ecology and Evolution, 11(3), 442–447.

Tikhonov, G., Ovaskainen, O., Oksane, J., Jonge, M. de, Opedal, O., & Dallas, T. (2021). Hmsc: Hierarchical Model of Species Communities. R package version 3.0-12.

Tjur, T. 2009. Coefficients of determination in logistic regression models - A new proposal: The coefficient of discrimination. - Am. Stat. 63: 366–372.

Walker, N. D. et al. 2017. Estimating efficiency of survey and commercial trawl gears from comparisons of catchratios. - ICES J. Mar. Sci. 74: 1448–1457.

WoRMS Editorial Board 2022. World Register of Marine Species.

Yool, A. et al. 2013. MEDUSA-2.0: An intermediate complexity biogeochemical model of the marine carbon cycle for climate change and ocean acidification studies. - Geosci. Model Dev. 6: 1767–1811.

3.3 Baltic Sea fish model

Authors: Tom Jimenez, Federico Maioli, Marcel Montanyes, Martin Lindegren

3.3.1. Study area and data availability

Fish abundance data was collected from the North Sea International Bottom Trawl Survey (NS-IBTS) and the Baltic International Trawl Survey (BITS) from the publicly available scientific monitoring survey database DATRAS, hosted by the International Council for the Exploration of the Sea (ICES) (www.datras.ices.dk). The data covered available surveys from 1993 to 2021 conducted during the winter, summer and autumn seasons, ensuring complete coverage of the entire study area ranging from Skagerrak and Kattegat to the Baltic proper (Figure 3.3.1). Taxa names were checked and verified following the World Register of Marine Species (WoRMS Editorial Board 2024). Taxa other than fish were excluded, retaining only organisms identified to species level in the following classes: Actinopterygii, Elasmobranchii, Holocephali, Myxini and Petromyzonti. Furthermore, we excluded rare species with less than 10 unique occurrence records in the entire data set. This resulted in a total of 78 species from 12,953 unique hauls. For each of the hauls we recorded the presence-absence of species, as well as their abundance standardized for sampling area (km²) and trawl gear catchability following (Walker et al. 2017; van Denderen et al. 2023).

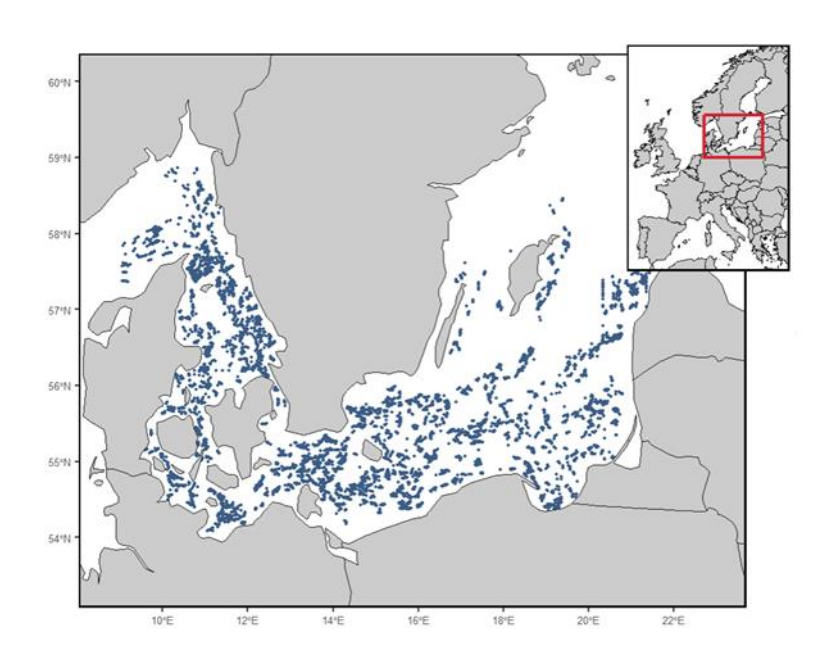


Figure 3.3.1. Position of all unique hauls of the bottom-trawl surveys performed in the Baltic Sea between 1993 and 2021 ranging from Skagerrak and Kattegat to the Baltic proper

In order to represent the broader ecology of species in terms of their morphology, life history, reproduction and diet we selected 10 ecological traits (Dencker et al. 2017) (Appendix 3; Table S1). Trait values for each species were collected from available trait data bases (Beukhof et al. 2019; Coulon et al. 2023). The species morphology is defined by body shape, caudal fin shape, and maximum length (cm). Life history traits include age at maturity (years) and the von Bertalanffy growth coefficient (K) (year-1). Reproductive characteristics cover spawning type, fecundity (number of eggs), and offspring size (egg diameter in mm). Dietary factor is represented by feeding mode while habitat indicates the general position in the water column. To reflect key environmental conditions affecting fish species distribution and composition we used the physics and biochemistry reanalysis products of the Baltic

(BALMFC CMEMS). The reanalysis products are based on the regionally downscaled Nemo-Nordic general circulation model (Hordoir et al. 2019) coupled with the SCOBI (Swedish Coastal and Ocean Biogeochemical) biogeochemistry model (Eilola et al. 2009; Almroth-Rosell et al. 2015). The environmental data extracted from Copernicus (www.marine.copernicus.eu) include bottom temperature, salinity, oxygen concentration, as well as surface chlorophyll-a concentration and depth. After checking for potential collinearity among variables (Appendix 3; Figure S1) all were included as candidate predictors in the subsequent modelling.

3.3.2. Model setup, fitting and validation

We used the HMSC framework to investigate drivers and community assembly rules in the Baltic Sea fish community (Ovaskainen et al. 2017; Tikhonov et al. 2020). HMSC quantifies variation in species distributions using environmental covariates and random effects, which capture spatio-temporal patterns and species-specific associations. These associations, reflecting ecological processes such as dispersal limitation and biotic interactions, are estimated using latent variables (Ovaskainen and Abrego 2020). We fitted a presence-absence HMSC model with a probit link function using individual hauls as sampling units. We also fitted a biomass model conditional on presence, but with the primary purpose to allow calculation of biodiversity indicators relying on such information. As fixed effects, we included bottom temperature, bottom salinity, bottom oxygen concentration, surface chlorophyll-a concentration, depth and season. Since species usually display non-linear environmental niches, especially for temperature, we also included a quadratic term for temperature and salinity in the models. Finally, we included year as a temporal random effect, and hexagonal grid cells (N=47) as spatially random effect. The latter random effect is introduced to accommodate spatial patterns that remain unexplained by environmental predictors. All random effects were treated independently, and the number of latent variables for each was constrained to a minimum of 1 and a maximum of 6. Two Markov chain Monte Carlo (MCMC) chains were run, each collecting 100 samples, resulting in 200 posterior samples. We applied a thinning of 1000, resulting in 150,000 iterations per chain of which the first 51,000 were discarded as burn-in. MCMC convergence was assessed by examining the potential scale reduction factors (PSRF; Gelman and Rubin 1992) of model parameters where convergence is considered satisfactory if the mean PSRF values do not exceed 1.1 (Tikhonov et al. 2020). The model performance was evaluated as both explanatory and predictive power (through a 2fold cross-validation) by means of the area under the receiver operating characteristic curve (AUC), Tjur R² and root mean square error (RMSE).

Table 3.3.1. Mean explanatory and predictive powers (from a 2-fold cross-validation) for the occurrence and biomass models.

Model		Occurrence	Biomass		
	AUC	Tjur R²	RMSE	R²	RMSE
Explanatory power	0.934	0.258	0.151	0.430	1.208
Predictive power	0.742	0.111	0.196	0.216	1.538

3.3.3. Model diagnostics and performance

The mean PSRF of the fitted gamma parameters was <1.1 for the presence-absence model, indicating satisfactory convergence (Appendix 3; Table S2 and Figure S2). In terms of the beta parameters, the values were slightly higher (1.29), indicating poor convergence for some taxa. The effective sample size of the MCMC was close to the number of posterior samples (200 samples), and we can therefore assume samples not being autocorrelated. These MCMC convergence statistics indicate a good reliability and validity of our model, which avoids the need to take more samples. The explanatory power of the model had a mean AUC of 0.93, Tjur R² of 0.26 and RMSE of 0.15, while the mean predictive power (based on a 2-fold cross-validation) was 0.74, 0.11 and 0.20, respectively (Table 3.3.1). While the AUC is generally high, the value of Tjur R² is relatively modest, suggesting a moderate capacity of the model to explain the variance in the data. Finally, the RMSE value based on cross-validation (0.196) is slightly higher, indicating a decrease in the accuracy of predictions on unobserved data. The values for the biomass model are slightly higher.

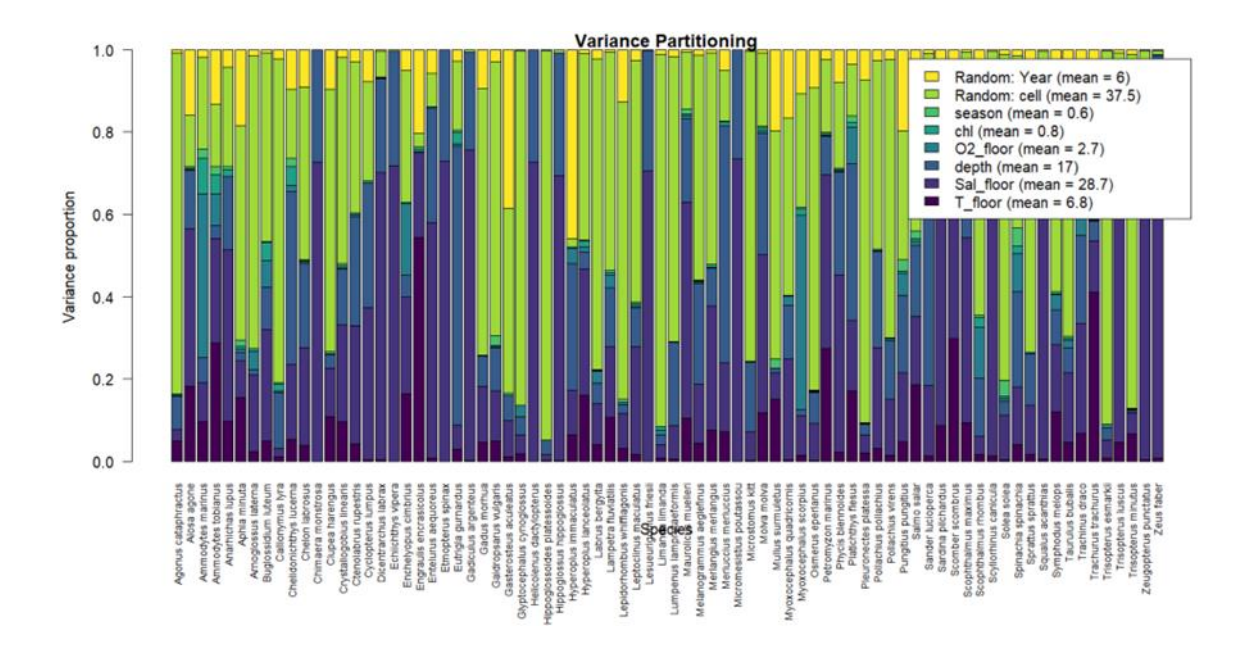


Figure 3.3.2. Variance by species explained by the fixed and random effects included in the model.

3.3.4. Species and trait responses to drivers

The variance in species' occurrence explained by the model was attributed to both fixed and random effects that explained on average 56.5% and 43.5% of the variance, respectively (Figure 3.3.2). This indicates that most of the explanatory power of the model is encapsulated by the environmental variables. However, the spatial random effect accounted for the largest portion of variability across species, explaining 37.5% of the total variance. Among the environmental covariates, salinity and depth explained 28.7% and 17% of the variance, while temperature and year explained 6.8% and 6%, respectively. The other variables, including bottom oxygen concentration, chlorophyll-a concentration and season, explained ~4% of the variance in species occurrences. Interestingly, the contribution of each of the variables varied markedly between species. For instance, some species, such as

Chimaera monstrosa, Echiichthys vipera and Micromesistius poutassou, were almost entirely explained by the fixed effects, while Hippoglossoides platessoides, Limanda limanda and Pleuronectes platessa were predominately explained by the spatial random effects.

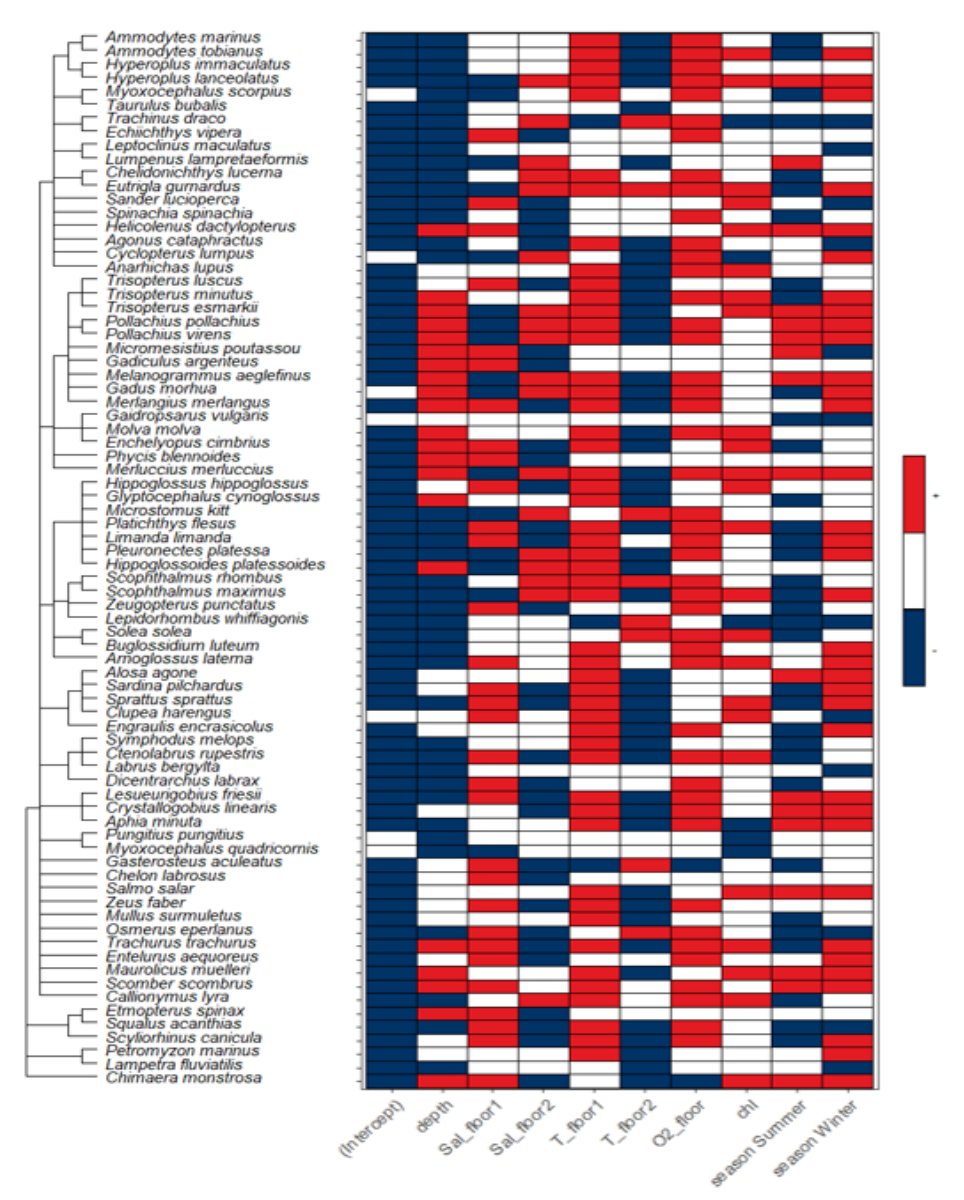


Figure 3.3.3. Heatmap of estimated beta coefficients indicating positive (red), negative (blue) or no relationships (blank) of species responses to the set of environmental covariates included (with at least a posterior probability of 0.95). Species are sorted vertically according to their taxonomic relatedness.

We observed a wide range of species-specific responses to all the environmental variables included in the model, including negative, positive and non-significant relationships (Figure 3.3.3). Among the environmental variables, bottom temperature, bottom salinity and depth show significant beta coefficients for many species, suggesting that these are critical variables determining the environmental niches for most species in the area. As an example, we found positive responses of the common and commercially important species herring (*Clupea harengus*) and sprat (*Sprattus sprattus*) to salinity and temperature, while the Atlantic cod (*Gadus morhua*) responded positively also to depth and bottom oxygen concentrations. The species responses to the environmental variables were partially explained by the set of traits

included in the model. More specifically, the proportion of species responses to the different environmental variables explained by traits varied from a maximum of 28% for bottom oxygen concentration, to a minimum of 4% for the winter season (Appendix 3; Figure S3). Among the ten environmental variables considered, traits explained more than 10% of the response in four. From the included traits, age at maturity, growth coefficient K, body shape, feeding mode and habitat show pairwise responses to at least one of the environmental covariates (Figure 3.3.4). For example, age at maturity shows a positive response to depth and summer season, while body shape shows a negative response to oxygen concentration. In addition, demersal and pelagic habitat types seem to react positively to temperature.

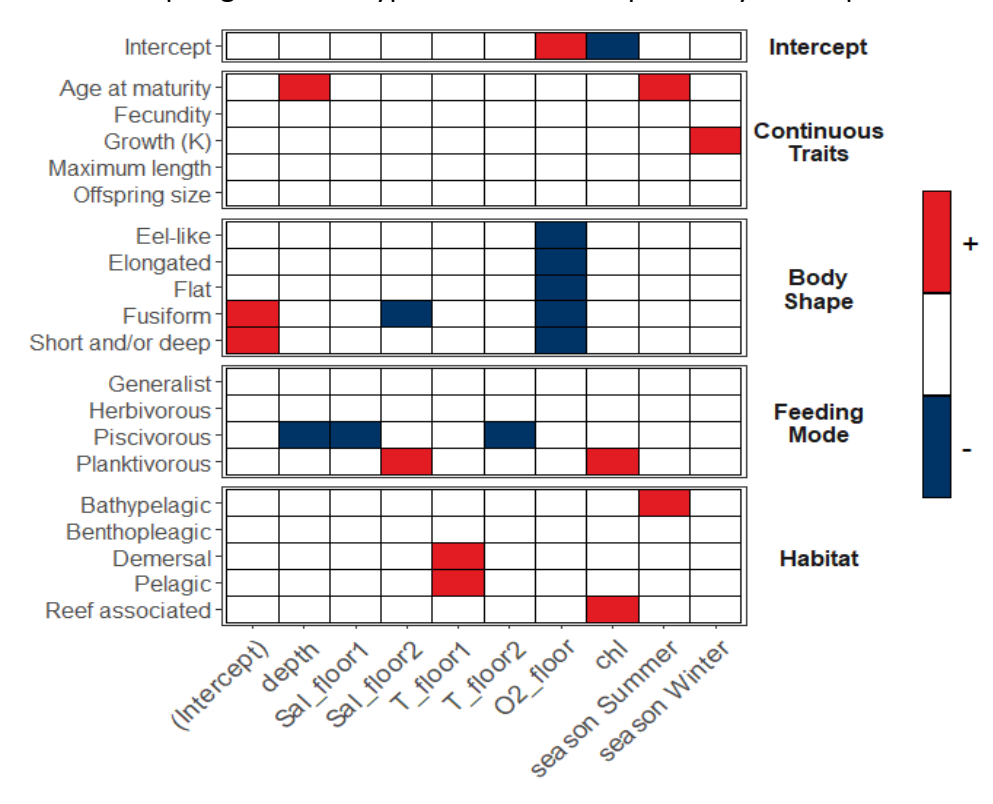


Figure 3.3.4. Heatmap of estimated gamma coefficients indicating positive (red), negative (blue) or no relationships (blank) of traits to the set of environmental covariates included (with at least a posterior probability of 0.90).

3.3.5. Patterns and trends in biodiversity

The biodiversity indicators estimated from model predictions of species occurrences and biomass show pronounced geographic variation within and among indicator (Figure 3.4.5). In terms of species richness, we found high values in the Kattegat/Skagerrak (~25 species) and a sharp decrease further south and east into the Baltic proper. The spatial gradient from west to east is relatively stable over time (Figure 7B), but with slight variations in the intensity and extent of change, particularly in the Kattegat where an increasing trend of up to 0.2 species/year can be observed. The Shannon index shows a similar spatial gradient with higher values in the Kattegat and in more coastal areas, while the lowest values are predicted in the eastern part, especially in the deeper basins of the Baltic proper. Similarly, there is moderate variation over time with most areas showing no directional (linear) trend. In terms of the functional indicators (using also trait information in the estimation), we found a rather similar overall spatial patterns as the taxonomic indicators. More specifically, the Hill's number 0 was higher in the Kattegat/Skagerrak, especially in the more coastal areas, while the lowest values

were found in the deeper basins of the Baltic proper. The temporal trend is rather modest, indicating only slight changes in trait richness, despite changes in the overall number of species. Similar to the Hill number the functional richness shows a similar spatial pattern, with highest values in the deeper areas the entrance to the North Sea. In terms of temporal trends, we found a positive rate of change in the inner Danish waters and along the Swedish west coast. With regard to functional divergence, a gradient opposite to that of functional richness was observed with slight variations over time.

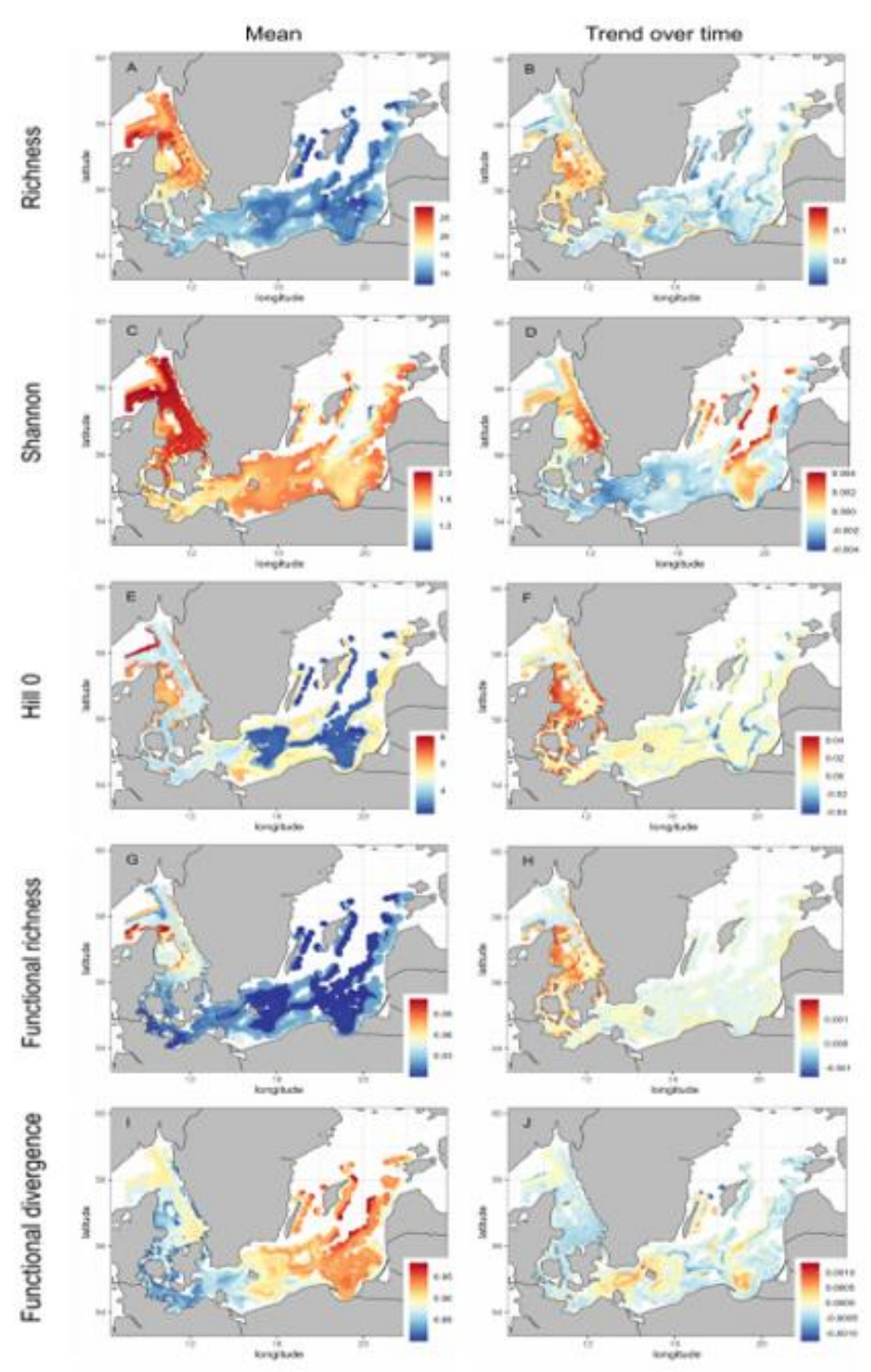


Figure 3.3.5. Spatial patterns and changes in taxonomic and functional biodiversity indicators, reflected by the mean (left) and linear trend (right) in each variable between 1993 and 2021. The bottom panels show biplots from a PCA, reflecting the loadings of each biodiversity indicators on the first two axis (PC1 and PC2) while using means (K) and linear trends (L) as input.

3.3.6. **Summary**

Our model predictions highlight patterns and changes in overall biodiversity throughout the study area, reflected by a complementary set of indicators of taxonomic and functional diversity. The patterns and trends reflect the underlying changes in species distribution and biomass in response to climate variability and change, as captured by the parameterized models. The large-scale spatial patterns of species richness and functional richness are similar to those observed in previous data-driven studies (Pecuchet et al. 2016). Notably, the most decisive gradient is that of salinity where areas with low salinity and functional richness can be explained by the presence of communities made up of species with similar traits, such as flatfish. Conversely, areas with high salinity and functional diversity include a greater number of species with more different traits (Pecuchet et al. 2016), which in turn is considered beneficial for the ecosystem at large (Cadotte et al. 2011). Understanding the environmental factors that shape species distribution and community composition enables us to predict changes in overall diversity in response to future environmental change (Mouillot et al. 2013). This can help us evaluate the effectiveness of conservation and management actions helping to safeguard biodiversity, notably the designation of an effective and well-connected system of protected areas jointly covering 30% of the land and oceans (Convention on Biological Diversity 2021; Hermoso et al. 2022).

3.3.7. References

Almroth-Rosell E, Eilola K, Kuznetsov I, Hall POJ, Meier HEM (2015) A new approach to model oxygen dependent benthic phosphate fluxes in the Baltic Sea. Journal of Marine Systems 144:127–141. doi: 10.1016/j.jmarsys.2014.11.007

Beukhof E, Frelat R, Pecuchet L, Maureaud A, Dencker TS, Sólmundsson J, Punzón A, Primicerio R, Hidalgo M, Möllmann C, Lindegren M (2019) Marine fish traits follow fast-slow continuum across oceans. Sci Rep 9:17878. doi: 10.1038/s41598-019-53998-2

Cadotte MW, Carscadden K, Mirotchnick N (2011) Beyond species: functional diversity and the maintenance of ecological processes and services. Journal of Applied Ecology 48:1079–1087. doi: 10.1111/j.1365-2664.2011.02048.x

Convention on Biological Diversity (2021) First draft of the post-2020 global biodiversity framework.

Coulon N, Lindegren M, Goberville E, Toussaint A, Receveur A, Auber A (2023) Threatened fish species in the Northeast Atlantic are functionally rare. Global Ecology and Biogeography 32:1827–1845. doi: 10.1111/geb.13731

Dencker TS, Pecuchet L, Beukhof E, Richardson K, Payne MR, Lindegren M (2017) Temporal and spatial differences between taxonomic and trait biodiversity in a large marine ecosystem: Causes and consequences. PLOS ONE 12:e0189731. doi: 10.1371/journal.pone.0189731

Eilola K, Meier HEM, Almroth E (2009) On the dynamics of oxygen, phosphorus and cyanobacteria in the Baltic Sea; A model study. Journal of Marine Systems 75:163–184. doi: 10.1016/j.jmarsys.2008.08.009

Gelman A, Rubin DB (1992) Inference from Iterative Simulation Using Multiple Sequences. Statistical Science 7:457–472. doi: 10.1214/ss/1177011136

Hermoso V, Carvalho S, Giakoumi S, Goldsborough D, Katsanevakis S, Leontiou S, Markantonatou V, Rumes B, Vogiatzakis I, Yates K (2022) The EU Biodiversity Strategy for 2030: Opportunities and challenges on the path towards biodiversity recovery. Environmental Science & Policy 127:263–271. doi: 10.1016/j.envsci.2021.10.028

Hordoir R, Axell L, Höglund A, Dieterich C, Fransner F, Gröger M, Liu Y, Pemberton P, Schimanke S, Andersson H, Ljungemyr P, Nygren P, Falahat S, Nord A, Jönsson A, Lake I, Döös K, Hieronymus M, Dietze H, Löptien U, Kuznetsov I, Westerlund A, Tuomi L, Haapala J (2019) Nemo-Nordic 1.0: a NEMO-based ocean model for the

Baltic and North seas – research and operational applications. Geoscientific Model Development 12:363–386. doi: 10.5194/gmd-12-363-2019

Mouillot D, Graham NAJ, Villéger S, Mason NWH, Bellwood DR (2013) A functional approach reveals community responses to disturbances. Trends in Ecology & Evolution 28:167–177. doi: 10.1016/j.tree.2012.10.004

Ovaskainen O, Tikhonov G, Norberg A, Guillaume Blanchet F, Duan L, Dunson D, Roslin T, Abrego N (2017) How to make more out of community data? A conceptual framework and its implementation as models and software. Ecology Letters 20:561–576. doi: 10.1111/ele.12757

Ovaskainen O, Abrego N (2020) Joint Species Distribution Modelling: With Applications in R. Cambridge University Press, Cambridge

Pecuchet L, Törnroos A, Lindegren M (2016) Patterns and drivers of fish community assembly in a large marine ecosystem. Marine Ecology Progress Series. doi: 10.3354/meps11613

Tikhonov G, Opedal ØH, Abrego N, Lehikoinen A, de Jonge MMJ, Oksanen J, Ovaskainen O (2020) Joint species distribution modelling with the r-package Hmsc. Methods Ecol Evol 11:442–447. doi: 10.1111/2041-210X.13345

WoRMS - World Register of Marine Species. https://www.marinespecies.org/. Accessed 28 Oct 2024

3.4 Baltic Sea benthos model

Authors: Baptiste Degueurce, Federico Maioli, Marcel Montanyes, Daniel van Denderen, Martin Lindegren

3.4.1. Study area and data availability

We collected available monitoring data on benthic invertebrates' distribution and abundance from the International Council for the Exploration of the Sea (ICES) zoobenthos data as provided by national data submitters for HELCOM (https://data.ices.dk) and from the Swedish Ocean Archive (https://sharkweb.smhi.se). The data set includes XXX unique sampling events throughout the time period from 1993-2020 for which we have good coverage in both benthic communities and environmental data over the study area (Figure 3.4.1). We excluded invalid samples and discarded species for which no traits data was available, thus limiting the number of species retained to 143. Furthermore, rare species with less than 100 occurrences over the 28 years of data, and species which were recorded in less than 10 different years were also excluded, reducing the total number of taxa considered in modelling to 88. The final data set included both the presence and absence of species per sampling events, as well as their densities reflected by the ash free dry weight (AFDW) per m².

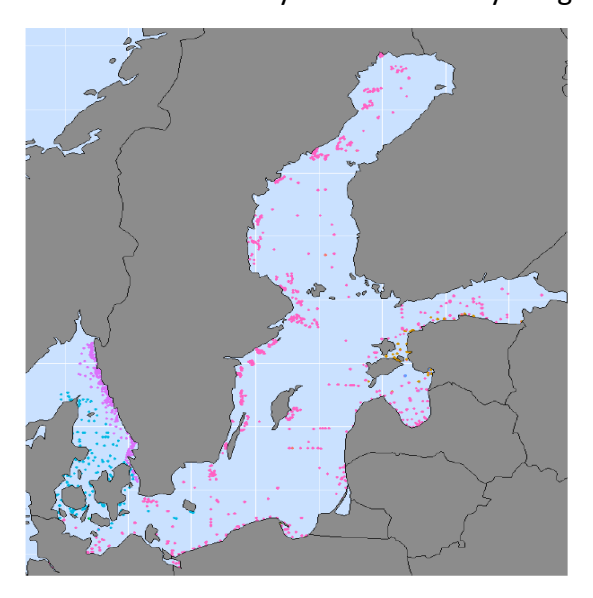


Figure 3.4.1. Position of all unique benthic invertebrate samples included in the study.

To represent the broader ecology of benthic species we extracted available trait data from the online traits data portals WoRMS (https://www.marinespecies.org/), (https://www.marlin.ac.uk/biotic/) and Polytraits (http://polytraits.lifewatchgreece.eu/). For size and adult lifespan, a number is assigned for each species between 1 and 5 representing an increasing size category or a life span duration, respectively. For the other traits, each trait is divided into a number of modalities, reflecting the presence or absence of the given modality for each taxa considered. All modalities and explanations for the traits are listed in the supplementary material. To avoid redundancy among traits we excluded highly correlated traits and thus retained 12 of the modalities present in the trait data set. To reflect key candidate drivers affecting benthic species distribution we extracted temperature (°C), depth and salinity (PSU) from the Copernicus physic re-analysis and forecast for the Baltic Sea (cmems mod bal phy anfc PT1H-i, https://data.marine.copernicus.eu/). Furthermore, we extracted oxygen (g per m3) and chlorophyll-A (mg per m3) concentration from the Copernicus Biogeochemistry analysis and forecast (cmems_mod_bal_bgc_anfc_P1M-m) (Huess et al., 2024). Finally, seabed sediment type and composition for each sampling site was extracted from EMODnet (European Marine Observation and Data network; www.emodnet-geology.eu; version November 2024).

3.4.2. Model setup, fitting and validation

To investigate key drivers and assembly process affecting benthic invertebrates we used the Hierarchical modelling of species communities (HMSC) framework (Ovaskainen and Abrego, 2017). More specifically, we fitted a presence absence model using the "probit" distribution and a biomass model conditional on presence using log-transformed AFDW as response. Both models use the assembled environmental conditions depth, bottom salinity, bottom temperature, mean chlorophyll-a, bottom oxygen, sediment type and gear type as predictors. The gear type is a fixed effect factor included to account for potential differences in sampling methods on the observed occurrence or biomass of species throughout the study area. To account for any unmeasured spatial effects not covered by the set of environmental predictors, or through biotic associations, reflecting potential interactions we also included a spatial random effect, representing hexagon grid cells amounting 75 km². For model fitting we ran a Markov chain Monte Carlo sampling (MCMC) to explore parameters and estimate the prior model parameters distribution. The MCMC sampling was configured with a thinning value (300), a transient value (50) and a sample value (100). This enabled us to reduce correlation between samples and to evaluate the model convergence using two independent chains. Furthermore, to evaluate the MCMC chains convergence we used the Gelman-Rubin diagnostic on two model parameters (β and γ) (Brooks and Gelman, 1998). This method compares the variance between the chains to the variance within the chains. If the potential scale reduction factor (PSRF) is close to 1, it suggests that the MCMC chains converged well.

3.4.3. Model diagnostics and performance

Mean PSRF (potential scale reduction factor) for the fitted gamma and beta parameters were <1.1, indicating satisfactory convergence of the model. The run of our cross-validation routine also provides us with AUC values above 0.9 for the explanatory power and 0.8 for the mean predictive power. These values are described as good according to Mandrekar (2010).

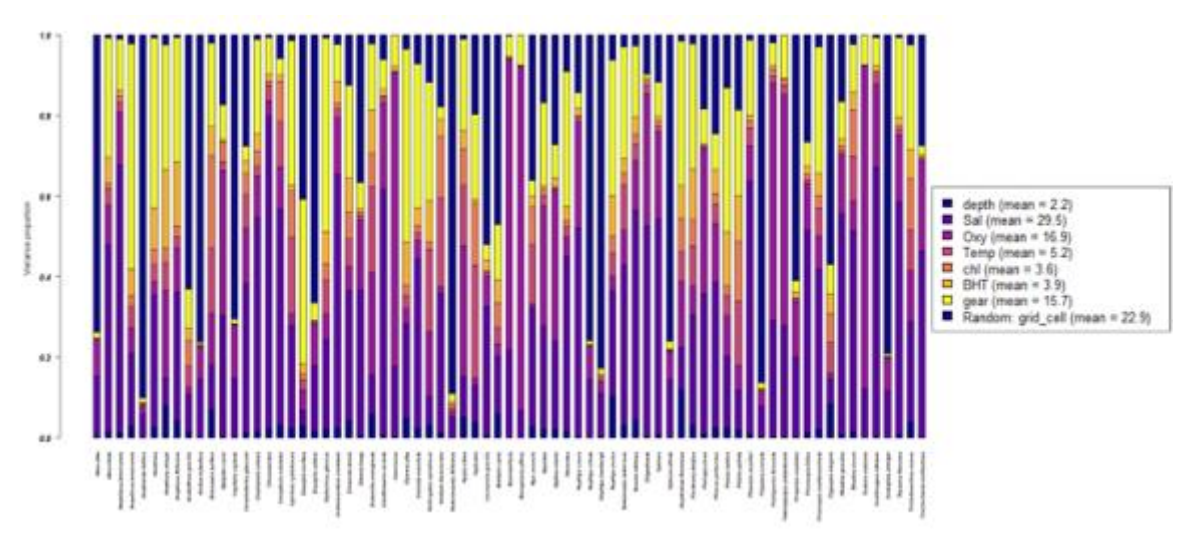


Figure 3.4.2. Variance by species explained by the fixed and random effects considered in the model.

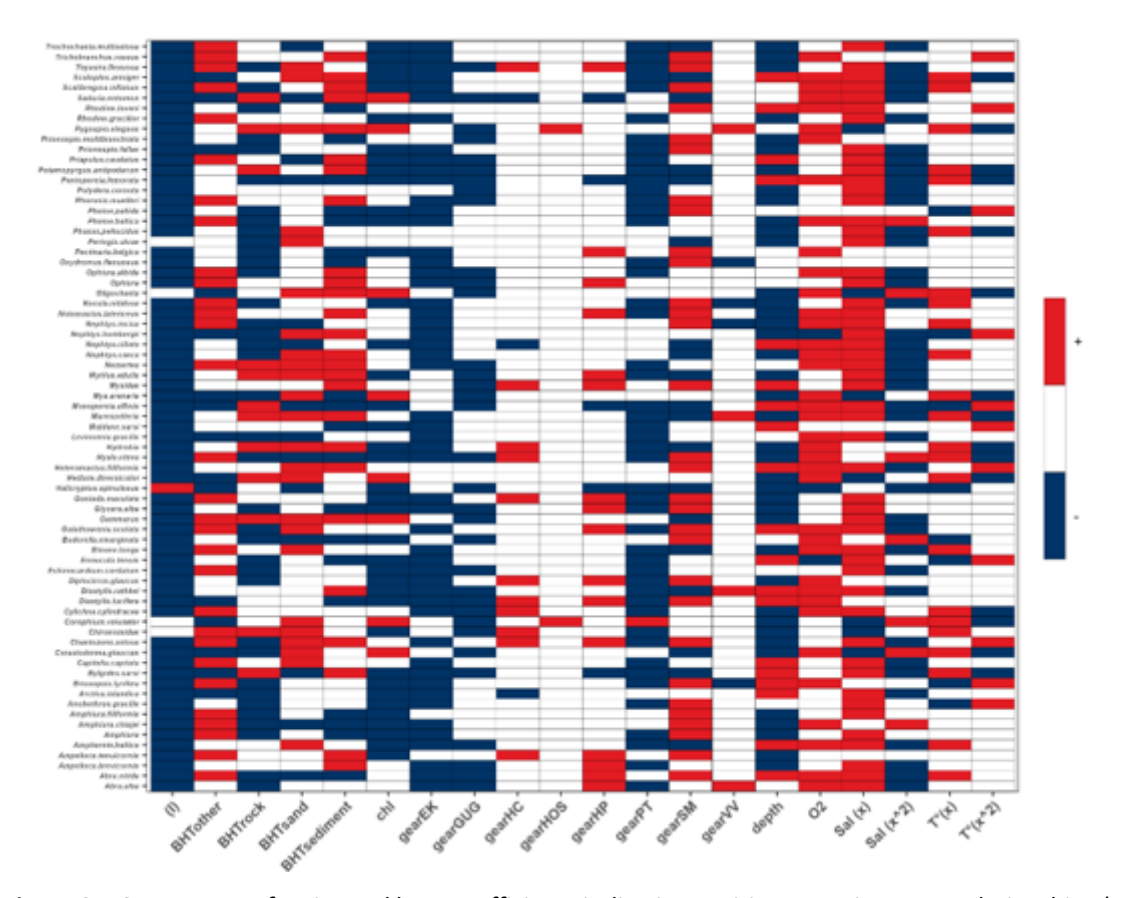


Figure 3.4.3. Heatmap of estimated beta coefficients indicating positive, negative or no relationships (red, blue, white respectively) of species responses to the set of fixed effects of our model with a posterior probability of 0.95.

3.4.4. Species and trait responses to drivers

The variance partitioning shows that the environment is explaining much of the variance, while the random effects account for only 23% of the total variance explained (Figure 3.4.2). However, there is considerable variation as some species distributions are fully explained by the environment (e.g. *Potamopyrgus antipodarum*), while others are mostly explained by the random effects (e.g. *Nephtys hombergii*). Among the environmental covariates, bottom

salinity and bottom oxygen concentration explains ~45% of the variance, while gear type explains 15%. The other environmental covariates, including temperature, chl a and sediment type account for only 12% of the total variance. The species responses to main environmental covariates show primarily positive saturating relationships to bottom salinity, as indicated by the positive linear and negative quadratic effect, while for oxygen a majority of positive or neutral responses are shown (Figure 3.4.3). In terms of the other covariates deemed less important based on the variance partitioning chl a show primarily negative relationships, while temperature, depth and sediment type show either positive, negative or non-significant relationships. In terms of potential trait effects, most of the responses to gear type is explained by traits (Figure 3.4.4). In addition, the responses of taxa to salinity (21%), temperature (20%) and chlorophyll-a rate (27%) are conditioned on the set of traits included. Among the specific pairwise interaction between traits and environmental factors (Figure 4), feeding mode is mainly responding positively to sediment type and salinity with a positive or negative response depending on the modality, while the bioturbation is mainly responding to depth and chlorophyll.

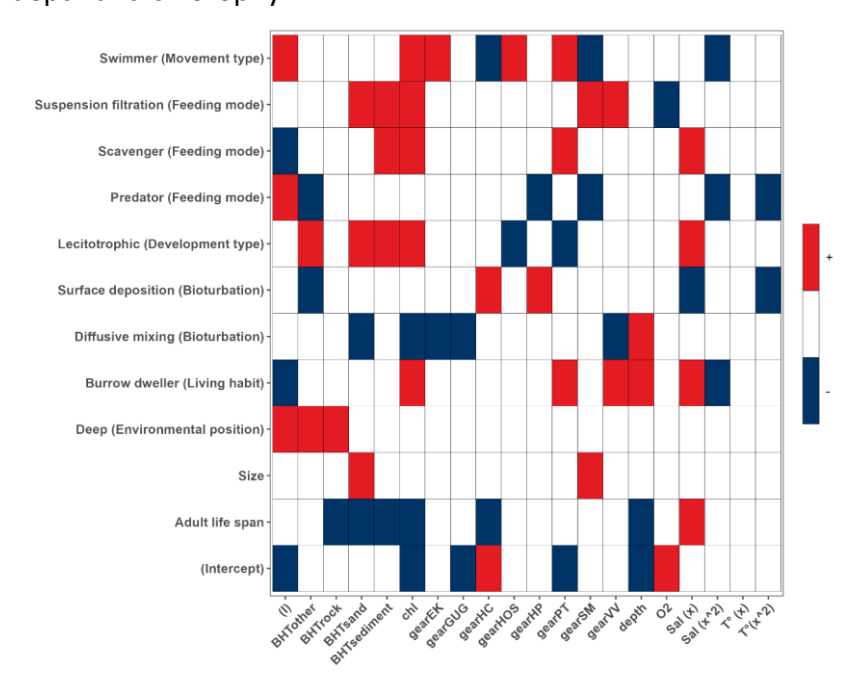


Figure 3.4.4. Heatmap of the estimated gamma coefficients indicating positive, negative or no relationship (red, blue, white respectively) of traits to the model fixed effects with a posterior probability of 0.85.

3.4.5. Patterns and trends in biodiversity

The overall biodiversity patterns and changes predicted from the final models demonstrate a pronounced gradient in species richness with a higher average number of taxa in Kattegat (>25 species), followed by a sharp decline towards the northeast to ~5 taxa on average when entering the Bothnian Sea (>60°N) (Figure 3.4.5). The same gradient is evident for functional richness, with high values in the Kattegat and declining values further east and northward. This general pattern is also visible in terms of functional dispersion, but with relatively higher values in coastal waters also in the eastern and northern areas, such as along the Finnish coast. In contrast to the abovementioned indices, the functional divergence, as well as functional and taxonomic evenness show patterns deviating from the general west to east gradient. More specifically, functional divergence show higher values in the Baltic proper and Gulf of

Finland and moderate to low values in the Kattegat and Bothnian Bay, respectively, while functional dispersion show higher values both in the western part and the coastal areas in the northeastern part around Finland. The latter indicates higher mean functional distances between species in terms of their traits, despite the different number of taxa present in these areas. Lastly, both evenness indicators show pronounced fine-scaled variability, but with generally lower values in the Kattegat, as well as deeper areas in the Baltic proper. In terms of temporal trends in biodiversity indicators throughout the time period, the model predictions show generally increasing slopes in species richness across the region, while functional richness, divergence and dispersion show rather stable, or slight overall increases, respectively. In contrast, both indicators of evenness show a general declining trend throughout the study area, except for the deeper pars of the Baltic proper where trends are showing increasing values.

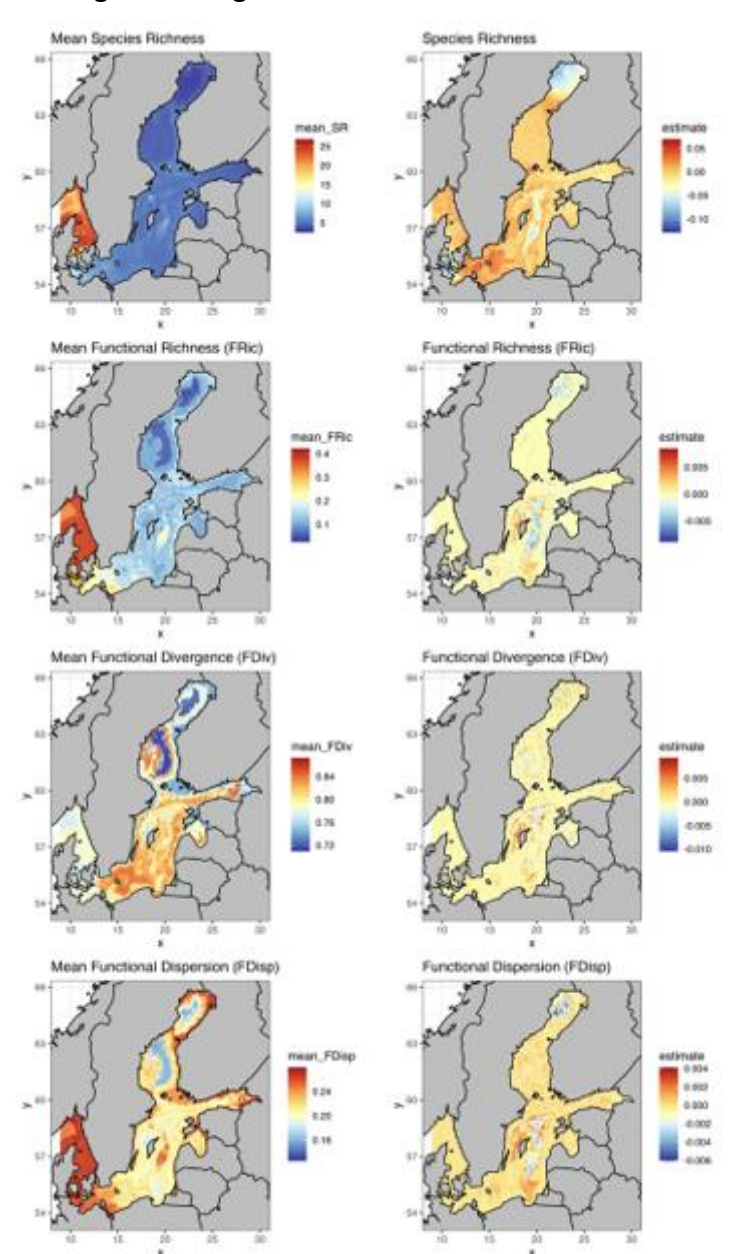


Figure 3.4.5. Mean (left) and linear trend (right) of some taxonomic and functional biodiversity indicators in the Baltic Sea between 1993 and 2020.

3.4.6. Summary

Our model results confirm the importance of environmental filtering channelled through both salinity and oxygen as a primary community assembly process influencing benthic species distributions and community composition by favouring more tolerant generalist species (Törnroos et al., 2015; Gogina et al., 2016; Gogina et al., 2020). More specifically, the significant responses of species to salinity and oxygen are consistent with Remane's tolerance curve for brackish and marine water species (Telesh et al., 2011) and corroborate findings by Diaz & Rosenberg (2008) affirming that highly oxygenated waters support a higher benthic biodiversity. Taken together, our results highlight the importance of multi-factors gradients (Levin et al., 2009), here reflecting both salinity and oxygen in benthos communities distribution and diversity in the Baltic Sea (Bonsdorff, 2006). The lower importance of other variables explaining species distributions, notably temperature, is consistent with previous studies in the area, indicating that the pronounced salinity gradient may mask potential temperature effects (Gogina and Zettler, 2010; Gogina et al., 2020), even if such temperature effects may play a substantial role determining the growth, metabolism and survival of benthic species.

3.4.7. References

Bonsdorff E (2006) Zoobenthic diversity-gradients in the Baltic Sea: Continuous post-glacial succession in a stressed ecosystem. J Exp Mar Biol Ecol 330: 383–391

Brooks SP, Gelman A (1998) General Methods for Monitoring Convergence of Iterative Simulations. J Comput Graph Stat 7: 434–455

Diaz RJ, Rosenberg R (2008) Spreading Dead Zones and Consequences for Marine Ecosystems. Science 321: 926–929

Gogina M, Nygård H, Blomqvist M, Daunys D, Josefson AB, Kotta J, Maximov A, Warzocha J, Yermakov V, Gräwe U, et al (2016) The Baltic Sea scale inventory of benthic faunal communities. ICES J Mar Sci 73: 1196–1213

Gogina M, Zettler ML (2010) Diversity and distribution of benthic macrofauna in the Baltic Sea. J Sea Res 64: 313–321

Huess V, Ringgard I, Korabel V, Spruch L, Lindenthal A (2024) © EU Copernicus Marine Service — Public Ref : CMEMS-BAL-PUM-003-006-007.

Levin LA, Ekau W, Gooday AJ, Jorissen F, Middelburg JJ, Naqvi SWA, Neira C, Rabalais NN, Zhang J (2009) Effects of natural and human-induced hypoxia on coastal benthos. Biogeosciences 6: 2063–2098

Mandrekar JN (2010) Receiver Operating Characteristic Curve in Diagnostic Test Assessment. J Thorac Oncol 5: 1315–1316

Ovaskainen O, Abrego N (2017) Joint Species Distribution Modelling. Camb. Univ. Press

Parmesan C, Yohe G (2003) A globally coherent fingerprint of climate change impacts across natural systems. Nature 421: 37–42

Telesh I, Schubert H, Skarlato S (2011) Revisiting Remane's concept: evidence for high plankton diversity and a protistan species maximum in the horohalinicum of the Baltic Sea. Mar Ecol Prog Ser 421: 1–11

Tikhonov G, Opedal ØH, Abrego N, Lehikoinen A, de Jonge MMJ, Oksanen J, Ovaskainen O (2020) Joint species distribution modelling with the r-package Hmsc. Methods Ecol Evol 11: 442–447

Törnroos A, Bonsdorff E, Bremner J, Blomqvist M, Josefson AB, Garcia C, Warzocha J (2015) Marine benthic ecological functioning over decreasing taxonomic richness. J Sea Res 98: 49–56

3.5 Icelandic fish model

Authors: Francesco Golin, Haseeb Randhawa, Federico Maioli, Martin Lindegren, Julian Burgos, Ingibjörg G. Jónsdóttir

3.5.1. Study area and data availability

The data for this study has been collected through bottom trawling as part of the Icelandic Groundfish Survey (SMB) and the Autumn Groundfish Survey (SMH), both of which are carried out by the Marine and Freshwater Research Institute of Iceland (Figure 3.5.1). The temporal span of the data is 1996 – 2024, while the sampling points span between 62° 12' 50.4" N and 68° 19' 43.2" N in latitude, 31° 32' 12.6" W and 9° 36' 49.8" W in longitude, and 30-1500 m in depth. For this study, only data concerning species belonging to the classes Actinopterygii, Elasmobranchii, Holocephali, Myxinii and Petromyzontii have been considered. The data went through a quality check procedure during which invalid hauls and invalid species records have been removed. Additionally, rare species with less than 10 occurrence records over space (ICES rectangles), time (years), and with less than 1% occurrence in the dataset have been removed (140 species). Pelagic and bathypelagic species (19 in total) were also removed from the analysis, as their lower catchability in bottom trawled gear can lead to the underestimation of their abundance (Walker et al. 2017). The benthopelagic species Clupea harengus, Cyclopterus lumpus and Mallotus villosus were also removed due to possible large geographical variability in abundance given by their mobility. Therefore, the analysis included 82 species found in 25 911 samples (Figure 3.5.1).

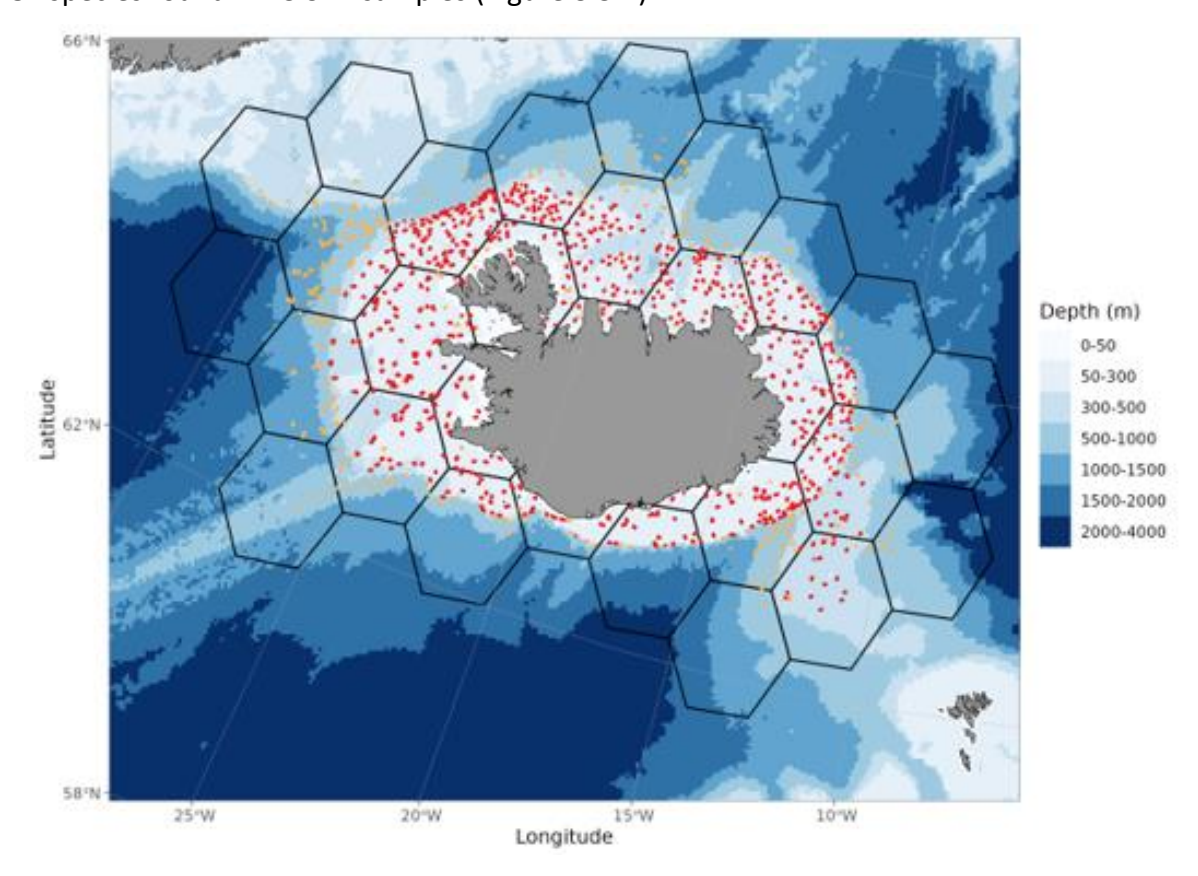


Figure 3.5.1. The location of the sampling points around Iceland, and the grid used as spatial random effect in the models. Red indicates the origin of the samples collected during the SMB, while orange indicates the origin of the samples collected during the SMH.

Species abundance was expressed as kg/km². These estimates of density were calculated using information on the species-specific number of individuals and length distribution found in each sample and the species-specific coefficients of the length-weight relationship available from FishBase (Froese and Pauly 2024). These estimates were then adjusted using coefficients of fishing gear efficiency provided in the Supplementary Information of Walker et al. (2017). To characterize species in terms of their morphology, life history, reproduction and diet (Dencker et al. 2017) we selected 7 ecological traits to be included in the models. Morphology was described by maximum length (m) and the aspect ratio of the caudal fin, which constituted a proxy for mobility. Life history was described by the age of maturity (years) and by the von Bertalanffy growth coefficient (K) (year⁻¹). Life history was described by the age of maturity and by fecundity (number of offspring), while dietary aspects were described by the trophic level. Finally, the position usually occupied in the water column was included as a categorical variable with three levels: demersal, bathydemersal and benthopelagic. Trait information was gathered for each species using available datasets (Beukhof et al. 2019, Thorson et al. 2017) and supplemented with information found in recent literature (Emblemsvåg et al. 2020). If no information could be found for a specific trait, the Genus or Family average was used. Furthermore, to estimate the influence of taxonomically structured traits on species niches, taxonomic information was retrieved from WoRMS (Ahyong et al. 2025) and included in the model.

Information on the physical and biogeochemical environment were sourced from data products by Copernicus Marine (Copernicus Marine Service 2025a and 2025b). These provided monthly averages of sea bottom temperature (SBT) (°C), sea bottom salinity (/10³), chlorophyll a concentration (at surface, mg/m³), dissolved oxygen (mmol/m³), nitrate concentration (at surface, mmol/m³), phosphate concentration (at surface, mmol/m³), silicate concentration (at surface, mmol/m³) and net primary production of biomass (at surface, expressed as mg carbon /m³/day). The annual standard deviation of sea bottom temperature (SD SBT) (°C) was included as a measure of seasonality and stability of the environmental conditions at each sampling location. Information on the site of sampling included depth (m), mean sea bottom slope for a 5km radius around the sampling site (°), and the mean fishing effort by bottom trawling for the year past the month of sampling and a 20 km radius. This was expressed as a ratio between the swept are and the area of a cell, following a methodology akin to the one found in Gerritsen et al. 2013. Data on sea bottom slope was calculated using bathymetric information by the R package marmap (Pante et al. 2023) and the package terra (Hijmans 2025), while data on fishing effort was retrieved from logbook data property of the Icelandic Ministry of Fishery (Fiskistofa 2025). To capture possible variability in occurrence and abundance due to diel migration, time of sampling (expressed as hours from solar noon) was included in the models. The above-mentioned environmental covariates were tested for multicollinearity, and when two variables had a correlation >0.7 or <-0.7, only the one least correlated with the other variables was kept for analysis (Figure S1). The only exception was nitrate concentration, which was excluded to avoid overfitting, since chlorophyll concentration was deemed sufficient to constitute a proxy of primary productivity. Therefore, the set of variables with limited reciprocal correlation were SBT, SD SBT, salinity, chlorophyll concentration, oxygen concentration, depth, mean slope, fishing effort, and time from solar noon.

3.5.2. Model setup, fitting and validation

To model the response of the selected species to the environment, the hierarchical modelling of species community (HMSC) framework was used (Ovaskainen et al. 2017). Due to the zero inflated nature of the data, a hurdle approach was used. This involves producing a presenceabsence model, denominated here as PA model, and an abundance conditional on presence model, the ABU model. The models were fitted using the default priors reported in the Supporting Information of Tikhonov et al. (2020). Four Markov chain Monte Carlo (MCMC) chains were run using the high-performance computing implementation described in Rahman et al. (2024). Each chain collected 250 samples, resulting in a total of 1000 posterior samples. We applied applied a thinning of 250, resulting in 93 750 iterations per chain, of which the first 31 250 were discarded as burn-in. MCMC convergence was evaluated using the potential scale reduction factor (PSRF) (Gelman and Rubin 1992), and it was considered satisfactory when it did not exceed 1.1 (Tikhonov et al. 2020). Three species (Centroscyllium fabricii, Deania calceus, Notacanthus chemnitzii) were removed at this step due to poor chain convergence for many of their parametres, which affected the overall performance of the models. As fixed effects we included SBT, SD SBT, salinity, chlorophyll concentration, depth, mean slope, fishing effort and time from solar noon. Oxygen concentration was ultimately excluded as its parameter estimates suffered from poor convergence. Anyway, it was deemed unlikely that oxygen concentration would have influenced the distribution of the chosen species, as no site had an estimated oxygen concentration close to hypoxic conditions (commonly defined as concentrations lower than 63 mmol/m³) (Rabalais et al., 2002), with the range of available measurements being included between 201 mmol/m³ and 358 mmol/m³. Furthermore, to accommodate non-linear responses in species niches to SBT and depth, quadratic terms were included for both of these variables. Finally, mean slope was logtransformed to stabilize variance and ensure model convergence. In addition to the fixed effects, the models included a spatial and a temporal random effect. The unit of the spatial random effect was constituted by hexagonal grid cells (n = 30) with a distance of 200km between their centres (see Figure 3.5.1). The year of sample collection constituted the unit of the temporal random effect. The random effects were treated independently from each other. The number of latent variables to be produced by the model was limited to a minimum of 1 and a maximum of 5. Latent variables are used in the HMSC framework to estimate the parameters of residual association between pairs of species (Ovaskainen and Abrego 2020). Model performance was evaluated both as explanatory and predictive power through a 5-fold cross-validation. The under the receiver operating characteristic curve (AUC), Tjur's R² and the root mean square error (RMSE) were used to evaluate the performance of the PA model, while R² and RMSE were used to evaluate the performance of the ABU model.

3.5.3. Model diagnostics and performance

The mean PSRF was <1.1 for both the PA and the ABU model, for both the *beta* and the *gamma* parameters. Only a few beta parameters were characterized by a PSRF higher than this threshold – 26 and 2 for the PA and the ABU model respectively, out of a total of 869. The effective sample size (ESS) of the models was close to the real number of posterior samples (1000), thus indicating low probability of samples autocorrelation. Nevertheless, some gamma parameters related to fecundity were characterized by an ESS of 0. Despite these exceptions, the MCMC convergence statistics indicate a good reliability and validity for the majority of the models' estimated parameters. The explanatory power of the PA model had a mean AUC of

0.93, a mean Tjur R² of 0.37 and a mean RMSE of 0.19. The explanatory power of the ABU model had a mean R^2 of 0.28 and an RMSE of 0.84. Regarding predictive power, in only two exceptions – the AUC score of *Phycis blennoides* and the Tjur R² of *Enchelyopus cimbrius* – it outperformed the explanatory power (Figure S4 and Figure S5). In all the other cases the explanatory power outperformed the predictive power, showing no major sign of overfitting.

3.5.4. Species and trait responses to drivers

The variance in species distribution was explained in part by the fixed effects (69% of the explained variance of the PA model, and 60% of the ABU model, on average) and in part by the random effects (31% of the explained variance of the PA model and 39% of the ABU model, on average) (Figure 3.5.2). In both models the most important fixed effect was depth, with 38 and 23 species for which >50% of the explained variance was attributable to this fixed effect in the PA and ABU model respectively (Figure S6). Grid cell identity was instead found to be the most important random effect in both models. Again in both models, SBT was the second most important fixed effect in explaining species distribution, while annual variation in temperature (SD SBT) explained a smaller but relevant portion of explained variance – with peaks of 16% for Centrophorus squamosus and 20% for Rajella fyllae in the PA and ABU model respectively. There were two main differences between the two models in the levels of variance explained by the chosen predictors. The first is the greater influence exerted by drivers related to sea water composition (salinity), seasonality in environmental conditions (SD SBT), time of capture (time from noon), topography of the sampling site (mean slope) productivity (chlorophyll) and exploitation levels (fishing effort by bottom trawling) in determining the abundance of the considered species (Figure 3.5.2). The second is the larger portion of variance explained by the random effects in the ABU model, indicating that unmeasured factors correlated with location and year of sample collection were more influential in determining species abundance than in determining species occurrence.

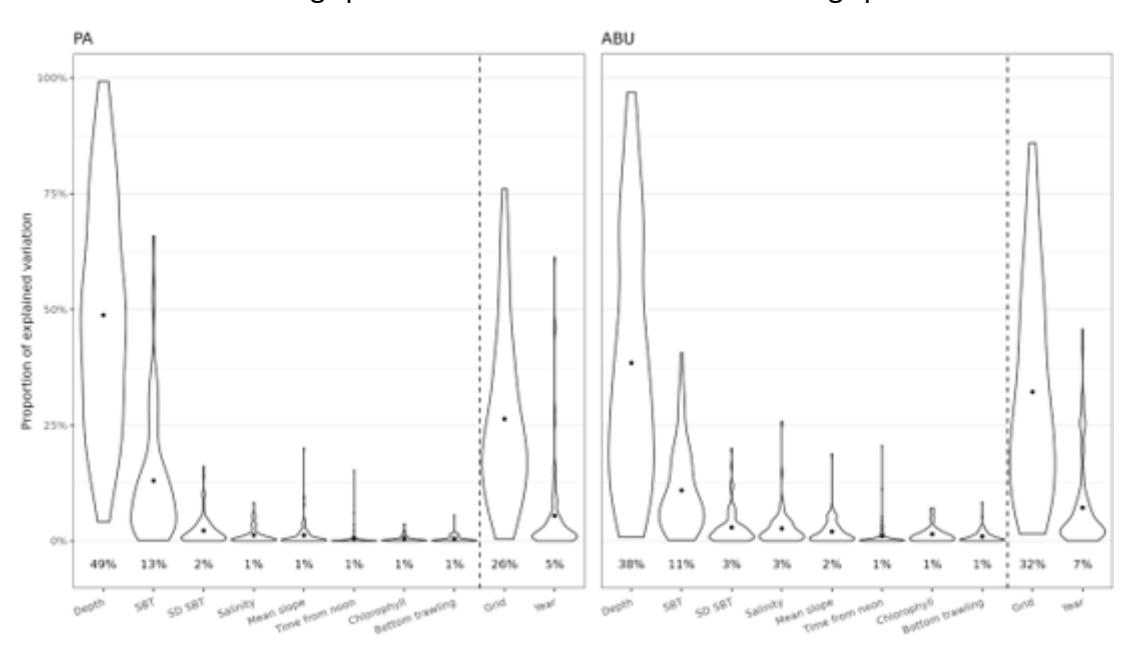


Figure 3.5.2. Proportion of the explained variation attributed to each one of the predictors, across species. The black dot denotes the average explained variation by each predictor (reported at the bottom of each violin plot). The dashed line separates between the fixed effects (to the left) and the random effects (to the right).

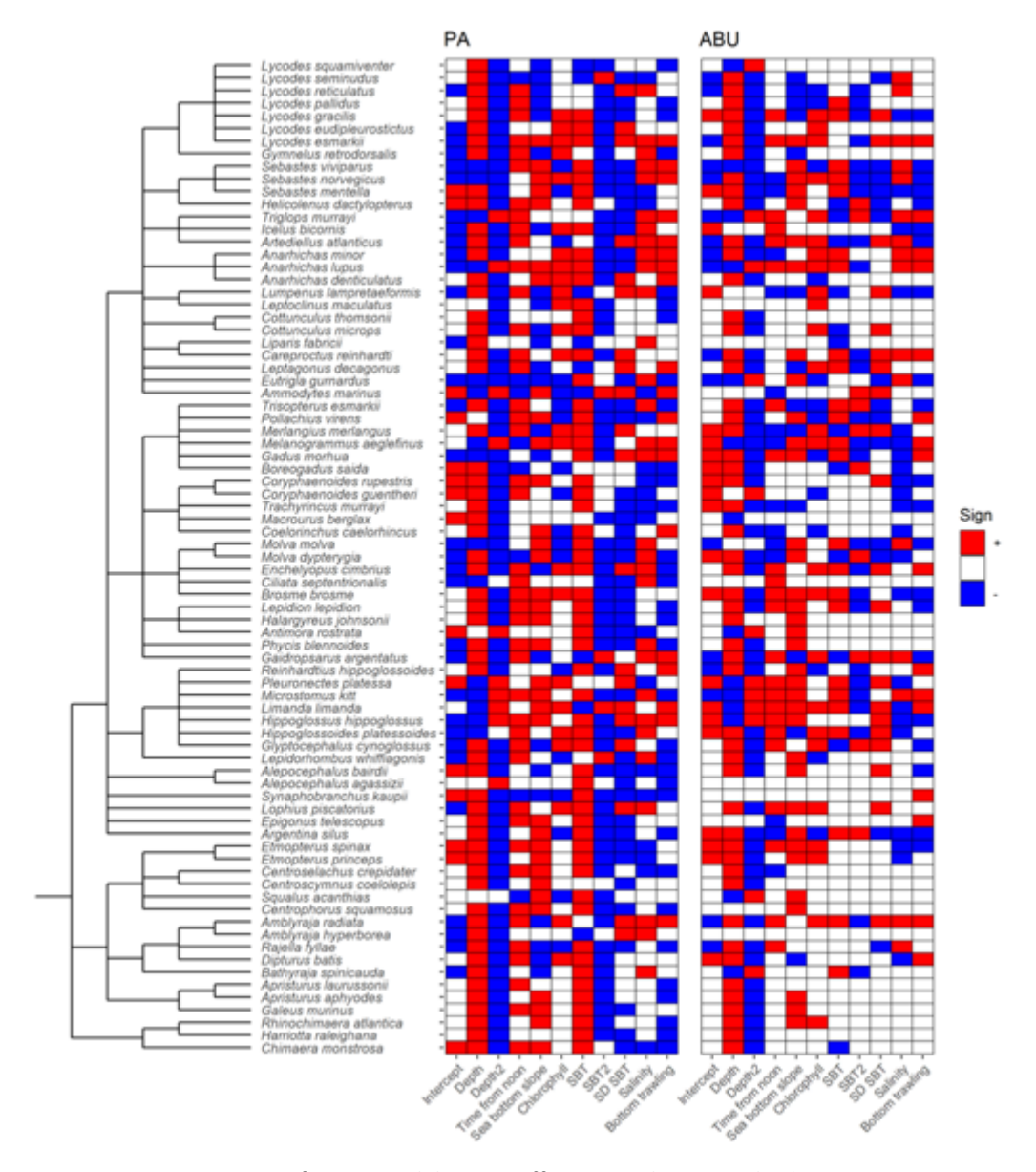


Figure 3.5.3. Heatmap of estimated beta coefficients indicating whether species response to the chosen environmental covariates was negative (blue), positive (red), or not statistically significant (<95% posterior support) (white). The taxonomic tree is displayed, illustrating species' taxonomic relatedness.

The importance of depth in determining both the occurrence and the abundance of most species considered in the study is attested by their response to this variable, with the majority (78 in the PA model and 67 in the ABU model) having a statistically significant response (with a >95% posterior support) with either the linear term Depth, the quadratic term Depth2, or both (Figure 3.5.3). Among these, the probability of occurrence of 58 species (PA model) and the abundance of 51 species (ABU model) were estimated to have a non-linear relationship with depth, with a species-specific optimal depth at which the highest probability of occurrence or abundance was estimated to be found (indicated by a positive 'Depth' term and a negative 'Depth2' term). SBT was also found to be a strong driver of species occurrence, with 76 species having a statistically significant (>95% posterior probability) relationship with the variable, while 50 of these were estimated to have a non-linear relationship with a temperature optimum (Figure 3). Conversely, SBT was found to exert a lesser influence on species abundance, with a smaller – but still prevailing – number of species (40) having a

statistically significant response to either the SBT term, the SBT2 term, or both (Figure 3.5.3). Among these, the trend of abundance of 21 of these were characterized by an SBT optimum (Figure 3.5.3). Concerning SD SBT, the majority of species (42) showed a decreasing probability of occurrence (PA model) with increasing annual temperature excursion, indicating a preference for most species to be found in areas where thermal excursions are limited. In the ABU model instead, overall species response to SD SBT appears to be weaker, with the majority of species (44) having no statistically significant response to the variable (Figure 3.5.3). Concerning traits, we found that 17.7% of the total variance in probability of occurrence (PA model) and 4.4% of the total variance in abundance (ABU model) was attributable to the ones included in the analysis. Only a few statistically significant responses (>95% posterior probability) to the included environmental variables were estimated (Figure 3.5.4); nonetheless, 5 and 4 traits (out of 9) had at least one significant relationship with any of the covariates, in the PA and ABU model respectively (Figure 3.5.4). We found a strong support for niche conservatism, with the taxonomic correlation parameter (rho) being 0.81 (95% credible interval: 0.67-0.92) in the PA model and 0.92 (95% credible interval: 0.80-0.99) in the ABU model. This indicates that there is likely a set of taxonomically structured traits beyond the ones included in the models, which are likely to be determining species' response to the environment.

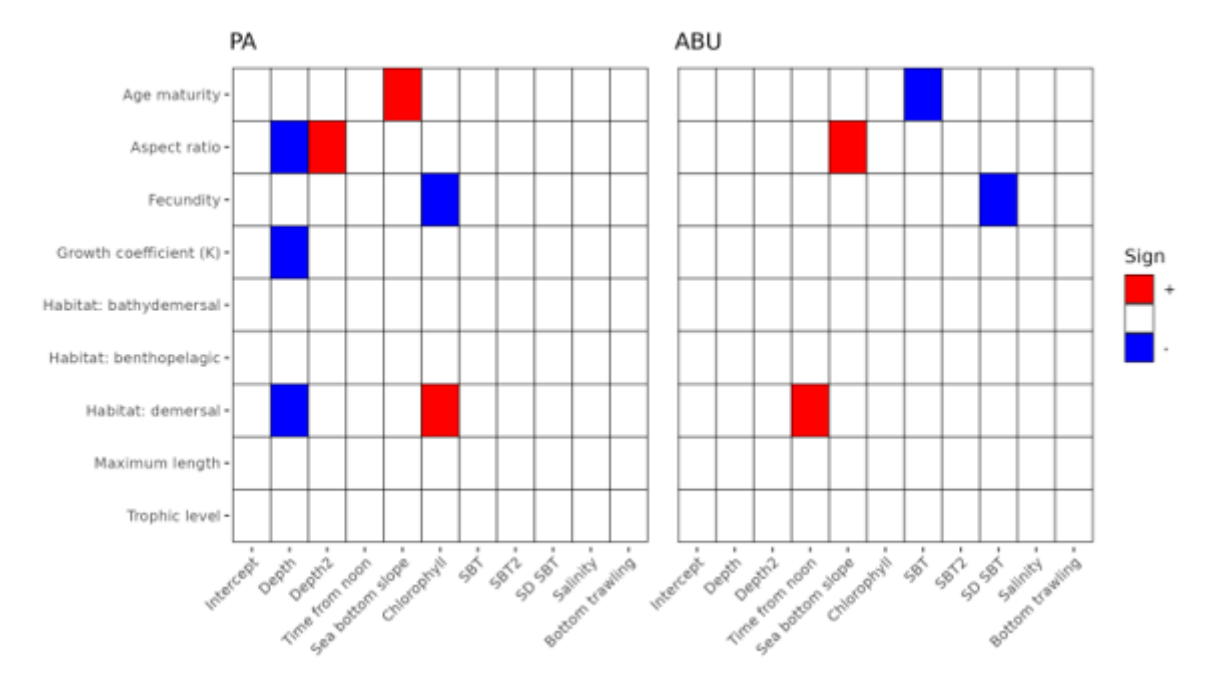


Figure 3.5.4. Heatmap of estimated gamma coefficients indicating whether traits' response to the chosen environmental covariates was negative (blue), positive (red), or not statistically significant (<95% posterior support) (white).

3.5.5. Patterns and trends in biodiversity

The biodiversity indicators estimated from the predictions given by the models for the period 1996-2024 show some spatial and temporal trends in the waters around Iceland (Figure 3.5.5). Different areas can be defined depending on common patterns in the evaluated EBVs, and some contrasting patterns can be identified. The first is the contrast between the northern portion of the study area, coinciding with the deep seabed of the Icelandic sea and the northern section of the Denmark strait, and the southern portion, coinciding with the shelf

break of the Greenlandic and Icelandic shelf in the west-southwest of the study area, the Reykjanes ridge, the shelf break of the Icelandic shelf in the south, and the south-central portion of the Iceland-Faroe ridge. In the north, species richness is particularly low, with a large fraction of the area predicted to not have any of the species considered in this study. In this area, species richness has been stable over time, with only the upper portion of the continental slope and lower portion of the continental shelf showing positive variations in species richness (Figure 3.5.5A).

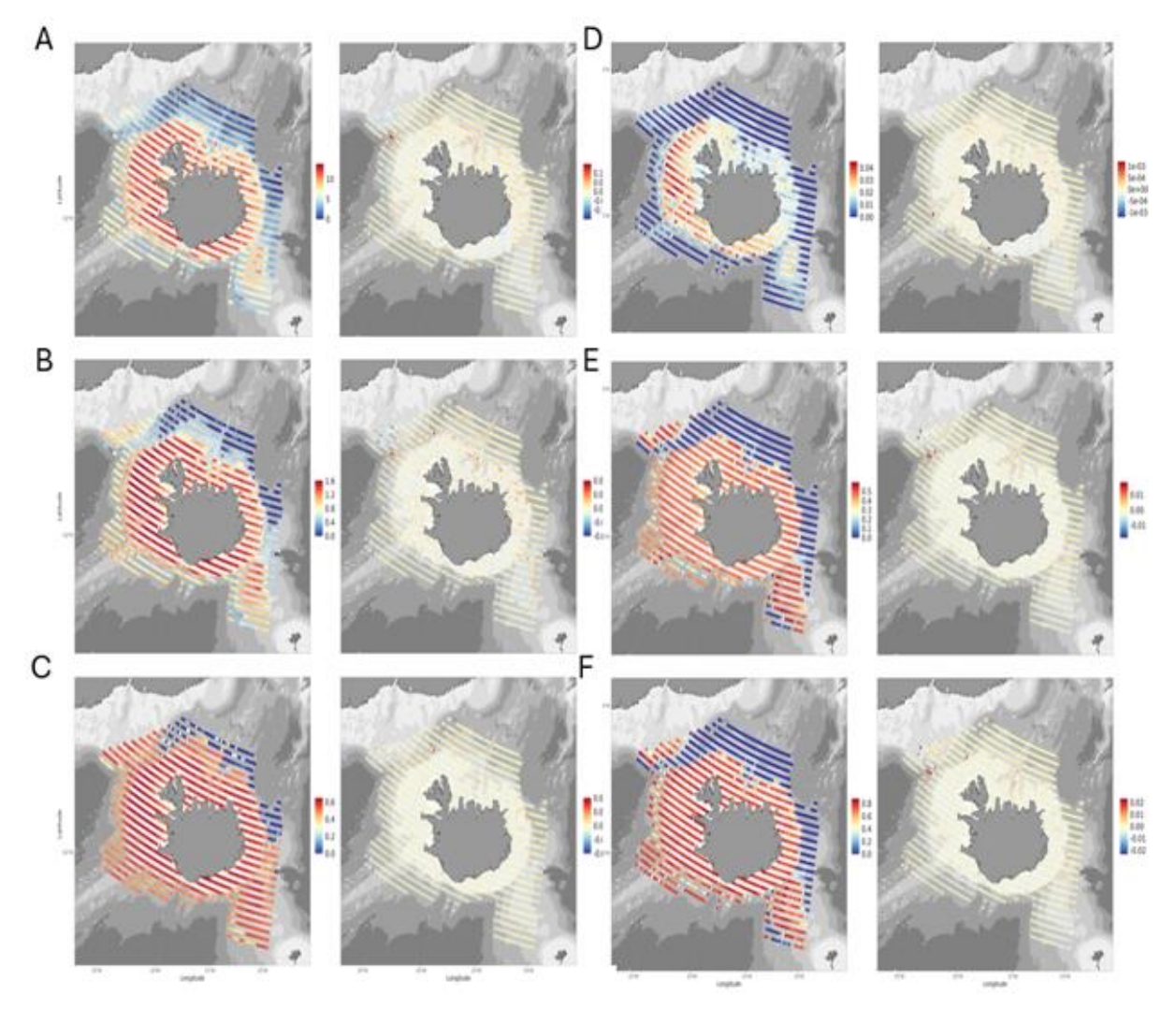


Figure 3.5.5. Patterns and trends in biodiversity indicators illustrated by mean value (left column) and yearly change (right column) in: A) species richness, B) Shannon index, C) species evenness, D) functional richness, E) functional evenness, F) functional dispersion.

Consequently, the Shannon index has been increasing in the same areas, indicating that species' abundance has been getting more evenly distributed (Figure 3.5.5B). However, when adjusted by the number of species (species evenness), no particular trends stand out in the area, with only limited and scattered increases (Figure 3.5.5C). Concerning functional diversity, the area in the north appears to be again characterized by the lowest functional richness of all the study area, and only limited increases in this EBV have been estimated for the lower portion of the coastal shelf (Figure 3.5.5D). Functional evenness and dispersion show a similar pattern, being generally low to very low with small increases in the lower continental shelf or upper continental slope (Figure 3.5.5E and 3.5.5F). In the south instead,

the values in all the EBVs are generally higher than the ones estimated for the north, albeit being lower than the ones found in the Icelandic coastal shelf (Figure 3.5.5A-F). In this area, only in a few locations the EBVs are estimated to increase in value, but in general they remained stable or underwent decreases during the study period (Figure 3.5.5A-F). For instance, for the southwestern portion of the Icelandic shelf break and the south-central portion of the Iceland-Faroe ridge decreases in species richness and in Shannon diversity were calculated, whereas the estimated values of every calculated EBV has been decreasing in the deeper portion of the Greenlandic coastal shelf (Figure 3.5.5A-F). Another contrast can be found between the north-northeast portion of the Icelandic coastal shelf versus the southsouthwest portion. In the south, the highest values of species and functional richness for the entirety of the study area can be found (Figure 3.5.5A and 3.5.5D). Also the Shannon index and species evenness values estimated for the area are the highest, even though they tend to be similar to the ones found in the north (Figure 3.5.5B and 3.5.5C). On the other hand, functional evenness and dispersion seem to be relatively homogeneous throughout the coastal shelf of Iceland (Figure 3.5.5E and 3.5.5F). Despite the lower values in species and functional richness, in the Shannon index and in species evenness, the EBVs in the northern portion show a more homogeneous increase in value, whereas in the southern portion the increase in EBV value was estimated to be more scattered – except for species evenness, which has been predicted to remain relatively stable or with limited increases through time (3.5.5A-D). Following the same trend, small increases in functional evenness and dispersion values have been predicted for the northern portion (3.5.5E-F). The differences in EBV patterns between the north and the south of the study area, in shallow water (coastal shelf) and deep water (shelf break and continental slope) alike, can probably be explained by the different community composition that distinguishes the north of the study area. Marine fish assemblages in the north of Iceland are known to possess a larger proportion of Arctic species than the assemblages found in the south (Mecklenburg et al., 2011). Arctic assemblages are generally characterized by lower species richness and functional diversity (Planque et al. 2014). This could explain the lower overall diversity found in the north, and the general increase in EBV values estimated for the area - possibly a result of the increase in temperatures reported for the area (Campana et al. 2020, Valdimarsson 2012, Sólmundsson et al. 2010, Sólmundsson et al. 2025), which can lead to the establishment and increase in abundance of Boreal and Atlantic species (Sólmundsson et al. 2025, Valdimarsson et al. 2012). Aside for this north-south main difference, some subareas show different patterns in EBV than the surroundings. For instance, species and functional richness have been estimated to decrease in the southeastern portion of the Icelandic coastal shelf, marking a spot of diversity loss in that area (3.5.5A and 3.5.5D).

3.5.6. Summary

Our models indicate the importance of depth and sea bottom temperature (SBT) in determining the distribution of the groundfish species that are found in the seas surrounding Iceland down to 1500 m of depth and that have been considered for the study. On average, depth explained the largest proportion of variance of all the selected predictors, and most species were estimated to possess a depth optimum at which the highest probability of their occurrence, or highest abundance, is to be found. Temperature was the second-most important predictor in determining species distribution, and again temperature optima were identified in the trends of probability of occurrence of most species. Furthermore, the

probability of occurrence for the majority of the considered species was found to be inversely related to the annual thermal excursion (SD SBT), indicating a general preference for smaller seasonal variability. Overall, these observations indicate that species distribution is likely to undergo changes with changes in sea bottom temperature, but that species distribution is unlikely to shift towards deeper waters due to a preference for a specific depth. Therefore, the range of marine groundfish species found around Iceland are likely shift horizontally, rather than vertically, with climate change. Localized changes in values of the calculated EBVs (species richness, Shannon index, species evenness, and functional richness, evenness and divergence) for the study period (1996-2024) might be an indication of this ongoing phenomenon, as changes in sea bottom temperatures have already been reported for the waters surrounding Iceland (Campana 2020, Sólmundsson 2025). These climate-induced shifts can, in the long run, alter patterns in biodiversity found across groundfish communities, possibly by reducing the north-south difference in EBVs reported in this study.

3.5.6. References

Ahyong, S., Boyko, C. B., Bernot, J., Brandão, S. N., ... Zullini, A. (2025). World Register of Marine Species (WoRMS).

Beukhof, E., Dencker, T.S., Palomares, M.L.D., Maureaud, A., 2019. A trait collection of marine fish species from North Atlantic and Northeast Pacific continental shelf seas. https://doi.org/10.1594/PANGAEA.900866

Campana, S.E., Stefánsdóttir, R.B., Jakobsdóttir, K., Sólmundsson, J., 2020. Shifting fish distributions in warming sub-Arctic oceans. Scientific Reports 10, 16448. https://doi.org/10.1038/s41598-020-73444-y

Copernicus Marine Service, 2025a. Global Ocean Physics Reanalysis. https://doi.org/10.48670/moi-00021

Copernicus Marine Service, 2025b. Global Ocean Biogeochemistry Hindcast. https://doi.org/10.48670/moi-00019

Dencker, T.S., Pecuchet, L., Beukhof, E., Richardson, K., Payne, M.R., Lindegren, M., 2017. Temporal and spatial differences between taxonomic and trait biodiversity in a large marine ecosystem: Causes and consequences. PLOS ONE 12, e0189731.

Emblemsvåg, M., Núñez-Riboni, I., HT, C., Nogueira, A., Gundersen, A., Primicerio, R., 2020. Increasing temperatures, diversity loss and reorganization of deep-sea fish communities east of Greenland. Marine Ecology Progress Series 654, 127–141.

Fiskistofa [WWW Document], 2025. . islands.is. URL https://island.is/s/directorate-of-fisheries

Froese, R., Pauly, D., 2024. FishBase [WWW Document]. URL www.fishbase.org

Gelman, A., Rubin, D.B., 1992. Inference from Iterative Simulation Using Multiple Sequences. Statistical Science 7, 457–472. https://doi.org/10.1214/ss/1177011136

Gerritsen, H.D., Minto, C., Lordan, C., 2013. How much of the seabed is impacted by mobile fishing gear? Absolute estimates from Vessel Monitoring System (VMS) point data. ICES Journal of Marine Science 70, 523–531. https://doi.org/10.1093/icesjms/fst017

Hijmans, R., 2025. terra: Spatial Data Analysis.

Mecklenburg, C.W., Møller, P.R., Steinke, D., 2011. Biodiversity of arctic marine fishes: taxonomy and zoogeography. Marine Biodiversity 41, 109–140. https://doi.org/10.1007/s12526-010-0070-z

Ovaskainen, O., Abrego, N., 2020. Joint Species Distribution Modelling: With Applications in R, Ecology, Biodiversity and Conservation. Cambridge University Press, Cambridge. https://doi.org/DOI: 10.1017/9781108591720

Ovaskainen, O., Tikhonov, G., Norberg, A., Guillaume Blanchet, F., Duan, L., Dunson, D., Roslin, T., Abrego, N., 2017. How to make more out of community data? A conceptual framework and its implementation as models and software. Ecology Letters 20, 561–576. https://doi.org/10.1111/ele.12757

Pante, E., Simon-Bouhet, B., Irisson, J., 2023. marmap: Import, Plot and Analyze Bathymetric and Topographic Data.

Planque, B., Primicerio, R., Johannesen, E., Dolgov, A., Wiedmann, M.A., Aschan, M., Certain, G., Greenacre, M., 2014. Functional diversity of the Barents Sea fish community. Mar Ecol Prog Ser 495, 205–218. https://doi.org/10.3354/meps10558

Rabalais, N.N., Turner, R.E., Wiseman, W.J., 2002. Gulf of Mexico Hypoxia, A.K.A. "The Dead Zone." Annual Review of Ecology, Evolution, and Systematics. https://doi.org/10.1146/annurev.ecolsys.33.010802.150513

Rahman, A.U., Tikhonov, G., Oksanen, J., Rossi, T., Ovaskainen, O., 2024. Accelerating joint species distribution modelling with Hmsc-HPC by GPU porting. PLoS Comput Biol 20, e1011914. https://doi.org/10.1371/journal.pcbi.1011914

Sólmundsson, J., Jonsson, E., Bjornsson, H., 2010. Phase transition in recruitment and distribution of monkfish (Lophius piscatorius) in Icelandic waters. Marine Biology 157, 295–305. https://doi.org/10.1007/s00227-009-1317-8

Sólmundsson, J., Sigurðsson, Ó.Á., Jónsdóttir, I.G., Jónsson, S., 2025. How different life-history strategies respond to changing environments: a multi-decadal study of groundfish communities. Scientific Reports 15, 20441. https://doi.org/10.1038/s41598-025-02204-7

Thorson, J.T., Munch, S.B., Cope, J.M., Gao, J., 2017. Predicting life history parameters for all fishes worldwide. Ecological Applications 27, 2262–2276. https://doi.org/10.1002/eap.1606

Tikhonov, G., Opedal, Ø.H., Abrego, N., Lehikoinen, A., De Jonge, M.M.J., Oksanen, J., Ovaskainen, O., 2020. Joint species distribution modelling with the R -package H MSC. Methods Ecol Evol 11, 442–447. https://doi.org/10.1111/2041-210X.13345

Valdimarsson, H., Astthorsson, O.S., Palsson, J., 2012. Hydrographic variability in Icelandic waters during recent decades and related changes in distribution of some fish species. ICES Journal of Marine Science 69, 816–825. https://doi.org/10.1038/278097a0

Walker, N.D., Maxwell, D.L., Le Quesne, W.J.F., Jennings, S., 2017. Estimating efficiency of survey and commercial trawl gears from comparisons of catch-ratios. ICES Journal of Marine Science 74, 1448–1457. https://doi.org/10.1093/icesjms/fsw250



3.6 Central-Eastern Mediterranean Sea model

Authors: Walter Zupa, Antonella Consiglio, Matteo Chiarini, Maria Teresa Spedicato

3.6.1. Study area and data availability

Data on the occurrence and abundance of demersal species were obtained from the Mediterranean International Bottom Trawl Survey MEDITS (Bertrand et al., 2002; Spedicato et al., 2019) conducted annually from May to July since 1994, recently under the EU Data Collection Framework (DCF; EU, (EU) 2017/1004). The survey applies a stratified random sampling scheme, with haul allocation proportional to the surface area of 5 depth strata (covering the bathymetrical range from 10m to 800m). The analyses focused on nine Geographical Sub-Areas (GSAs; GFCM, 2009) of the Central and Eastern Mediterranean Sea, specifically: GSA 15 (Malta), GSA 16 (Southern Sicily), GSA 17 (Northern Adriatic Sea), GSA 18 (Southern Adriatic Sea), GSA 19 (Western Ionian Sea), GSA 20 (Eastern Ionian Sea), GSA 22 (Aegean Sea), GSA 23 (Crete), and GSA 25 (Cyprus), as illustrated in Figure 3.6.1. The selected spatial domain covers approximately 378,852 km2 with, on average, about 577 sampling stations per year. The selected temporal range for the analysis spans from 1999 to 2021 to provide comprehensive coverage of environmental drivers used in modeling. Although the MEDITS survey has been conducted regularly on an annual basis, some gaps in temporal continuity occurred in some GSAs, such as GSA 15 and GSA 25, where sampling began in 2005, and some annual gaps between 2009 and 2013 in GSAs 20, 22, and 23. The survey is conducted in each GSA using the GOC 73 trawl gear, which is equipped with a 20 mm stretched mesh codend (Bertrand et al., 2002; Spedicato et al., 2019), allowing for the capture of small-sized individuals. Once onboard, all specimens exceeding 1 cm in size are taxonomically identified, and both their number and total biomass are recorded. This procedure generates a consistent dataset that supports the calculation of standardized abundance indices (expressed as N/km²) across hauls.

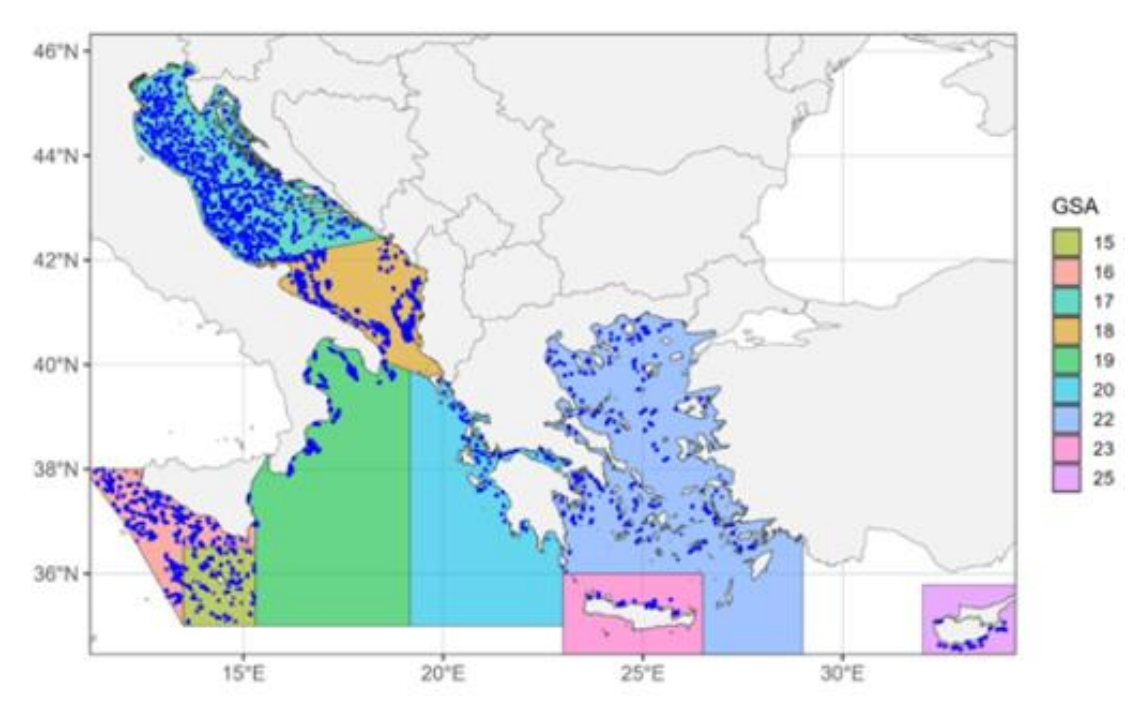


Figure 3.6.1. Position of all unique hauls designed for the MEDITS survey within Adriatic, Ionian, and Eastern Mediterranean Seas (GSAs 15, 16, 17, 18, 19, 20, 22, 23, 25).

To ensure the quality of data used for the analysis, a multiple and comprehensive data validation procedure was applied on MEDITS data using the R package RoME (https://github.com/COISPA/RoME), routinely adopted by the MEDITS coordination group and embedded in the newly developed Med&BS RDBFIS regional database in the Mediterranean (https://medbsrdb.eu/), extensively checked by experts in the QualiTrain EU project (EASME/EMFF/2020/OP/021). This process allows the users to easily identify the presence of inconsistencies in the source data, such as haul position, taxonomic classification, measure units, number of individuals caught, and their relative weights, which could likely affect the results of the modeling analysis. Consequently, data correction procedures were carried out, particularly oriented to address issues linked to the estimation of the sampling positions and of the abundance indices at the species level. To define the species pool used in the HMSC modeling, we calculated the occurrence and frequency of all taxa recorded in the catches of the dataset across all hauls of the geographical domain of the study. Species belonging to fish (A), decapod crustaceans (B), and cephalopods (C) were retained. The initial MEDITS dataset covering the study area comprised a total of 599 taxa, including 371 fish species (of which 321 were teleosts and 50 elasmobranchs) alongside 47 cephalopod species and 181 crustacean taxa. For the main analysis, we selected species with frequency of occurrence > 1%, resulting in a final list of 184 taxa. A subsequent screening based on the availability of trait information led to a further reduction of the dataset, retaining 158 taxa for modeling purposes (120 fish, 18 crustaceans, and 20 cephalopods).

In parallel with the species occurrence and abundance, a comprehensive life-history trait database was developed ad hoc, as reported in the Deliverable D2.2 (https://buseful.eu/library/deliverables/; Spedicato et al., 2024), including 15 different traits (9 continuous and 6 categorical). Trait databases for crustaceans and cephalopods were compiled, drawing primarily from SeaLifeBase (Palomares & Pauly, 2022), while for fish, the trait dataset was assembled mostly based on Beukhof et al. (2019) complemented by FishBase (Froese, 2005), and through phylogenetic imputation using the R package phylosem (Thorson & van der Bijl, 2023). The traits database was finally composed of references for 363 fish taxa, 72 crustaceans, and 62 cephalopods. To characterize the environmental conditions at each sampling location, we extracted a comprehensive set of physical and biogeochemical variables from Marine the Copernicus Environment Monitoring Service (CMEMS) (https://marine.copernicus.eu) using the reanalysis products with a monthly temporal resolution and a spatial resolution of 1/24° (~0.042°). Specifically, we used the product MEDSEA MULTIYEAR PHY 006 004 (Escudier et al., 2021) to retrieve sea surface and bottom temperature (°C) and salinity (PSU), and the product MEDSEA_MULTIYEAR_BGC_006_008 (Cossarini et al., 2021) for surface chlorophyll-a concentration (mg m⁻³), net primary production (mmol N m⁻³ day⁻¹), nitrate (mmol N m⁻³), phosphate (mmol P m⁻³), dissolved oxygen (mmol O₂ m⁻³), and phytoplankton concentration (mmol N m⁻³). In addition, current velocity data were used to derive eastward and northward components of horizontal circulation. Furthermore, seabed substrate classification was retrieved from EMODnet Geology (European Marine Observation and Data network; www.emodnet-geology.eu), using the EUSeaMap 2023 Broad-Scale Predictive Habitat Map for Europe product (Vasquez et al., portal, 2023), whereas bathymetry product tiles (EMODnet Bathymetry http://www.emodnet-bathymetry.eu) were used to retrieve depth information. In addition, other pressure drivers were explored in the models' setup, such as the gravity index (Cinner et al., 2018), the fishing pressure index (FPI) estimated with the application of multi-criteria decision analysis (MCDA) (Kavadas et al., 2015) and the fishing effort information provided by DCF Fisheries Dependent Information (FDI), spatially disaggregated by means of a fishing footprint derived from Global Fishing Watch (GFW). Before the model fitting, collinearity among environmental covariates was assessed using Pearson's correlation matrix (Annex 6, Figure S1). Only predictors with pairwise correlation coefficients below 0.7 were retained as a conservative rule of thumb (Dormann et al., 2013), to minimize redundancy and avoid strong collinearity.

3.6.2. Model setup, fitting and validation

The HMSC framework was employed to model and investigate the drivers and community responses acting on the Mediterranean demersal communities through the R package Hmsc version 3.3-4 (Ovaskainen et al., 2017; Tikhonov et al., 2020). Due to the zero-inflated distribution of the data, a hurdle approach involving two separate models was adopted: a presence-absence model (occurrence) based on a probit distribution combined with an abundance conditional on presence model (abundance model). The abundance models were tested using different distributions, although the normal distribution was retained as it provided the best fitting performance. Two different hurdle models were finally produced: one using the whole time series (WTS), spanning from 1999 to 2021, and another using a shortened time series (2012-2021) that allowed the inclusion of fishing effort (FE) derived from DCF FDI data, spatially disaggregated using the GFW fishing footprint, which was not tested in the WTS models. Each model included both random and fixed effects. The former was selected to account for the spatial and temporal variations (by means of the inclusion of the grid cells and the year effects) not directly incorporated as fixed components. As fixed effects, bottom temperature, bottom salinity, depth, and chlorophyll-a concentration were finally retained in both WTS and FE models. To account for potential non-linear speciesenvironment relationships, for both models, a second-degree polynomial function was applied to depth, for the occurrence sub-models, and extended to all other environmental covariates for the abundance models, except for chlorophyll-a. Chlorophyll-a concentration and fishing effort (for the FE model) were log-transformed to reduce variability and to improve the linearity of their relationship with the species response.

To account for interspecific variation in ecological strategies to environmental variables and reduce computational performance, a set of biologically meaningful traits was selected and incorporated into the models. The retained traits included maximum length, longevity, depth preference, temperature preference, and trophic level, and were applied consistently across taxonomic groups, including fishes, crustaceans, and cephalopods. These traits were selected based on their ecological relevance in structuring demersal communities and mediating responses to external pressure drivers. Maximum body length and longevity are key life-history traits associated with species' reproductive output, population turnover, and sensitivity to exploitation (Hiddink et al., 2019; Quesne & Jennings, 2012). Depth and temperature preferences reflect species' niche and are critical traits determining the spatial distribution (Polo et al., 2025; Stuart-Smith et al., 2015). Trophic level situates species within the food web and is important for understanding predator—prey interactions (Romanuk et al., 2011). Four Markov Chain Monte Carlo (MCMC) chains were run, each drawing 250 posterior samples, for a total of 1000 samples. Thinning intervals were thus adjusted for each model individually to optimise convergence diagnostics, while ensuring computational feasibility,

finally adopting a thinning interval of 2000. To ensure that the chains reached their stationary distribution before posterior sampling, a burn-in phase of 250,000 iterations (transients) was applied. As a result, each chain executed a total of 750,000 iterations (250,000 burn-in + 500,000 sampling), yielding an overall computational effort of 3 million iterations across the four chains. This modeling setup adheres to widely accepted practices in Bayesian inference, where sufficient burn-in and thinning are essential to reduce the impact of initialisation and autocorrelation (Geyer, 2011; Margossian et al., 2023). Convergence of the MCMC was assessed by evaluating the Potential Scale Reduction Factor (PSRF; Gelman & Rubin, 1992) of model parameters, with convergence considered satisfactory when the mean PSRF values do not exceed 1.1 (Tikhonov et al., 2020). Convergence of the MCMC chains was further assessed using the Geweke diagnostic (Geweke, 1992) for each model parameter, and convergence was considered satisfactory when |z| < 1.96. The model performances were evaluated as both explanatory and predictive power through a 4-fold cross-validation. In each fold, the models were trained on 75% of the data and tested on the remaining 25%, iteratively covering the entire dataset. To quantify model performance, a set of complementary metrics was used, tailored to the nature of the models. For the occurrence model the following metrics were used: the area under the operating characteristic curve (AUC) and Tjur's coefficient of discrimination (Tjur R²), a robust measure for binary response models that reflects the difference in predicted probabilities between observed presences and absences (Tjur, 2009). For the abundance (conditional-on-presence) model, the R² was used instead, while in both models the root mean square error (RMSE) was estimated as an indicator of the average deviation between observed and predicted values. All the statistical analyses were conducted in R software version 4.4.1 (R Core Team, 2024). The model runs and the cross-validation were performed on the DRAGO high-performance computing (HPC) cluster hosted by the Consejo Superior de Investigaciones Científicas (CSIC), exploiting the HMSC-HPC implementation using NVIDIA A100 40GB GPUs. For each cross-validation fold and MCMC chain, independent jobs were launched in parallel, allowing efficient scaling of the workload across the cluster.

Based on the models' predictions a set of biodiversity indicators was estimated. Taxonomic richness was assessed as the total number of species present at each site, considering only those species with an occurrence probability equal to or greater than 0.2. This threshold was chosen to avoid excluding rare species that typically exhibit low predicted occurrence probabilities, aligning with other studies that favor more inclusive thresholds (Chou et al., 2020; Linhoss and Mickle, 2022). The Shannon diversity index (H') was calculated using the R package vegan. Pielou's evenness index (J') was computed as the ratio between the Shannon index and the natural logarithm of species richness. To quantify functional diversity, we calculated functional richness (FRic) and functional evenness (FEve) by constructing a multidimensional trait space. This was achieved through a Principal Coordinates Analysis (PCoA) based on Gower distances between species traits (Legendre and Legendre, 1998). These metrics describe the extent to which species occupy the available functional trait space within the community, and the uniformity of biomass distribution across that space (Mouillot et al., 2013). We retained the first three Principal Coordinates (PCs), with a cumulative explained variance of 83%.

Table 3.6.1 Mean explanatory and predictive powers (from a 4-fold cross-validation) for the occurrence and abundance sub-models for the Whole Time Series and Fishing effort models.

		Occurrence			Abundance	
Model		AUC	Tjur R²	RMSE	R ²	RMSE
Whole Time Series	Explanatory power	0.898	0.294	0.239	0.239	1.144
	Predictive power	0.897	0.293	0.241	0.215	1.161
Fishing effort	Explanatory power	0.9	0.309	0.241	0.264	1.111
	Predictive power	0.895	0.303	0.245	0.207	1.151

3.6.3. Model diagnostics and performance

MCMC convergence diagnostics indicated robust convergence for both the occurrence and abundance sub-models, either for both WTS and FE Models (Appendix 4, Fig. S2). Despite the presence of a few outlier values, the overall mean PSRF remained well below the commonly accepted threshold of 1.1, confirming good chain mixing. Effective Sample Size (ESS) values were also consistently high, with mean values exceeding 995 for all parameter groups, indicating highly efficient sampling and low autocorrelation. These results were further supported by the Geweke diagnostic, with 90.4% and 93.2% of the parameters passing the test in the occurrence and abundance sub-models, respectively for the WTS model, and 91.5% and 91.3% respectively, for the FE model. The combination of diagnostics provides strong evidence of reliable posterior estimation. Both the occurrence models showed excellent discriminatory ability, with AUC values close or equal to 0.9 for both explanatory and predictive components, and consistent Tjur's R² and RMSE values (Table 3.6.1). The nearidentical performance metrics between the explanatory and predictive assessments further highlight that the cross-validation procedure demonstrated the robustness of the models' predictive capabilities. In particular, the negligible decline in AUC, R², Tjur's R², and RMSE from training to testing supports the idea that the model is generalizable and not overfitted to the dataset. The abundance model exhibited a slightly lower explanatory strength and predictive accuracy in both cases, with only moderate reductions in performance across validation folds.

In the WTS model, variance partitioning (Figure 3.6.2, upper panel) revealed that in the occurrence sub-model, the fixed effect with the highest explanatory power was depth, which accounted on average for 55.1% of the explained variation across species. This was followed by spatial random effects, which contributed 34.1%, and temporal variation with 4.8%. Other environmental covariates such as bottom temperature (3.3%), chlorophyll-a (1.6%), and bottom salinity (1.2%) had limited contribution. On the other side, in the abundance model, explained variance was more evenly distributed. The fixed effect of depth explained 39.6% of the variation, closely followed by spatial random effects (38.7%), while bottom temperature, salinity and chlorophyll-a contributed 6.7%, 5.2% and 2.6% respectively, indicating a more balanced partitioning of ecological drivers compared to the occurrence model (14.5% vs. 6.1%). In the FE model as well (Figure 3.6.2, lower panel), depth was the most influential fixed effect in both abundance (43%) and occurrence (54%) sub-models, followed by cell and year random effects (respectively 36% and 0.6% for the abundance sub-model and 38% and 4% for

the occurrence one). The other environmental covariates had a limited influence, as well as the fishing effort pressure variable, which scored 1% in both sub-models. At faunal group level, depth was consistently the dominant driver of species responses in the abundance sub-model, especially among bony fishes and chondrichthyans, where it explained, on average, more than 39% of the variance, in the WTS model. In contrast, environmental covariates other than depth gained less importance in decapod crustaceans and cephalopods. For example, in crustaceans, bottom temperature and salinity explained on average 9.65% and 9.41% of the variance, respectively, suggesting, anyway, a moderate physiological sensitivity to water mass properties, influencing abundance distribution. Similarly, in cephalopods, with temperature accounting for 8.54% of the explained variance, possibly reflecting their more limited capacity for thermal regulation and stronger environmental dependence. In the occurrence sub-model, however, the influence of depth was markedly dominant across all taxa, and especially in fishes. In some species, such as Serranus hepatus and Trachinus draco, depth alone explained more than 99% of the occurrence variance, indicating an extremely narrow bathymetric niche and strong habitat specificity. These sharp patterns underscore how bathymetry shapes the distributional boundaries of many demersal species, with environmental gradients playing a more nuanced role in determining abundance patterns once presence is established. Similar patterns have been reported accordingly even for the FE model.

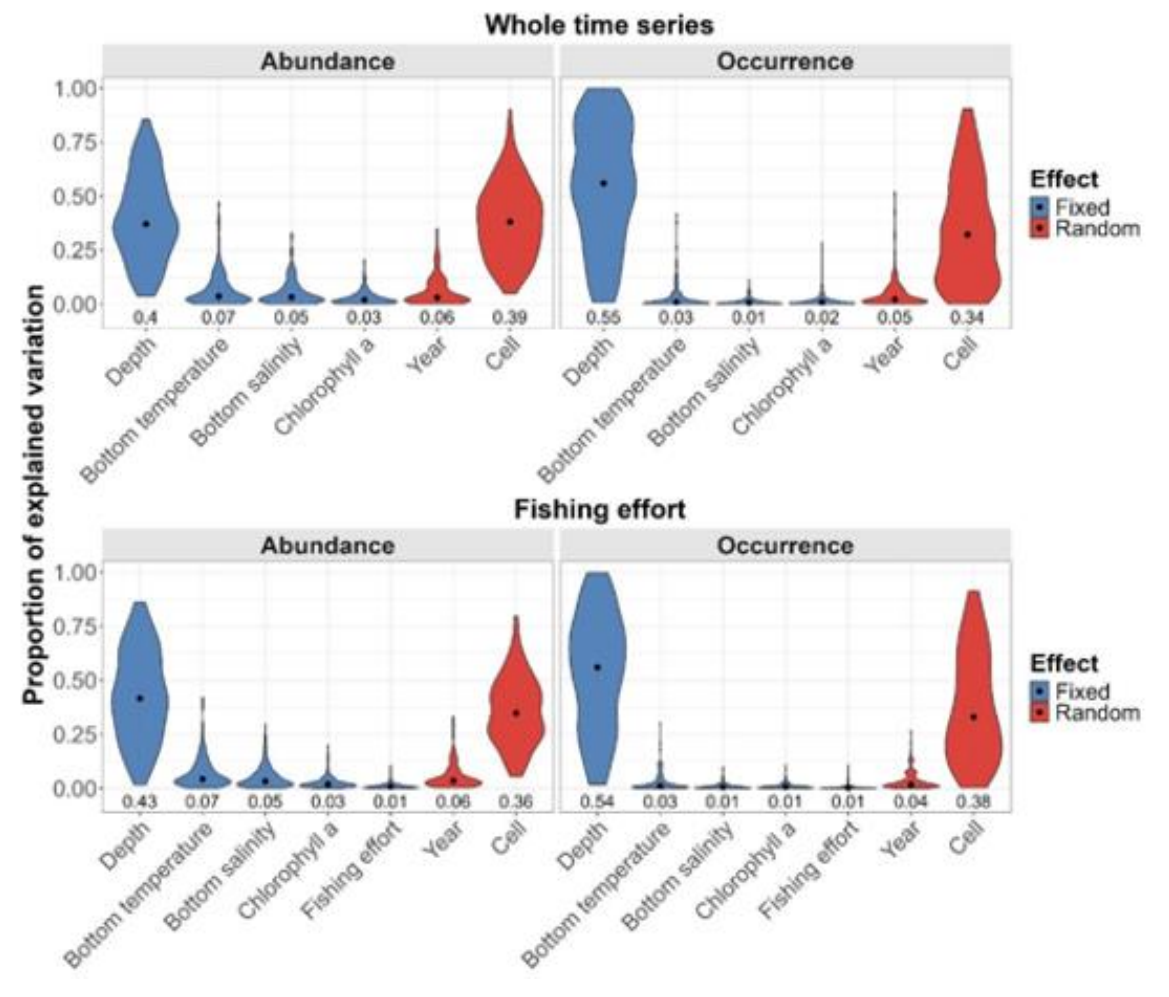


Figure 3.6.2. Variance partitioning of fixed (blue) and random (red) effects for abundance (left) and occurrence (right) for both models (Whole Time Series, upper panel; Fishing Effort, lower panel). The mean value for each violin plot is denoted by a black dot, with the corresponding value indicated on the X axis.

3.6.4. Species and trait responses to drivers

Across the Mediterranean demersal assemblage, the two models drew a coherent picture of how environmental gradients shape taxa distributions and abundances (Fig. 3.6.3). In both cases, depth emerged as the overarching driver. In the WTS occurrence sub-model 78% of taxa reacted significantly to both the linear and the quadratic terms of depth, indicating an overall unimodal curve that peaks at mid-slope depths. Such bell-shaped patterns, evident for species as diverse as Merluccius merluccius and Dipturus oxyrinchus, confirm that most demersal taxa concentrate their realised niches within a constrained bathymetric zone rather than at the extremes of the continental shelf or slope covered by the survey. The remaining environmental predictors affected species occurrence in a less even way. Bottom temperature shoed significant effects in 122 taxa (77 % of the total), but negative coefficients were twice as common as positive ones, suggesting that many taxa could be potentially penalised when temperatures rise above their preferred range. Salinity influenced 112 taxa (71 %), and here, positive and negative effects were almost balanced, suggesting that each group tolerates only a limited salinity range. Chlorophyll-a affected 119 taxa (75 %), and a slight prevalence of negative coefficients suggests decreasing presence towards the more productive coastal zone. When we looked at responses by taxonomic group, clear contrasts emerged: cephalopods were the only group in which positive salinity effects prevailed (≈ 45 % positive vs 10 % negative), whereas negative responses dominated in elasmobranchs and crustaceans (both > 50 %), while bony fishes showed a more balanced pattern (\approx 25 % positive and 19 % negative).

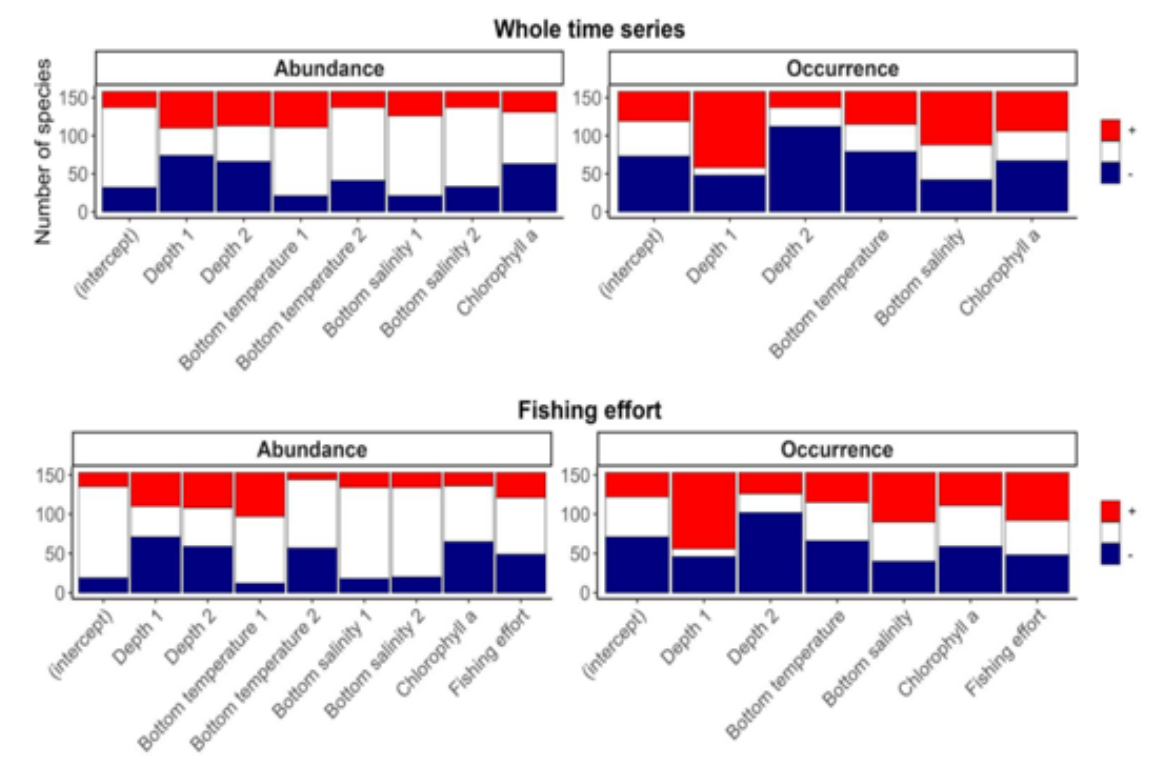


Figure 3.6.3. Number of species with positive (red), negative (blue), or no response (white) to each environmental variable, for the abundance (left) and occurrence (right) environment-only WTS (upper panel) and FE (lower panel) models. Covariates labelled with indices 1 and 2 correspond to the linear and quadratic components, respectively, of the second-order polynomial transformation applied to the variables.

In terms of the abundance sub-model, where each continuous covariate (except the log-transformed chlorophyll-a) was represented by a second-order polynomial, the picture

became more variable. Bell-shaped relationships were detected in 29% of taxa for depth, 25% for bottom temperature, and 20% for salinity, showing that only some taxa adjust their abundance pattern to remain within their ecological optima. The pattern remained, however, taxonomically structured: one half of the cephalopod taxa displayed a unimodal response to bottom temperature, suggesting a tight coupling between abundance and preferred temperature range in this group, whereas two-thirds of crustacean taxa modulated abundance following a bell-shaped pattern with depth, indicating that crustacean taxa show a clear niche preference with bathymetrical distribution. Regarding fishing effort, the occurrence FE model (Fig. 3.6.3, lower panel) indicated that 31% of all taxa responded negatively to this variable, particularly elasmobranchs (76%) and bony fish to a lesser extent (31%). Similarly, the abundance FE model revealed a comparable proportion of negative responses to fishing effort (32%). These results suggest a heterogeneous effect of fishing effort across taxa, with particularly notable impacts on vulnerable species such as elasmobranchs (e.g., Galeus melastomus, Scyliorhinus canicula, Raja clavata, Dipturus oxyrinchus) but also commercially targeted species such as Mullus barbatus and Sardina pilchardus.

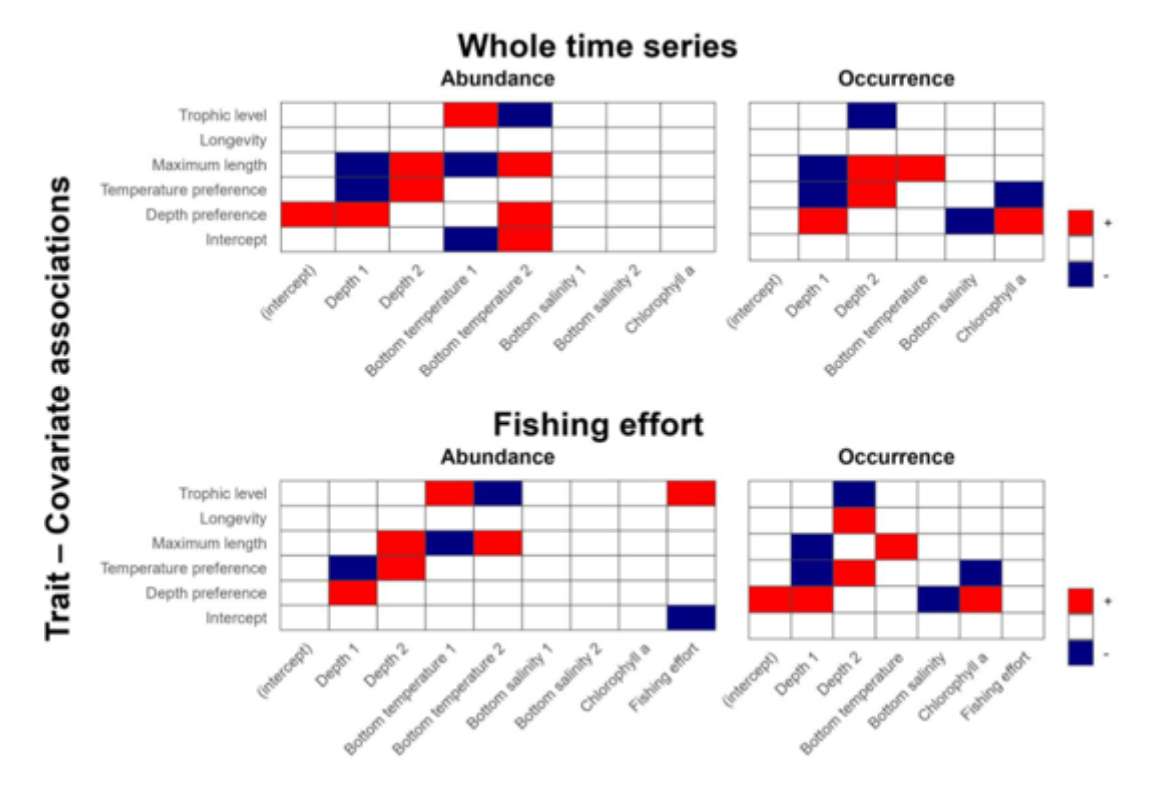


Figure 3.6.4. Heatmap of the estimated γ parameters (posterior probability \geq 0.9) indicating positive (red), negative (blue), or no response (white) of traits to the environmental coefficients. Covariates labelled with indices 1 and 2 correspond to the linear and quadratic components, respectively, of the second-order polynomial transformation applied to the variables.

Other important information is derived from the variance-partitioning analysis conducted on both WTS and FE models. In the WTS model, the analysis (Annex 6, Figure S3, upper panel) showed that species traits explain a substantial share of the differences in how taxa respond to environmental variables. In particular, in the occurrence sub-model, traits explained 55.8 % of the responses to the environmental variables. Most of this was driven by depth (34.0 %), with chlorophyll-a contributing 17.9 %, while temperature and salinity had smaller effects (2.8

% and 1.1 %). The abundance sub-model showed a similar total contribution of traits (55.3 %), but with a different pattern: temperature explained 27.8 %, depth accounted for 18.9 %, salinity for 6.8 %, and chlorophyll-a for 1.9 %. In short, traits explain most of the variation in where taxa occur, primarily through depth, emerging as the first-order gradient structuring demersal fish assemblages, determining multiple abiotic constraints (light attenuation, pressure, substrate and hydrography) (Colloca et al., 2003; Peristeraki et al., 2017) and chlorophyll-a, as an indirect proxy for energy supply (Matek and Ljubešić, 2024), while much of the variation in how abundant they are, mostly through temperature (Crozier and Hutchings, 2014) and depth. Other environmental factors play only a minor role. Additionally, for the FE model (Annex 6, Figure S3, lower panel), species traits explained 3.17% of the variance in the abundance sub-model and 2.32% in the occurrence sub-model for the fishing effort variable, suggesting that traits may mediate species' sensitivity to fishing effort slightly more in terms of abundance than in terms of presence/absence.

The gamma parameters calculated with a support level ≥ 0.9 (Fig. 3.6.4) reveal a concise yet balanced set of responses between traits and environmental coefficients. Ten trait-driver pairs exceeded the 0.9 support threshold in the occurrence sub-model in WTS. Maximum length trait showed a negative relationship with the linear depth term (Depth 1, capturing the monotonic trend) but a positive one with the quadratic term (Depth 2, captures the curvature of the relationship) and the bottom temperature, meaning that larger taxa have relatively lower occurrence at mid-depths (and intermediate temperature as well) and relatively higher occurrence toward either shallow or deep ends of the depth ranges (and temperature as well), according to the species beta parameters. Depth preference was positively linked with linear depth and chlorophyll-a, but negatively with bottom salinity, indicating that taxa preferring deeper habitats tend to have a more positive linear occurrence response along the depth gradient and to respond more positively to higher productivity, while being less frequent in areas with relatively higher bottom salinity. Temperature preference showed a negative association with the linear depth term and chlorophyll-a, but a positive association with the quadratic depth term; consequently, warm-water taxa tend to exhibit depth non-linear responses, with higher occurrence skewed toward shallower waters, and, at the same time comparatively less frequent under higher-productivity (high chl-a) conditions. Thirteen traitdriver associations were detected in the abundance sub-model, providing a more complex picture of the traits' influence on species abundance responses to environmental conditions. The results describe that depth preference mainly shows positive effects on depth (linear component) and bottom temperature (quadratic component). The trophic level predominantly guides the species' response to temperature, following a bell-shaped pattern. On the other side, traits as temperature preference and maximum length were negatively associated with the linear terms of depth and bottom temperature but positively with the corresponding quadratic terms, implying non-linear relationships skewed towards the extremes of both gradients. No other trait-driver combinations exceed the 0.9 support threshold, underscoring that only a subset of ecological traits meaningfully modulates specieslevel responses to the key environmental gradients considered here. Additionally, in the FE occurrence sub-model, no trait-fishing effort associations provided any significant evidence that gamma parameters systematically modulate species' responses to fishing effort over 2012–2021 period. In the abundance sub-model, the mean (intercept-level) effect of fishing effort was negative. However, the positive trait-effort association for trophic level indicates that higher-trophic taxa show weaker declines with increasing effort. Finally, the phylogenetic signal echoed these ecological patterns for both models. Species occurrences were strongly structured (see Annex 4, Table S1), λ indicating that closely related taxa tend to occupy similar portions of the environmental space. Abundances, in contrast, carried a weaker phylogenetic imprint, implying some divergence within groups, allowing congeners to attain markedly different densities even when they co-occur.

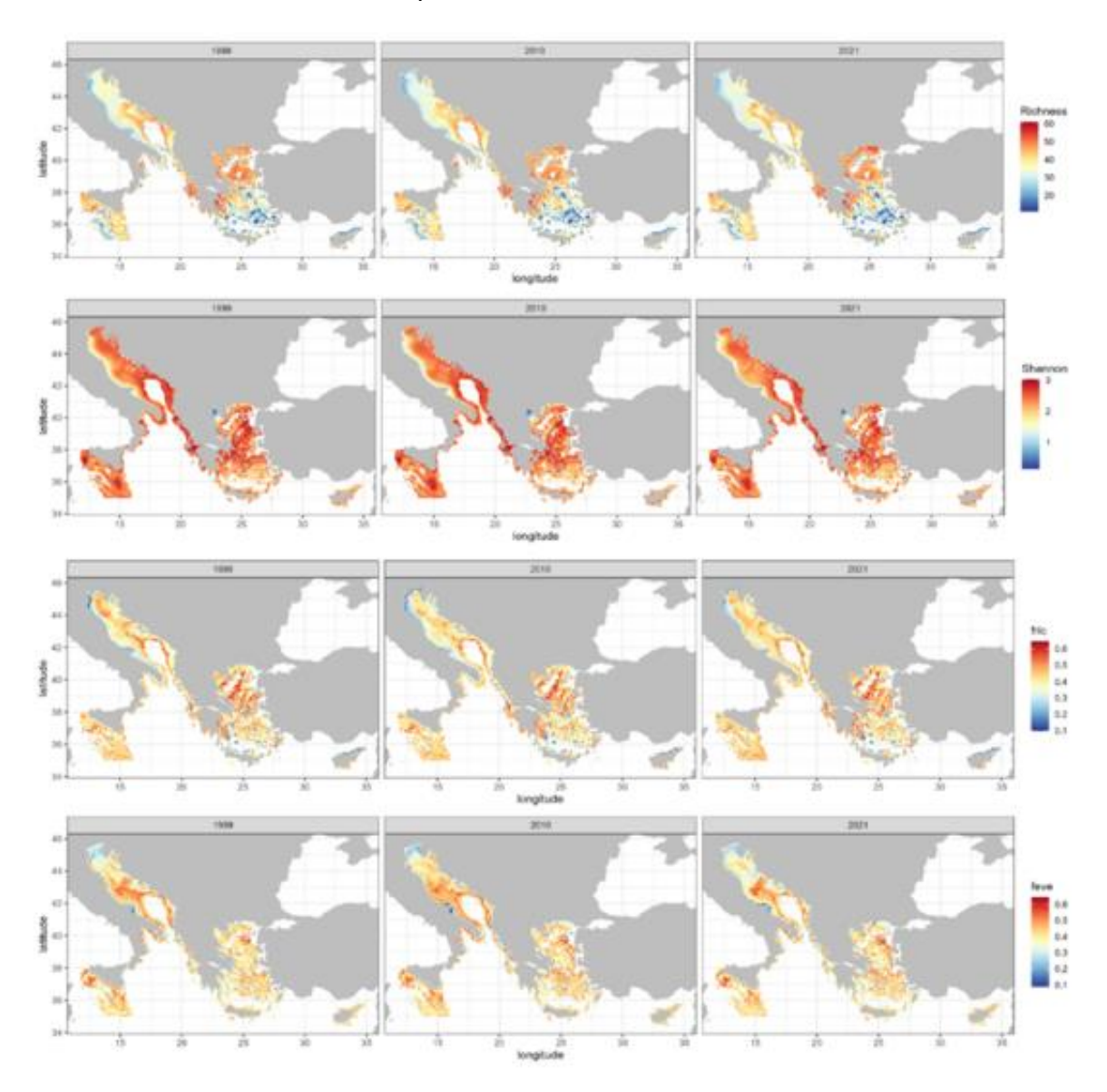


Figure 3.6.5. Spatial patterns of taxonomic and functional biodiversity indicators, including species richness (1st row), Shannon index (2nd row), functional richness (3rd row), and functional evenness (4th row). The indicators are based on model predictions for three selected years: 1999 (left column), 2010 (middle column), and 2021 (right column).

3.6.5. Patterns and trends in biodiversity

The indicators of taxonomic and functional diversity showed a pronounced spatial variability across different areas of the Mediterranean basin (Figure 3.6.5). The depth gradient appears to be the main driver of such a variability, structuring specific spatial patterns across the Mediterranean Sea, especially in relation to the assemblages of demersal and benthopelagic species (e.g. Tecchio et al. 2011; Carlucci et al. 2018). Based on the Species richness and

Shannon diversity indices, biodiversity patterns in the Mediterranean Sea typically peak at 200-400 m depth and decline beyond this range, with different rates for different faunal components (Danovaro et al., 2010; Keller et al., 2016; Tecchio et al., 2011). At these depths, on the slope, the presence of Vulnerable Marine Ecosystems (VMEs) as cold-water coral communities acts as biodiversity refugia for commercially important and protected species (Carbonara et al., 2022; Savini et al., 2014). Concerning the temporal trends observed over the period of 23 years (from 1999 to 2021) of our analysis in the WTS model, a slight decline in all the biodiversity indicators was detected over time. The FE model showed the same patterns and trends, increasing the contrast at the maximum and minimum values of the indicators (Annex 6, Figure S4). In terms of species richness, the highest values were estimated in the Thracian Sea (the northernmost part of the Aegean Sea) and the Myrtoan Sea (located between the Cyclades and Peloponnese peninsula), as well as around the Ionian Islands (east part of the Ionian Sea); relevant values were also found off the eastern coast of Pantelleria Island (south of Sicily), in the southern-eastern part of the Gulf of Taranto (Western Ionian Sea) and along the continental slope of the Southern Adriatic Sea. These values resulted in the deeper fishable strata of the continental slope, approximately between 200 and 400 m depth, consistent with depth-related spatial biodiversity patterns previously observed in the Mediterranean Sea (Keller et al., 2016; Tecchio et al., 2011). These peaks in richness are associated with a mosaic of habitats shaped by complex bathymetry patterns, mass-transport deposits, and local hydrodynamic conditions (Cataudella & Spagnoli, 2011; Savini et al., 2016). These factors contribute to increased habitat heterogeneity, supporting biodiversity at this depth. On the contrary, the lowest values were observed in the Northern Adriatic Sea as well as in the Southern Aegean Sea, and around Cyprus, accordingly to Granger et al. (2015). This is probably linked to the water masses circulation within the areas (Peristeraki et al. 2017).

The diversity of demersal species depicted by the Shannon index showed similar spatiotemporal patterns to species richness with some exceptions: in the northernmost part of the Adriatic Sea as well as around Cyprus and Crete Islands, the Shannon index resulted in medium/high values opposite to the richness ones; on the other side, within the Thermaic Gulf (south of Thessaloniki) this pattern is reversed showing low Shannon index values combined to medium species richness level. This specific pattern is likely related to fishing activities that have impacted species composition over the years in this area, with few commercially important species dominating in shallower waters and non-commercial species prevailing below 200 meters, as is the case in the Aegean Sea (Labropoulou and Papaconstantinou, 2005). The geographic patterns observed in the species richness are even more reflected in the corresponding functional indicator. For instance, the distinct pattern observed between the western and eastern sides of the Adriatic Sea is likely associated with the basin's water-mass circulation, characterized by colder water masses on the western side and an incoming of warmer, saltier waters on the eastern side; such a supply of water masses from the lower Adriatic induces a hyaline and thermal increase with probable consequences on basin productivity and biodiversity (Cataudella and Spagnoli, 2011; Taviani et al., 2015). The highest values of functional richness observed in the study area suggest that a greater number of species is also associated with a more diverse community in terms of species traits, especially within the Adriatic basin and in the Aegean Sea. Regarding the functional evenness estimated by the model, the trend showed a gradual decline of the indicator over time, indicating that current demersal communities (e.g., 2021) have lower resilience and stability in facing external drivers, such as environmental changes and fishing pressure, compared to

the past (e.g., 1999). Indeed, a decline of both diversity and evenness indices has also been noticed in the north-western Ionian Sea over the period from 2012 to 2020 (Maiorano et al., 2022). It is important to highlight that the biodiversity complexity observed in the study area is shaped by the combined, and often synergistic, effects of environmental factors (e.g., climate change) and anthropogenic pressures (e.g., fishing effort), which together influence the capacity of communities to cope with external stressors. Indeed, where natural variability in environmental conditions is high, species may be more resilient to additional stressors, whereas communities in more stable settings tend to be less tolerant and thus more vulnerable to anthropogenic pressures (Dutertre et al., 2013; Jennings and Kaiser, 1998). Consistent with this, high diversity of demersal assemblages in the Mediterranean has been observed in the continental shelves of Sicily and the Aegean Sea, which are associated with reduced bottom trawl fishing effort (Farriols et al., 2019).

3.6.6. Summary

The joint hierarchical modelling of demersal communities conducted across the Central-Eastern Mediterranean Sea over a 23-year period reveals that environmental features play a key role in shaping species distributions and abundance patterns for both WTS and FE models. Model convergence diagnostics confirmed robust posterior estimates, and cross-validation demonstrated strong predictive performance, especially for species occurrence sub-models. Moreover, the abundance sub-models exhibited slightly lower explanatory and predictive power, though they still captured relevant ecological signals, especially when evaluated through trait-environment relationships and variance partitioning. Depth significantly influenced the structuring of demersal assemblages, particularly in terms of species composition, as also demonstrated in previous studies (Carlucci et al., 2018; Evagelopoulos et al., 2021; Valente and Maiorano, 2025). In our case study, depth alone accounted for a significant share of explained variation, particularly in the occurrence sub-models, also influencing trait responses to environmental variables. In contrast, abundance patterns were shaped by additional covariates, particularly temperature and salinity. Similar results were reported by Maioli et al. (2023) in an HMSC analysis of the Adriatic elasmobranch community, where depth emerged as the dominant driver of occurrence, supported by temperature in determining abundance. These findings are consistent with previous studies in the Eastern Mediterranean, which identified temperature and salinity as the primary environmental drivers shaping benthic species distributions under climate change scenarios (Moraitis et al., 2019; Rubino et al., 2024). Although the FE model has a limited time series, it was implemented to provide a direct evaluation of fishing effort effects in modulating biodiversity patterns. Despite a limited overall variance explained by fishing effort (~1% in both FE submodels), significant species-level responses were observed: approximately one-third of the taxa responded negatively to fishing effort, with elasmobranchs and several commercially exploited species being particularly impacted. Taxon-specific patterns and trait—environment relationships in the Mediterranean Sea highlight the crucial role of functional traits, particularly body size, depth preference, and temperature tolerance, in shaping species' ecological responses. Studies indicate that body size often correlates with depth distribution, with medium to large-bodied species dominating at intermediate depths (Moranta et al., 2004).

Across faunal groups, traits such as bathymetric and temperature preferences emerge as defining factors shaping species abundance, with many exhibiting narrow depth niches (Agnetta et al., 2025; Colloca et al., 2003; Givan et al., 2018). Additionally, the FE model showed that traits such as trophic level can contribute in modulating species' sensitivity to fishing pressure. Hence, these traits help explain why certain species are more resilient or vulnerable to environmental change, offering critical insight into biodiversity patterns and ecosystem functioning (Pecuchet et al., 2018). Temporal trends from 1999 to 2021 revealed a subtle but consistent decline in biodiversity indicators, including species richness, Shannon diversity, functional richness, and functional evenness (Albano et al., 2021; Coll et al., 2010). The decrease in functional evenness suggests growing ecological imbalance and reduced resilience in demersal assemblages, likely driven by environmental changes. Functional redundancy in Mediterranean demersal communities is generally low, meaning that declines in evenness may significantly compromise ecosystem stability and recovery capability. This pattern is particularly pronounced in some areas of the Aegean and Ionian Seas and along the Italian Adriatic coast (Tsikopoulou et al., 2021; Valente et al., 2023). The use of biodiversity indices derived from HMSC model outputs, rather than raw survey data, represents another methodological advancement of this study. These model-derived indices help correct sampling bias and improve comparisons of biodiversity patterns across different areas under certain environmental conditions, which can be a very useful base for exploring future forecasting of specific scenarios. These model-derived spatial and temporal patterns observed in both taxonomic and functional diversity provide important ecological baselines that can inform targeted conservation actions, sustainable fisheries management, and effective marine spatial planning in this rapidly changing region. Importantly, these patterns may serve as early-warning signals for ecosystem shifts, emphasising the need for integrative, traitinformed approaches in future biodiversity assessments and policy development.

3.6.7. References

Agnetta, D., Vascotto, I., Panzeri, D., Celić, I., Solidoro, C., Fortibuoni, T., Raicevich, S., & Libralato, S. (2025). Bottom trawling and environmental variables drive the biodiversity of mediterranean demersal assemblages. Scientific Reports, 15(1), 27188.

Albano, P. G., Steger, J., Bošnjak, M., Dunne, B., Guifarro, Z., Turapova, E., Hua, Q., Kaufman, D. S., Rilov, G., & Zuschin, M. (2021). Native biodiversity collapse in the eastern Mediterranean. Proceedings of the Royal Society B, 288(1942), 20202469.

Bertrand JA, Gil de Sola L, Papaconstantinou C, Relini G, Souplet A. (2002). The general specifications of the MEDITS surveys. Sci. mar.;66(S2):9-17. https://scientiamarina.revistas.csic.es/index.php/scientiamarina/article/view/605

Beukhof E., T. S., Dencker, M. L. D., Palomares & A., Maureaud A. (2019) Trait collection of marine fish species from North Atlantic and Northeast Pacific continental shelf seas. PANGAEA https://doi.org/10.1594/PANGAEA.900866

Carbonara, P., Zupa, W., Follesa, M. C., Cau, A., Donnaloia, M., Alfonso, S., Casciaro, L., Spedicato, M. T., & Maiorano, P. (2022). Spatio-temporal distribution of Isidella elongata, a vulnerable marine ecosystem indicator species, in the southern Adriatic Sea. Hydrobiologia, 849(21), 4837–4855.

Carlucci, R., Bandelj, V., Ricci, P., Capezzuto, F., Sion, L., Maiorano, P., Tursi, A., Solidoro, C., & Libralato, S. (2018). Exploring spatio-temporal changes in the demersal and benthopelagic assemblages of the northwestern Ionian Sea (central Mediterranean Sea). Marine Ecology Progress Series, 598, 1–19. https://doi.org/10.3354/meps12613

Cataudella S. & Spagnolo M. (eds), 2011 - The state of Italian marine fisheries and aquaculture. Ministero delle Politiche Agricole, Alimentari e Forestali (MiPAAF), Rome (Italy), 620 p.

Chou, E., Kershaw, F., Maxwell, S. M., Collins, T., Strindberg, S., & Rosenbaum, H. C. (2020). Distribution of breeding humpback whale habitats and overlap with cumulative anthropogenic impacts in the Eastern Tropical Atlantic. Diversity and Distributions, 26(5), 549–564. https://doi.org/10.1111/ddi.13033

Cinner, J. E., Maire, E., Huchery, C., MacNeil, M. A., Graham, N. A. J., Mora, C., McClanahan, T. R., Barnes, M. L., Kittinger, J. N., Hicks, C. C., D'Agata, S., Hoey, A. S., Gurney, G. G., Feary, D. A., Williams, I. D., Kulbicki, M., Vigliola, L., Wantiez, L., Edgar, G. J., ... Mouillot, D. (2018). Gravity of human impacts mediates coral reef conservation gains. Proceedings of the National Academy of Sciences, 115(27).

Coll, M., Piroddi, C., Steenbeek, J., Kaschner, K., Ben Rais Lasram, F., Aguzzi, J., Ballesteros, E., Bianchi, C. N., Corbera, J., Dailianis, T., & others. (2010). The biodiversity of the Mediterranean Sea: estimates, patterns, and threats. PloS One, 5(8), e11842.

Colloca, F., Cardinale, M., Belluscio, A., & Ardizzone, G. (2003). Pattern of distribution and diversity of demersal assemblages in the central Mediterranean Sea. Estuarine, Coastal and Shelf Science, 56(3–4), 469–480. https://doi.org/10.1016/S0272-7714(02)00196-8

Cossarini, G., Feudale, L., Teruzzi, A., Bolzon, G., Coidessa, G., Solidoro, C., Biagio, V. Di, Amadio, C., Lazzari, P., Brosich, A., & Salon, S. (2021). High-Resolution Reanalysis of the Mediterranean Sea Biogeochemistry (1999–2019). Frontiers in Marine Science, 8.

Crozier, L. G., & Hutchings, J. A. (2014). Plastic and evolutionary responses to climate change in fish. Evolutionary Applications, 7(1), 68–87. https://doi.org/10.1111/EVA.12135;CTYPE:STRING:JOURNAL

Danovaro, R., Company, J. B., Corinaldesi, C., D'Onghia, G., Galil, B., Gambi, C., Gooday, A. J., Lampadariou, N., Luna, G. M., Morigi, C., Olu, K., Polymenakou, P., Ramirez-Llodra, E., Sabbatini, A., Sardà, F., Sibuet, M., & Tselepides, A. (2010). Deep-Sea Biodiversity in the Mediterranean Sea: The Known, the Unknown, and the Unknowable. PLoS ONE, 5(8), e11832.

Dormann, C. F., Elith, J., Bacher, S., Buchmann, C., Carl, G., Carré, G., Marquéz, J. R. G., Gruber, B., Lafourcade, B., Leitão, P. J., & others. (2013). Collinearity: a review of methods to deal with it and a simulation study evaluating their performance. Ecography, 36(1), 27–46.

Dutertre, M., Hamon, D., Chevalier, C., & Ehrhold, A. (2013). The use of the relationships between environmental factors and benthic macrofaunal distribution in the establishment of a baseline for coastal management. ICES Journal of Marine Science, 70(2), 294–308.

Escudier, R., Clementi, E., Cipollone, A., Pistoia, J., Drudi, M., Grandi, A., Lyubartsev, V., Lecci, R., Aydogdu, A., Delrosso, D., Omar, M., Masina, S., Coppini, G., & Pinardi, N. (2021). A High Resolution Reanalysis for the Mediterranean Sea. Frontiers in Earth Science, 9.

Evagelopoulos, A., Batjakas, I. E., & Koutsoubas, D. (2021). Structure and Diversity of the Demersal Fish Assemblages off Psara Island (Central Aegean Sea) Caught by Experimental Bottom Trawling. *Thalassas*, *37*(1), 379–391. https://doi.org/10.1007/S41208-020-00277-X/FIGURES/2

Farriols, M. T., Ordines, F., Carbonara, P., Casciaro, L., Lorenzo, M. Di, Esteban, A., Follesa, C., García-Ruiz, C., Isajlovic, I., Jadaud, A., Ligas, A., Manfredi, C., Marceta, B., Peristeraki, P., Vrgoc, N., & Massutí, E. (2019). Spatio-temporal trends in diversity of demersal fish assemblages in the Mediterranean. Scientia Marina, 83(S1), 189–206. https://doi.org/10.3989/scimar.04977.13A

Froese, R. (2005). FishBase. world wide web electronic publication. https://www.fishbase.se

Gelman, A., & Rubin, D. B. (1992). Inference from iterative simulation using multiple sequences. Statistical Science, 7(4), 457–472.

Geweke, J. (1992). Evaluating the accuracy of sampling-based approaches to the calculations of posterior moments. Bayesian Statistics, 4, 641–649.

Geyer, C. J. (2011). "Introduction to markov chain monte carlo." Handbook of markov chain monte carlo : Vol. 20116022(45).

Givan, O., Edelist, D., Sonin, O., & Belmaker, J. (2018). Thermal affinity as the dominant factor changing Mediterranean fish abundances. *Global Change Biology*, *24*(1), e80–e89.

Granger, V., Fromentin, J. M., Bez, N., Relini, G., Meynard, C. N., Gaertner, J. C., Maiorano, P., Garcia Ruiz, C., Follesa, C., Gristina, M., Peristeraki, P., Brind'Amour, A., Carbonara, P., Charilaou, C., Esteban, A., Jadaud, A., Joksimovic, A., Kallianiotis, A., Kolitari, J., ... Mérigot, B. (2015). Large-scale spatio-temporal monitoring highlights hotspots of demersal fish diversity in the Mediterranean Sea. Progress in Oceanography, 130, 65–74. https://doi.org/10.1016/j.pocean.2014.10.002

Hiddink, J. G., Jennings, S., Sciberras, M., Bolam, S. G., Cambiè, G., McConnaughey, R. A., Mazor, T., Hilborn, R., Collie, J. S., Pitcher, C. R., Parma, A. M., Suuronen, P., Kaiser, M. J., & Rijnsdorp, A. D. (2019). Assessing bottom trawling impacts based on the longevity of benthic invertebrates. Journal of Applied Ecology, 56(5), 1075–1084. https://doi.org/10.1111/1365-2664.13278

Jennings, S., & Kaiser, M. J. (1998). The effects of fishing on marine ecosystems. In Advances in marine biology (Vol. 34, pp. 201–352). Elsevier.

Kavadas, S., Maina, I., Damalas, D., Dokos, I., Pantazi, M., & Vassilopoulou, V. (2015). Multi-Criteria Decision Analysis as a tool to extract fishing footprints and estimate fishing pressure: application to small scale coastal fisheries and implications for management in the context of the Maritime Spatial Planning Directive. Mediterranean Marine Science, 16(2), 294. https://doi.org/10.12681/mms.1087

Keller, S., Bartolino, V., Hidalgo, M., Bitetto, I., Casciaro, L., Cuccu, D., Esteban, A., Garcia, C., Garofalo, G., Josephides, M., Jadaud, A., Lefkaditou, E., Maiorano, P., Manfredi, C., Marceta, B., Massutí, E., Micallef, R., Peristeraki, P., Relini, G., ... Quetglas, A. (2016). Large-Scale Spatio-Temporal Patterns of Mediterranean Cephalopod Diversity. PLOS ONE, 11(1), e0146469. https://doi.org/10.1371/journal.pone.0146469

Labropoulou, M., & Papaconstantinou, C. (2005). Effect of fishing on community structure of demersal fish assemblages. Belgian Journal of Zoology, 135(2), 191.

Legendre, P., Legendre, L., & others. (1998). Numerical ecology: developments in environmental modelling. Developments in Environmental Modelling, 20(1), 1–853.

Linhoss, A., & Mickle, P. (2022). A Field Validated Model of Temporal Variability in Oyster Habitat Suitability. Frontiers in Marine Science, 9. https://doi.org/10.3389/fmars.2022.778936

Maioli, F., Weigel, B., Chiarabelli, E., Manfredi, C., Anibaldi, A., Isailović, I., Vrgoč, N., & Casini, M. (2023). Influence of ecological traits on spatio-temporal dynamics of an elasmobranch community in a heavily exploited basin. Scientific Reports, 13(1), 1–14. https://doi.org/10.1038/S41598-023-36038-7
Y;SUBJMETA=158,631,704;KWRD=ECOLOGY

Maiorano, P., Ricci, P., Chimienti, G., Calculli, C., Mastrototaro, F., & D'Onghia, G. (2022). Deep-water species assemblages on the trawlable bottoms of the Central Mediterranean: Changes or not over time? Frontiers in Marine Science, 9. https://doi.org/10.3389/fmars.2022.1007671

Margossian, Gelman, A., & C., C. (2023). For how many iterations should we run Markov chain Monte Carlo? ArXiv Preprint ArXiv:2311.02726. https://doi.org/10.48550/arXiv.2311.02726

Matek, A., & Ljubešić, Z. (2024). Primary production research in the Adriatic Sea-a review. Acta Adriatica, 65(2).

Moraitis, M. L., Valavanis, V. D., & Karakassis, I. (2019). Modelling the effects of climate change on the distribution of benthic indicator species in the Eastern Mediterranean Sea. *Science of the Total Environment*, 667, 16–24. https://doi.org/10.1016/j.scitotenv.2019.02.338

Moranta, J., Palmer, M., Massutí, E., Stefanescu, C., & Morales-Nin, B. (2004). Body fish size tendencies within and among species in the deep-sea of the western Mediterranean. *Scientia Marina*, *68*(S3), 141–152. https://doi.org/10.3989/SCIMAR.2004.68S3141

Mouillot, D., Graham, N. A. J., Villéger, S., Mason, N. W. H., & Bellwood, D. R. (2013). A functional approach reveals community responses to disturbances. Trends in Ecology & Evolution, 28(3), 167–177.

Ovaskainen, O., Tikhonov, G., Norberg, A., Guillaume Blanchet, F., Duan, L., Dunson, D., Roslin, T., & Abrego, N. (2017). How to make more out of community data? A conceptual framework and its implementation as models and software. Ecology Letters, 20(5), 561–576.

Palomares, M. D., & Pauly, D. S. (2022). World Wide Web electronic publication. Version (08/2021).

Pecuchet, L., Reygondeau, G., Cheung, W. W. L., Licandro, P., van Denderen, P. D., Payne, M. R., & Lindegren, M. (2018). Spatial distribution of life-history traits and their response to environmental gradients across multiple marine taxa. Ecosphere, 9(10), e02460.

Peristeraki, P., Tserpes, G., Lampadariou, N., & Stergiou, K. I. (2017). Comparing demersal megafaunal species diversity along the depth gradient within the South Aegean and Cretan Seas (Eastern Mediterranean). PLOS ONE, 12(9), e0184241. https://doi.org/10.1371/JOURNAL.PONE.0184241

Polo, J., López-López, L., Engelhard, G. H., Punzón, A., Hidalgo, M., Rutterford, L. A., Bariáin, M. S., González-Irusta, J. M., Esteban, A., García, E., Vivas, M., & Pecuchet, L. (2025). Trait-Based Indicators of Marine Communities' Sensitivity to Climate Change and Fishing. Diversity and Distributions, 31(1).

Quesne, W. J. F. Le, & Jennings, S. (2012). Predicting species vulnerability with minimal data to support rapid risk assessment of fishing impacts on biodiversity. Journal of Applied Ecology, 49(1), 20–28.

R CoreTeam (2024). R: A Language and Environment for Statistical Computing. R Foundation for Statistical Computing. https://www.R-project.org/

Romanuk, T. N., Hayward, A., & Hutchings, J. A. (2011). Trophic level scales positively with body size in fishes. Global Ecology and Biogeography, 20(2), 231–240.

Rubino, C., Adelfio, G., Abbruzzo, A., Bosch-Belmar, M., Lorenzo, M. di, Fiorentino, F., Gancitano, V., Colloca, F., & Milisenda, G. (2024). Exploring the effects of temperature on demersal fish communities in the Central Mediterranean Sea using INLA-SPDE modeling approach. Environmental and Ecological Statistics, 31(3), 629–647. https://doi.org/10.1007/S10651-024-00609-7/FIGURES/5

Savini, A., Marchese, F., Verdicchio, G., & Vertino, A. (2016). Submarine slide topography and the distribution of vulnerable marine ecosystems: a case study in the Ionian Sea (Eastern Mediterranean). Submarine Mass Movements and Their Consequences: 7th International Symposium, 163–170.

Savini, A., Vertino, A., Marchese, F., Beuck, L., & Freiwald, A. (2014). Mapping cold-water coral habitats at different scales within the Northern Ionian Sea (Central Mediterranean): an assessment of coral coverage and associated vulnerability. PLoS One, 9(1), e87108.

Spedicato, M. T., Massutí, E., Mérigot, B., Tserpes, G., Jadaud, A., & Relini, G. (2019). The medits trawl survey specifications in an ecosystem approach to fishery management. Scientia Marina, 83(S1), 9–20.

Spedicato M. T., Zupa W., Adriana Villamor, Vaishav Soni, Patricia Puerta, Fabien Moullec, Heino Fock, Manuel Hidalgo, Antonio Punzó, Lucia López-López, Bastien Mérigot, Teresa Moura, Sofia Henriques, Paulo Oliveira, Corina Chaves, Rita Vasconcelos, Louise Rutterford, Clement Garcia, Murray Thompson, Georg Engelhard, Esther Beukhof, Laurene Pecuchet, Panagiota Peristeraki, Marcel J.C. Rozemeijer, Ingibjörg G. Jónsdóttir, Lise Cronne, Neil Holdsworth, Martin Lindegren (2024) - B-USEFUL. Report of available metadata and data gaps across case studies. Technical University of Denmark. (https://b-useful.eu/library/deliverables/, accessed September 2025).

Stuart-Smith, R. D., Edgar, G. J., Barrett, N. S., Kininmonth, S. J., & Bates, A. E. (2015). Thermal biases and vulnerability to warming in the world's marine fauna. Nature, 528(7580), 88–92.

Taviani, M., Angeletti, L., Beuck, L., Campiani, E., Canese, S., Foglini, F., Freiwald, A., Montagna, P., & Trincardi, F. (2015). On and off the beaten track: Megafaunal sessile life and Adriatic cascading processes. Mar. Geol, 375.

Tecchio, S., Ramírez-Llodra, E., Sardà, F., & Company, J. B. (2011). Biodiversity of deep-sea demersal megafauna in western and central Mediterranean basins. Scientia Marina, 75(2), 341–350.

Thorson, J. T., & van der Bijl, W. (2023). phylosem: A fast and simple R package for phylogenetic inference and trait imputation using phylogenetic structural equation models. Journal of Evolutionary Biology, 36(10), 1357–1364. https://doi.org/10.1111/jeb.14234

Tikhonov, G., Opedal, Ø. H., Abrego, N., Lehikoinen, A., de Jonge, M. M. J., Oksanen, J., & Ovaskainen, O. (2020). Joint species distribution modelling with the r-package Hmsc. Methods in Ecology and Evolution, 11(3), 442–447. https://doi.org/10.1111/2041-210X.13345

Tjur, T. (2009). Coefficients of determination in logistic regression models—A new proposal: The coefficient of discrimination. The American Statistician, 63(4), 366-372.

Tsikopoulou, I., Dimitriou, P. D., Karakassis, I., Lampadariou, N., Papadopoulou, N., & Smith, C. J. (2021). Temporal Variation in the Ecological Functioning of Benthic Communities After 20 Years in the Eastern Mediterranean. *Frontiers in Marine Science*, *8*, 768051.

Valente, S., Moro, S., Di Lorenzo, M., Milisenda, G., Maiorano, L., & Colloca, F. (2023). Mediterranean fish communities are struggling to adapt to global warming. Evidence from the western coast of Italy. *Marine Environmental Research*, 191, 106176. https://doi.org/10.1016/J.MARENVRES.2023.106176

Vasquez, M., Ségeat, B., Cordingley, A., Tilby, E., Wikström, S., Ehrnsten, E., Hamdani, Z. Al, Agnesi, S., Andersen, M. S., Annunziatellis, A., & Askew, N. (2023). EUSeaMap 2023, A European broad-scale seabed habitat map.

3.7. Western Mediterranean model

Authors: Patricia Puerta, Alicia Gran, Manuel Hidalgo

3.7.1. Study area and data availability

We used annual data of the Mediterranean International Bottom Trawl surveys (MEDITS) from 1999-2021 for the Western Mediterranean sub-basin (Fig. 3.7.1). This region covers from the Strait of Gibraltar to the Strait of Sicily and includes 9 fisheries management areas (i.e., Geographical Sub-Areas, GSA) assessed by the General Fisheries Commission for the Mediterranean (GFCM). MEDITS data collection follows standardized protocols that account for gears, sampling scheme and biological procedures for data collection; details in Spedicato et al. 2019, 2024. A total of 12.666 locations were sampled over 23 years in pre-defined locations following a depth-stratified scheme. This study focuses only on the presence and abundance (individuals · km⁻²) of main demersal macrofaunal species and, therefore we only consider fish (Elasmobranchii and Teleostei), cephalopods (Cephalopoda) and decapod crustaceans (Malacostraca) groups. Additionally, we compile information on different functional traits from FishBase (Froese & Pauly, 2023; Boettinger, 2012), SeaLifeBase (Palomares and Pauly, 2023) and primary literature (see details Spedicato et al. 2024). Continues traits include body length, life span, larval and juvenile development, vertical biological zone, depth range and temperature preferences and diet as categorical traits. For the feasibility of the statistical analyses, we only selected the species that fullfil with the following criteria: i) occurred in at least 1% of the hauls (approximately 200 occurrences) across the complete time series and, ii) information on life-history and ecological traits was available. Final species selection accounts for a total of 191 species, including 146 fish, 24 cephalopods and 21 crustaceans.

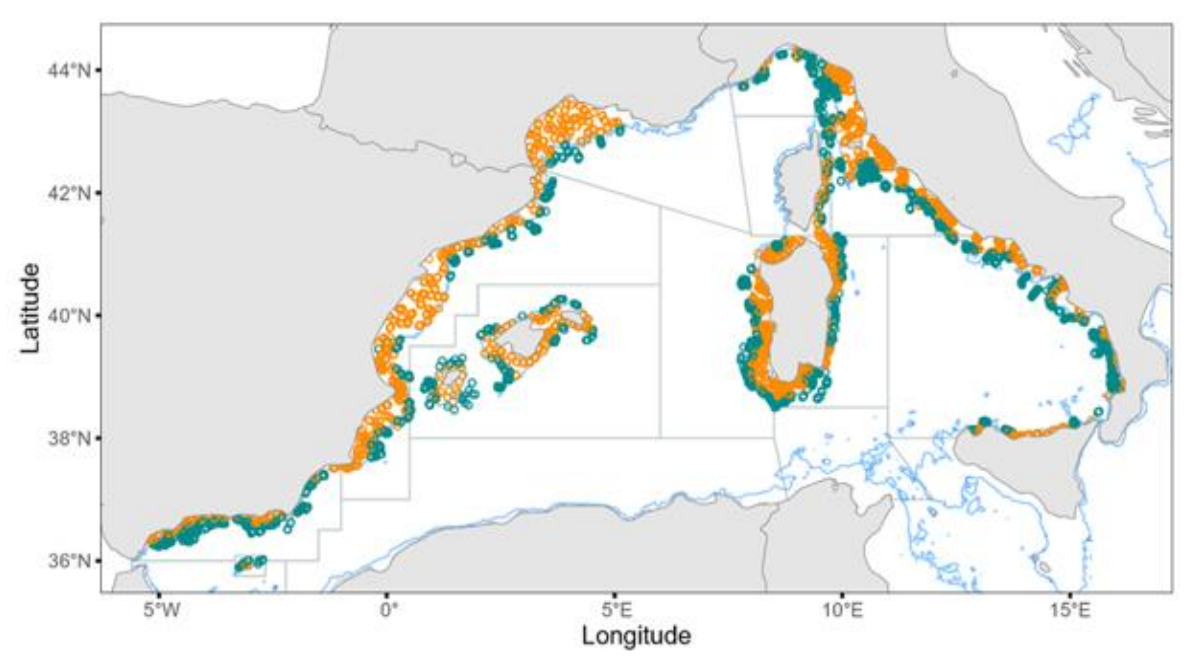


Figure 3.7.1. Position of all unique locations (hauls) of the Mediterranean International Bottom Trawl surveys (MEDITS) from 1999-2021 in the Western Mediterranean. Continental shelf and slope hauls are denoted in orange and green, respectively. The 200m isobath is shown in blue. Geographical Sub-Areas (GSA) assessed by the General Fisheries Commission for the Mediterranean (GFCM) are indicated by gray polygons.

We combined seabed, oceanographic and fishing pressure variables to account for spatial environmental and local anthropogenic impact gradients. The selection of the 6 final variables was based on Pearson correlations <0.65 and Variance Inflation Factor values <3 (VIF, Zuur et al. 2010) to avoid cross-correlation and collinearity, respectively. Main seabed substrate was obtained from the broad-scale seabed habitat map for Europe (EUSeaMap; Vasquez et al. 2023) of the European Marine Observation Data Network (EMODnet), re-scaled to 0.042° grid cell, and simplified to five categories: posidonia (*Posidonia oceanica* meadows), hard-substrate (rock or other hard-substrates), sand, mud and mixed sediment (coarse and mixed sediment). As oceanographic variables, monthly average of surface (SST) and bottom (botTemp) temperatures (°C), surface (so) and bottom (botso) salinity and chlorophyl (Chl) concentration (μ g l⁻¹) were obtained from the Copernicus Marine Service Data at 0.042° hexagonal grid cell (Nigam et al. 2021, Teruzzi et al. 2021). Finally, a fishing pressure index (FPI) to account for trawling, purse-seine and small-scale fisheries footprint was included (Kavada et al. 2015).

3.7.2. Model fitting, validation and predictions

HMSC was used to model demersal communities using the hurdle approach by modeling independently presence-absence (PA model) from abundance data (AB model), using probit and log-linear regression, respectively. Both models used the same setup and parameterization, assuming the default prior distribution, and including as linear fixed effects all the environmental variables (substrate, SST, botTemp, so, botso, chl, FPI). We included second-order polynomial terms for temperature and salinity variables, since many species may display optimum ranges in their environmental niches. The rest of the explanatory variables were assumed to display linear relationship. As random effects, we included the year of the survey and a fixed hexagonal grid of 0.042° as spatial units (N=1121; instead of haul

locations) to reduce the complexity of the spatial structure. Models were fitted independently with the Markov chain Monte Carlo (MCMC) method implemented in 'Hmsc' R-package (Tikhonov et al. 2020). Each of the four MCMC included 250 samples with a thinning of 100 with the first 12.500 discarded as burn in, therefore, running 37.500 iterations and returning 1000 posterior samples in total for each model. Convergence was assessed with the Gelman-Rubin potential scale reduction factor (psrf; Gelman and Rubin 1992). Explanatory power was estimated using root mean square error (RMSE), as well as the area under the curve (AUC; Pearce & Ferrier 2000) and the coefficient of discrimination (Tjur R2; Tjur 2009) values for presence-absence model and, using R² in the abundance model. To compute predictive power, 4-fold cross-validation was performed in each of the models. Final predictions were the product of the two model predictions, as an estimate of species abundance conditioned on presence over the 0.042° spatial grid. Prior computing final predictions, species presence (i.e., threshold between zero and one values) was set using a species-specific threshold that maximize the Percentage of Correct Classification (PCC) using "PresenceAbsence" R package (Manel et al. 2001, Wilson et al. 2004, Freeman and Moisen 2008). Final predictions were used to compute a suite of biodiversity indicators including taxonomic and functional richness, evenness and dispersion.

3.7.3. Model diagnostics and performance

The convergence of PA and AB models was satisfactory as indicated by psfr (mean < 1.1) for beta and gamma parameters, which indicate consistent results among the MCMC simulations. The effective sample size of the MCMC was very close to the number of posterior samples (mean difference < 8%), indicating no autocorrelation in the samples. Explanatory power in the PA model was good (RMSE=0.249, AUC=0.854 and Tjur R²=0.190), while it was slightly lower for the AB model (RMSE=1.176, R²=0.172). However, the explanatory power was much larger for up to 15 species in PA model (e.g., Hymenocephalus italicus, Plesionika martia, Lampanyctus crocodilus; Appendix 5) and 5 in the AB model (e.g., Heptranchias perlo, Dentex maroccanus, D. macrophthalmus), with the corresponding Tjur/R² values> 0.4. As the model includes a spatially structured random effect, its predictive power is based on both the fixed and the random effects, resulting in a predictive power with near-identical or slightly outperformed metrics as for explanatory power. The variance partitioning indicates similar explanatory variables influence species variability in both, PA and AB, models (Fig. 3.7.2), with salinity (i.e., so and botso) and temperature (i.e., SST and botTemp) variables exhibiting the largest influence, accounting for 37.3 and 31.4 % of the total variance explained in the community, respectively, in the PA model and, 29.1 and 28.9 % in the AB model. Most of these explained variability was attributed to the second-order polynomial terms of bottom salinity and bottom temperature. Substrate type showed larger explained variance for AB (11.2%) than PA model (7.6%), while ChI and FPI have more marginal contributions (~7%) in both models. The temporal and spatial random effects had, overall, a small contribution to the explained variance in all cases (Fig. 3.7.2).

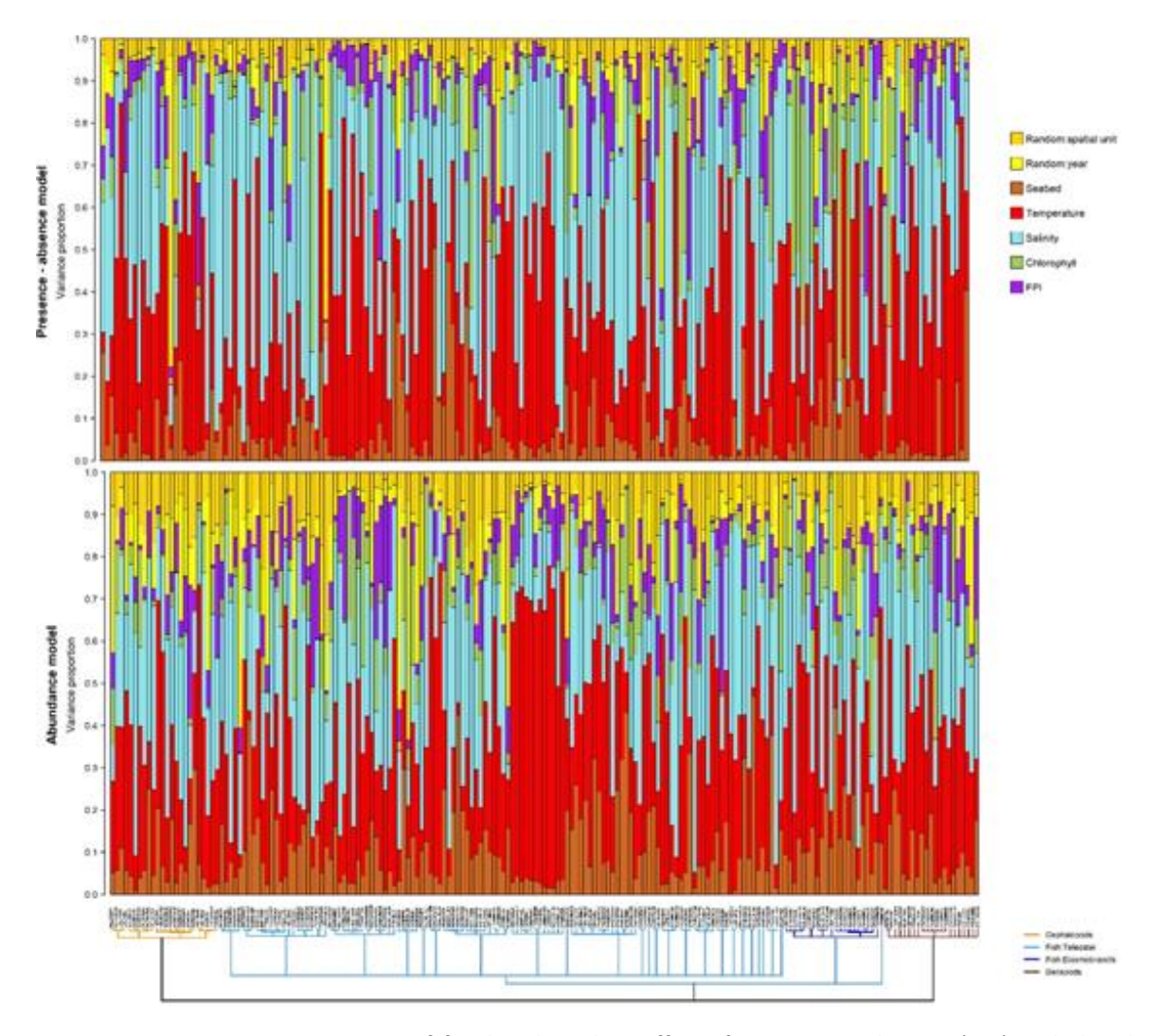


Figure 3.7.2. Variance partitioning of fixed and random effects for presence-absence (top) and abundance (bottom) models and each of the species. Species are ordered phylogenetically as denoted by the phylogenic tree.

Temperature and FPI have larger influence on decapods occurrence (explained variance was double as in the whole community or in the two other groups) and therefore, slightly higher Tjur R²= 0.24 was obtained for this group. By contrast, the variance explained for cephalopods and fish were closer to the community mean value. In the case of AB models, total and partitioning variance values were slightly lower for cephalopods, with substrate and Chl showing lower influence than in the other groups. Interestingly, the influence of temperature and substrate type in the community variability was largely explained by the trait combination (Fig. 3.7.3). Thus, traits explained 80% of the responses to temperature in PA model, while 50% in the AB model. Additionally, up to 55% and 45% of the responses to substrate types in PA and AB model, respectively, can be also attributed to traits.

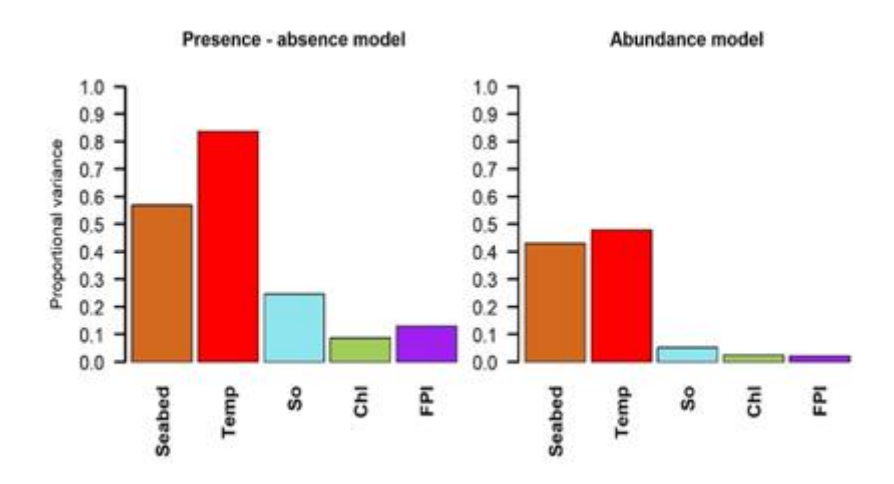


Figure 3.7.3. Percentage of explained variance by grouped covariates attributed to traits combinations in the demersal community.

3.7.4. Species and trait responses to drivers

The responses of species to covariates are in general larger and more widespread (both positive and negative effects) in the PA model than in the AB (Fig. 3.7.4), with negative effects predominating in both. Substrate type, botTemp, so and, to a lesser extent, FPI are the most influential covariates in both models, although their effects are considerably larger and involve more species in the PA model. For instance, bottom temperature showed negative effects in >70% of the Teleostei and Cephalopoda classes in the PA model, whereas in the AB model significant responses to this variable accounted for only about 40% of species when combining both positive and negative effects. Such large negative effect of bottom temperature may indicate a reduction in the habitat suitability due to warming, where demersal species with cold-water preferences may be more sensitive to changes in temperature conditions (Burrows et al. 2019, Sanz-Martin et al. 2024). SST displayed a clear asymmetry in the responses, with linear effect (sst1) mainly associated to positive effects and second polynomial responses (sst2) dominated by negative responses (Fig. 4). This asymmetry was observed in both models (and also in other European regions, see section 3.1), although more pronounced in the AB model. As aforementioned, this reflects the different temperature niches of marine species (e.g., optimum, range, tolerance) associated with the presence of warm- and cold-water species in the demersal communities, and their contrasting responses to warming. Chlorophyll and FPI showed remarkable effects in the AB model compared to the rest of the variables, but in general, they affect a larger number of species in the PA model. However, only a few significant relationships between traits and drivers were found in both models, mainly associated with depth and temperature preferences.

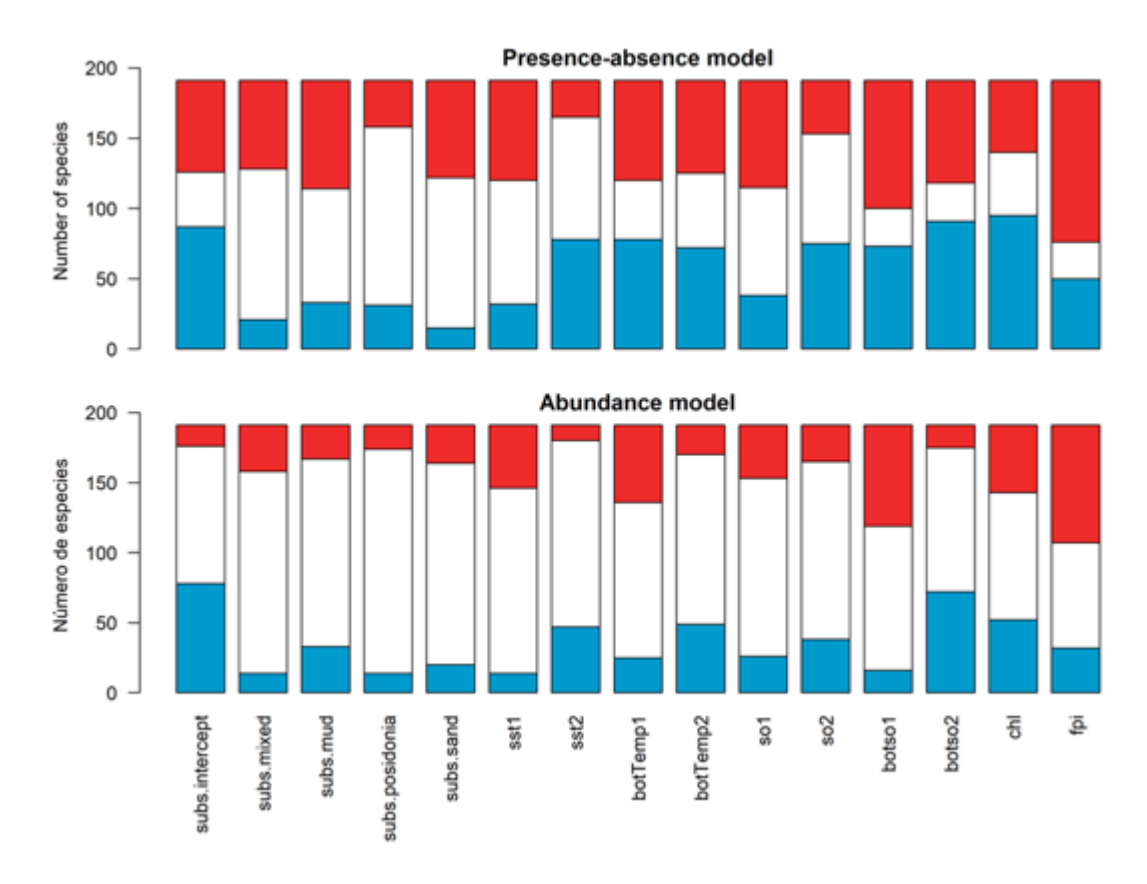


Figure 3.7.4. Number of species with positive (red), negative (blue) or no significant (white) response to each variable included in the model, for the presence-absence (top) and abundance (bottom) models. Note that fixed effect with linear (1) and polynomial (2) effects are displayed independently.

3.7.5. Patterns and trends in biodiversity

From a total of eleven taxonomic (4), functional (3) and multidimensional functional (4) biodiversity indicators calculated, we present the results for those accounting for relevant spatial differences and patterns, including taxonomic richness, functional richness (FD q0), functional Shannon-like index (FD q1), and multidimensional functional evenness (feve), dispersion (fdis) and divergence (fdiv) (Fig. 4; details on indicators can be found in Magneville et al. 2022). Overall, a clear East-West gradient, where values increase, can be observed in most indicators (Fig. 3.7.5). Taxonomic and functional (FD q0) richness and functional Shannon-like (FD q1) displayed similar patterns with larger values in the Alboran Sea and the Balearic Islands, particularly in the slope and deep-water areas. The lower impact of fishing pressure in the Balearic Islands (Colloca et al. 2017) and the transitional role of the Alboran Sea between Atlantic and Mediterranean systems that account for a high species turn-over (Real et al. 2021) are likely to be responsible of the high diversity observed in these regions. Intermediate to high values followed the slopes of the Catalan coast, the Gulf of Lion towards the west of Corsica and Sardinia. In contrast, the Thyrrhenian Sea presented more homogeneous values, with a hot-spot of diversity north of Sicily. Overall, coastal areas with extensive continental shelves such as the Gulf of Valencia, the Gulf of Lions or the Northern Tyrrhenian exhibited the lower diversity values for these indicators. However, the opposite pattern was observed for multifunctional evenness. Functional dispersion highlighted the East-West gradient more strongly, with particular high values observed in the Alboran Sea and the south of the Balearic

Islands. In contrast, functional divergence only showed high values for the Alboran Sea and intermediate ones for the southern Balearic Islands and northern Tyrrhenian coast.

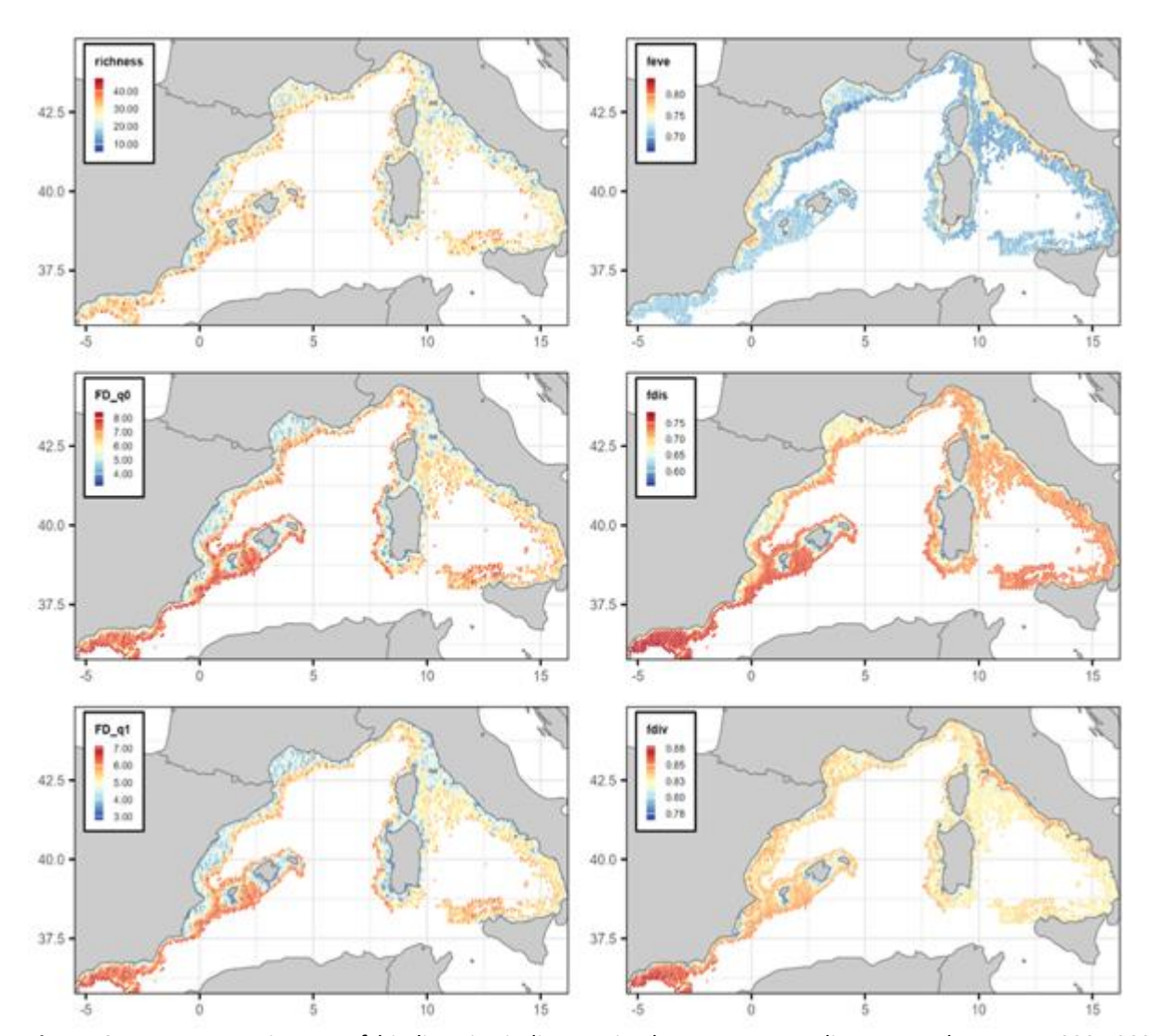


Figure 3.7.5. Mean estimates of biodiversity indicators in the Western Mediterranean between 1999 -2021, including: taxonomic richness (richness), functional richness (FD_q0), functional Shannon-like index (FD_q1), and multidimensional functional evenness (feve), dispersion (fdis) and divergence (fdiv).

Temporal variability in biodiversity indicators across the Western Mediterranean revealed quite steady trends, probably due to the larger spatial heterogeneity. Temporal linear trends for multidimensional functional indicators slightly vary across space, with slopes variability <|0.01|. A notable temporal change was only observed for taxonomic richness and the functional indicators (FD_q0, FD_q1, FD_q2) (Fig. 3.7.6). Significant temporal changes are patchy and disperse in space, but overall, an increase in functional diversity indicators over time occurred more frequently in the continental shelves, while a decrease is observed in the slope and deep-water areas (Fig. 5). In contrast, taxonomic richness did not show any clear pattern.

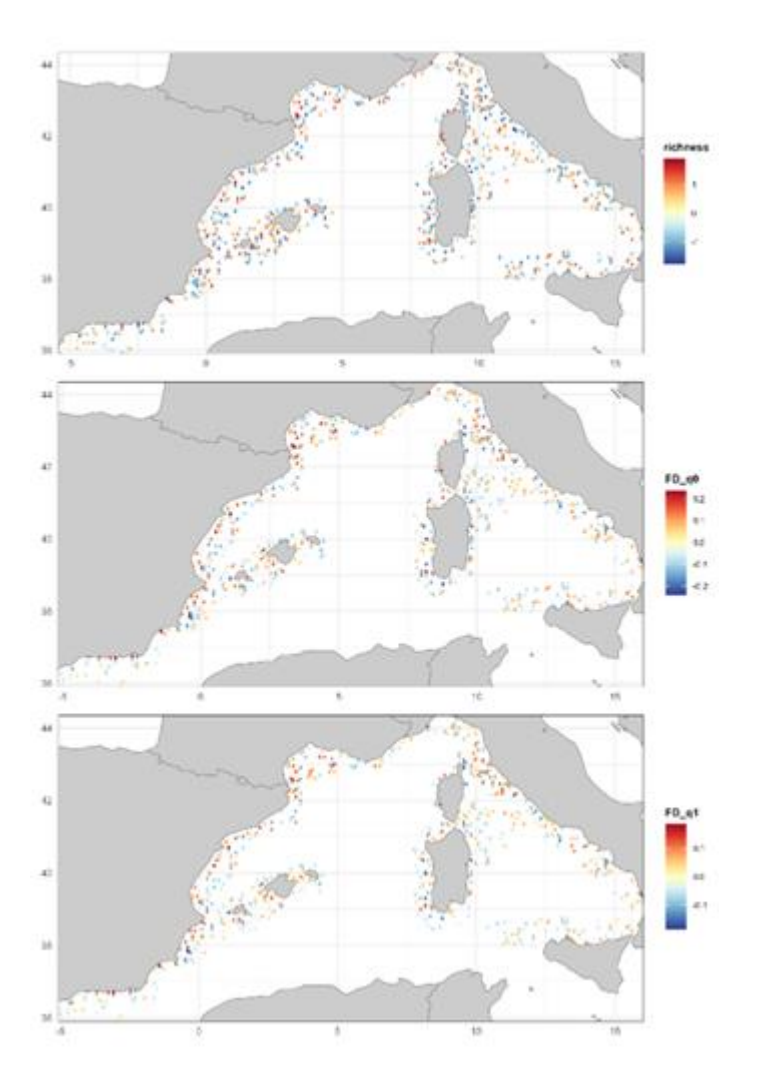


Figure 3.7.6. Temporal trends in biodiversity indicators, showing the linear regression slope of taxonomic richness, functional richness (FD_q0) and functional Shannon-like indicator (FD_q1) for the time period 1999 – 2021.

3.7.6. Summary

The large-scale modelling of demersal communities in the Western Mediterranean showed the importance of environmental variability for the community composition and species distribution, mainly mediated by temperature, salinity and to a lesser extent, substrate type. The role of fishing impact and primary production seems lower. However, the different groups of organisms responded differently to environmental conditions, which may differ from the community average response. Importantly, these responses to main environmental drivers are largely mediated by traits, reflecting the long-term adaptation to different environmental niches. Regarding biodiversity patterns, large heterogeneity is observed across the spatial scale, while temporal changes are minor in comparison. A clear overall East-West pattern was identified with biodiversity indicators decreasing from the Alboran Sea towards the Thyrrhenian Sea, in agreement with previous studies (Coll et al. 2010, Piroddi et al. 2022). On top of this pattern, slopes and deep-water areas and extensive continental shelves displayed opposite patterns in magnitude and temporal changes of biodiversity. Such difference can be attributed to the different composition, spatial configuration and ecosystem functioning previously described in these two realms (Hidalgo et al. 2017, Farriols et al. 2019) that also influence differently the spatial connectivity and the temporal stability of the shelf and slope demersal communities. Taxonomic richness showed the largest changes across space and time but without clear trends, while functional biodiversity indicators showed more modest but consistent changes following the overall large-scale spatial patterns. Thus, on one hand, high species richness may not necessarily reflect community conservation or ecosystem stability. On the other hand, functional diversity may better reflect adaptations and long-term ecosystem changes than species counts alone. Trait-based approaches are increasingly recognized as a tool for understanding ecosystem functioning and conservation under intensifying global change (Green et al. 2022), where the Mediterranean Sea is one of the most strongly impacted areas worldwide due to cumulative impacts of multiple pressures.

3.7.7. References

Boettiger C, Lang DT, Wainwright PC. 2012. rfishbase: exploring, manipulating and visualizing FishBase data from R. Journal of Fish Biology 81(6), 2030-2039.

Coll M, Piroddi C, Steenbeek J, Kaschner K, Lasram FBR, Aguzzi J, Ballesteros E, Bianchi CN, Corbera J, Dailianis T, Danovaro R, Estrada M, Froglia C, Galil BS, Gasol JM, Gertwage R, Gil J, Guilhaumon F, Kesner-Reyes K, ... Voultsiadou E. 2010. The biodiversity of the Mediterranean Sea: estimates, patterns, and threats. PLoS ONE 5(8), e11842. DOI: 10.1371/journal.pone.0011842.

Colloca F, Scarcella G, Libralato S. 2017. Recent trends and impacts of fisheries exploitation on Mediterranean stocks and ecosystems. Frontiers in Marine Science 4, 244. DOI: 10.3389/fmars.2017.00244.

Farriols MT, Ordines F, Carbonara P, Casciaro L, Di Lorenzo M, Esteban A, Follesa C, García-Ruiz C, Isajlovic I, Jadaud A, Ligas A, Manfredi C, Marceta B, Peristeraki P, Vrgoc N, Massutí E. 2019. Spatio-temporal trends in diversity of demersal fish assemblages in the Mediterranean. Sciencia Marina, 83(S1):189-206.

Freeman EA, Moisen G. 2008. PresenceAbsence: An R Package for Presence Absence Analysis. Journal of Statistical Software 23(11), 1–31. https://doi.org/10.18637/jss.v023.i11

Froese R, Pauly D. 2023. FishBase. World Wide Web electronic publication. www.fishbase.org, version (10/2023).

Gelman A, Rubin DB. 1992. Inference from iterative simulation using multiple sequences. Statistical Science 7, 457–472. DOI: 10.1214/ss/1177011136.

Green SJ, Brookson CB, Hardy NA, Crowder LB. 2022 Trait-based approaches to global change ecology: moving from description to prediction. Proceedings of the Royal Society B: Biological Sciences 289: 20220071. https://doi.org/10.1098/rspb.2022.0071

Hidalgo M, Quetglas A, Ordines F, Rueda L, Punzón A, Delgado M, Gil de Sola L, Esteban A, Massutí E. 2017. Size-spectra across geographical and bathymetric gradients reveal contrasting resilient mechanisms of recovery between Atlantic and Mediterranean fish communities. Journal of Biogeography, 44(9), 1939–1951. https://doi.org/10.1111/jbi.12976

Kavadas S, Maina I, Damalas D, Dokos I, Pantazi M, Vassilopoulou V. 2015. Multi-criteria decision analysis as a tool to extract fishing footprints: application to small scale fisheries and implications for management in the context of the maritime spatial planning directive. Mediterranean Marine Science 16(2), 294–304. https://doi.org/10.12681/mms.1087.

Magneville C, Loiseau N, Albouy C, Casajus N, Claverie T, Escalas A, Leprieur F, Maire E, Mouillot D, Villéger S. 2022. mFD: an R package to compute and illustrate the multiple facets of functional diversity. Ecography 45(10), 1–13. https://doi.org/10.1111/ecog.05904

Manel S, Williams HC, Ormerod SJ. 2001. Evaluating presence—absence models in ecology: The need to account for prevalence. Journal of Applied Ecology 38, 921–931.

Nigam T, Escudier R, Pistoia J, Aydogdu A, Omar M, Clementi E, Cipollone A, Drudi M, Grandi A, Mariani A, Lyubartsev V, Lecci R, Cretí S, Masina S, Coppini G, Pinardi N. 2021. Mediterranean Sea Physical Reanalysis

INTERIM (CMEMS MED-Currents, E3R1i system) (Version 1) [Data set]. Copernicus Monitoring Environment Marine Service (CMEMS). https://doi.org/10.25423/CMCC/MEDSEA MULTIYEAR PHY 006 004 E3R1I

Palomares MLD, Pauly D. 2023. SeaLifeBase. World Wide Web electronic publication. www.sealifebase.org.

Pearce J, Ferrier S. 2000. Evaluating the predictive performance of habitat models developed using logistic regression. Ecological Modelling 133, 225–245. DOI: 10.1016/S0304-3800(00)00322-7.

Piroddi C, Coll M, Macias D, Steenbeek J, Garcia-Gorriz E, Mannini A, Vilas D, Christensen V. 2022. Modelling the Mediterranean Sea ecosystem at high spatial resolution to inform the ecosystem-based management in the region. Scientific Reports 12(1), 19680. DOI: 10.1038/s41598-022-18017-x.

Sanz-Martín M, Leprieur F, Albouy C, Mouillot D, Villéger S. 2024. Functional traits explain species' responses to environmental gradients in marine communities. Global Ecology and Biogeography, 33(2), 345–359. https://doi.org/10.1111/geb.13321

Real R, Gofas S, Altamirano M, Salas C, Báez JC, Camiñas JA, García Raso JE, Gil de Sola L, Olivero J, Reina-Hervás JA, Flores-Moya A. 2021. Biogeographical and macroecological context of the Alboran Sea. In: Báez JC, Vázquez JT, Camiñas JA, Malouli Idrissi M (eds). *Alboran Sea – Ecosystems and Marine Resources*. Springer International Publishing, Cham, 431–457.

Spedicato MT, Massutí E, Mérigot B, Tserpes G, Jadaud A, Relini G. 2019. The MEDITS trawl survey specifications in an ecosystem approach to fishery management. Sciencia Marina, 83(S1), 9-20. https://doi.org/10.3989/scimar.04915.11X

Spedicato MT, Zupa W, Villamor A, Soni V, Puerta P, Moullec F, Fock H, Hidalgo M, Punzó A, López-López L, Mérigot B, Moura T, Henriques S, Oliveira P, Chaves C, Vasconcelos R, Rutterford L, Garcia C, Thompson M, Engelhard G, Beukhof E, Pecuchet L, Peristeraki P, Rozemeijer MJC, Jónsdóttir IG, Cronne L, Holdsworth N, Lindegren M. 2024. B-USEFUL. Report of available metadata and data gaps across case studies. Technical University of Denmark. Available at: https://b-useful.eu/b-useful/uploads/D2.1-B-USEFUL report.pdf

Teruzzi A, Di Biagio V, Feudale L, Bolzon G, Lazzari P, Salon S, Coidessa G, Cossarini G. 2021. Mediterranean Sea Biogeochemical Reanalysis (CMEMS MED-Biogeochemistry, MedBFM3 system) (Version 1) [Data set]. Copernicus Monitoring Environment Marine Service (CMEMS).

https://doi.org/10.25423/CMCC/MEDSEA MULTIYEAR BGC 006 008 MEDBFM3

Tikhonov G, Opedal ØH, Abrego N, Lehikoinen A, de Jonge MMJ, Oksanen J, Ovaskainen O. 2020. Joint species distribution modelling with the R-package Hmsc. Methods in Ecology and Evolution 11(3), 442–447. https://doi.org/10.1111/2041-210X.13345.

Tjur T. 2009. Coefficients of determination in logistic regression models – a new proposal: the coefficient of discrimination. The American Statistician 63, 366–372. DOI: 10.1198/tast.2009.08210.

Vasquez M, Ségeat B, Cordingley A, Tilby E, et al. 2023. EUSeaMap 2023, a European broad-scale seabed habitat map, Technical Report. Ref. EASME/EMFF/2020/3.1.11/Lot3/SI2.843624 – EMODnet Thematic Lot n° 3 – Seabed Habitats - D1.15. EMODnet. https://doi.org/10.13155/97116.

Wilson KA, Westphal MI, Possingham HP, Elith J. 2004. Sensitivity of conservation planning to different approaches to using predicted species distribution data. Biological Conservation 22(1), 99–112.

Zuur AF, Ieno EN, Elphick CS. 2010. A protocol for data exploration to avoid common statistical problems. Methods in Ecology and Evolution 1(1), 3–14. DOI: 10.1111/j.2041-210X.2009.00001.x.

3.8 Barents Sea fish model

Authors: Shannon Moore, Laurene Pecuchet

3.8.1. Study area and data availability

The Barents Sea is a sub-Arctic shelf sea situated in the transition zone between the Northeast Atlantic and the Arctic Ocean. This high latitude sea has a maximum depth of 500m and an average depth of 230m (Kolås et al., 2024; Loeng, 1991; Eriksen et al., 2018). It is influenced by two dominant water masses, namely relatively warm (>3° C) and saline (>34.9) Atlantic Water flowing in from the southwest and cooler (<0° C), fresher (34.4-34.8) Arctic Water entering from the north (Eriksen et al., 2018; Kolås et al., 2024). The colder northern region of the Barents Sea is also characterized by its sea ice cover, which varies seasonally — with a minimum in September (0-30%) and a maximum in April (35-85%) — and interannually (Eriksen et al., 2018). These spatial differences in temperature, salinity, and sea ice provide more Arctic conditions in the northern Barents Sea and more boreal conditions in the southern Barents Sea. Where these two water masses meet in the Barents Sea is called the Polar Front, a rather stable oceanographic front preventing colder Arctic water from dispersing further south (Eriksen et al., 2018; Kolås et al., 2024).

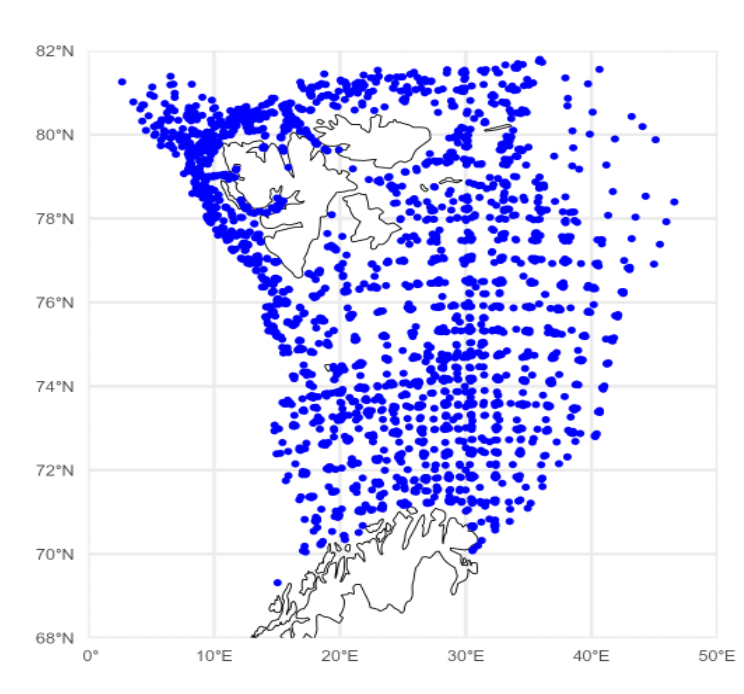


Figure 3.8.1. Map of the Barents Sea region included in this study with sampling stations marked with blue dots. This map includes all sampling stations that were sampled throughout the entire survey period (2004-2022).

Data used in this analysis were collected as part of the Barents Sea Ecosystem Survey (BESS) supported by the cooperation between Norway's Institute for Marine Research (IMR, Bergen) and Russia's Knipovich Polar Research Institute of Marine Fisheries and Oceanography (PINRO, Murmansk). The annual survey takes place from August through October (the period with the lowest sea ice cover) throughout the Barents Sea and its adjacent waters (Eriksen et al., 2018; Michalsen et al., 2013). Stations are distributed along a 35x35 nautical mile (about 65 km²) grid and are sampled yearly when possible. Here, we use fish community data from bottom-trawl survey from 2004 to 2022 in the Western part of the Barents Sea (Figure 3.8.1). Individuals were identified to the lowest possible taxa (the species level whenever possible) and counted. This resulted in abundance data available for a total of 108 fish taxa. We further constrained this taxa list by excluding rare taxa, which we defined as taxa with fewer than 10 occurrences over time (year) and space (haul). One additional low-occurring fish species, the

Greenland argentine (Nansenia groenlandica), was removed from the final taxa list due to the lack of trait data necessary for this analysis. Therefore, our final taxa list consisted of 88 fish taxa. To characterize the environmental niche of fish taxa, we used daily modeled environmental covariates available from Copernicus Marine Data Store's Arctic Ocean Physics Reanalysis model. For this analysis, we included a set of seven physical and chemical environmental covariates that were hypothesized to be important for demersal fish community composition, namely depth (m), sea surface temperature (SST, °C), sea bottom temperature (SBT, °C), sea surface salinity (SSS), sea bottom salinity (SBS), the number of annual sea ice days, and mixed layer depth (m). The number of annual sea ice days was calculated from sea ice concentration values provided by Copernicus. If sea ice concentration (or the percentage of a grid cell covered by sea ice) amounted to 15% or higher, the area was considered ice-covered. We then summed the number of ice-covered days in each grid cell over the course of each year to calculate the number of annual sea ice days. Seasonality was calculated for temperature (SST, SBT) and salinity (SSS, SBS) as the standard deviation of each modelled point and year. Each covariate was provided at the spatial resolution of 12.5km² as a daily average value, with surface and bottom measurements reported for salinity and temperature variables. To better understand the role of traits in structuring fish communities in the Barents Sea, we included three traits that are believed to inform fish responses to their environment, namely, maximum length, fecundity, and trophic level. These three functional traits were related to life history strategies, diet, morphology, and reproduction and deemed important for determining the spatio-temporal patterns of fish distributions. Demersal fish traits were obtained from Wiedmann et al. (2014), who gathered Barents Sea-specific fish trait values and were further supplemented with trait data from Beukhof et al. (2019).

3.8.2. Model setup, fitting and validation

We fitted joint species distribution models (JSDMs), specifically applying the HMSC framework to the Barents Sea demersal fish community data using the R package 'Hmsc' version 3.0-13 (Ovaskainen et al., 2017; Ovaskainen & Abrego, 2020; Tikhonov, et al., 2020). To allow for quicker computing times associated with model fitting of such a large and complex model, we opted to implement the Hmsc-HPC method as outlined in Rahman et al. 2024. We conducted all statistical analyses in Visual Studio Code version 1.96 using R version 4.4.1 (R Core Team, 2024). To account for the 0-inflated abundance data, a hurdle model approach was applied in which we first fit a model using presence/absence data with a probit regression (hereafter referred to as the occurrence model) and then fit a model using logged abundance data conditional on presence via a normal regression (hereafter referred to as the abundance model) (Leandro et al., 2023; Piirainen et al., 2023). While HMSC can explain variation in communities produced via environmental filtering based on the covariates provided in the model, it can also account for any spatial and temporal autocorrelation in the taxa occurrence/abundance data through random effects, which are accounted for as latent factors in the model. We developed a spatially explicit random effect by constructing a hexagonal grid covering our study area with cells measuring approximately 300km across using the R package 'dggridR' version 3.1.0 (Barnes & Sahr, 2024). Sample year was used as a temporal unstructured random effect. We used the default prior values for our models. The posterior distribution was sampled with four Markov chain Monte Carlo (MCMC) simulations. Each chain ran 37,500 samples with the first 12,500 samples discarded as burn-in. We applied a thinning of 100 to each chain which resulted in 250 posterior samples for a total of 1,000

posterior samples total. To assess model fit and ensure adequate independence of these modeled MCMC samples, MCMC convergence was evaluated by comparing the effective sample size of each parameter (beta, gamma, and omega) to the total number of modeled samples collected from the four MCMC chains and by assessing if the potential scale reduction factors for each parameter were centered around 1.00 (Gelman & Rubin, 1992). To assess model performance, we evaluated both explanatory and predictive power for each of the models. The performance of the occurrence model was assessed via root mean square error (RMSE), Tjur's coefficient of discrimination (Tjur R²), and area under the curve (AUC). RMSE reports how close the modeled values are to the true values and is a measure of precision. Tjur R² and AUC are both measures of the model's ability to discriminate between the presence and absence of a taxon in a specific community (Fielding & Bell, 1997; Pearce & Ferrier, 2000; Tjur, 2009). The abundance model was also assessed via RMSE as well as the coefficient of discrimination (R²), which provides an average of how well the model fits for each species. Predictive power was assessed through a twofold cross-validation and evaluated using the same methods as listed above for both models (occurrence and abundance).

Table 3.8.1. Mean explanatory and predictive powers (from a 5-fold cross-validation) across all modelled species measured as AUC, Tjur R2 and RMSE.

Model	Occurrence			Abundance (based on occurrence)	
	AUC	Tjur R²	RMSE	R ²	RMSE
Explanatory power	0.86	0.14	0.21	0.29	0.78

3.8.3. Model diagnostics and performance

MCMC convergence for both the occurrence model and the abundance model showed satisfaction as demonstrated by the potential scale reduction factor being <1.1 for beta and gamma parameters, respectively, in both models (occurrence = 1.000 and 1.008; abundance = 1.000 and 0.990). This, along with visual inspection of the trace plots, confirmed that our four chains provided consistent results. Additionally, the effective sample size of the beta and gamma parameters, respectively, were similar to the number of posterior samples calculated (occurrence = 855 and 779; abundance = 1044 and 1063), and we are, therefore, confident in the models' lack of autocorrelation between modeled MCMC samples. The mean explanatory power for the occurrence model as measured by Tjur's R², AUC, and RMSE were 0.14, 0.86, and 0.21, respectively (Table 3.8.1). The abundance model's explanatory power was 0.78 (RMSE) and 0.29 (R²).

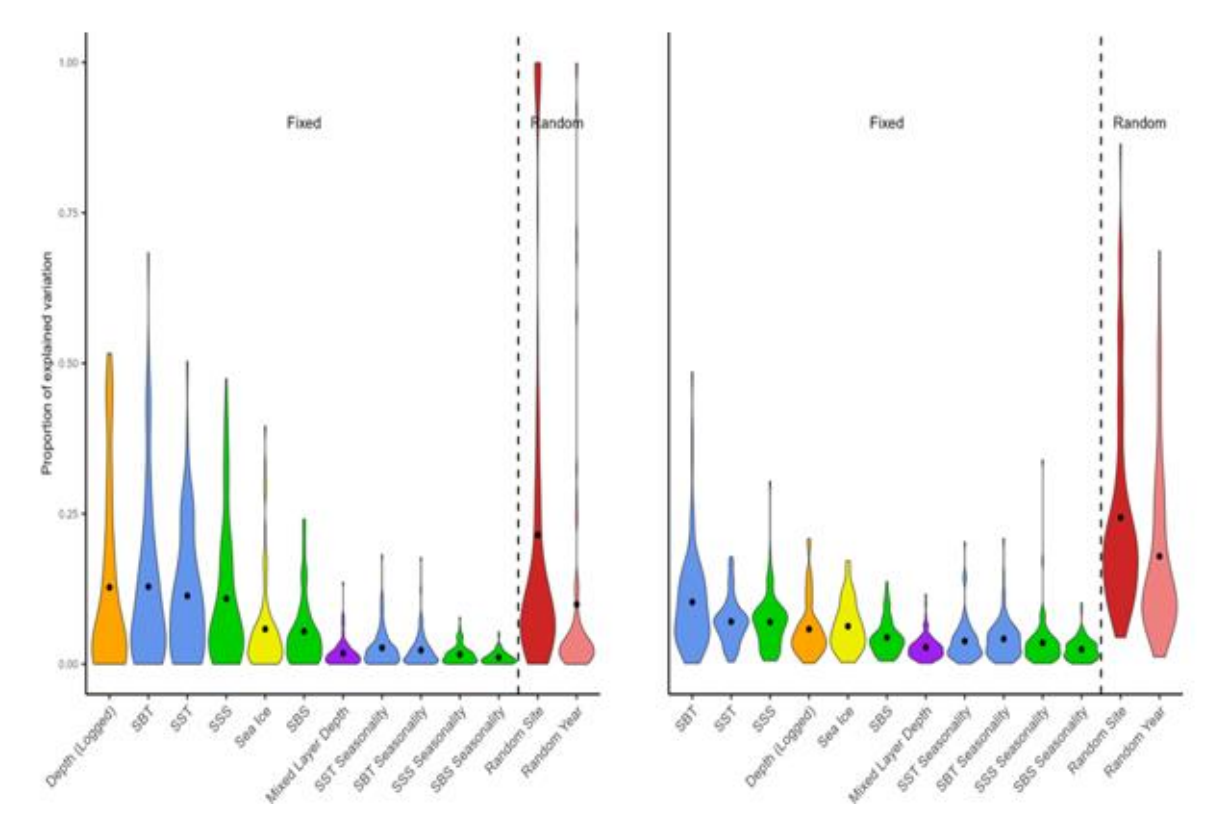


Figure 3.8.2. The distribution of the proportion of the total variation in species (a) occurrence and (b) abundance explained by each of the environmental variables and random effects (space and time) across all species. Mean values for each environmental variable are depicted with a black dot.

All the components of our model, including environmental variables, spatial and temporal effects, traits, and taxonomy, were able to explain 64% of the total variation in species occurrences and 9% of the total variation in species abundances. On average, the environmental variables explained 68% (occurrence model) and 58% (abundance model) of the variance in species distributions explained by our models. The rest of the variance was explained by the two included random effects (spatial and temporal), with the spatial random effect contributing the most of the two with 21% in the occurrence model and 24% in the abundance model. Both the occurrence model and the abundance model exhibited similar patterns relating to the importance of each environmental variable in determining species composition. The environmental variable having the most influence on both species occurrence and abundance was temperature (occurrence = 32%, abundance = 25%). Salinity was the next most important environmental variable in both models, accounting for 18% of the variation in species occurrences and 17% in species abundances. Depth was also important in determining species' occurrence (12%), but it was much less influential for species' abundances (6%). Sea ice was not particularly important in either model (occurrence = 5%, abundance = 7%), and the effect of mixed layer depth on species occurrence and abundance was also negligible (occurrence = 1% and abundance 3%). When breaking down temperature and salinity, we saw that sea bottom temperature was more important than sea surface temperature by a small margin in both models (occurrence = 13% vs. 11%, abundance = 10% vs. 7%) (Figure 3.8.2). However, the opposite trend was observed for salinity where sea surface salinity was always more important in explaining both species occurrence and species abundance patterns than sea bottom salinity.

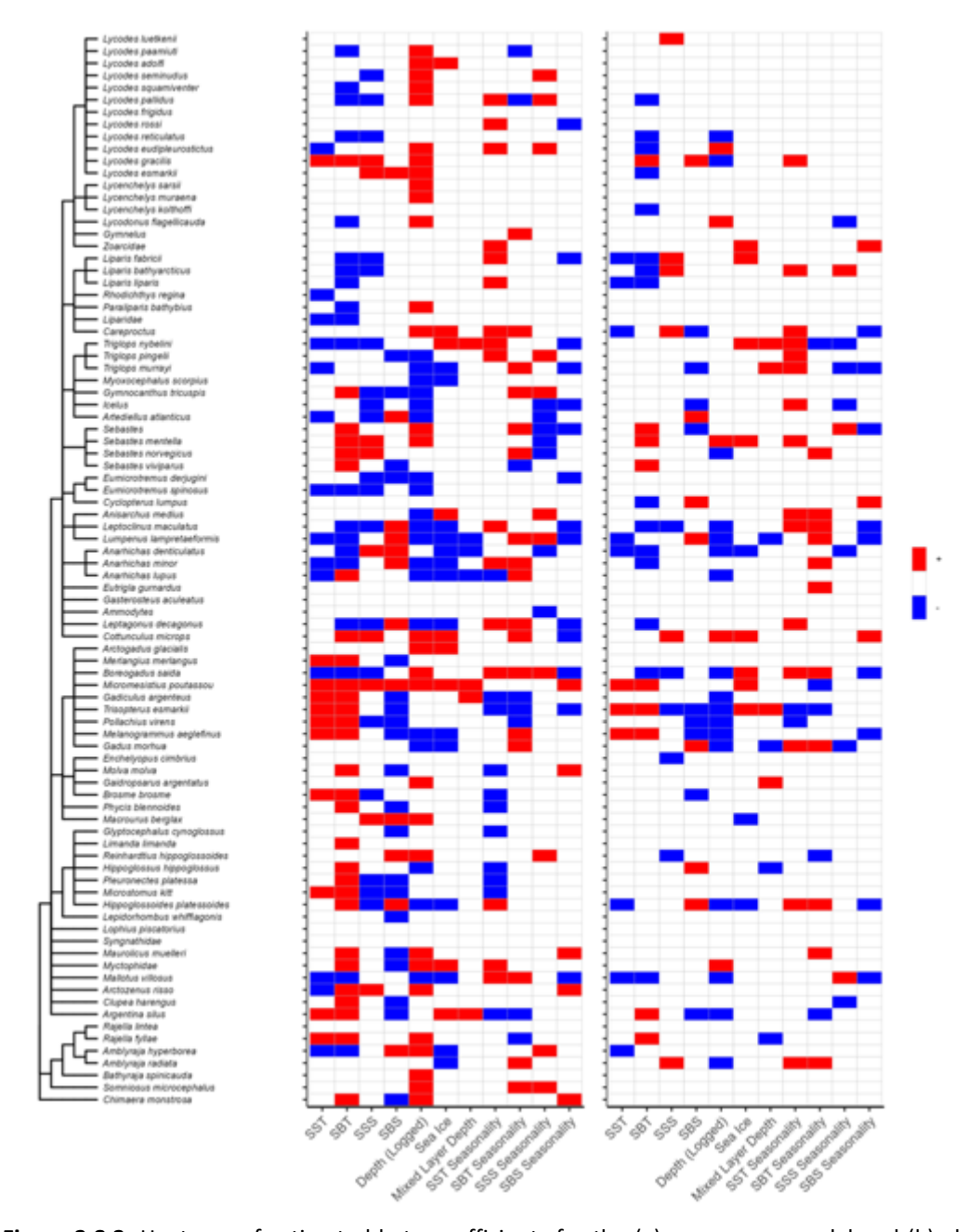


Figure 3.8.3. Heatmap of estimated beta coefficients for the (a) occurrence model and (b) abundance model indicating positive (red), negative (blue) or no relationships (white) of species responses to the set of environmental covariates included in the models (with at least a posterior probability of 0.95). Species are sorted vertically according to their taxonomic relatedness.

3.8.4. Species and trait responses to drivers

Both models displayed diverse species-specific responses to the environmental variables with at least 95% posterior probability. However, these species-specific niches varied depending on whether we were analyzing occurrence or abundance patterns (Figure 3.8.3). In general, the occurrence model provided more statistically significant species-specific responses than the abundance model. The environmental factors that significantly affected the highest number of species' occurrence values were depth and SBT. Species occurrence probabilities increased in deeper waters for 30 species and species occurrence increased in shallower waters for 19 species. SBT also affected the occurrence of an equal number of species in the

community (49), with the occurrence probability of 29 species increasing in warmer waters and 20 species increasing in cooler waters. Depth and SBT were also responsible for the highest degree of species' variation in abundance. However, increased depth only led to a higher abundance in 5 species while it decreased the abundance of 17 species. Meanwhile, warmer waters resulted in a higher abundance of 9 species and decreased the abundance of 15 species.

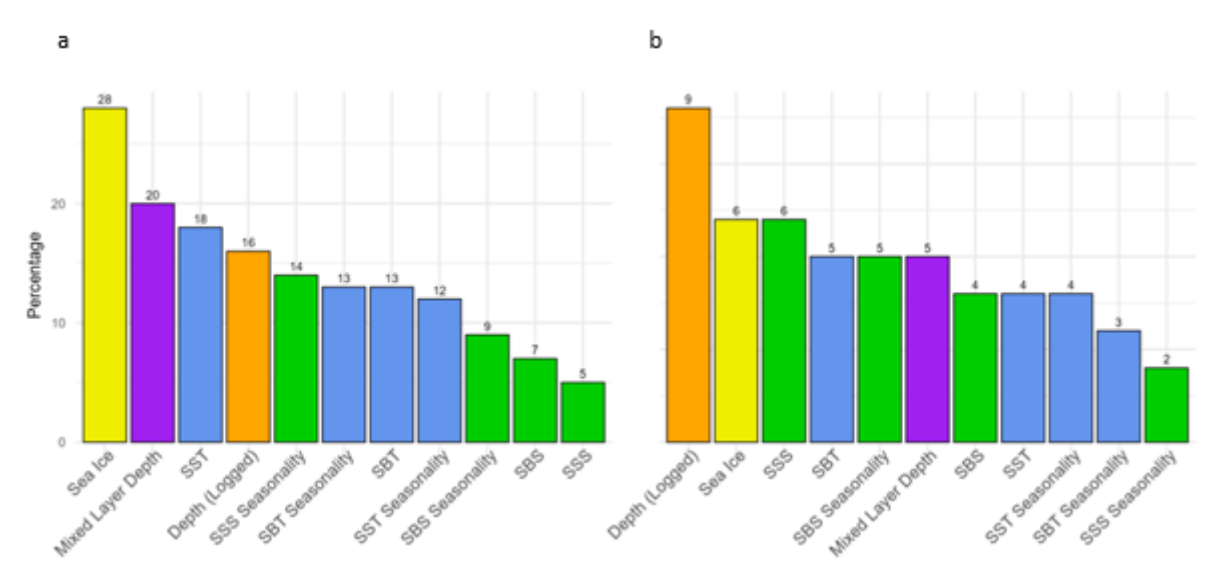


Figure 3.8.4. The proportion of the species response to environmental covariates mediated by traits in both our (a) occurrence model and (b) abundance model.

Traits were responsible for an average of 14% of the examined variance in species occurrence related to a species' niche, with traits mediating the largest proportional response of species occurrence for number of ice days (28%), while it was the lowest for SSS (5%) (Figure 3.8.4). Therefore, traits influence the response of species to sea ice variation more than for any other environmental variable. However, when plotting a heatmap of the gamma responses (the relationships between traits and the environment) in the occurrence model (Figure 3.8.5), we observed that only one trait, maximum body size, was shown to mediate the occurrence responses to sea ice (with at least 95% posterior support). Maximum body size also mediated the responses to SBT and SBT seasonality, while fecundity mediated the responses to depth. The direction (positive or negative) of these relationships suggests that we are more likely to find larger species in regions with cooler, yet more seasonal, SBT and fewer days of ice and that more fecund taxa are more negatively influenced by depth than less fecund taxa. As opposed to the occurrence model, traits only mediated an average of about 5% of the relationships between species abundances and the environment were mediated by traits. Depth was the environmental variable most mediated by traits in the abundance model, however, it was still mediated by traits to a lesser degree in this model than in the occurrence model (Figure 3.8.4). Additionally, no traits were found to mediate the response of species abundances to any of the environmental variables with at least 95% posterior support (Figure 3.8.5). Therefore, the abundance of certain trait values are not more or less expected under specific environmental conditions.

a b

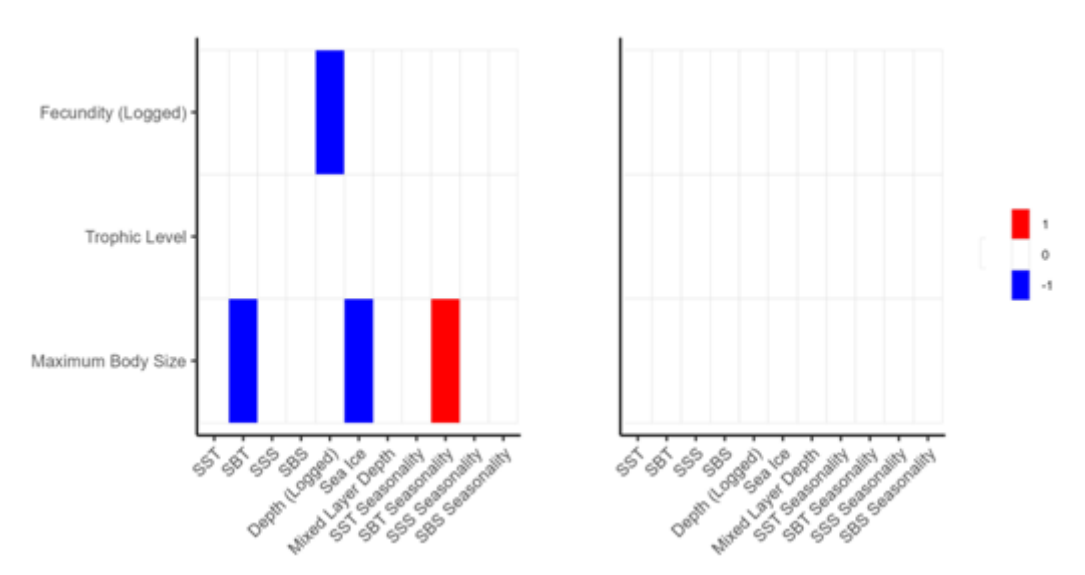


Figure 3.8.5. Heatmap of estimated gamma coefficients for the (a) occurrence model and (b) abundance model indicating positive (red), negative (blue) or no relationships (white) of traits to the set of environmental covariates included in the models (with at least a posterior probability of 0.95).

3.8.5. Patterns and trends in biodiversity

Shannon's diversity index map and the Bray-Curtis dissimilarity index map displayed clear spatial patterns, but with values shown to be, in general, the opposite of each other. Community diversity was highest across the middle of the Barents Sea and wrapping up around the northwest coast of Svalbard, while remaining lower in the southwest corner of the Barents Sea where it meets the Norwegian Sea and in the northeast region where it meets the Arctic Ocean (Figure 3.8.6). Meanwhile, community dissimilarity is shown to be highest in the southwest region, out near the continental slope in the northwest corner, and along the north and east edges of the Barents Sea, while it remained lower in the middle of the Barents Sea (Figure 3.8.6).

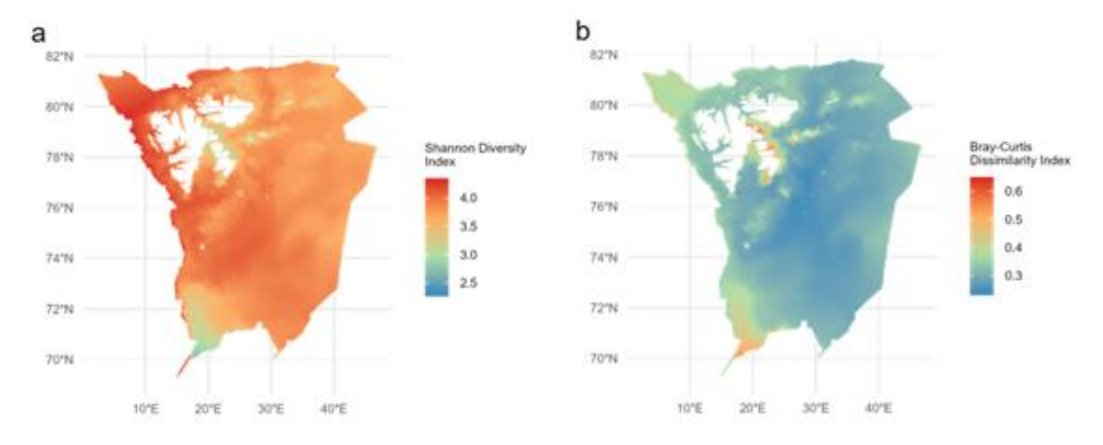


Figure 3.8.6. Maps displaying (a) Shannon's diversity index and (b) Bray-Curtis dissimilarity index across the study area based on predictions made from the abundance model.

The community weighted mean trait maps displayed a similar clear spatial pattern for each of the three traits (Figure 3.8.7). Community-weighted mean body size ranged from 31.6 to 80.4, and, on average, larger demersal fish can be found along the southeast to northwest diagonal

line across the Barents Sea and much smaller both northeast and southwest of this diagonal line. Individuals higher up in the food web are generally found in the southwest half of the Barents Sea and wrapping up around the west and northwest corner of Svalbard. Meanwhile, lower trophic level individuals were found further north throughout the Barents Sea. The community weighted-mean trophic level varied from 3.26 to 4.00. A similar pattern was observed for fecundity, which ranged from 8.60 to 13.6 (logged), but with more fecund individuals extending slightly further north than the pattern observed for trophic level. Interestingly, all three trait values dramatically decreased upon entering the slope to the Arctic Ocean just northwest of Svalbard (smaller individuals, lower trophic level individuals, and less fecund individuals).

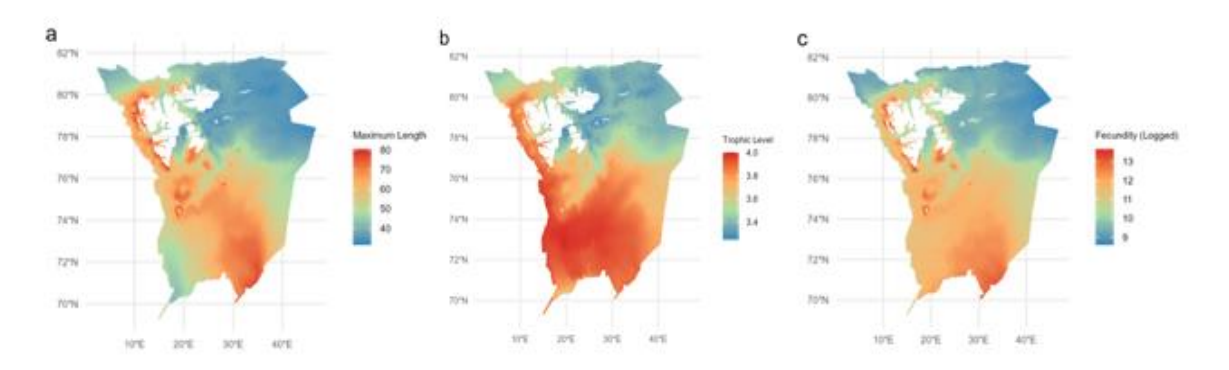


Figure 3.8.7. Predicted community-weighted mean trait values across the study area, including (a) maximum body size, (b) trophic level, and (c) logged fecundity. Predictions were based on the product of the predicted occurrence probability (calculated from the occurrence model) and the predicted abundance conditional on occurrence values (calculated from the abundance model).

3.8.6. **Summary**

Our models depict the importance of both environmental variables and the trait values species possess in influencing demersal fish community distributions in the Barents Sea. Specifically, temperature, salinity, and depth explained the largest proportion of the variance in both species' occurrences and abundances. As the location of the Polar Front can be defined from year to year by the temperature and salinity of the Arctic and Atlantic water masses in the north and the south, respectively, this would suggest that the communities on either side of the Polar Front are different. This supports the idea of a more characteristically Arctic community in the north and a more characteristically boreal community in the south, with some mixing in the middle. Our study supports previous findings on the drivers of fish community composition in the Barents Sea (see Johannesen et al., 2012, Aschan et al., 2013, and Johannesen et al., 2017). However, the inclusion of traits and taxonomy in such a rigorous way via HMSC adds for a richer understanding of how these communities respond to their environment. In fact, the division between Arctic communities and boreal communities is further evidenced by the patterns we see with traits amongst the taxa in our study. Sea ice is the environmental variable to which species distributions respond the most (and second most) to as a result of the traits they possess. Additionally, the mapped community-weighted mean trait values display distinct gradients in values for all three traits explored in this study. Based on these maps, one could even argue for a third demersal fish community in the Barents Sea, besides the arctic and boreal, that exists in the middle near the Polar Front that consists of both arctic and boreal fish. This was and briefly discussed by Fossheim et al. (2015) and

implied by Frainer et al (2021) but corroborated in the present study. A third arcto-boreal community is further substantiated by Shannon's diversity index map and the Bray-Curtis dissimilarity index map. The regions with high Shannon's and low Bray-Curtis, found mostly in the region where this third arcto-boreal community is found, share many species with similar abundances, whereas those regions with low Shannon's and high Bray-Curtis, found mostly in the northern and southern tips of the study area, have distinct species compositions with little overlap. We therefore stress the importance of a trait-based approach for community distribution studies, as they provide a more holistic view of what is driving community composition.

3.8.7. References

Arctic Ocean Physics Reanalysis. E.U. Copernicus Marine Service Information (CMEMS). Marine Data Store (MDS). DOI: 10.48670/moi-00007 (Accessed in Aug-2024)

Aschan, M., M. Fossheim, M. Greenacre, and R. Primicerio. 2013. Change in fish community structure in the Barents Sea. PloS one **8**:e62748.

Barnes, R., and K. Sahr. 2024. dggridR: Discrete Global Grids. R package version 3.1.0. https://cran.r-project.org/package=dggridR.

Beukhof, E., T. S. Dencker, M. L. Palomares, and A. Maureaud. 2019. A trait collection of marine fish species from North Atlantic and Northeast Pacific continental shelf seas. Pangaea 1:12.

Eriksen, E., H. Gjøsæter, D. Prozorkevich, E. Shamray, A. Dolgov, M. Skern-Mauritzen, J. E. Stiansen, Y. Kovalev, and K. Sunnanå. 2018. From single species surveys towards monitoring of the Barents Sea ecosystem. Progress in Oceanography **166**:4-14.

Fielding, A. H., and J. F. Bell. 1997. A review of methods for the assessment of prediction errors in conservation presence/absence models. Environmental conservation **24**:38-49.

Frainer, A., R. Primicerio, S. Kortsch, M. Aune, A. V. Dolgov, M. Fossheim, and M. M. Aschan. 2017. Climate-driven changes in functional biogeography of Arctic marine fish communities. Proceedings of the National Academy of Sciences **114**:12202-12207.

Fossheim, M., R. Primicerio, E. Johannesen, R. B. Ingvaldsen, M. M. Aschan, and A. V. Dolgov. 2015. Recent warming leads to a rapid borealization of fish communities in the Arctic. Nature Climate Change **5**:673-677.

Gelman, A., and D. B. Rubin. 1992. Inference from iterative simulation using multiple sequences. Statistical science **7**:457-472.

Johannesen, E., Å. S. Høines, A. V. Dolgov, and M. Fossheim. 2012. Demersal fish assemblages and spatial diversity patterns in the Arctic-Atlantic transition zone in the Barents Sea. PloS one **7**:e34924.

Johannesen, E., L. L. Jørgensen, M. Fossheim, R. Primicerio, M. Greenacre, P. A. Ljubin, A. V. Dolgov, R. B. Ingvaldsen, N. A. Anisimova, and I. E. Manushin. 2017. Large-scale patterns in community structure of benthos and fish in the Barents Sea. Polar Biology **40**:237-246.

Kolås, E. H., T. M. Baumann, R. Skogseth, Z. Koenig, and I. Fer. 2024. Circulation and hydrography in the northwestern Barents Sea: insights from recent observations and historical data (1950–2022). Journal of Geophysical Research: Oceans 129:e2023JC020211.

Leandro, C., M. Jones, W. Perrin, P. Jay-Robert, and O. Ovaskainen. 2023. Dung beetle community patterns in Western Europe: responses of Scarabaeinae to landscape and environmental filtering. Landscape Ecology **38**:2323-2338.

Loeng, H. 1991. Features of the physical oceanographic conditions of the Barents Sea. Polar Research 10:5-18.

Michalsen, K., P. Dalpadado, E. Eriksen, H. Gjøsæter, R. B. Ingvaldsen, E. Johannesen, L. L. Jørgensen, T. Knutsen, D. Prozorkevich, and M. Skern-Mauritzen. 2013. Marine living resources of the Barents Sea–Ecosystem understanding and monitoring in a climate change perspective. Marine Biology Research **9**:932-947.

Ovaskainen, O., G. Tikhonov, A. Norberg, F. Guillaume Blanchet, L. Duan, D. Dunson, T. Roslin, and N. Abrego. 2017. How to make more out of community data? A conceptual framework and its implementation as models and software. Ecology letters **20**:561-576.

Ovaskainen, O., and N. Abrego. 2020. Joint species distribution modelling: With applications in R. Cambridge University Press.

Pearce, J., and S. Ferrier. 2000. Evaluating the predictive performance of habitat models developed using logistic regression. Ecological modelling **133**:225-245.

Piirainen, S., A. Lehikoinen, M. Husby, J. A. Kålås, Å. Lindström, and O. Ovaskainen. 2023. Species distributions models may predict accurately future distributions but poorly how distributions change: A critical perspective on model validation. Diversity and Distributions **29**:654-665.

R Core Team (2023). R: A Language and Environment for Statistical Computing. R Foundation for Statistical Computing, Vienna, Austria. http://www.R-project.org/.

Rahman, A. U., G. Tikhonov, J. Oksanen, T. Rossi, and O. Ovaskainen. 2024. Accelerating joint species distribution modelling with Hmsc-HPC by GPU porting. PLOS Computational Biology **20**:e1011914.

Tikhonov, G., Ø. H. Opedal, N. Abrego, A. Lehikoinen, M. M. de Jonge, J. Oksanen, and O. Ovaskainen. 2020. Joint species distribution modelling with the R-package Hmsc. Methods in ecology and evolution **11**:442-447.

Tjur, T. 2009. Coefficients of determination in logistic regression models—A new proposal: The coefficient of discrimination. The American Statistician **63**:366-372.

Wiedmann, M. A., M. Aschan, G. Certain, A. Dolgov, M. Greenacre, E. Johannesen, B. Planque, and R. Primicerio. 2014. Functional diversity of the Barents Sea fish community. Marine Ecology Progress Series **495**:205-218.

4. Alternative approaches to biodiversity assessments

4.1. Biodiversity assessment across organism groups in the Greater North Sea

Authors: Murray Thompson, Lily Greig, Keith Cooper and Georg Engelhard

4.1.1. Study area and data

Phytoplankton and zooplankton data were obtained from the Continuous Plankton Recorder survey (CPR, https://www.cprsurvey.org/data/our-data/; Batten et al., 2003). Samples were collected using a Continuous Plankton Recorder that is towed behind ships and continuously filters plankton from the water column using a moving band of silk gauze (270 µm mesh) at a depth of around 7 m. Observations with unique spatial and temporal information correspond to a tow length of approximately 10 nautical miles and a volume of 3 m³ of seawater (henceforth, plankton samples). Because it is unfeasible to count all phytoplankton in each sample, sample counts per taxa were derived by statistically resampling to estimate mean sample-level abundance. Phytoplankton counts were then rescaled to approximate the initial subsample counts (i.e. with many singletons which are typical of community samples and are required to estimate the effective number of species, see below) by dividing each count per taxa by the lowest count per taxa within each sample and rounded to the nearest whole number. Larger zooplankton counts were estimated at the sample-level, meaning no statistical resampling nor rescaling was required. We make use of phytoplankton (n taxa = 173) and zooplankton (n taxa = 119) data available from 1980-2021 for the northeast Atlantic downloaded on 09/07/2024, including information from 114925 samples. Benthic macrofaunal data sourced from the OneBenthic database were (https://rconnect.cefas.co.uk/onebenthic_portal/) with all publicly downloaded on 07/11/2024, including information on 3700 taxa from 29403 comparable grab and core samples (henceforth benthic samples, i.e., sampled using a 0.1 m² grab or core and

processed using a 1 mm sieve) collected between 1985-2023 from shelf waters of the northeast Atlantic. Fish observations from 38363 otter trawl surveys from across the northeast Atlantic spanning years 1983-2020 and including 513 taxa were obtained from Lynam & Ribeiro (2022) who collated multiple surveys stored on the ICES database of trawl surveys (DATRAS). Hauls (henceforth, fish samples) had a mean swept area of 0.7 km² (sd = 0.02; had a mean duration of 31.7 minutes). All data on biota incorporate taxonomic information from the World Register of Marine Species (WoRMS Editorial Board, 2024), with each taxon uniquely identified by its 'aphiaID', allowing data to be outputted using standardized nomenclature. Taxonomic resolution varied considerably among groups. Phytoplankton were identified with the lowest precision (15% to species, 46% to genus, none to family, and 39% only to class or higher). Most zooplankton records were resolved to species (69% to species, 6% to genus, 6% to family, and 19% to class or above), this precision was higher for benthic invertebrates (79% to species, 14% to genus, 3% to family, and 4% to class or higher). Fish achieved the highest resolution, with nearly all records (99%) identified to species and only 1% to genus or higher. Given this variability, we used the lowest (i.e. ideally species) available taxonomic resolution for phytoplankton, zooplankton, and benthos, retaining records identified to species, genus, and family, while restricting fish to species-level data. This approach maximizes the retention of both taxonomic detail and abundance information across assemblages, while acknowledging that diversity indices, particularly for phytoplankton, capture broader taxonomic richness rather than species richness alone.

4.1.2. Methods and indicators

Rarefaction and extrapolation based on Hill numbers provide a unified framework for estimating α -, β -, and γ -diversity that corrects for biases arising from variable sample sizes and sampling effort, and is applicable across different assemblages (Chao et al., 2014; Chao et al. 2023; Jost, 2007). Diversity estimates were all generated per assemblage. To estimate α -diversity, we calculated the effective number of species for each sample at twice the mean sample count for that assemblage (20 for phytoplankton, 42 for zooplankton, 365 for benthos, and 15933 for fish) using individual-based rarefaction and extrapolation. γ -diversity for each assemblage was estimated using the following approach: at the time and location of each sample estimates were generated by incorporating nine surrounding samples (selected at random where more than 9 were available) collected within 6 months and within 75 km of that sample and applying sample-based rarefaction and extrapolation to 20 samples. Where <9 surrounding samples were available, γ -diversity estimates were dropped because variation in the number of samples can incorporate more or less β -diversity, biasing estimates (Thompson et al. 2021). β -diversity is an estimate of the effective number of communities in a given area and was calculated as:

$$\beta = \gamma / \overline{\alpha} \tag{1}$$

where $\overline{\alpha}$ represents mean α -diversity (Jost, 2007; Tuomisto, 2010).

All α -, β -, and γ -diversity estimates were made for q0 (the effective number of species; i.e. species richness), q1 (the effective number of typical species; i.e. exponential of Shannon entropy) and q2 (the effective number of dominant species; i.e. inverse Simpson index), yielding 9 taxa-based biodiversity indices. These were supplemented with three abundance-based biodiversity indices of sample count, coefficient of variation in sample-count (Wang et

al. 2014), and sum of counts (i.e. α -, β -, and γ -diversity equivalents for abundance, respectively), yielding 12 biodiversity indices in total. All rarefaction and extrapolation analyses were conducted using the R package *iNEXT* (Hsieh et al., 2014). To assess temporal changes in biodiversity we used Kendall's tau trend analysis between annual means of our biodiversity indices for ICES statistical rectangles. Kendall's tau scores are presented for each rectangle to show regions of temporal change and thus explore contrasting directions of change across assemblages. Kendall's tau scores of -1 to +1 represent a 100% probability of a decreasing or increasing trend, respectively. Kendall's tau trend analysis is rank-based and non-parametric because our response variables were not normally distributed. Using Kendall's tau has the added benefit of detecting correlations which may be non-linear, since temporal change in the responses could take any smoothly varying (curving) function.

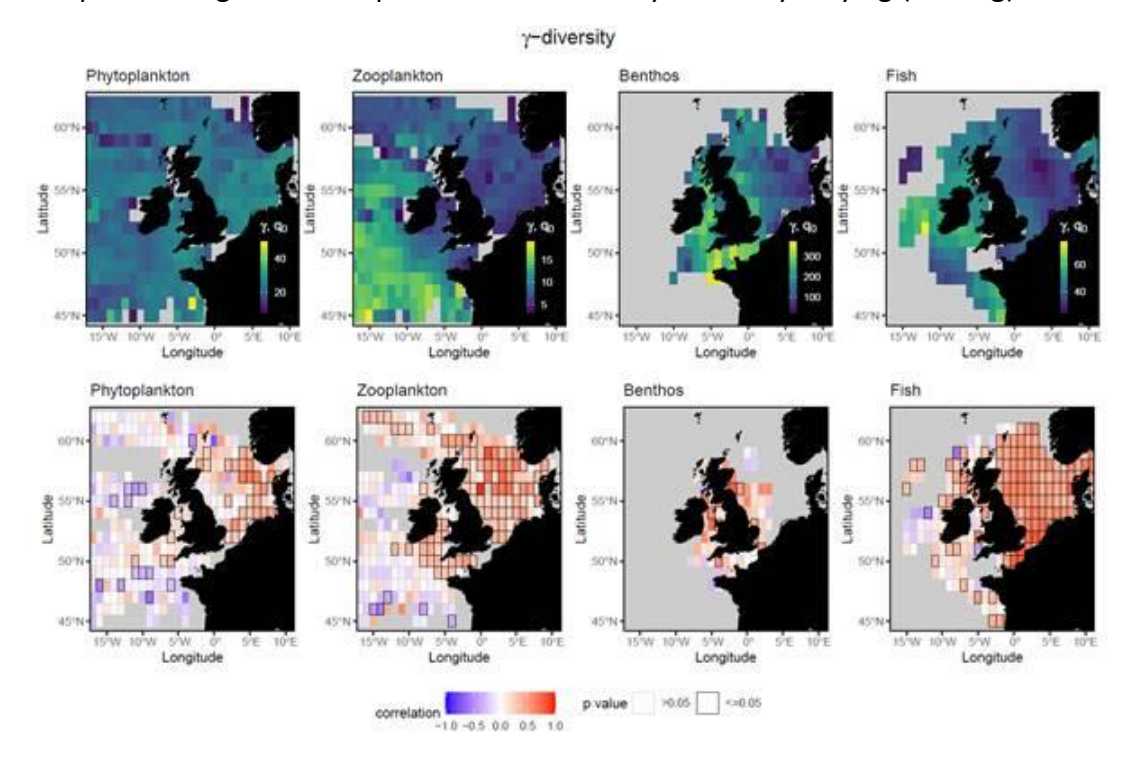


Fig. 4.1.1. Mean (top row) and temporal change (bottom row) in γ -diversity across assemblages. Temporal increases are shown by red cells (Kendall's tau correlation values between 0 and +1), declines by blue cells (correlation values between 0 and -1), and cells with significant correlations have a black border. Observations span 1980-2021 for plankton, 1985-2023 for benthos, and 1983-2021 for fish.

4.1.3. Results

There were widespread increases in fish γ -diversity, followed by widespread increasing trends for zooplankton and then phytoplankton, with increases also detected for benthos where sufficient time series existed (Figure 4.1.1). Increases in γ -diversity largely occurred in the North Sea, where fish and zooplankton had relatively low mean values, whereas phytoplankton mean γ -diversity was relatively high (Fig. 4.1.1; there were insufficient spatially extensive time-series for benthos for a similar comparison). Temporal change in α -diversity largely reflected the direction of change in γ -diversity for fish, benthos and zooplankton, but with weaker and more patchy correlations (Fig. 4.1.2). There was limited temporal change in phytoplankton α -diversity and no regions clearly changing in the same direction (Fig. 4.1.2). Where temporal change in β -diversity was detected, trends were broadly positive for

phytoplankton and zooplankton, decreasing for benthos and with contrasting directions of change for fish (Fig. 4.1.3).

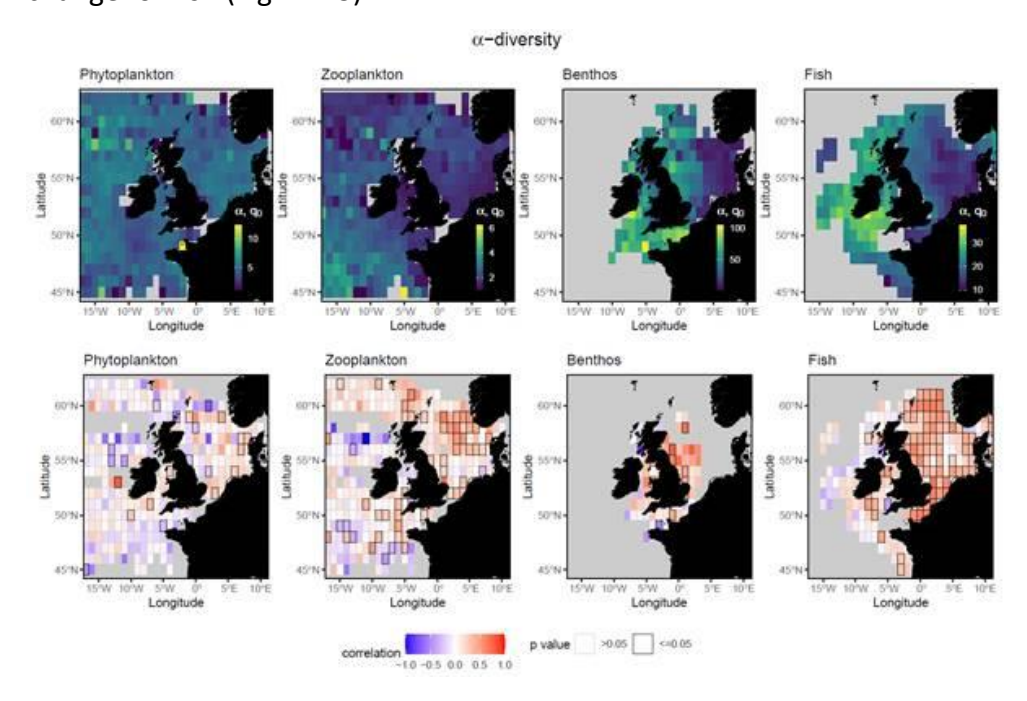


Fig. 4.1.2. Mean (top row) and temporal change (bottom row) in α -diversity across assemblages. Temporal increases are shown by red cells (Kendall's tau correlation values between 0 and +1), declines by blue cells (correlation values between 0 and -1), and cells with significant correlations have a black border. Observations span 1980-2021 for plankton, 1985-2023 for benthos, and 1983-2021 for fish.

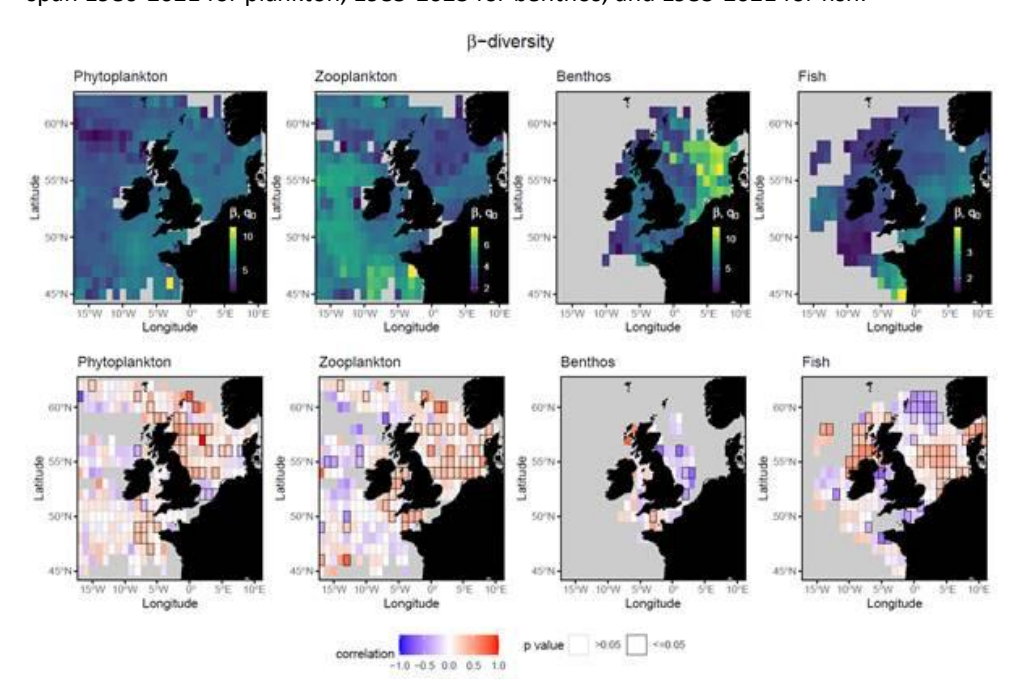


Fig. 4.1.3. Mean (top row) and temporal change (bottom row) in β-diversity across assemblages. Temporal increases are shown by red cells (Kendall's tau correlation values between 0 and +1), declines by blue cells (correlation values between 0 and -1), and cells with significant correlations have a black border. Observations span 1980-2021 for plankton, 1985-2023 for benthos, and 1983-2021 for fish.

4.1.4. Summary

Our analysis of more than 180,000 samples across phytoplankton, zooplankton, benthos, and fish shows that biodiversity in the northeast Atlantic has undergone widespread changes within and across assemblages since the 1980s. The most consistent signal was widespread increases in fish γ -diversity (i.e. regional species richness), with more patchy but generally increasing trends for zooplankton and phytoplankton with changes largely in the North Sea. Benthic time-series were more limited spatially, but show some temporal increases in γ -diversity and α -diversity (i.e. sample scale species richness), with decreasing β -diversity (i.e. differences in species composition between samples). Patterns of α -diversity broadly reflected those of γ -diversity, while β -diversity exhibited contrasting trajectories among assemblages, highlighting the multidimensional nature of biodiversity change across assemblages. We provide a unified, multidimensional biodiversity assessment across marine assemblages using rarefaction and extrapolation based on Hill numbers. This approach corrects for sampling biases and yields comparable α -, β -, and γ -diversity indices across groups.

4.1.5. References

Batten, S. D., Clark, R., Flinkman, J., Hays, G., John, E., John, A. W. G., Jonas, T., Lindley, J. A., Stevens, D. P., & Walne, A. (2003). CPR sampling: the technical background, materials and methods, consistency and comparability. Progress in Oceanography, 58(2–4), 193–215. https://doi.org/10.1016/J.POCEAN.2003.08.004

Chao, A., Chiu, C.-H., Hu, K.-H., van der Plas, F., Cadotte, M. W., Mitesser, O., Thorn, S., Mori, A. S., Scherer-Lorenzen, M., Eisenhauer, N., Bässler, C., Delory, B. M., Feldhaar, H., Fichtner, A., Hothorn, T., Peters, M. K., Pierick, K., von Oheimb, G., & Müller, J. (2024). Hill–Chao numbers allow decomposing gamma multifunctionality into alpha and beta components. Ecology Letters, 27(1), e14336.

Chao, A., Gotelli, N. J., Hsieh, T. C., Sander, E. L., Ma, K. H., Colwell, R. K., & Ellison, A. M. (2014). Rarefaction and extrapolation with Hill numbers: a framework for sampling and estimation in species diversity studies. Ecological Monographs, 84(1), 45–67. https://doi.org/10.1890/13-0133.1

Hsieh, T. C., Ma, K. H., & Chao, A. (2016). iNEXT: an R package for rarefaction and extrapolation of species diversity (Hill numbers). Methods in Ecology and Evolution, 7(12), 1451–1456. https://doi.org/10.1111/2041-210X.12613

Jost, L. (2007). Partitioning diversity into independent alpha and beta components. Ecology, 88(10), 2427–2439. https://doi.org/10.1890/06-1736.1

Lynam, C. P., & Ribeiro, J. (2022). A data product derived from Northeast Atlantic groundfish data from scientific trawl surveys 1983-2020. https://doi.org/https://doi.org/10.14466/CefasDataHub.126

Thompson, M. S. A., Couce, E., Webb, T. J., Grace, M., Cooper, K. M., & Schratzberger, M. (2021). What's hot and what's not: Making sense of biodiversity 'hotspots.' Global Change Biology, 27(3), 521–535. https://doi.org/10.1111/gcb.15443

Tuomisto, H. (2010). A diversity of beta diversities: Straightening up a concept gone awry. Part 1. Defining beta diversity as a function of alpha and gamma diversity. Ecography, 33(1), 2–22. https://doi.org/10.1111/j.1600-0587.2009.05880.x

Wang, S., & Loreau, M. (2014). Ecosystem stability in space: α , β and γ variability. Ecology Letters, 17(8), 891–901. https://doi.org/10.1111/ele.12292

WoRMS Editorial Board. (2020). World Register of Marine Species. https://doi.org/10.14284/170

4.2 Data driven analysis on biodiversity indicators of North Sea invertebrates

Authors: Justin Tiago, Marcel Rozemeijer

Biodiversity indicators provide essential information on the state and dynamics of marine ecosystems, and are increasingly used to inform conservation, management, and policy. Understanding how biodiversity varies across space and time is essential for assessing ecosystem resilience, identifying vulnerable species and habitats, and informing sustainable management. Within the North Sea, benthic communities are subject to multiple anthropogenic and climate pressures, and long-term monitoring surveys offer a unique opportunity to assess trends in biodiversity at multiple spatial and temporal scales (Callaway et al., 2002; Reiss et al., 2010; Kröncke et al., 2011). For this task we applied a suite of empirical biodiversity indicators derived from the ICES Beam Trawl Survey (BTS) between 2000 and 2024. Specifically, we quantified species richness, Pielou's evenness, Shannon and Simpson diversity indices per haul, and beta diversity across ICES rectangles. To examine compositional shifts, we identified the most abundant species per decade and evaluated changes in dominant taxa over time. In addition, we explored relationships between biodiversity patterns and environmental drivers through co-inertia analysis (Dolédec & Chessel, 1994; Dray & Dufour, 2007), linking species composition with gradients in depth, sediment characteristics, trawling effort, temperature, nutrients, and chlorophyll-a. This combination of biodiversity indicators, dominant species trends, and multivariate analyses provides a comprehensive picture of how benthic communities in the North Sea have changed in the 21st century, and of the environmental and anthropogenic factors that structure these communities.

4.2.1. Study area and data availability

This analysis focused on temporal and spatial patterns in biodiversity indicators of North Sea benthic invertebrates, using data from the annual ICES Beam Trawl Survey (BTS) collected between 2000 and 2024. Survey coverage extended from 51°N to 58°N and 3°W to 9°E, encompassing the central and southern North Sea. All invertebrate records were extracted from the ICES DATRAS database for Quarter 3 hauls conducted by the Netherlands, Germany, the United Kingdom, and Belgium. Belgian BTS data for 2000–2009, 2010, and 2016 were excluded due to closed species lists that limited detection of rare taxa. Only epibenthic invertebrates and cephalopods were retained for analysis. For each haul, biodiversity indicators were calculated using the vegan package in R. Indicators included:

- Species richness (number of taxa per haul)
- Pielou's evenness
- Shannon diversity index
- Simpson diversity index
- Beta diversity, calculated as mean Bray—Curtis dissimilarity per ICES rectangle across vears

Spatial patterns in biodiversity indicators were mapped for three time periods (2000–2009, 2010–2019, 2020–2024). Temporal trends were analyzed across the full time series (2000–2024) using generalized additive models (GAMs) fitted with smoothing splines. Furthermore, to examine how environmental variables covaried with species composition, a co-inertia analysis was performed using the ade4 package (Dolédec and Chessel, 1994; Dray and Dufour, 2007). Species abundance data were Hellinger-transformed and ordinated with principal

component analysis (PCA), while environmental covariates (including depth, sediment grain size, orbital current velocity, sea surface temperature, chlorophyll-a, nitrogen, phosphorus, and trawling effort) were standardized. Co-inertia analysis was then applied to quantify the shared co-structure between species and environmental ordinations, with results visualized as biplots. Statistical significance was assessed with Monte Carlo permutation tests (n = 999). All plotting and statistical analyses were performed in R (R Core Team 2025).

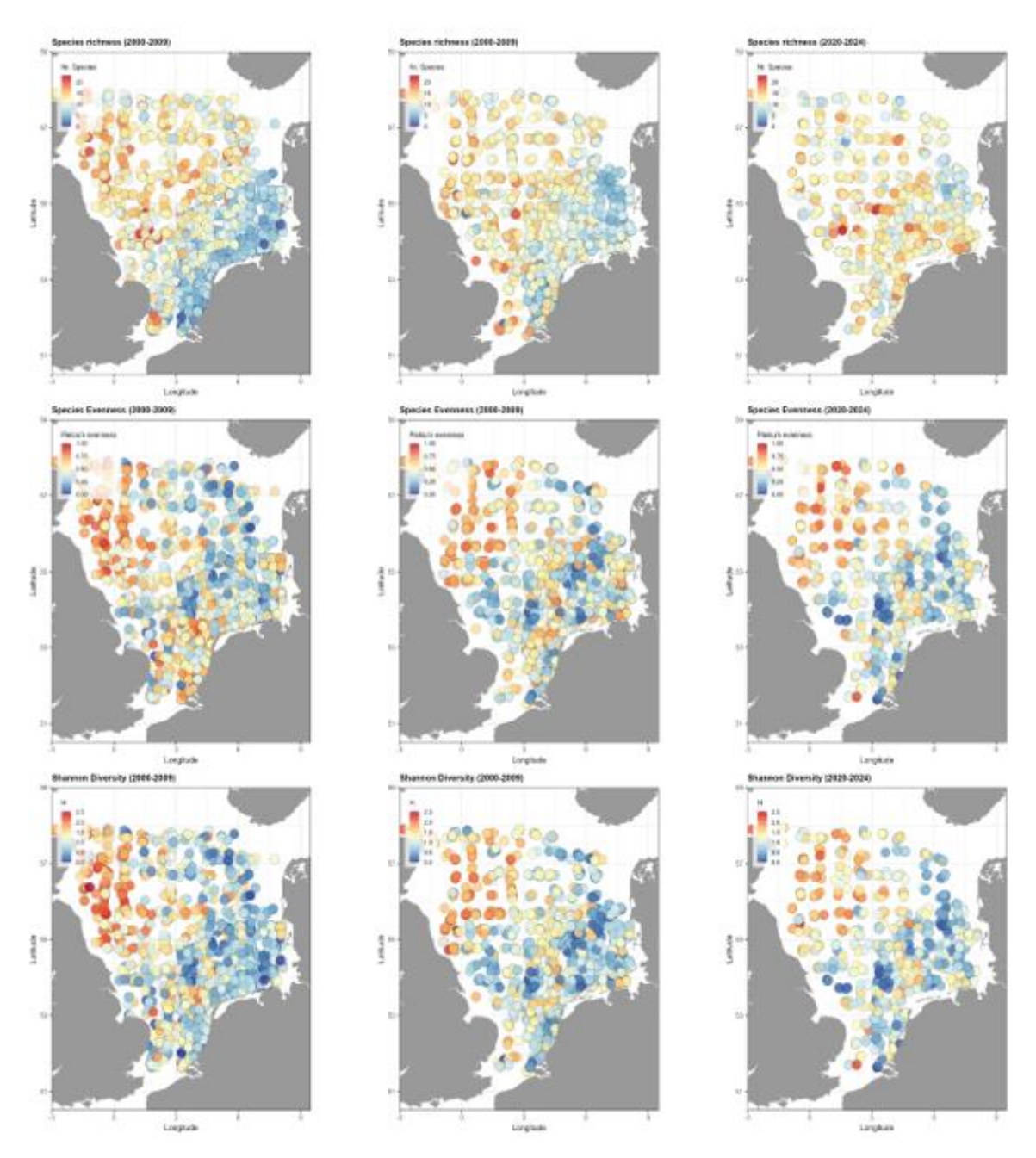


Figure 4.2.1. Maps of North Sea spatial locations for biodiversity indicators: species richness, species evenness, and Shannon diversity, from 2000-2009 (left), 2010-2019 (middle), and 2020-2024 (right).

4.2.2. Results

Spatial patterns of biodiversity indicators showed marked changes in benthic community structure across the North Sea from 2000–2024 (Figure 4.2.1). Species richness was highest in the northern and northwestern North Sea during 2000–2009, while the southern and central basin generally supported lower richness. Over the subsequent decades, richness expanded southward and eastward, such that by 2010-2019 and especially 2020-2024, higher richness was more evenly distributed across the basin, with notable increases in the German Bight and southern coastal areas. Species evenness showed an opposite tendency. Evenness was relatively high across much of the basin during 2000–2009, with particularly strong values in the north and northwest. Over time, however, evenness declined in southern and eastern regions, coinciding with the expansion of richness. By 2020-2024, high evenness remained mostly confined to the northwestern North Sea, while many southern sites showed lower values. Shannon diversity, which integrates richness and evenness, showed persistently high values in the northwestern North Sea across all decades. In contrast, the central and southern North Sea showed more moderate diversity, with limited increases through time.

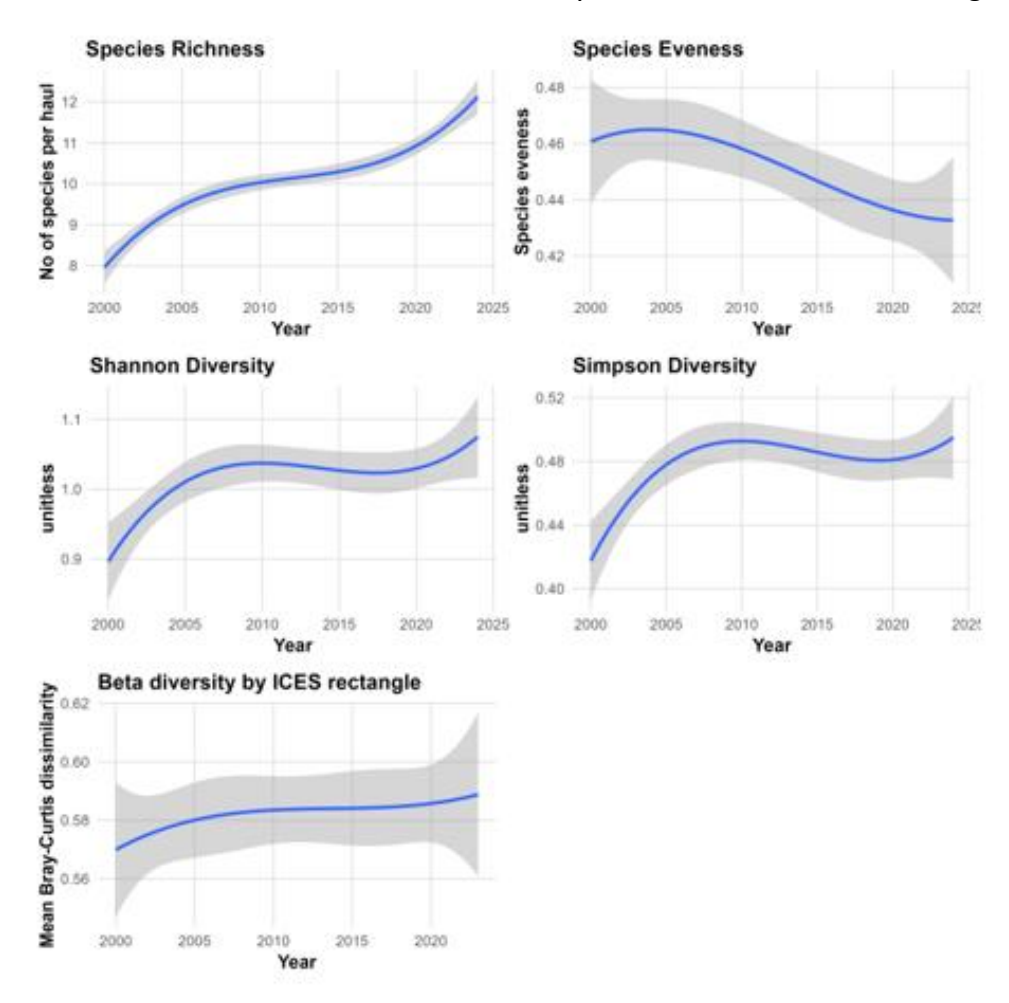


Figure 4.2.1. Temporal trends in biodiversity indicators in North Sea BTS hauls from 2000–2024, based on GAM smoothed splines with 95% confidence intervals (grey shading). Indicators shown are species richness, species evenness, Shannon diversity, Simpson diversity, and beta diversity (mean Bray–Curtis dissimilarity across ICES rectangles).

Time-series analyses of biodiversity indicators revealed clear but contrasting temporal trajectories across the 2000–2024 period (Figure 4.2.2). Species richness increased steadily throughout the time series, rising from an average of ~7–8 species per haul in the early 2000s to >12 species per haul in the most recent years. In contrast, species evenness declined gradually, from around 0.46 in the early 2000s to ~0.43 by 2024. Shannon diversity and Simpson diversity, which combine richness and evenness, both showed initial increases up to ~2010–2012, followed by relative stability and slight fluctuations in recent years. Despite declining evenness, the continued rise in richness appears to have maintained moderate-to-high values of Shannon and Simpson indices through the later years of the series. Finally, beta diversity (mean Bray–Curtis dissimilarity across ICES rectangles) showed a weak but consistent upward trend, indicating a gradual increase in spatial turnover of species composition.

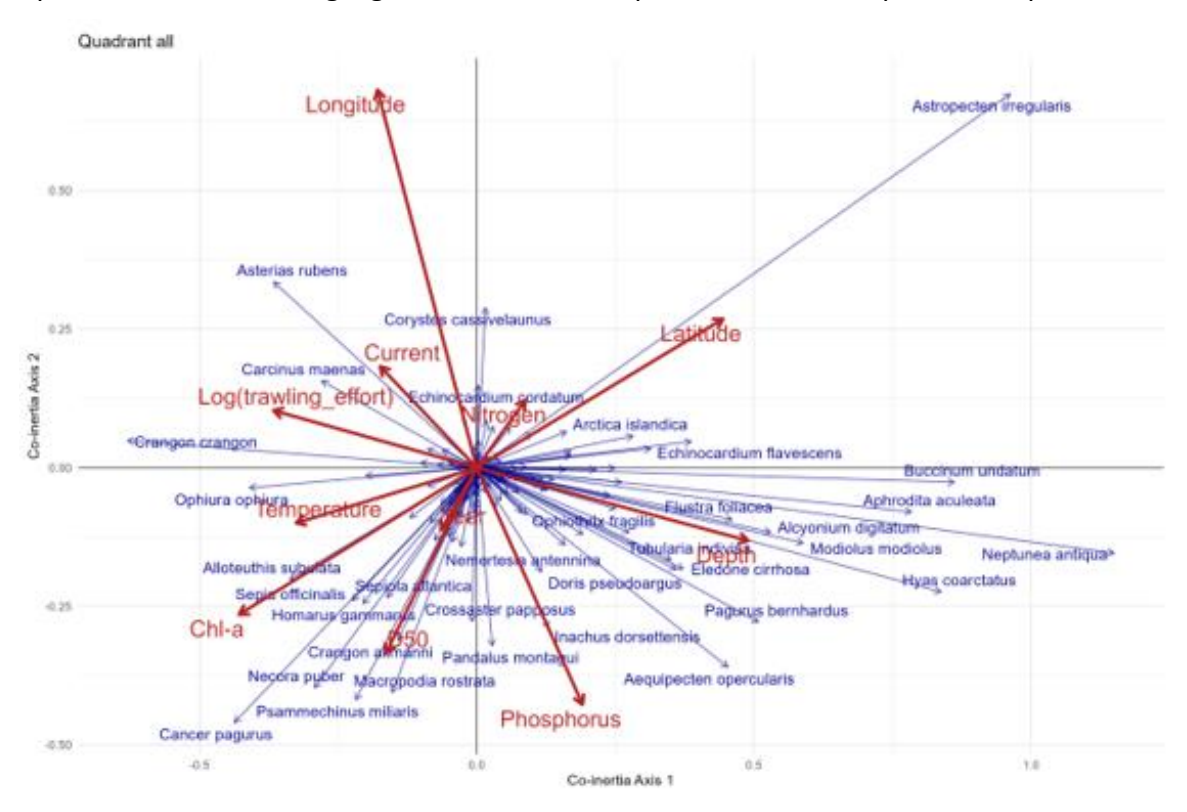


Figure 4.2.3. Co-inertia analysis of relationships between environmental variables (red arrows) and species composition (blue arrows) across the North Sea

A co-inertia analysis was performed to explore the joint structure between species composition and environmental variables across the North Sea (Figure 4.2.3). The analysis revealed a significant overall co-structure (Monte-Carlo test, p = 0.001). The first two axes together explained 88.4% of the total projected inertia (Axis 1: 66.7%; Axis 2: 21.7%). Species and environmental variables were strongly structured along these axes, with a subset of species (e.g. *Carcinus maenas, Ophiura ophiura*) aligning closely with trawling intensity and current speed, while others (e.g. *Alloteuthis subulata, Sepia officinalis*) showed positive association with chlorophyll-a. A distinct cluster of taxa including *Neptunea antiqua, Hyas coarctatus, Buccinum undatum* and *Aphrodita aculeata* were opposed to trawling gradients and instead associated with greater depth. Sediment characteristics (D50) also structured another set of species aligned with sandy habitats (e.g. *Cancer pagarus, Psammechinus miliaris, Necora puber* and others).

The BTS hauls revealed that a small group of benthic species consistently dominated catches across decades (Table 4.2.1). Astropecten irregularis and Asterias rubens were the two most consistently abundant species, appearing at the top of all three time periods. Several other taxa were also common throughout, including Ophiura ophiura, Echinocardium cordatum, Pagurus bernhardus, and Crangon crangon, indicating a core group of widespread and persistent species in the North Sea benthic community. At the same time, there were some temporal shifts in the composition of the most common species. Overall, the results suggest that while the North Sea benthic community is structured around a stable core of dominant species, there are also decadal shifts in the relative prominence of certain taxa, notably a decline in Ophiothrix fragilis and an increase in Spisula subtruncata and Ophiura albida in recent years.

Table 4.2.1. Top ten most abundant species per decade (2000-2024).

Period	Species	Period	Species	Period	Species
	Astropecten irregularis		Astropecten irregularis		Astropecten irregularis
	Asterias rubens		Asterias rubens		Ophiura ophiura
	Ophiothrix fragilis		Ophiura ophiura	-	Asterias rubens
	Ophiura ophiura		Echinosardium cordatum		Spisula subtruncata
2000-2009	Cranzon cranzon	2010-2019	Cranzon cranzon	2020-2024	Esammeshinus miliaris
	Echinosardium cordatum		Pagurus <u>bernhardus</u>		Echinocardium cordatum
	Pandalus montagui		Spisula subtruncata		Pagurus bernhardus
	Pagurus bernhardus		Psammechinus miliaris		Ophiura albida
	Carvstes cassivelaunus		Ophiura albida		Corxstes. cassixelaunus
	Esammeshinus miliaris		Landalus montagui		Crangon crangon

3.7.3. Discussion

Our analysis revealed clear spatio-temporal shifts in benthic biodiversity indicators across the North Sea between 2000 and 2024. The most obvious pattern was the steady increase in species richness, which expanded from northern and northwestern regions into southern and eastern parts of the basin. This redistribution suggests a gradual broadening of species-rich

assemblages away from historically diverse northern areas (Callaway et al., 2002; Frid et al., 2009; Reiss et al., 2010) into coastal and shelf areas of the southern North Sea and the German Bight. This geographical expansion of richness parallels similar findings of climate-associated increases in species richness for North Sea fishes (Hiddink and ter Hofstede, 2008) and predicted north-south benthic distributional shifts under climate change (Weinert et al. 2016). However, this expansion was accompanied by declines in species evenness, particularly in southern and eastern areas. By 2020–2024, these sites supported more species overall, yet communities were increasingly dominated by a smaller subset of taxa. This trade-off was also evident in the Shannon and Simpson diversity indices, which remained relatively stable with rising richness offsetting declines in evenness. The trade-off between increased richness and decreased evenness is consistent with long-term benthic monitoring showing greater community dominance despite overall rising species numbers (Clare et al. 2015; Frid et al. 2009). The persistence of high Shannon diversity in the northwestern North Sea highlights the importance of this region as a long-term reservoir of both richness and balanced community structure. In contrast, the more variable diversity in central and southern regions reflects uneven trajectories, with rising richness but also growing dominance by a few widespread species. Collectively, these patterns indicate that while benthic biodiversity has expanded geographically, communities have become more uneven and heterogeneous. The modest but consistent rise in beta diversity further supports this view, suggesting that differences in community composition among ICES rectangles have become slightly more pronounced over time. The co-inertia analysis provided further insight into how community change aligns with environmental pressures and gradients. The significant shared structure between species composition and environmental covariates indicates that community dynamics are not random but strongly shaped by environmental forcing. Trawling effort and current speed were associated with taxa such as Carcinus maenas and Ophiura ophiura, while high chlorophyll-a and temperatures were linked to certain cephalopod species including Alloteuthis subulata and Sepia officinalis. Depth and sediment characteristics structured another set of species, with taxa such as Neptunea antiqua, Hyas coarctatus, and Buccinum undatum more prevalent in deeper, less disturbed habitats, and others (Cancer pagurus, Psammechinus miliaris) aligned with sandy sediments. Links between trawling disturbance, temperature, and benthic biomass (Rijnsdorp et al. 2020; Tiano et al., 2020; Clare et al. 2021) provide mechanistic support for the observed co-inertia signals. These relationships highlight the role of both anthropogenic (e.g. trawling) and environmental (e.g. productivity, depth, substrate) drivers in shaping benthic assemblages.

The analysis of dominant species further illustrates the balance between stability and change in North Sea benthic communities. A small core group of taxa (*Astropecten irregularis*, *Asterias rubens*, *Ophiura ophiura*, *Echinocardium cordatum*, *Pagurus bernhardus*, *Crangon crangon*) remained abundant throughout the two decades, pointing to their resilience and ecological dominance in the region. However, shifts in the prominence of other taxa, such as the decline of *Ophiothrix fragilis* and *Pandalus montagui*, and the rise of *Spisula subtruncata*, *Psammechinus miliaris*, and *Ophiura albida*, reflect ongoing turnover within the broader community. These changes may reflect climate-driven shifts in temperature tolerance, changes in habitat availability, or responses to fishing pressure and eutrophication. Taken together, our results suggest that North Sea benthic communities are undergoing a process of redistribution and restructuring. Richness has increased and spread into new areas, but this expansion is often accompanied by reduced evenness and subtle increases in spatial turnover.

Core species remain widespread, but changes in the prominence of secondary taxa indicate that communities are not static. This has implications for ecosystem resilience: while higher richness may buffer communities against disturbance, declining evenness and increasing dominance can reduce functional redundancy and make systems more vulnerable to specific pressures. The strong links observed between community composition and environmental drivers further highlight the need to consider both anthropogenic pressures and natural gradients when assessing benthic biodiversity risk.

3.5.6. **Summary**

This analysis shows that benthic biodiversity in the North Sea has undergone substantial changes in the previous two decades. Species richness has increased and spread into southern and coastal regions, while evenness has declined, indicating a trend toward more uneven community structures dominated by a subset of taxa. Diversity in the northwestern North Sea has remained comparatively stable, reinforcing its historical pattern of supporting balanced and diverse benthic assemblages (Reiss et al., 2010). A small set of core species persisted throughout the study, but decadal changes in other taxa suggests the gradual turnover within communities. Multi-variate co-inertia analysis further demonstrated strong links between species composition and environmental drivers, including trawling, depth, sediment, and productivity. These findings suggest that North Sea benthic ecosystems are simultaneously expanding in richness and diversifying geographically, but are also becoming more uneven. This pattern has important implications for ecosystem functioning and resilience, supporting the need to account for both anthropogenic pressures and natural gradients in future management and conservation strategies.

3.7.6. References

Callaway, R., Alsvåg, J., de Boois, I., Cotter, J., Ford, A., Hinz, H., Jennings, S., Kröncke, I., Lancaster, J., Piet, G., Prince, P., & Ehrich, S. (2002). Diversity and community structure of epibenthic invertebrates and fish in the North Sea. *ICES Journal of Marine Science*, 59(6), 1199–1214. https://doi.org/10.1006/jmsc.2002.1288

Clare, D. S., Robinson, L. A., & Frid, C. L. J. (2015). Community variability and ecological functioning: 40 years of change in the North Sea benthos. *Marine Environmental Research*, 107, 24-34. https://doi.org/10.1016/j.marenvres.2015.03.012

Clare, D. S., Robinson, L. A., & Birchenough, S. N. R. (2021). A temperature-dependent relationship between benthic invertebrate biomass and trawling pressure. *ICES Journal of Marine Science*, 78(1), 82–88. https://doi.org/10.1093/icesjms/fsaa191

Dolédec, S., & Chessel, D. (1994). Co-inertia analysis: an alternative method for studying species—environment relationships. *Freshwater Biology*, 31(3), 277–294. https://doi.org/10.1111/j.1365-2427.1994.tb01741.x

Dray, S., & Dufour, A.-B. (2007). The ade4 package: Implementing the duality diagram for ecologists. *Journal of Statistical Software*, 22(4), 1–20. https://doi.org/10.18637/jss.v022.i04

Hiddink, J. G., & ter Hofstede, R. (2008). Climate-induced increases in species richness of marine fishes. *Global Change Biology*, *14*(3), 453-460. https://doi.org/10.1111/j.1365-2486.2007.01518.x

Frid, C. L. J., Garwood, P. R., & Robinson, L. A. (2009). The North Sea benthic system: a 36 year time-series. Journal of the Marine Biological Association of the United Kingdom, 89(1), 1-10. https://doi.org/10.1017/S0025315408002956 Kröncke, I., Reiss, H., Eggleton, J. D., Aldridge, J., Bergman, M. J. N., Cochrane, S., Craeymeersch, J. A., Degraer, S., Desroy, N., Dewarumez, J. M., Duineveld, G. C. A., Essink, K., Hillewaert, H., Lavaleye, M. S. S., Moll, A., Nehring, S., Newell, R., Oug, E., Pohlmann, T., Rachor, E., & Rees, H. L. (2011). Changes in North Sea macrofauna communities and species distribution between 1986 and 2000. *Estuarine, Coastal and Shelf Science*, 94(1), 1-15. https://doi.org/10.1016/j.ecss.2011.04.008

Jetz, W., McGeoch, M. A., Guralnick, R., Ferrier, S., Beck, J., Costello, M. J., Fernandez, M., Geller, G. N., Keil, P., Merow, C., Meyer, C., Muller-Karger, F. E., Pereira, H. M., Regan, E. C., Schmeller, D. S., & Turak, E. (2019). Essential biodiversity variables for mapping and monitoring species populations. *Nature Ecology & Evolution*, 3, 539–551. https://doi.org/10.1038/s41559-019-0826-1

Reiss, H., Degraer, S., Duineveld, G. C. A., Kröncke, I., Aldridge, J., Craeymeersch, J., Eggleton, J. D., Hillewaert, H., Lavaleye, M. S. S., Moll, A., Pohlmann, T., Rachor, E., Robertson, M., vanden Berghe, E., van Hoey, G., & Rees, H. L. (2010). Spatial patterns of infauna, epifauna, and demersal fish communities in the North Sea. *ICES Journal of Marine Science*, 67, 278–293.

R Core Team. (2025). R: A language and environment for statistical computing (Version 4.4.1). R Foundation for Statistical Computing. https://www.R-project.org/

Rijnsdorp, A. D., Depestele, J., Eigaard, O. R., Hintzen, N. T., Ivanović, A., Molenaar, P., et al. (2020). Mitigating seafloor disturbance of bottom trawl fisheries for North Sea sole (Solea solea) by replacing mechanical with electrical stimulation. *PLOS ONE*, 15(11), e0228528. https://doi.org/10.1371/journal.pone.0228528

Tiano J.C., S. O'Flynn, K.J. van der Reijden, T. Ysebaert, K. Soetaert, (2020). Experimental bottom trawling finds resilience in large-bodied infauna but vulnerability for epifauna and juveniles in the Frisian Front, *Marine Environmental Research*, 159, July 2020 104964. doi.org/10.1016/j.marenvres.2020.104964

Weinert, M., Mathis, M., Kröncke, I., Neumann, H., Pohlmann, T., & Reiss, H. (2016). Modelling climate change effects on benthos: Distributional shifts in the North Sea from 2001 to 2099. *Estuarine, Coastal and Shelf Science*, 175, 157-168. https://doi.org/10.1016/j.ecss.2016.03.024

4.3 Data driven analysis on fish biodiversity in the Iberian Coasts

Authors: Sofia Henriques, André Martins, Corina Chaves, Rita Vasconcelos, Teresa Moura

4.3.1. Study area and data availability

In the Iberian coast, demersal communities (mostly fish but also some invertebrate species) were sampled with a bottom otter trawl during the Portuguese Autumn Groundfish Survey (International Bottom Trawl Survey) that takes place along the Portuguese continental waters from 20 to 500 m depth (more details in ICES, 2017). The time periods 2005-2011, 2013-2018 and 2021-2023 were considered for the analysis of spatial and temporal patterns and changes of taxonomic and functional diversity of demersal communities of the Iberian Coast. For the analysis of functional diversity, the following traits were used to characterize each species caught: age at first maturity, body length, maximum depth, fecundity, trophic level, vertical biological zone (bathydemersal, bathypelagic, demersal, benthopelagic, pelagic-neritic, pelagic-oceanic, reef-associated), thermal tolerance (0-2.5, 2.5-5, 5-7.5, 7.5-10, 10-15, >15), mobility (sedentary, territorial, moderately mobile, highly mobile), diet (generalist, benthivorous, herbivorous, piscivorous, planktivorous). Data sources used for characterizing species traits were: Beukhof et al. 2019, Rfishbase (Boettiger et al. 2006), Henriques 2008, Henriques 2013, Polo et al. 2024,, Koutsidi et al. 2019, Butt et al. 2022, and finally expert judgement to fill gaps. Three taxonomic diversity indices (species richness, Shannon diversity index, Pielou evenness index) and two functional diversity indices (functional richness and functional evenness) were used. Functional diversity indices were computed using Gower

distance, due to the use of both continuous and categorical/ordinal traits, with R package mFD (Magneville et al. 2022).

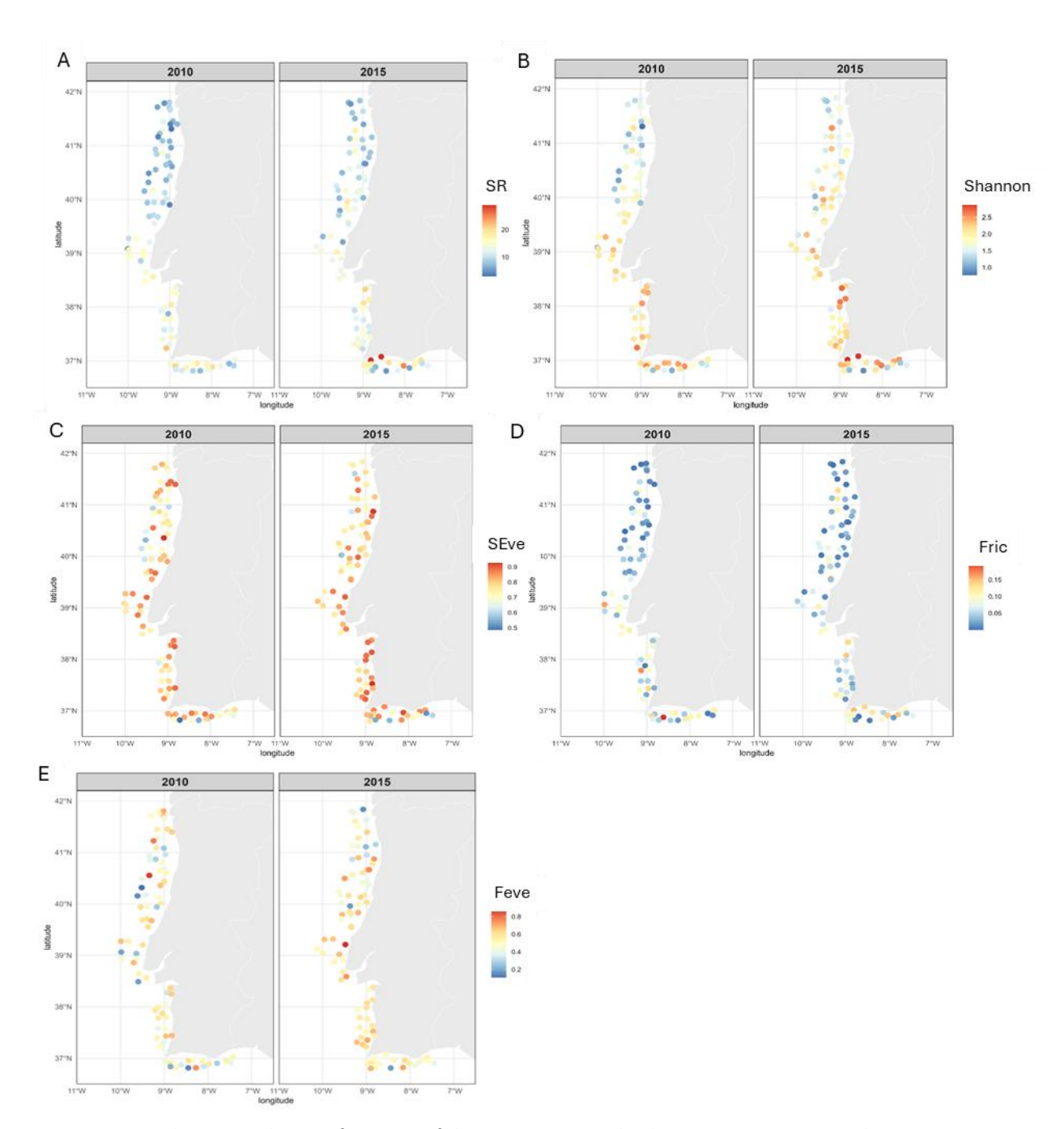


Figure 4.3.1. Biodiversity indicators for marine fish communities in the Iberian Coast in 2010 and 2015 including: Species Richness (A), Shannon Wiener evenness (B), Pielou evenness (C), as well as the functional diversity indices functional richness (D) and functional evenness (E).

4.3.2. Results

Species richness generally decreased from higher to lower latitudes along the Iberian coast, which is in agreement with macroecological patterns for marine communities globally (Figure 4.3.1A). The large-scale spatial pattern of Shannon diversity throughout the Iberian coast was quite similar to the spatial pattern of species richness (Figure 4.3.1B). On the other hand,

Pielou evenness index did not show an evident latitudinal pattern of spatial variation (Figure 4.3.1C). Functional richness also generally showed a decrease from higher to lower latitudes along the Iberian coast, though less evident than for species richness (Figure 4.3.1D). Similarly to taxonomic evenness, functional evenness did not show an evident latitudinal pattern of spatial variation (Figure 4.3.1E).

4.3.3. References

C. Boettiger, D. T. Lang and P. C. Wainwright (2012). rfishbase: exploring, manipulating and visualizing FishBase data from R. Journal of Fish Biology 81(6), pp. 2030-2039. DOI: 10.1111/j.1095-8649.2012.03464.x

Beukhof E., Dencker T. S., Palomares M. L. D. and Maureaud A. (2019): A trait collection of marine fish species from North Atlantic and Northeast Pacific continental shelf seas [dataset]. PANGAEA, https://doi.org/10.1594/PANGAEA.900866

Henriques S. (2008) Comparative analysis of the efficacy of multimetric indices based on fish communities in order to assess the ecological quality of coastal waters. MSC Thesis. Faculty of Sciences of the University of Lisbon. http://hdl.handle.net/10451/1404

Henriques S. (2013) Marine fish assemblages as indicators of anthropogenic pressures:identifying sensitive metrics. PhD Thesis. University of Lisbon. http://hdl.handle.net/10451/8913

ICES (2017). Manual of the IBTS North Eastern Atlantic Surveys. Series of ICES Survey Protocols SISP 15. 92 pp. http://doi.org/10.17895/ices.pub.3519

Magneville C., Loiseau N., Albouy C., Casajus N., Claverie T., Escalas A., Leprieur F., Maire E., Mouillot D. and Villéger S. (2022). mFD: an R package to compute and illustrate the multiple facets of functional diversity. Ecography, 2022(1).

Polo J., López-López L., Engelhard G.H., Punzón A., Hidalgo M., Rutterford L.A., Bariáin M.S., González-Irusta J.M., Esteban A., García, E. Vivas, M. and Pecuchet L. (2025, Trait-Based Indicators of Marine Communities' Sensitivity to Climate Change and Fishing. Diversity and Distributions, 31: e13959. https://doi.org/10.1111/ddi.13959

Koutsidi M., Moukas C. and Tzanatos E. (2020) Trait-based life strategies, ecological niches, and niche overlap in the nekton of the data-poor Mediterranean Sea. Ecol Evol. 10: 7129–7144. https://doi.org/10.1002/ece3.6414

Butt N., Halpern B.S., O'Hara C.C., Allcock A.L., Polidoro B., Sherman S., Byrne M. et al. 2022. A Trait-Based Framework for Assessing the Vulnerability of Marine Species to Human Impacts. Ecosphere 13(2): e3919. https://doi.org/10.1002/ecs2.3919

5. Summary and perspectives

The statistical modelling of marine species distribution, composition and overall diversity featured within this deliverable report represent a broad range of marine ecosystems and organisms sampled along European shelf seas from the Eastern Mediterranean Sea to Greenland and Barents Sea. Consequently, the organisms and areas considered are exposed to very different regional and local environmental conditions, both in terms of climate and hydrography, but also with regards to the type and level of human activities and their associated pressures. Furthermore, the model development relies on available monitoring data that may differ in terms of the spatio-temporal extent, as well as the amount and resolution of species occurrence and abundances data and their associated trait information. Despite these differences, the model results generated allows us to compare key outputs across areas and organism groups, as well as between more local or regional applications of the model framework. Below we briefly elaborate on outcomes in terms of the underlying drivers and responses of species to environmental conditions, as well as the overall patterns and trends in a number of biodiversity indicators (i.e., representing EBVs useful for informing MSP in general and placement of MPAs in particular). For a more detailed discussion regarding findings in each area and the relation to previous studies on the region and organism group in question we refer the readers to the discussion in each sub-section of chapter 3 and 4.

In terms of environmental drivers we found that ocean climate and hydrography are primary determinants of species distributions and community composition (Table 5.1). Among these bottom temperature stands out as a key predictor throughout most areas with species responding both positively and negatively to increasing temperature, reflecting that community composition is generally composed of a broad range of species with different tolerances to the range of temperature variation within each area. Hence, while the mean temperature and degree of seasonality various markedly along the pronounced latitudinal gradient from sub-tropical to temperate and sub-polar conditions, the regional communities generally contain a mix of species adapted to relatively warmer or colder waters. In addition to the broad and ubiquitous effect of temperature, we found a number of environmental variables with more regional and local impacts, conditioned on the specific conditions of each study area. For instance, depth was found a strong determinant of species distribution and composition, especially in areas where monitoring surveys cover both the continental shelf, as well as the shelf break towards greater depths (e.g., Iceland, Mediterranean). Consequently, community composition contains a mix of taxa with either more shallow or deeper depth distributions as reflected by their different affinities and responses to depth. Salinity was also found a key determinant of species distributions and composition but mainly in the Baltic Sea where the pronounced gradient from marine to brackish conditions cause a sharp decline in overall richness and composition. Other examples include ice cover which was found a strong determinant of species distribution only in the sub-polar Barents Sea. Taken together, the broad range of studies indicate that environmental filtering, conditioned on drivers and conditions operating across both larger and local spatial scales is a primary community assembly process determining the past, current, but also future distribution and composition of marine organisms throughout European Seas. However, while a large degree of variation in species distribution and abundance can be explained by the set of environmental conditions included, the importance of spatial random effects across our models underscore the importance of other drivers and assembly processes. These include a

range of largely unmeasured environmental covariates not yet accounted for in our modelling setup, but also potential biotic effects channelled through competitive or predator-prey interactions. Hence, we recommend further efforts compiling long-term and high-quality data on such candidate drivers (e.g., fine-scaled habitat and fishing effort information resolved by gears and over longer time horizons), but also stress the need for a better understanding of the role and relative importance of local biotic interactions, partly reflected by the pair-wise residual associations, reflecting species found more or less frequently than expected from their environmental affinities.

The set of biodiversity indicators estimated from the fitted and validated models, or from data analysis, include both species and community EBVs (i.e., reflecting the overall taxonomic and functional richness, evenness and dispersion). These indicators show marked spatial variation in terms of patterns and trends both within and among regions and metrics. Overall, the metrics of taxonomic and functional richness are interlinked and therefore show generally similar spatial patterns and gradients across areas. However, the latter is generally less constrained in space with higher values over larger areas, indicating that the presence and composition of traits can be conserved, despite absences or declines of individual species. The metric of evenness show generally different, or even opposite spatial patterns compared to richness. This suggests that areas and local assemblages with relatively high number of species and traits are often composed of both highly abundant and very rare taxa, leading to pronounced differences in densities and therefore a larger degree of dominance and lower evenness. In terms of temporal trends, we observe similar differences between metrics within and across areas. For instance, many regions (e.g., North Sea, North-East Atlantic) show increasing taxonomic and functional richness, especially towards higher latitudes, but often with declining community evenness, suggesting an increasing dominance by a few species. While the time frame of the presented analysis is generally constrained to the most recent decade(s), our findings show recent responses to climate variability and change in many areas, reflecting underlying changes in the distribution and composition of species in response to warming. Taken together, the differences and similarities in patterns and trends among EBVs may challenge end-users and managers involved in MSP and MPA planning, especially since hotspots or broader regions of "high biodiversity" may seem contingent on the set of indicators and metrics considered. Hence, we will advocate and adopt a broader and holistic perspective aiming to embrace this complexity when identifying candidate locations and areas for protection under different scenarios of change. This will be followed up in WP5-WP6 and will involve the joint considerations across a suite of both community and species EBVs (for instance reflecting taxa of particular conservation status), combined with more composite metrics and indicators, such as Hill numbers.

Finally, the overall performance and explanatory power of the models are generally well capable of representing and explaining the past and current distributions of species in terms of occurrence, as reflected by high values of overall AUC (~0.9). However, the models are generally worse in terms of explain variation in species abundance or biomasses (r2~0.2 to 0.4), likely due to an inadequate representation of key processes that regulate the productivity and population dynamics of species, notably growth, reproduction and survival. Despite the lower performance of predicting biomass, it is likely less of an issue in terms of overall biodiversity predictions. This because most of the indicators rely either on presence-absence

predictions only (e.g., richness), or account for relative biomasses in their estimation (e.g., evenness), rather than the absolute values predicted by the model. Besides, the modelling framework used provide standard errors for all predicted variables, allowing for formal sensitivity testing and accounting for uncertainty in model predictions. Taken together we are confident that the models provides not only increased process understanding of the drivers and assembly rules structuring marine communities, but also a means to predict, visualize and map patterns and changes in overall EBVs relevant for conservation and protection within the broader context of MSP under the upcoming WP5-WP6.

Table 4.1. Summary of key results of modelling representing individual analysis carried out on selected organisms groups and regions.

Area	Group	# of taxa	Method	Skill	Drivers	Patterns	Trends
NE Atlantic	Fish	151	JSDM	0.91 (AUC) 0.21 (R2)	Temp> Chla> Salinity	Highly variable between regions and metrics	Variable, increase/decrease in SR and Fric towards higher/lower latitudes
North Sea	Fish	67	JSDM	0.89 (AUC) 0.20 (RMSE)	Temp>> Shla> Fishing	Variable across metrics, difference between N (higher) and S (lower)	Variable, weak trends (short time frame)
Baltic Sea	Fish	78	JSDM	0.93 (AUC) 0.43 (R2)	Salinity> Depth> Temp	Variable across metrics, decline from W to E	Variable, slight increase in W, decline in E
Baltic Sea	Benthos	143	JSDM	0.91 (AUC)	Sal>> Oxygen> Temp	Variable across metrics, decline from W-E	Variable, but generally weak positive trends across metrics
Iceland	Fish	82	JSDM	0.93 (AUC) 0.37 (R2)	Depth>> Temp>	Variable across metrics, difference between N and S and on-/ offshore	Variable, but <u>slight</u> <u>increase</u> in N
Central/ East Med. Sea	Fish, Decapod, Ceph.	120, 18, 20	JSDM	0.89 (AUC) 0.24 (R2)	Depth>> Temp> Salinity	Variable across metrics, highest Eggan Sea	Variable, slight general decline in richness and evenness
West Med. Sea	Fish, Decapod, Cepb.	146, 21, 24	JSDM	0.89 (AUC) 0.24 (R2)	Temp> Seabed> Salinity	Variable across metrics, difference W- E and on-/offshore	Variable, no overall trends across metrics
Barents Sea	Fish	88	JSDM	0.86 (AUC) 0.29 (R2)	Temp> Depth> Salinity> Sea ice	Variable, difference between N and S (in terms of alpha and beta diversity)	No trends
Greater North Sea	Phytopl, Zoopl, Benthos, Fish	All obs. In survey	Data driven	NA	No analysis	Variable across groups, difference between Atlantic and North Sea	General increase in North Sea, slight decline in Atlantic (gamma)
North Sea	benthos	All obs. In survey	Data driven	NA	Fishing, currents, depth, Chi	Marked difference between N (high) and S (low)	Variable, general increase in S part (at least for species richness and shannon).
Iberian Coast	Fish	All obs. In survey	Data driven	NA	No analysis	Variable, <u>slight</u> <u>difference</u> between N (lower) <u>and S</u> (higher)	No general trend (short duration)

6. Appendices

The *Appendices* linked to this report comprise auxiliary material regarding data and modelling for each of the sections presenting model results for different areas and organism groups.

Version History

	HISTORY OF CHANGES						
Version	Date	Changes					
1	01/06/2025	Report structure and core text: Martin Lindegren					
2	15/09/2025	Updated version including contributions from all co- authors					
3	30/09/2025	Final version prepared for upload (by Martin Lindegren)					

Appendix 1. North East Atlantic fish model

Table A.1. Bottom trawl surveys included in the study.

Survey	Area	Year	Months	Number of Hauls	Source	Reference
EVHOE	Bay of Biscay & Celtic Sea	1997 - 2021	OctDec.	3415	(ICES, 2022)	(ICES, 1997)
FR-CGFS	English channel	1998 - 2021	SepNov.	911	(ICES, 2022)	(ICES, 2017)
Gre-GFS	Greenland	1989 - 2020	SepDec	3.121	N/A	(Fock, 2007)
Ice-GFS	Iceland	1989 - 2021	FebApr.	18.542	N/A	(Sólmundsson et al., 2010)
IE-IGFS	Ireland Shelf Sea	2003 - 2021	SepDec.	3.037	(ICES, 2022)	(ICES, 2017)
NIGFS	Northern Ireland	2006 - 2021	FebApr, Oct Nov.	1.589	(ICES, 2022)	(ICES, 2017)
Necells	Norwegian Sea, Barents Sea and northern North Sea	1989 - 2017	JanDec.	29.993	(Institute of Marine Research, 2021)	(Mjanger et al., 2006)
NS-IBTS	North Sea	1989 - 2021	JanMar., Jun Sep.	18.959	(ICES, 2022)	(ICES, 2020)
PT-IBTS	Portugal shelf sea	2002 - 2021	SepNov.	1.100	(ICES, 2022)	(ICES, 2017)
ROCKALL	Rockall plateau	1999 - 2020	AugSep.	779	(ICES, 2022)	(ICES, 2017)
SP-ARSA	Gulf of Cadiz	1996 - 2020	FebApr., Oct Dec.	1.419	(ICES, 2022)	(ICES, 2017)
SP-NORTH	Cantabrian Sea	1990- 2021	AugNov.	3.433	(ICES, 2022)	(ICES, 2017)
SWC-IBTS	Scotland Shelf Sea	1989 - 2021	FebApr., Oct Dec.	3.731	(ICES, 2022)	(ICES, 2017)
TOTAL				90.029		

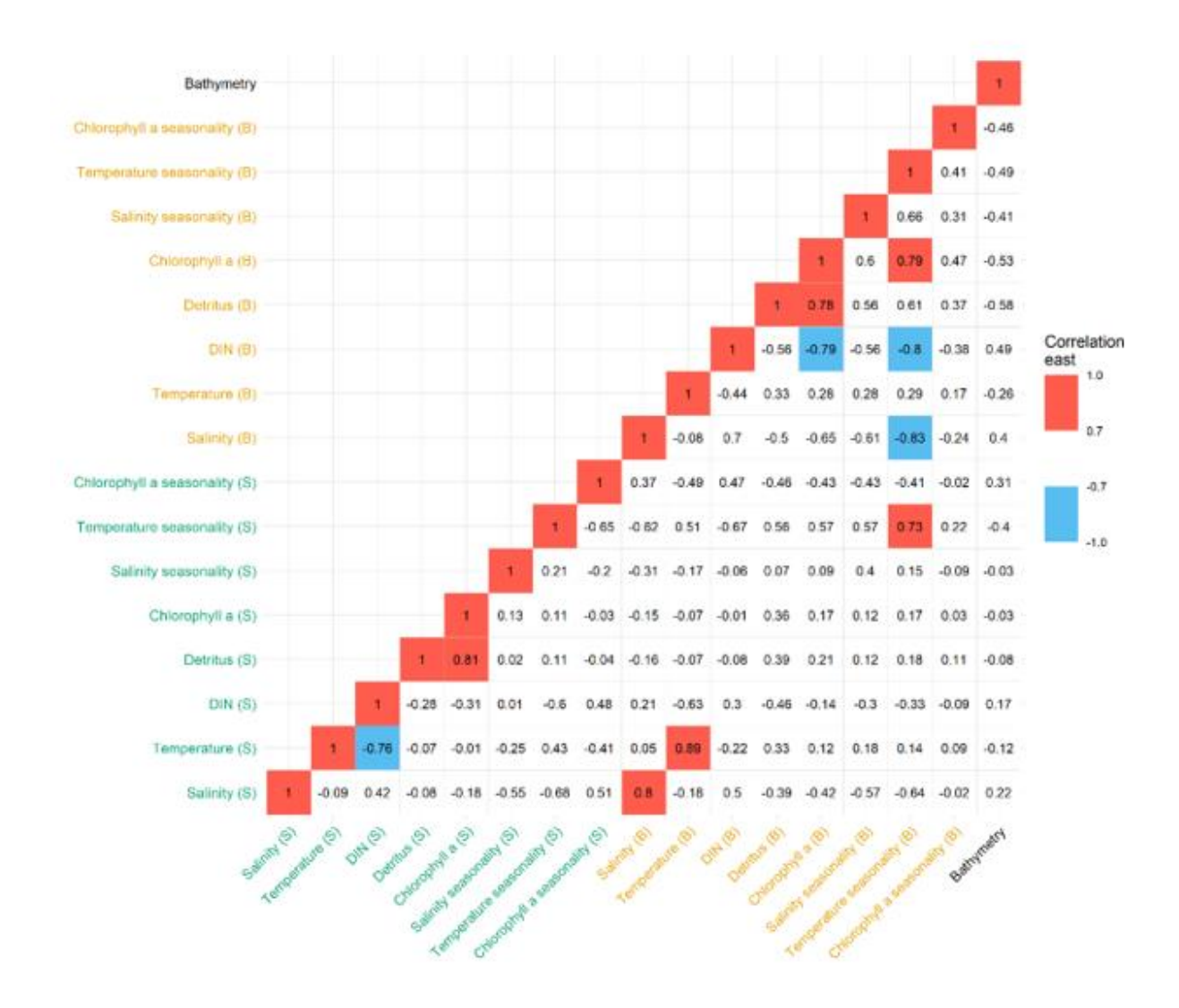


Figure S1. Correlation matrix between candidate environmental variables. Highly positively correlated variables (> 0.7) are shown in red; highly negatively correlated variables (< -0.7) in blue. Variable label colors denote whether the variable is from the sea surface (green), sea bottom (orange) or where this distinction is not applicable (black).

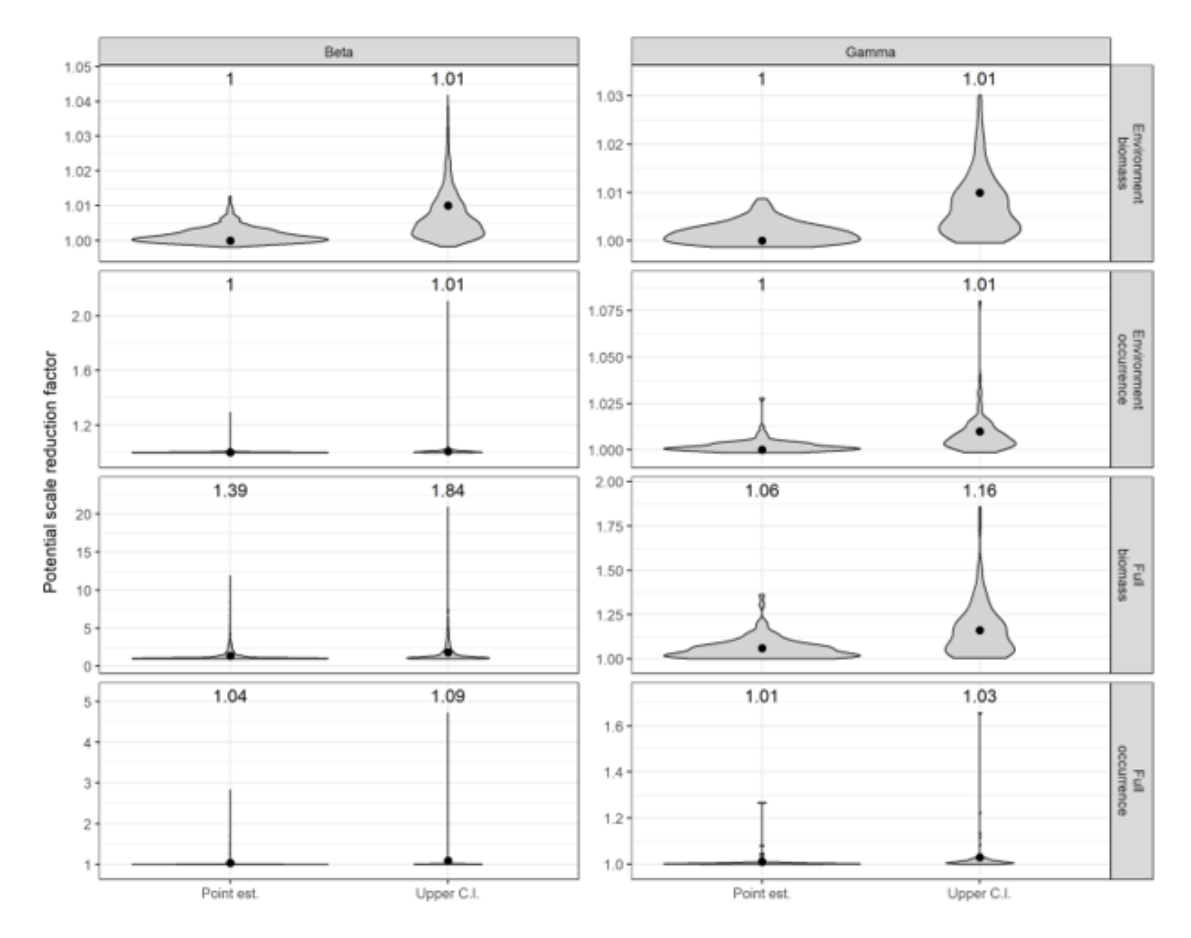


Figure S2. Whole-period models MCMC convergence from the Beta (left column) and Gamma (right column) parameters. Each row shows each model's distribution of the potential scale reduction factor values and its mean (value at the top of each panel) for the point estimate and the upper confidence interval.

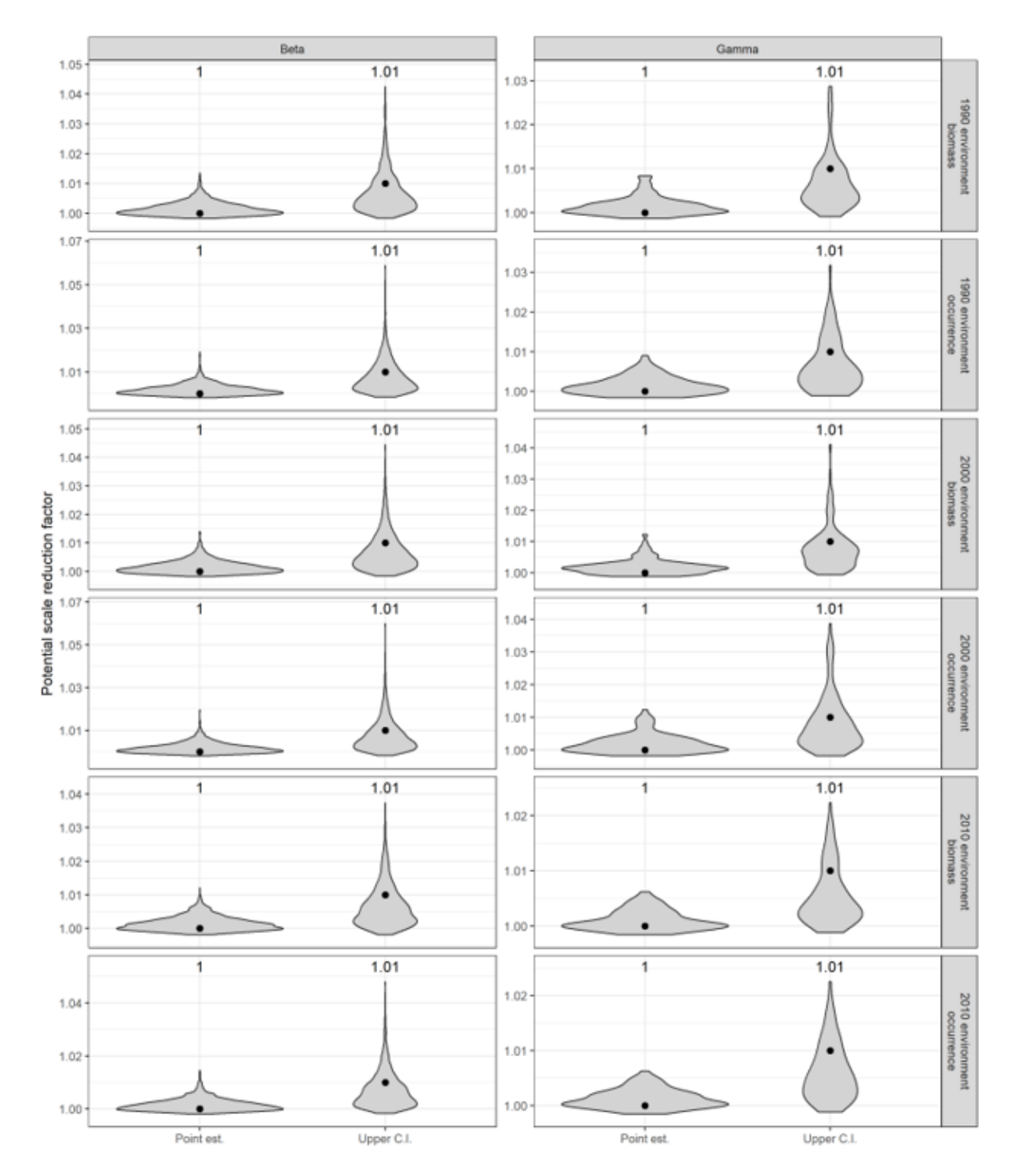


Figure S1. Decade models MCMC convergence from the Beta (left column) and Gamma (right column) parameters. Each row shows each model's distribution of the potential scale reduction factor values and its mean (value at the top of each panel) for the point estimate and the upper confidence interval.

Supplementary sources and references:

Fock, H. O. (2007). Driving-forces for Greenland offshore groundfish assemblages: Interplay of climate, ocean productivity and fisheries. Journal of Northwest Atlantic Fishery Science, 39, 103–118. https://doi.org/10.2960/J.v39.m588

Gurvan, M., Bourdallé-Badie, R., Chanut, J., Clementi, E., Coward, A., Ethé, C., Iovino, D., Lea, D., Lévy, C., Lovato, T., Martin, N., Masson, S., Mocavero, S., Rousset, C., Storckey, D., Müeller, S., Nurser, G., Bell, M., Samson, G., ... Moulin, A. (2022). NEMO ocean engine. In Note du Pôle de modélisation. https://doi.org/10.5281/zenodo.1464816

ICES. (1997). The EVHOE survey (France). In ICES documents.

ICES. (2017). Manual of the IBTS North Eastern Atlantic Surveys. In Series of ICES Survey Protocols SISP 15. http://doi.org/10.17895/ices.pub.3519

ICES. (2020). Manual for the North Sea International Bottom Trawl Surveys. In Series of ICES Survey Protocols: Vol. SISP 10-IB (p. 102). https://doi.org/10.17895/ices.pub.7562

ICES. (2022). Database of Trawl Surveys (DATRAS).

https://datras.ices.dk/Data_products/Download/Download_Data_public.aspx

Institute of Marine Research. (2021). IMR bottom trawl data 1980-2020. https://doi.org/10.21335/NMDC-328259372

Mjanger, H., Hestenes, K., Olsen, E., Svendsen, B. V., & De Lange Wenneck, T. (2006). Manual for sampling of fish and crustaceans.

Sólmundsson, J., Steinarsson, B. Æ., Jónsson, E., Karlsson, H., Björnsson, H., Pálsson, J., & Bogason, V. (2010). Manuals for the Icelandic bottom trawl surveys in spring and autumn (Enskar útgáfur handbóka stofnmælinga með botnvörpu að vori og hausti). Fjölrit nr. 156. https://www.hafogvatn.is/static/research/files/fjolrit-156.pdf

Yool, A., Popova, E. E., & Anderson, T. R. (2013). MEDUSA-2.0: An intermediate complexity biogeochemical model of the marine carbon cycle for climate change and ocean acidification studies. Geoscientific Model Development, 6(5), 1767–1811. https://doi.org/10.5194/gmd-6-1767-2013

Appendix 2. North Sea fish model

Table S1: Categories of biological traits used to assess functional composition.

Trait	Categories	Label	Description
Growth coefficient (K)	Continuous	log_growth	Growth coefficient K estimated from the Von Bertalanffy equation
Fecundity	Continuous	log_fecundity.	Number of offspring per female per batch or per year
Offspring size	Continuous	log_offspring_size	Diameter if the released eggs, length of the egg case or length of the young (mm)
Maximum length	Continuous	log_length.max	Maximum reported length
Age at maturity	Continuous	log_age_maturity	First age at which the individual is able to reproduce
Habitat	Bathydemersal Bathypelagic	habitatbathydemersal habitatbathypelagic	Zone of the water column used by the species

	Benthopelagic	habitatbenthopelagic	
	Demersal	habitatdemersal	
	Pelagic	habitatpelagic	
	Reef-associated	habitatreef-associated	
Feeding mode	Benthivorous	feeding.modebenthivorous.	Main food source from stomach contents and
	Herbivorous	feeding modeherbivorous	biological descriptions of
	Generalist	feeding modegeneralist	adults
	Piscivorous	feeding modepiscivorous	
	Planktivorous	feeding modeplanktivorous	
Body shape	Compressiform.	body.shapecompressiform	Shape of the body
	Eel-like	body shapeeel-like	
	Elongated	body.shapeelongated	
	Flat	body.shapeflat	
	Fusiform	body.shapefusiform	
	Short and/or deep	body shapeshort and/or deep	
Fin shape	Pointed	fin.shapepointed	Shape of the caudal fin
	Rounded	fin.shaperounded	
	Truncate	fin.shapetcuncate	
	Lunate	fin.shapelunate	
	Heterocercal	fin.shapeheterocercal	
	Forked	fin_shapeforked	
Spawning type	Guarder	spawning.typeguarder	Type of spawning related to
	Non-guarder	spawning typenon-guarder	parental care
	Bearer	spawning typebearer	

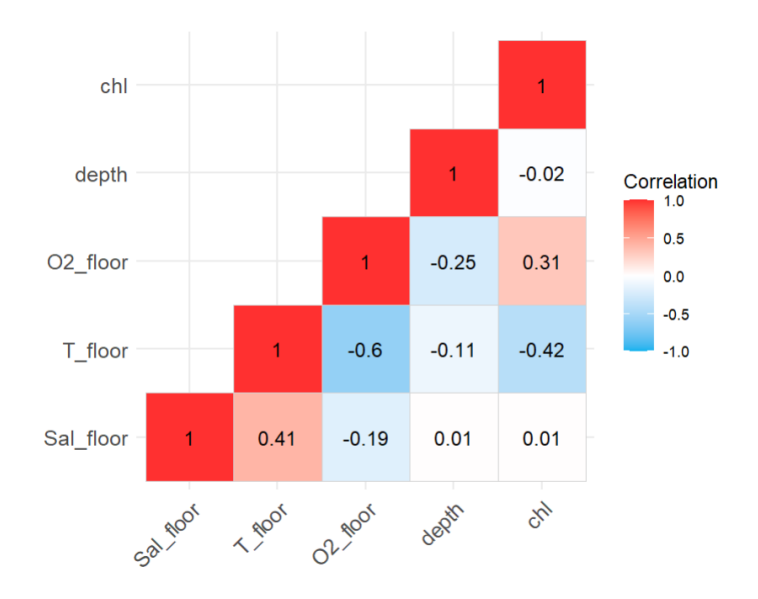


Figure S1: Correlation matrix for the environmental parameters

Table S2: MCMC convergence metrics.

Model		Beta parameter	Gamma parameter
Occurrence	Mean potential scale reduction factor	1.285	1.041
ı	Mean effective sample size	180.942	200.415
Biomass	Mean potential scale reduction factor	1.301	1.087
	Mean effective sample size	144.725	199.479

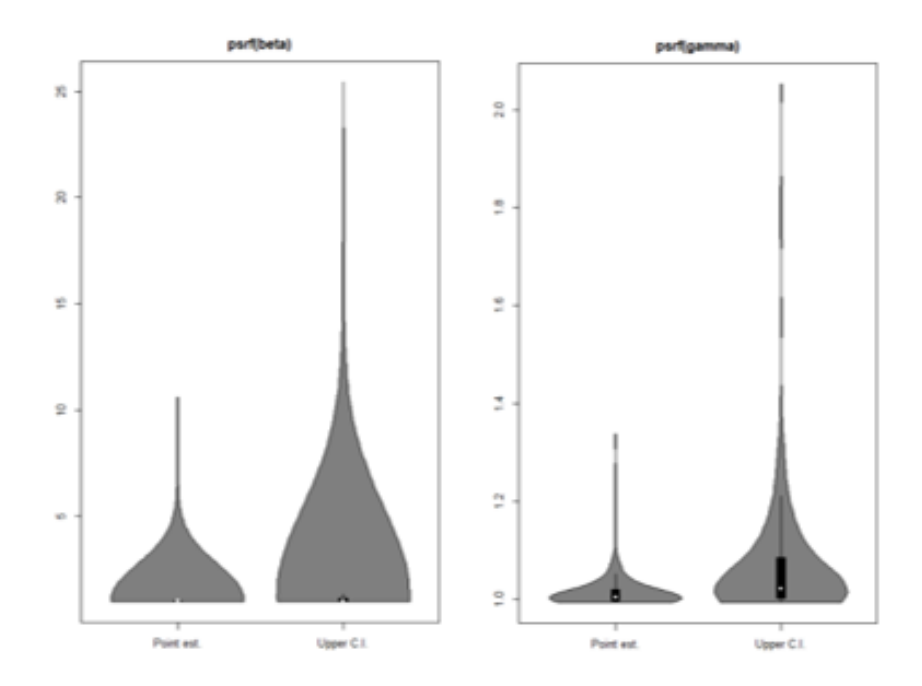


Figure S2: Violin plots of the potential scale reduction factor (psrf) for beta and gamma parameters.

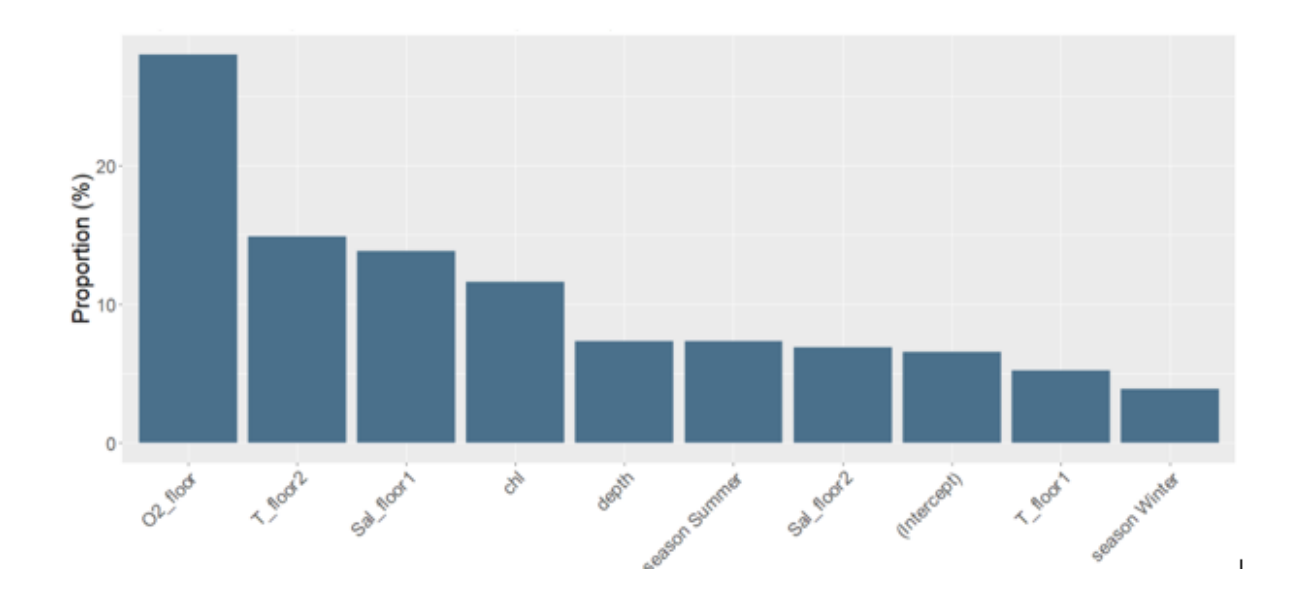


Figure S3: Proportion of the species response to environmental covariates explained by traits

Appendix 3. Baltic Sea fish model

Table S1: Categories of biological traits used to assess functional composition'

Trait	Categories	Label	Description	
Growth coefficient (K)	Continuous	les scowth	Growth coefficient K estimated from the Von Bertalanffy equation	
Fecundity	Continuous	los_fecundity	Number of offspring per female per batch or per year	
Offspring size	Continuous	les effserins size.	Diameter if the released eggs, length of the egg case or length of the young (mm)	
Maximum length	Continuous	los_lensth.max	Maximum reported length	
Age at maturity	Continuous	los_ass_maturity	First age at which the individual is able to reproduce	
Habitat	Bathydemersal Bathypelagic Benthopelagic Demersal Pelagic Reef-associated	habitatbathydemecsal. habitatbathydelagic. habitatbenthodelagic. habitatdemecsal habitatdelagic. habitatreef-associated	Zone of the water column used by the species	
Feeding mode	Benthivorous Herbivorous Generalist Piscivorous Planktivorous	feeding.modebenthixorous, feeding.modeberbixorous, feeding.modeseneralist feeding.modepiscixorous, feeding.modeplanktixorous	Main food source from stomach contents and biological descriptions of adults	
Body shape	Compressiform Eel-like Elongated Flat Fusiform Short and/or deep	body.shapesompressiform body.shapesel-like body.shapeslongated body.shapeslat. body.shapeslat. body.shapeshort.and/or deep	Shape of the body	
Fin shape	Pointed Rounded Truncate Lunate	fin.shapecointed fin.shapecounded fin.shapetruncate fin.shapelunate	Shape of the caudal fin	

	Heterocercal Forked	fin.shapeheterosercal fin.shapeforked	
Spawning type	Guarder Non-guarder Bearer	Spanning.typepun-guarder Spanning.typepun-guarder Spanning.typebearer	Type of spawning related to parental care

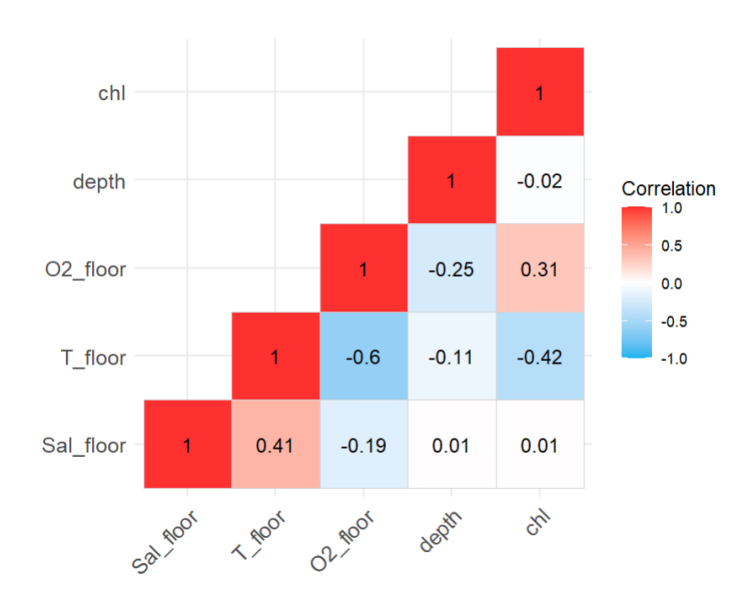


Figure S1: Correlation matrix for the environmental parameters

Table S2: MCMC convergence metrics

Model		Beta parameter	Gamma parameter
Occurrence	Mean potential scale reduction factor	1.104	1.015
	Mean effective sample size 880.6	880.659	1003.481
Biomass	Mean potential scale reduction factor	1.207	1.026
	Mean effective sample size	925.818	1043.748

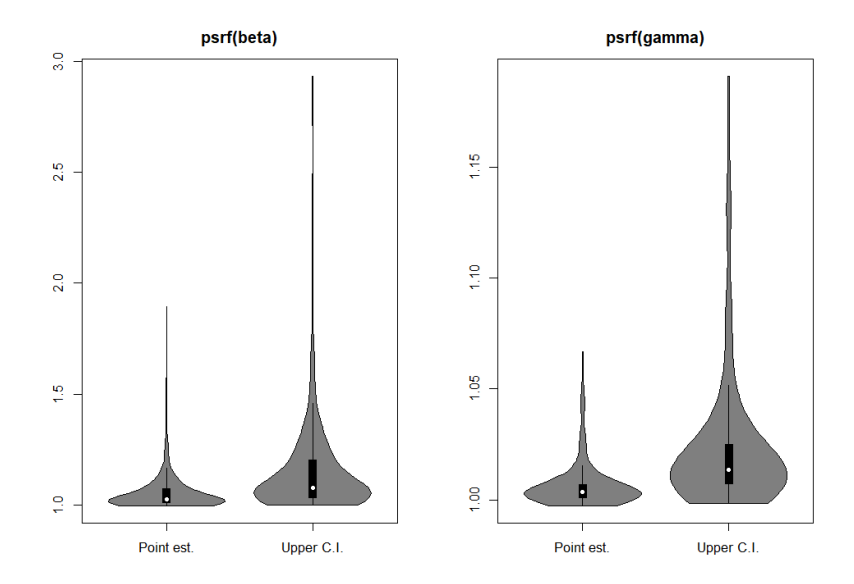


Figure S2: Violin plots of the potential scale reduction factor (psrf) for beta and gamma parameters.

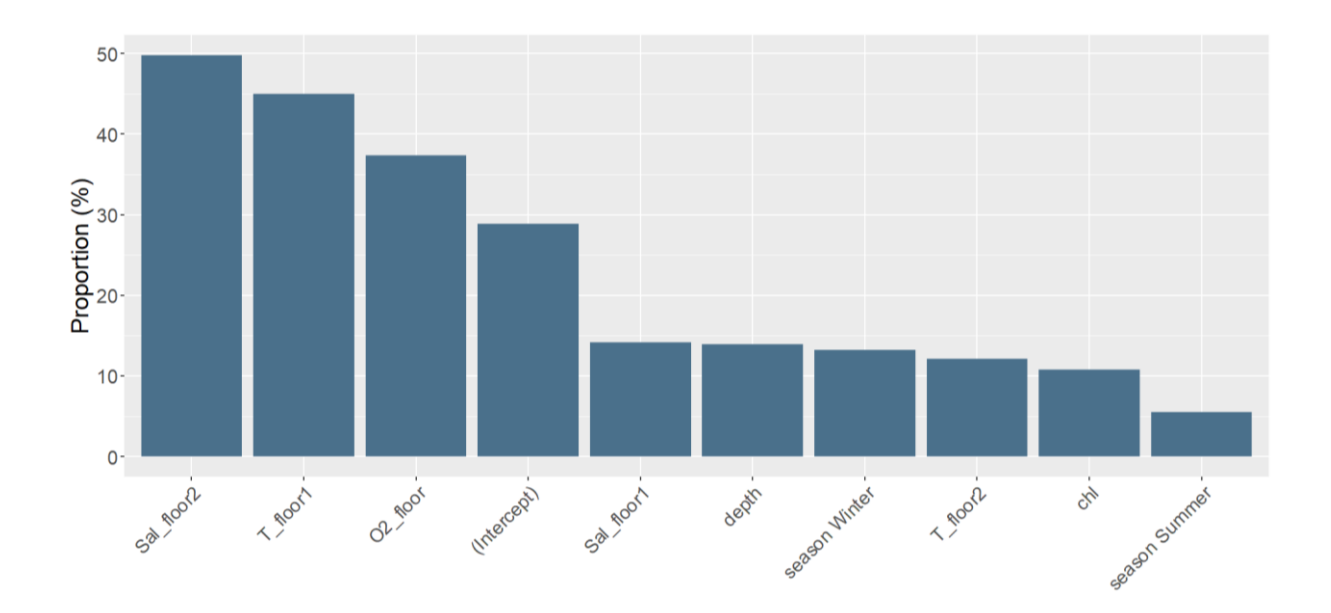


Figure S3: Proportion of the species response to environmental covariates explained by traits

Appendix 4. Central-Eastern Mediterranean Sea model

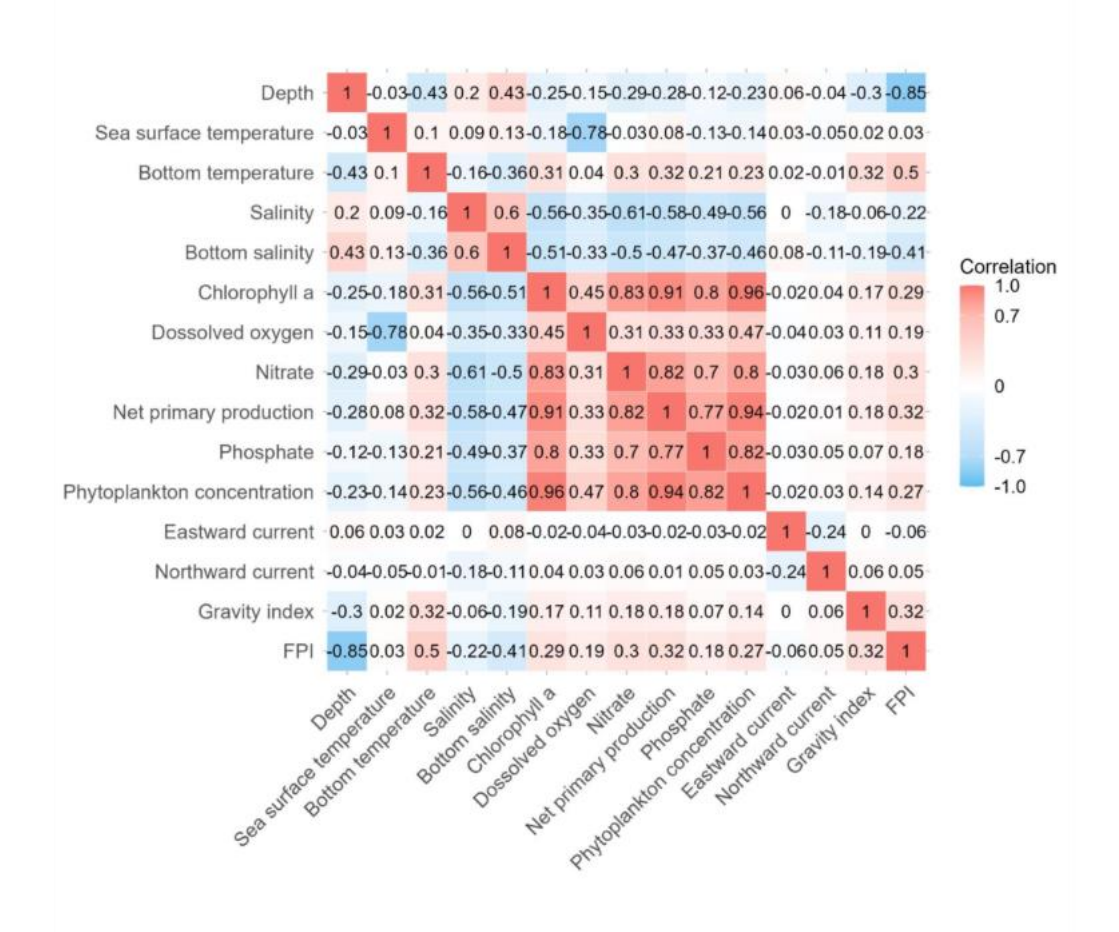


Figure S1. Pearson correlation matrix of the environmental and physical covariates included in the HMSC models. Each cell displays the pairwise Pearson correlation coefficient between covariates. The background colour gradient highlights the direction and magnitude of the correlation (blue for negative, red for positive), while numerical values allow precise interpretation.

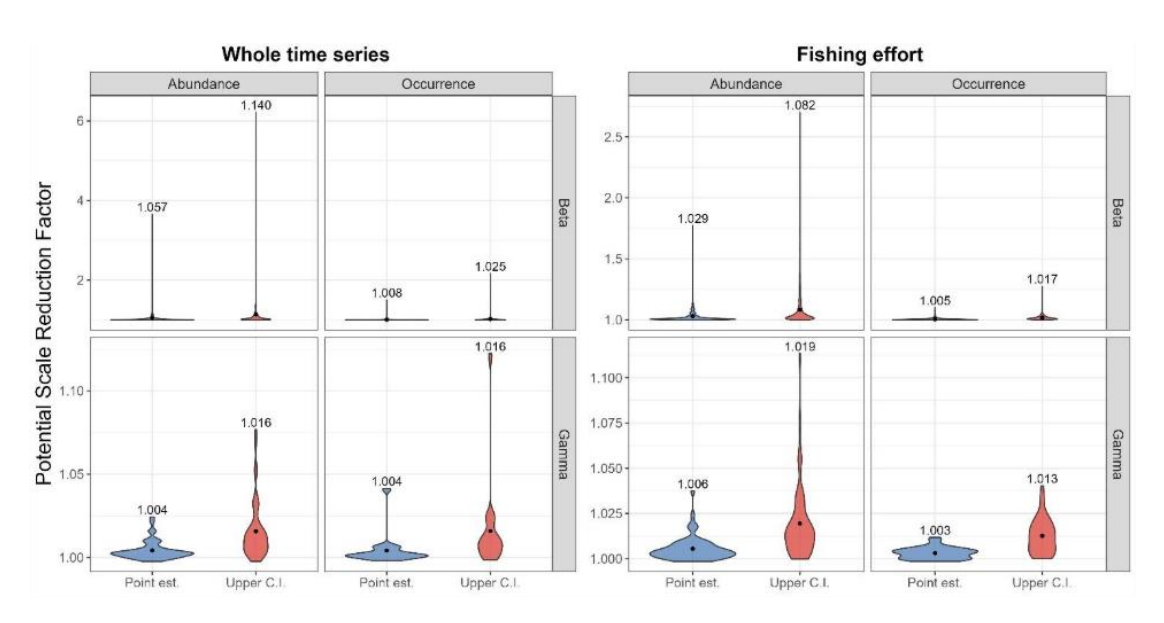


Figure S2. Convergence diagnostics for the MCMC models of Abundance (left column) and Occurrence (right column), showing the distribution of Potential Scale Reduction Factor (PSRF) values for the beta (first row) and gamma (second row) parameters. For each panel, distributions are shown separately for the point estimate and the upper confidence limit, with the corresponding mean PSRF value reported at the top.

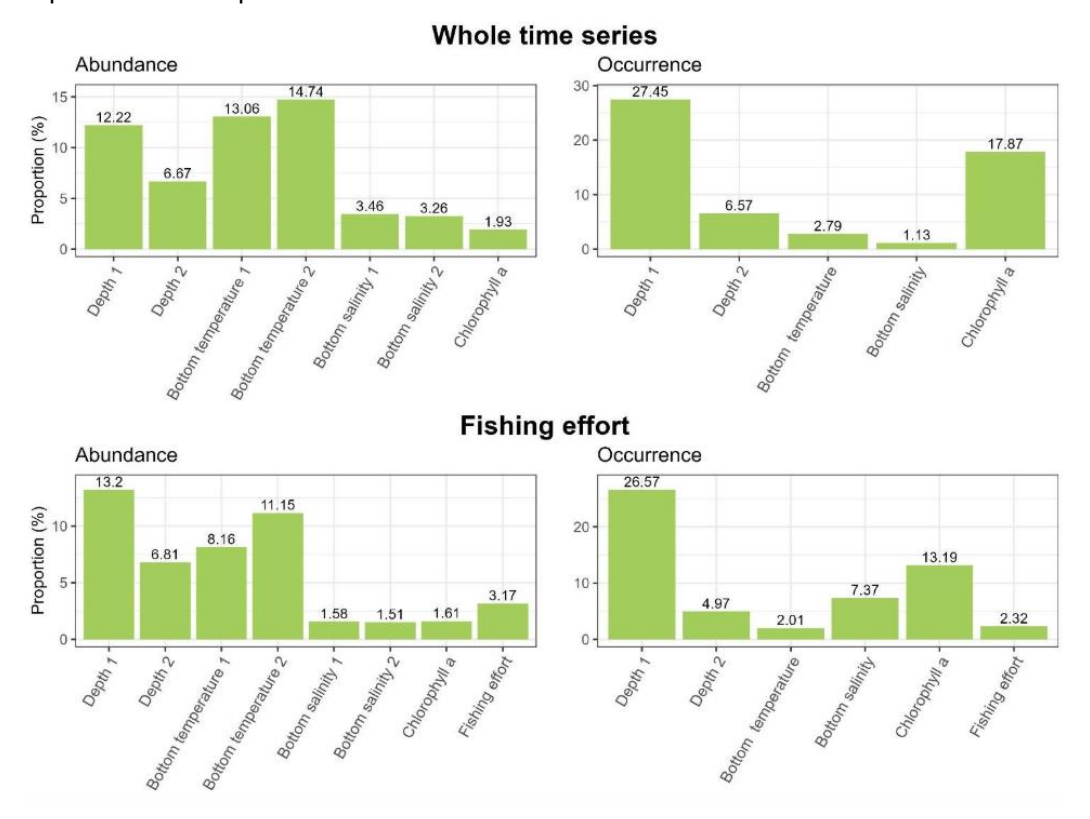


Figure S3. Proportion of the species' responses to environmental covariates explained by life history traits in the WTS (upper panel) and FE (lower panel) models.

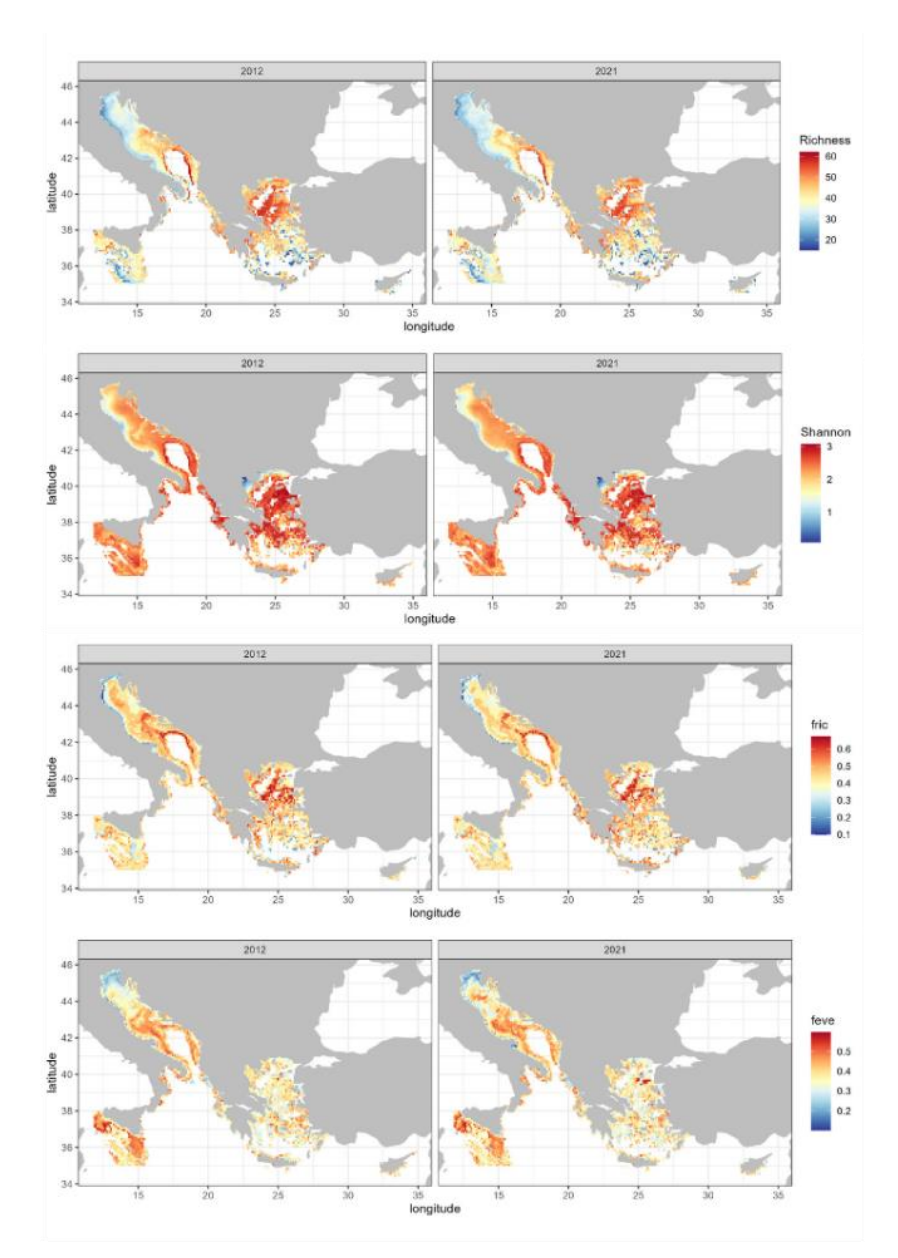


Figure S4. FE models' spatial patterns of taxonomic and functional biodiversity indicators, including species richness (1st row), Shannon index (2nd row), functional richness (3rd row), and functional evenness (4th row). The indicators are based on model predictions for two selected years, including 2012 (left column), and 2021 (right column).

Table S1. Posterior estimates (2.5%, 50%, and 97.5% quantiles) of the phylogenetic signal (λ) for both occurrence and abundance data of the WTS and FE models.

	Occurrence			Abundance		
Model	2.50% 50% 97.50%			2.50%	50%	97.50%
WTS	0.54	0.7	0.84	0.3	0.49	0.66
FE	0.58	0.72	0.84	0.44	0.63	0.78

Appendix 5 Western Mediterranean Sea model

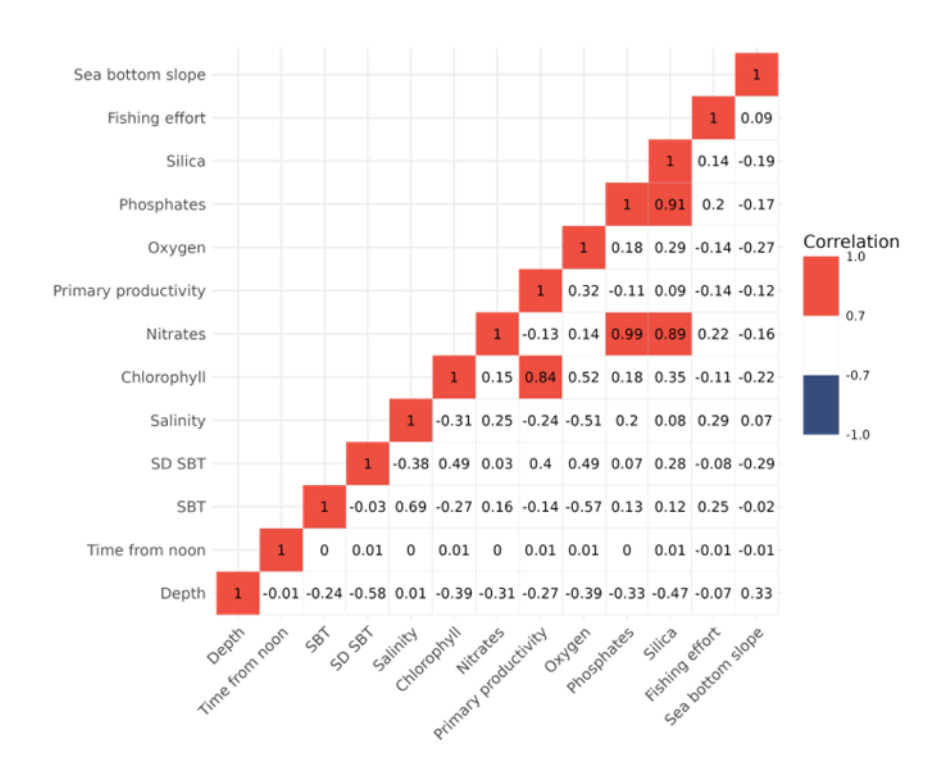


Figure S1: correlation matrix between the environmental predictors considere for the study. A correlation >0.7 is indicates in red, while a correlation <-0.7 is indicate in blue.

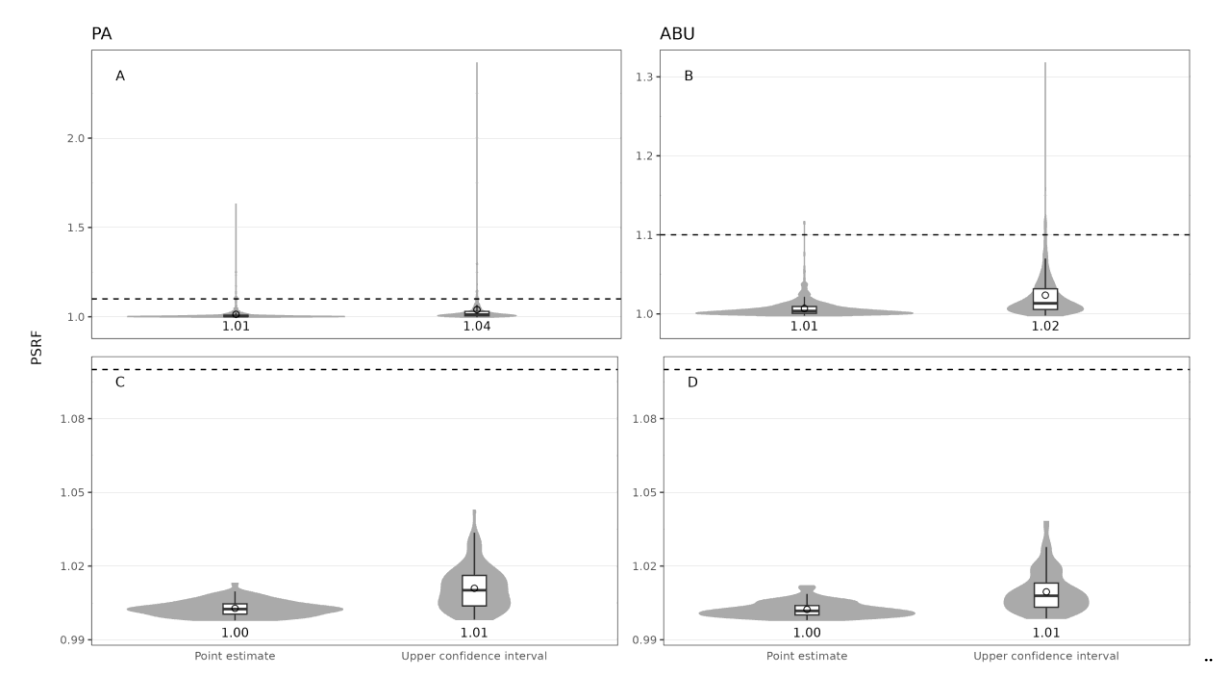


Figure S2: distribution of the potential scale reduction factors and related upper confidence interval of the beta (A-B) and gamma (C-D) parametres estimated for both models. The circle indicates the average value, which is noted at the bottom of each violin and boxplot.

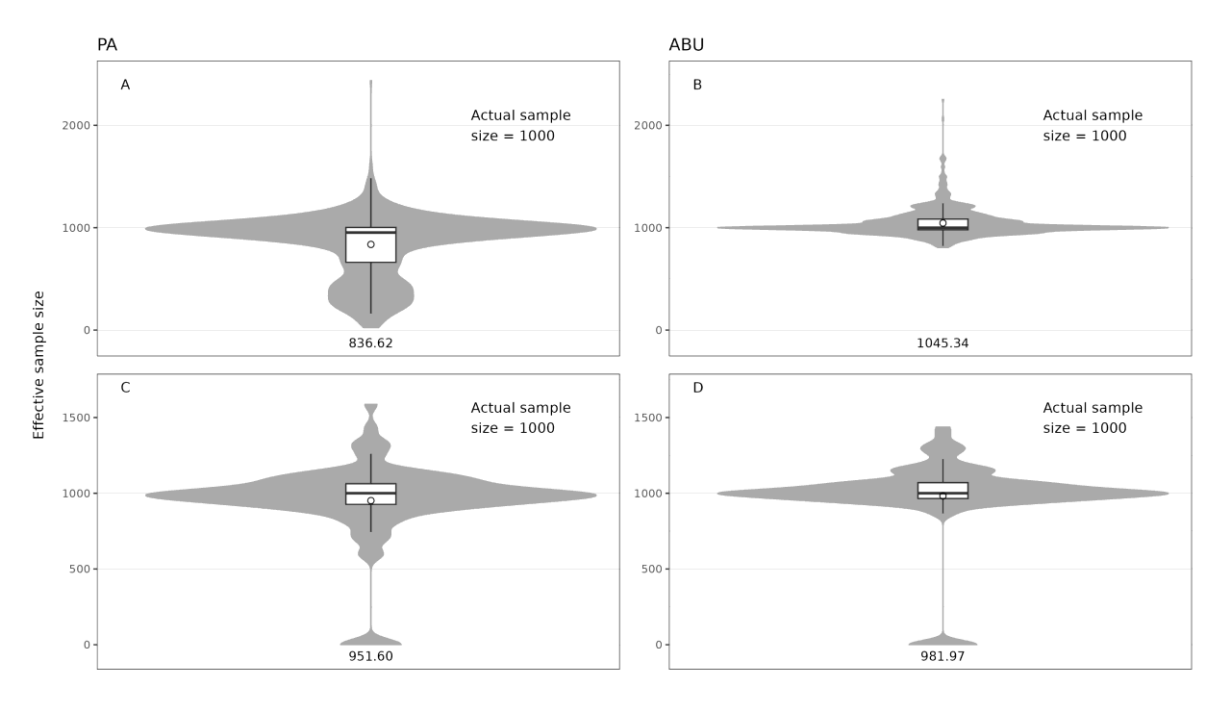


Figure S3: distribution of the effective sample size of the beta (A-B) and gamma (C-D) parametres estimated for both models. The circle indicates the average value, which is noted at the bottom of each violin plot.

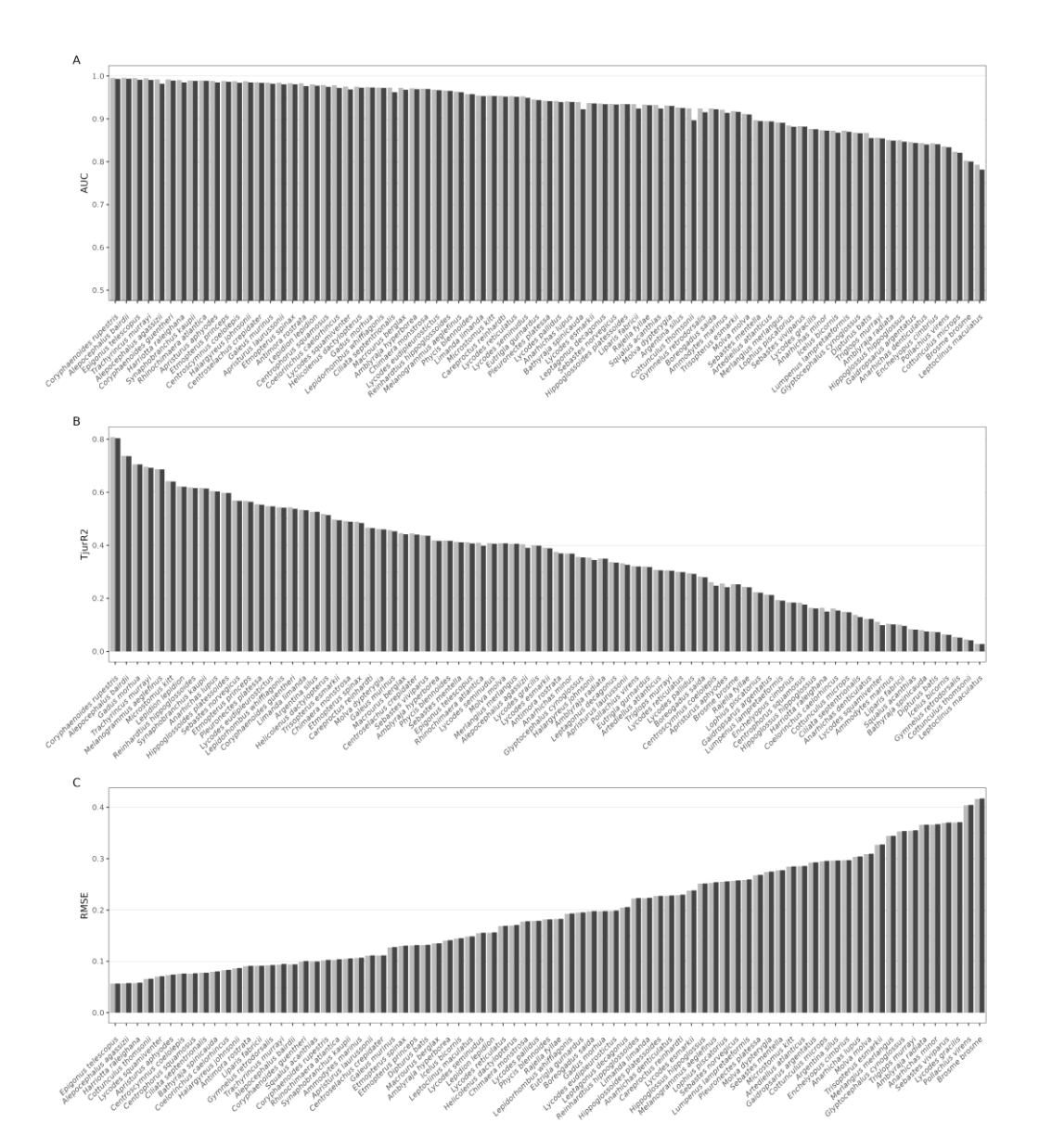


Figure S4: explanatory (light grey) and predictive (dark grey) power for each of the species included in the PA model, in terms of under the receiver operating characteristic curve (AUC) (A), Tjur's R2 (B) and the root mean square error (RMSE) (C)

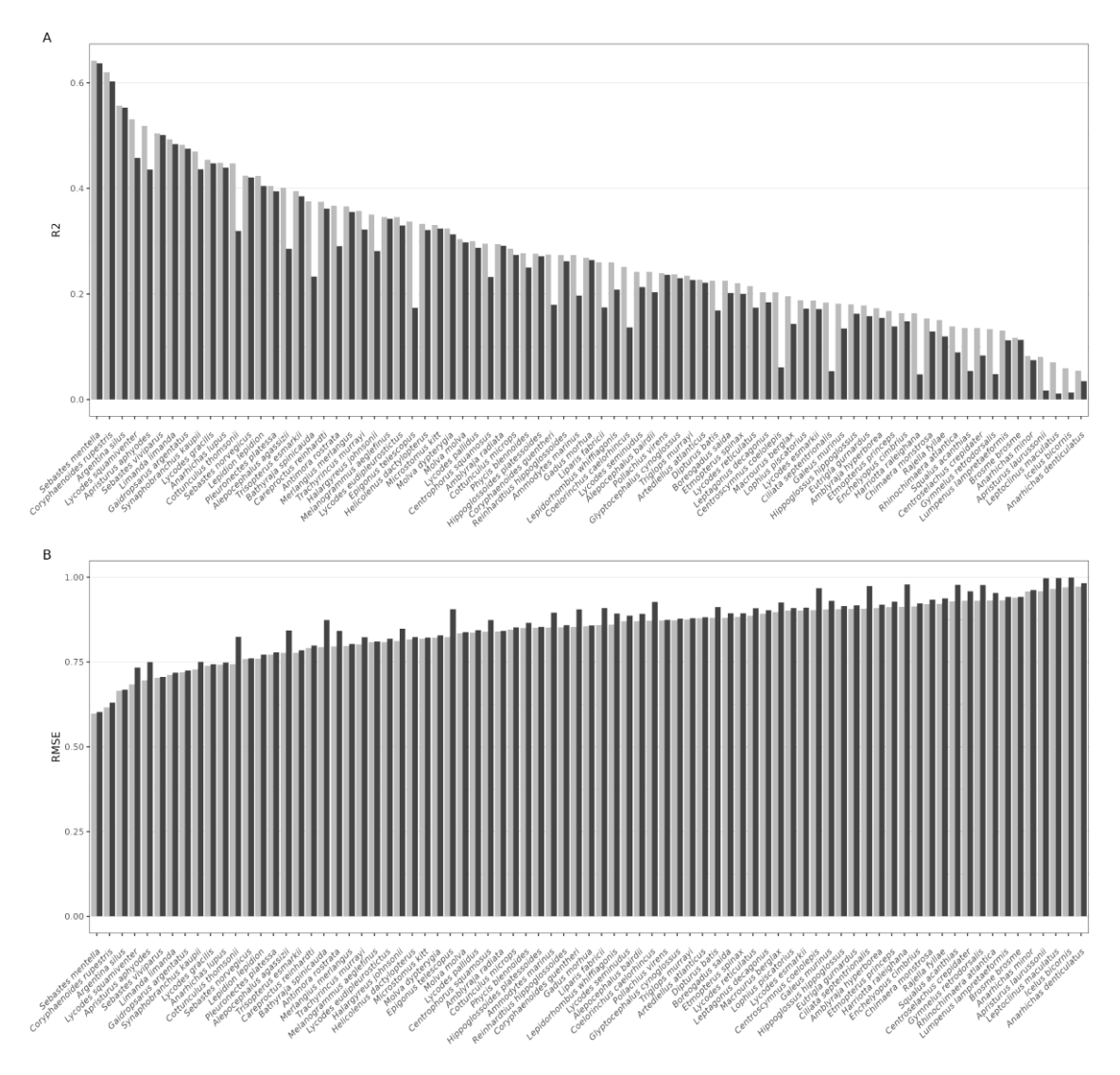


Figure S5: explanatory (light grey) and predictive (dark grey) power for each of the species included in the ABU model, in terms R2 (A) and the root mean square error (RMSE) (B)

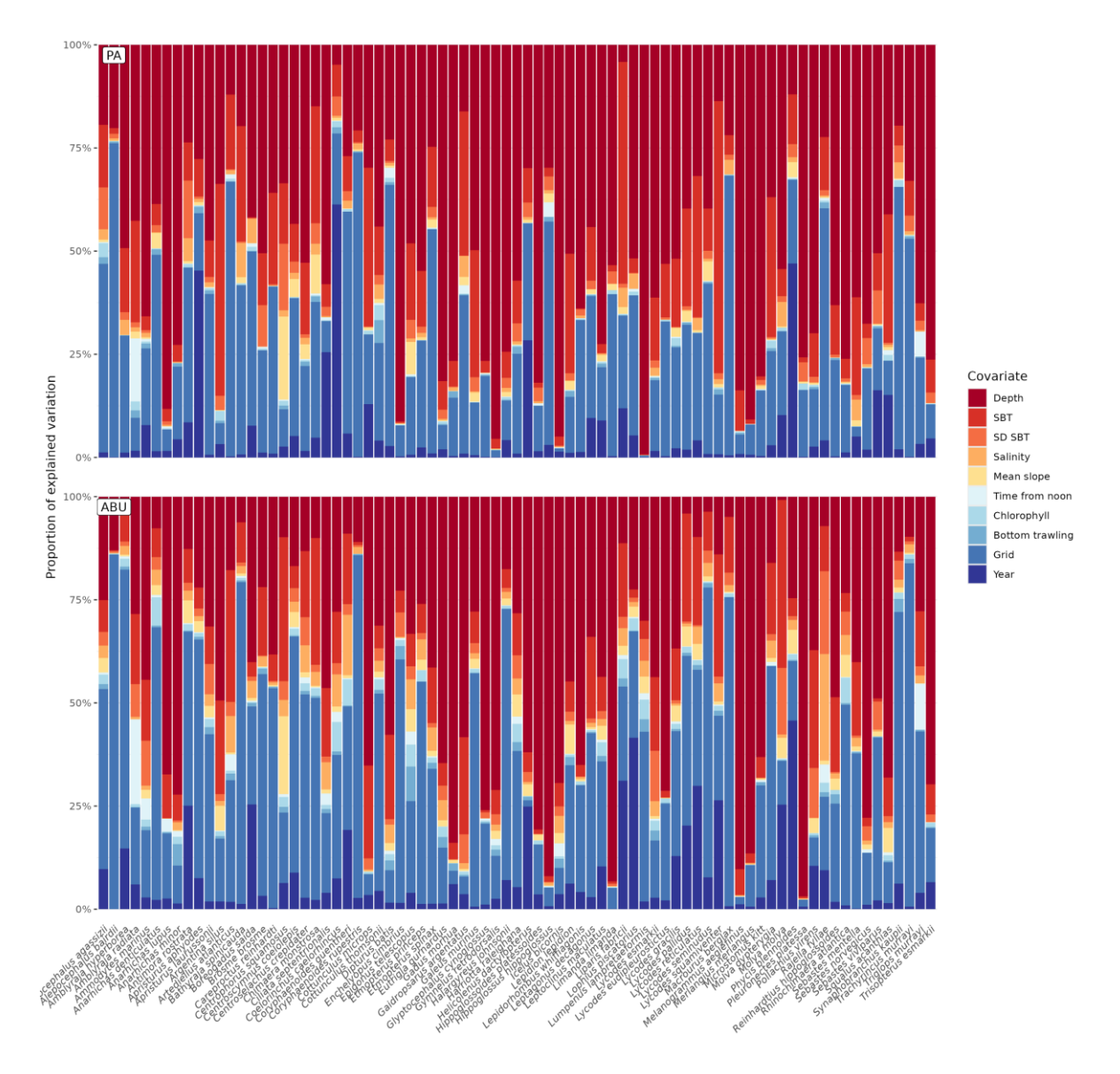


Figure S6: proportion of explained variance attributable to each one of the predictors included in the study, by species.